MICROCOPY RESOLUTION TEST CHART

NATIONAL BUREAU OF STANDARDS-1963-A

CHARACTERIZATION OF NAVY FUELS
USING SUPERCRITICAL FLUID ANALYTICAL METHODOLOGIES
23111 06392

Bob W. Wright, Henry T. Kalinoski, Andrew J. Kopriva,
Harold R. Udseth and Richard D. Smith

Chemical Methods and Separations Group
Chemical Technology Department
Battelle, Pacific Northwest Laboratories
Richland, WA 99352

DTIC
SELECTE**D**
NOV 0 4 1986
D

Final Report to:

Naval Research Laboratory
Washington, D.C.

August 1986

AD-A174 064

DTIC FILE COPY

AD-A174064

REPORT DOCUMENTATION PAGE

1a. REPORT SECURITY CLASSIFICATION UNCLASSIFIED	1b. RESTRICTIVE MARKINGS
2a. SECURITY CLASSIFICATION AUTHORITY	3. DISTRIBUTION / AVAILABILITY OF REPORT
2b. DECLASSIFICATION / DOWNGRADING SCHEDULE	Unlimited

4. PERFORMING ORGANIZATION REPORT NUMBER(S) 23111 06392	5. MONITORING ORGANIZATION REPORT NUMBER(S) ----

6a. NAME OF PERFORMING ORGANIZATION Battelle Pacific Northwest Laboratories	6b. OFFICE SYMBOL (If applicable) 052400	7a. NAME OF MONITORING ORGANIZATION U. S. Naval Res. Lab., Code 6180
6c. ADDRESS (City, State, and ZIP Code) Richland, WA 99352		7b. ADDRESS (City, State, and ZIP Code) Washington, DC 20375-5000

8a. NAME OF FUNDING / SPONSORING ORGANIZATION DTNSRDC/A	8b. OFFICE SYMBOL (If applicable) 387682	9. PROCUREMENT INSTRUMENT IDENTIFICATION NUMBER Contract No. N00014-84-C2306

8c. ADDRESS (City, State, and ZIP Code) Annapolis, MD 21402	10. SOURCE OF FUNDING NUMBERS			
	PROGRAM ELEMENT NO. 63724N	PROJECT NO.	TASK NO. Z0838-SL	WORK UNIT ACCESSION NO. 61-0079-06

11. TITLE (Include Security Classification)

Characterization of Navy Fuels Using Supercritical Fluid Analytical Methodologies

12. PERSONAL AUTHOR(S)
B. W. Wright, H. T. Kalinoski, A. J. Kopriva, H. R. Udseth and R. D. Smith

13a. TYPE OF REPORT Final	13b. TIME COVERED FROM 10/84 TO 6/86	14. DATE OF REPORT (Year, Month, Day) 1986,8,22	15. PAGE COUNT 170

16. SUPPLEMENTARY NOTATION

17.	COSATI CODES		18. SUBJECT TERMS (Continue on reverse if necessary and identify by block number)
FIELD	GROUP	SUB-GROUP	Polar Fuel Fractions, Supercritical Fluid Chromatography-MS, Fuel Sediments, Supercritical Fluid Extraction-MS, Chemical Class Fractionation, Antioxidant Analysis

19. ABSTRACT (Continue on reverse if necessary and identify by block number)

The purpose of this investigation was to develop and apply new analytical supercritical fluid methodologies for the improved characterization of Navy fuels. These studies addressed three specific areas which included the analysis of polar fuel components and sediment material; the development of a rapid and reliable chemical class fractionation methodology; and the development of simplified antioxidant analysis methodology. The main emphasis was directed at obtaining an improved understanding of the chemical composition of the polar fuel components that may lead to sediment formation in fuels and in elucidating the composition of fuel sediment material itself. Capillary supercritical fluid chromatography (SFC) and SFC-mass spectrometry (SFC-MS) were utilized for fuel analysis and direct supercritical fluid extraction-mass spectrometry (SFE-MS) was used to characterize intractable sediment material. An SFC/FID chemical class fractionation method was developed and applied to several middle distillate fuels and SFE-GC was examined for antioxidant analysis.

20. DISTRIBUTION / AVAILABILITY OF ABSTRACT ☐ UNCLASSIFIED/UNLIMITED ☒ SAME AS RPT. ☐ DTIC USERS	21. ABSTRACT SECURITY CLASSIFICATION Unclassified	
22a. NAME OF RESPONSIBLE INDIVIDUAL R.N. Hazlett	22b. TELEPHONE (Include Area Code)	22c. OFFICE SYMBOL 251950

DD FORM 1473, 84 MAR

83 APR edition may be used until exhausted.
All other editions are obsolete

86 11 3 019

CONTENTS

SUMMARY

The purpose of this investigation was to develop and apply new analytical supercritical fluid methodologies for the improved characterization of Navy fuels. These studies addressed three specific areas which included the analysis of polar fuel components and sediment material, the development of a rapid and reliable chemical class fractionation methodology, and the development of simplified antioxidant analysis methodology.

The main emphasis was directed at obtaining an improved understanding of the chemical composition of the polar fuel components that may lead to sediment formation in fuels and in elucidating the composition of fuel sediment material itself. To adequately characterize the polar fuel components it was necessary to develop improved supercritical fluid chromatography (SFC) and supercritical fluid chromatography - mass spectrometry (SFC-MS) capabilities. This included the development of procedures to prepare highly inert chromatographic capillary columns and the development of high polarity and high solvating power supercritical fluid mixtures for use as mobile phases. These developments allowed the successful SFC and SFC-MS analyses of the polar fractions to be obtained from unstable diesel fuel marine samples. Sediments from the same fuel were subjected to on-line supercritical fluid extraction - mass spectrometry with tandem MS/MS analyses. Alkyl indoles and carbazoles were found to be major components in the sediment material with the matrix consisting of a pyrrole-like polymer with molecular weights extending to over 900 daltons.

The development of a chemical class fractionation methodology designed to rapidly quantify the aliphatic, monocyclic, and dicyclic components in fuels was investigated. Various approaches utilizing low resolution supercritical fluid chromatography with flame ionization detection to facilitate direct quantification were explored. Several fuels were analyzed to demonstrate the utility of this approach.

On-line supercritical fluid extraction-gas chromatography was explored for the analysis of trace levels of antioxidants in fuels. With this approach the fuel additives were selectively extracted from the fuel matrix, concentrated

1

in the chromatographic column and subsequently analyzed by high resolution gas chromatography. The various approaches utilized in this investigation are described.

Finally, recommendations for future work are presented.

TASK A. CAPILLARY COLUMN TECHNOLOGY DEVELOPMENT

Introduction

A tremendous amount of effort has been expended in the development of capillary column technology for gas chromatography (1-2). Years of research have been devoted to capillary column deactivation, methods for efficient stationary phase coating, and recently, stabilization of the stationary phase polymers by in-situ crosslinking. Much of this technology has been easily adapted for use in capillary supercritical fluid chromatography (SFC). However, the requirements of SFC place different demands on column technology. One of the major differences results from the use of small diameter fused silica columns (10-50 μm) which leads to physical problems in various preparational procedures. Another important difference results from the extra stress applied to the stationary phase by the solvating influence of the supercritical fluid mobile phase.

To achieve high chromatographic efficiency of polar materials in capillary SFC it is imperative to have an inert silica surface on which to coat the stationary phase. For a time it was not considered important to have a deactivated surface (because of slower mass transfer), but experience has shown that deactivation is essential in SFC. One reason for this is that smaller diameter columns exhibit higher surface activities due to the higher drawing temperature needed for fabrication. Another reason is that SFC typically operates at lower temperatures where adsorption interactions are stronger. The major sources of surface activity for fused silica are surface impurities deposited or which segregate at surfaces during fabrication, silanol groups, and strained siloxane structures. Activity can also be imparted from the chemical nature of stationary phases and crosslinking procedures. The most successful deactivation procedures in capillary GC employ either polymeric (3) or monomeric siloxanes (4,5) which are thermally rearranged to cover the surface. These procedures are not generally amenable to small diameter SFC columns due to plugging that occurs during the treatment. High temperature silylations that were successful for glass capillary columns are not generally applicable for any fused silica column due to degradation of the polyimide sheath (6). Consequently, new treatments for

3

the deactivation of small diameter columns have been devised. Such treatments include modified silylations using established reagents (7) and use of more reactive silylation reagents (8). Unfortunately, deactivation procedures are highly dependent on the silica surface structure of a specific batch of fused silica and continual optimization studies are necessary.

Another requirement for efficient SFC columns is the formation of a thin and uniform film of stationary phase during the coating procedure. The static coating method (9) is typically used to obtain maximum coating efficiency. With this method the column is filled with a solution of the stationary phase in a volatile solvent. To achieve even thin films (i.e., ~0.20 μm) the stationary phase solution is usually sufficiently concentrated and viscous that it is difficult to fill the column. Furthermore, during the coating procedure in which the volatile solvent is pumped off under vacuum, the pressure drop along the small diameter column length can become great enough to drastically slow down (and even stop) the coating procedure. These problems have been partially overcome by using high pressure techniques to fill the column with stationary phase solution and elevated temperatures (usually above the solvent's boiling point) during solvent evaporation (10).

A critical aspect of column technology for SFC is the surface bonding and crosslinking of the stationary phase polymers. Without such measures the stationary phase would be readily removed by the solvating influences of supercritical mobile phases. Unfortunatey, more polar and higher critical temperature fluids usually exert stronger and more deleterious effects on the polysiloxane polymers currently used. This is a major problem for polar fluid SFC and is usually overlooked. The free-radical crosslinking procedures developed for GC (11) are also applicable for SFC. With these techniques, a free-radical generator such as an aromatic peroxide or an azo compound is doped into the stationary phase and heated to initiate the production of free-radicals which in turn crossslinks (form bonds with) adjacent vinyl and aliphatic groups on the polysiloxane chain. Excessive crosslinking, however, can lead to poor mass transfer properties and poor efficiency in GC, but since diffusion rates are slower in SFC, excessive crosslinking is rarely a problem. In fact, methods of achieving more extensive crosslinking is an active area of research in SFC column technology.

The work described in this section discusses the approaches taken to optimize and form effective deactivation layers in small-bore fused silica columns. Methods of achieving sufficient crosslinking and stationary phase stability to wit stand the stresses of more polar and binary fluid systems are also described. Due to the nature and magnitude of the specific methods used for these processes, a more generalized description and summary will be given.

Experimental

Several fused silica capillary columns were prepared using various deactivation procedures. Generally, short column lengths of 5-10 meters of 50 μm i.d. fused silica (Spectran Corp., Sturbridge, MA, and Polymicro Technologies, Inc., Phoenix, AZ) were used. Essentially two types of deactivation processes and various optimizations of each were evaluated. The first deactivation process utilized monomeric silylation procedures and the second method used reactive polymeric siloxanes for surface reactions. The quality of the deactivations were evaluated chromatographically with various test probes.

Surface impurities such as nitrates and chlorides deposited during fabrication of the capillary tubing were removed, and the surface moisture content adjusted by purging the columns with dry nitrogen at elevated temperatures. Temperatures ranging from 200°C to 375°C with purge times between 30 minutes and several hours were used. For some columns, attempts were made to increase the surface silanol concentration. This was done by rinsing the columns with methanol at room temperature followed by a nitrogen purge at 200°C. More severe hydroxylation reactions were accomplished by purging the columns with wet nitrogen at 350°C followed by dehydration with dry nitrogen at 200°C.

Monomeric silylations utilized hexamethyldisilazane, chlorotrimethylsilane, and a 60/40 mixture of the two reagents. Both liquid and vapor phase methods of introducing the reagents were used. Reaction times and temperatures ranged from 4-12 hours and 300-400°C, respectively. Excess reagent and

5

decomposition products were removed by purging with nitrogen at 350°C for approximately an hour.

Mixtures of 10-25% of a polymethylhydrosiloxane fluid in either methylene chloride or pentane were used for the polymeric surface reactions. These mixtures were dynamically coated in the columns to provide thin surface films. After purging with nitrogen the columns were sealed and heated from 200 to 300°C for one to several hours. After reaction, excess reagent and any decomposition products were removed by washing with methylene chloride. In some cases, an additional treatment with chlorotrimethylsilane was used to cap any unreacted hydro groups on the polymeric siloxane. This reaction was accomplished by passing a small plug of the reagent through the column, filling it with nitrogen, and reacting at 350°C for several hours. Excess reagent and any decomposition products were removed by purging with nitrogen at 350°C.

After deactivation, the columns were statically coated with a ~ 0.25 μm film of a 5% phenyl methylphenylpolysiloxane (SE-54) or a 50% phenyl methylphenylpolysiloxane (OV-17) stationary phase. Crosslinking of the coated stationary phase was achieved using azo-t-butane as a free radical initiator. Azo-t-butane was partitioned into the stationary phase by purging saturated nitrogen vapors through the column at room temperature for one to several hours. The columns were sealed and heated to 220°C to induce free-radical production. After 30 minutes at 220°C columns were purged with a nitrogen flow. In some instances, the columns were washed with either pentane or methylene chloride and then given duplicate crosslinking treatments.

Column deactivation was evaluated chromatographically using various polarity mixtures. In general, finished (e.g. deactivated, coated, and crosslinked) columns were evaluated, but in some instances the columns were evaluated after deactivation to decouple any stationary phase effects. The most often used test mixture contained n-decane, 1-octanol, 1,6-hexanediol, octanoic acid, n-dodecane, 2,4,5-trichlorophenol, p-nitrophenol, and n-octadecane. In some instances, a basic mixture containing n-decane, 1-octylamine, n-dodecane, 1-decylamine, and 1-dodecylamine was also used. A less sensitive mixture containing n-decane, acetophenone, N-ethylaniline, naphthalene, 1-decanol, p-chlorophenol, and n-pentadecane was also used to

6

probe surface activity. Both gas and supercritical fluid chromatography were used for evaluation analyses. Chromatographic operating conditions were chosen to provide a rigorous evaluation (e.g. slow program rates, lower temperatures, and low sample loadings; <1 ng). GC evaluations were obtained on a Carlo Erba 4160 instrument using split injection. The gas chromatograph was modified to allow 300 psi operation of the carrier gas.

Stationary phase stability was monitored by comparing gas chromatography capacity ratio data obtained before and after various solvent and supercritical fluid conditioning treatments. Loss of stationary phase was proportional to the decrease in the capacity factor. Less subtle changes could be detected by drastic decreases in column performance and in certain extremes by actual plugging of the column.

Results and Discussion

Deactivation

Column deactivation is an important parameter in capillary preparation. Due to the highly variable surface characteristics of fused silica no single approach has been developed that allows efficient and successful deactivation of all silica surfaces. Indeed, slightly different environmental conditions during fabrication can alter the final surface characteristics and its response to different deactivation methods. Thus, to obtain deactivated columns it is necessary to optimize the deactivation parameters for each batch and type of silica used until more uniform column materials become available. This behavior was particularly evident when using fused silica from the two different manufacturers (e.g., Spectran and Polymicro).

Fused silica is intrinsically acidic which greatly complicates the elution of basic compounds. Acidic compounds that can experience hydrogen bonding are also adversely affected by the active silica surface. Surface activity is manifested by chromatographic peak tailing and, in many instances, by complete adsorption of the compounds. High surface activity and/or poorly executed deactivations can also lead to very poor coating of the stationary phase, and hence low chromatographic efficiency. An example of a poorly deactivated column is illustrated by the chromatogram shown in Figure 1.
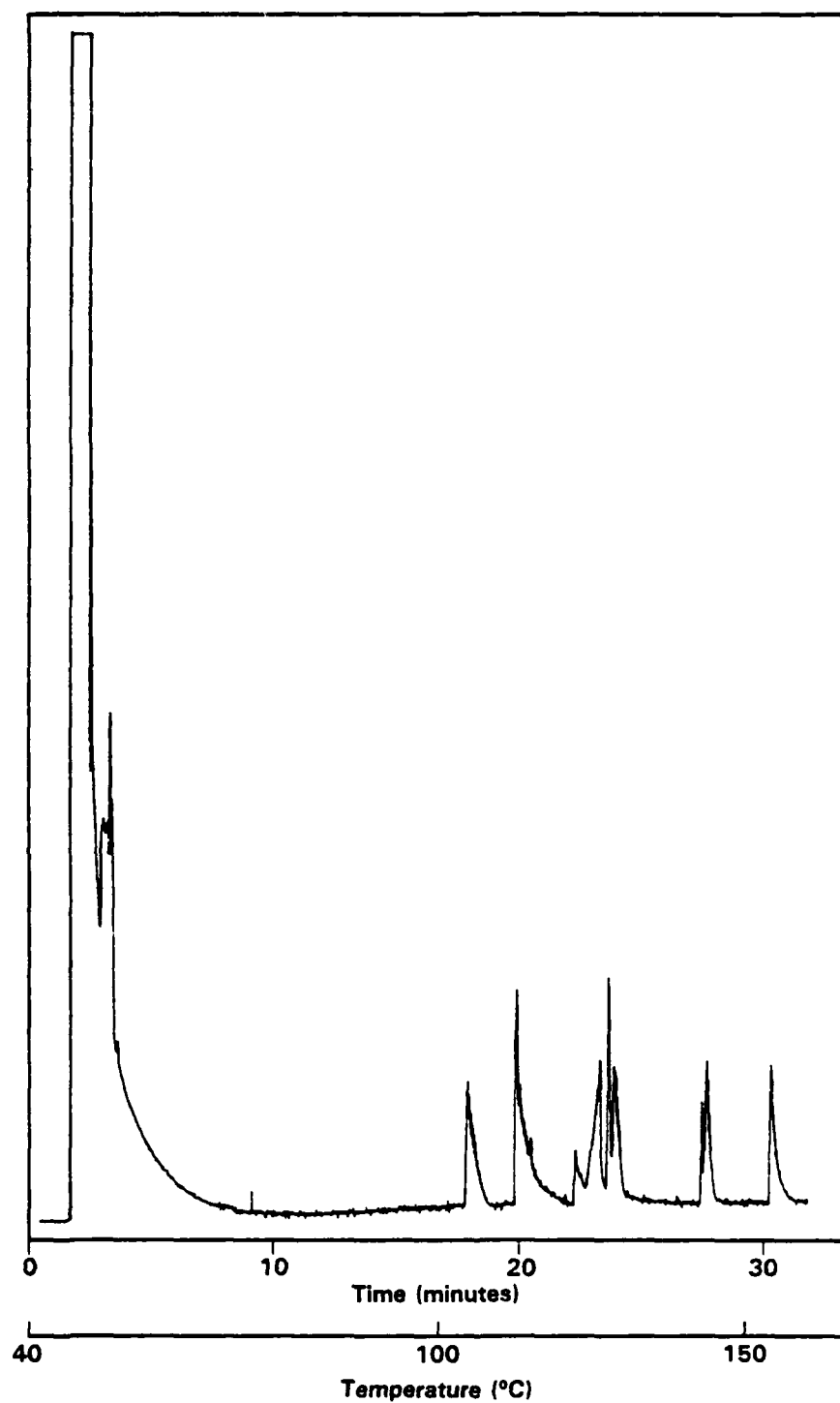
Figure 1.   Capillary GC test chromatogram of a polarity mixture obtained on a poorly deactivated column. Chromatographic conditions: 10 m x 50 μm column coated with SE-54, temperature programmed at 4°C/min from 40°C, 300 psi He carrier gas.

This separation of a polarity mixture was obtained by gas chromatography under temperature programmed conditions and illustrates both poor efficiency and high surface activity.

Monomeric Silylations

Successful approaches for column deactivation usually include some provision for removal of any reactive surface contaminants by chemical reaction with the active surface structures. Studies conducted during this investigation have shown that removal of the surface contaminants (including water) with a nitrogen purge at 350°C for several hours produced the optimum surface for reaction with monomeric silanes. The best silylations were obtained using a mixture (60/40) of hexamethyldisilazane and chlorotrimethylsilane reacted at temperatures in excess of 350°C for a minimum of eight hours. A dynamic vapor phase method of introducing the silylation agent in which new reagent continually flowed in to the column was found to provide better results than the static method in which the reagents were coated in the column prior to heat treatments. Reaction temperatures were limited to slightly less than 400°C, since serious oxidation of the polyimide occurred at higher temperatures. An example of a test chromatogram obtained on a column prepared in this manner is shown in Figure 2. The chromatogram was obtained using SFC (rather than GC) with a carbon dioxide mobile phase at 100°C and a 3 atm/min pressure ramp. High gain detection (which accounts for the noisy baseline) was used so very low (< 1 ng) solute loadings could be used to obtain as rigorous of evaluation as possible. Most of the compounds exhibited very good peak shape, but the most polar components still experienced some adsorptive influences. In fact, the diol was completely adsorbed and was not eluted. A basic test mixture was also evaluated and although the alkylamines were eluted, the peaks tailed badly. Clearly, however, this deactivation provides much better performance than observed in Figure 1.

Polymeric Deactivations

To obtain more inert surfaces, a polymeric siloxane was used for deactivation. Polymeric materials usually provide better deactivation than monomeric reagents because a thicker layer and more complete surface
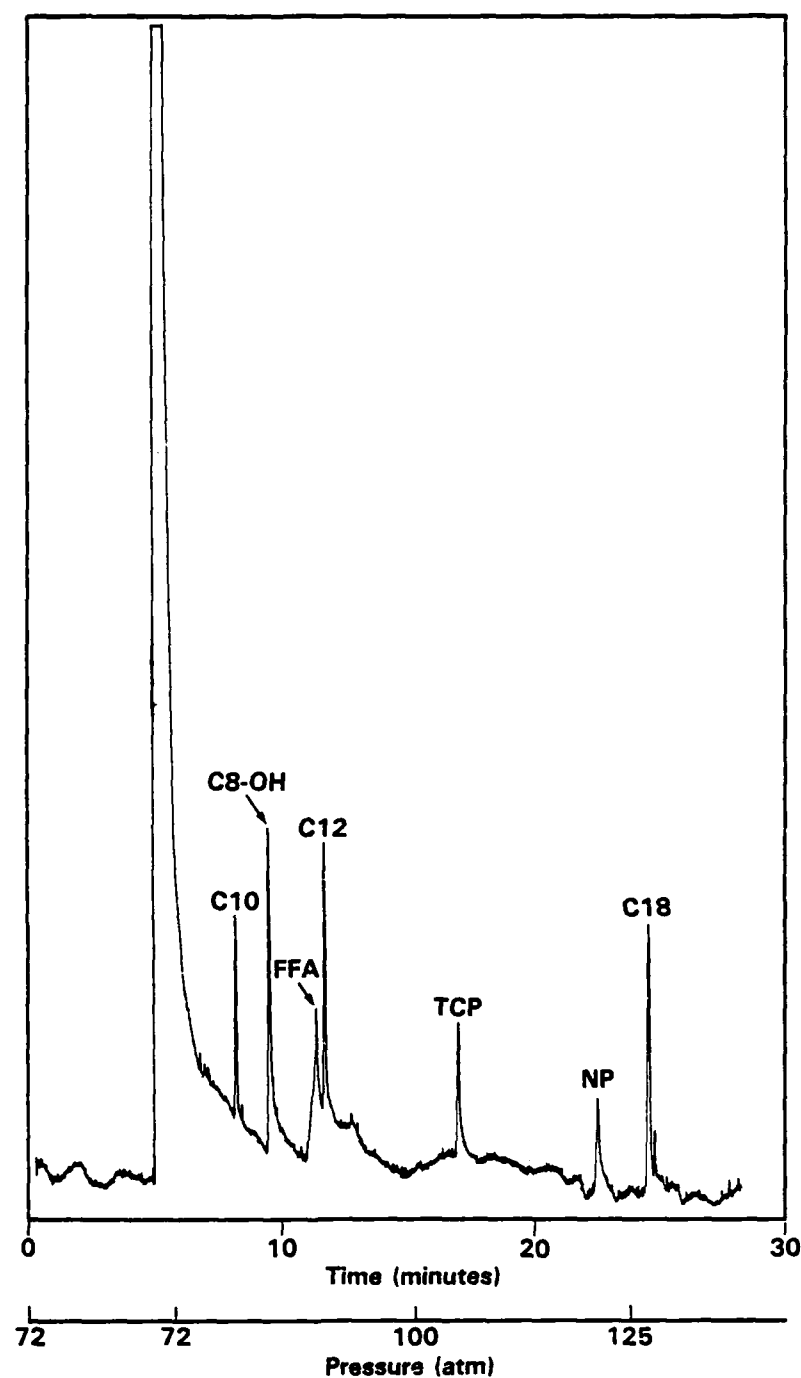
9

Figure 2.   Capillary SFC test chromatogram of a polarity mixture
             obtained on a column deactivated with monomeric silanes.
             Chromatographic conditions: 10 m x 50 μm column coated
             with SE-54, carbon dioxide mobile phase at 100°C,
             pressure ramped from 72 atm at 3 atm/min following elution
             of the solvent peak. Peak identifications: C10 = n-
             decane, C8-OH = 1-octanol, DIOL = 1,6-hexanediol, FFA =
             1-octanoic acid, TCP = 2,4,5-trichlorophenol, NP = p-
             nitrophenol, and C18 = n-octadecane.

10

coverage is obtained. The polymeric materials attach to the readily accessible silanol groups and provide an effective shield for any remaining unreacted groups (due either to steric hindrance or incomplete reaction). Monomeric reagents, on the other hand, only block those groups with which they react. In many cases the polymeric silica backbone is also active or intraglobular hydroxyl groups that lie immediately under the surface, and are not available for reaction, are also a source of surface activity. The polymeric materials cover these sites and produce an inert surface layer.

For successful deactivation in small diameter columns it is necessary to use dilute solutions of the polymeric reagents to prevent plugging. The lower concentration and correspondingly lower viscosity minimizes plugging but it also lowers the reactivity. To improve reactivity and also allow much lower treatment temperatures (since reaction is initiated by thermal degradation), a polymeric siloxane with chemically reactive groups is advantageous. The silylhydride group in polymethylhydrosiloxane reacts with silanol groups to form a siloxane bridge with the elimination of hydrogen gas (12). This reaction occurs at modest temperatures of approximately 250°C.

To achieve optimum surface coverage (and hence better deactivation and stability) it was found that more mild conditions were needed for the initial thermal treatment used to clean the surface of impurities. A nitrogen purge for thirty minutes at 300°C was found to provide the best results. The lower temperature and shorter time was probably sufficient to remove any contaminants but did not completely remove the surface water which could catalyze the reaction. A 20% mixture of the polymethylhydrosiloxane fluid in pentane reacted at 250°C for 1-2 hours provided optimum silylation conditions. A test chromatogram of a polarity mixture obtained from a column deactivated in this manner is shown in Figure 3. This chromatogram was obtained by gas chromatography under temperature programmed conditions. Although the diol peak tailed slightly, the rest of the polar compounds exhibited excellent symmetry indicating that good deactivation was obtained. The alkylamines were also eluted and exhibited only slight peak tailing.

A potential problem with deactivations using polymethylhydrosiloxane is incomplete reaction of the hydro groups. To eliminate this possibility a silylation treatment using chlorotrimethylsilane was applied after the
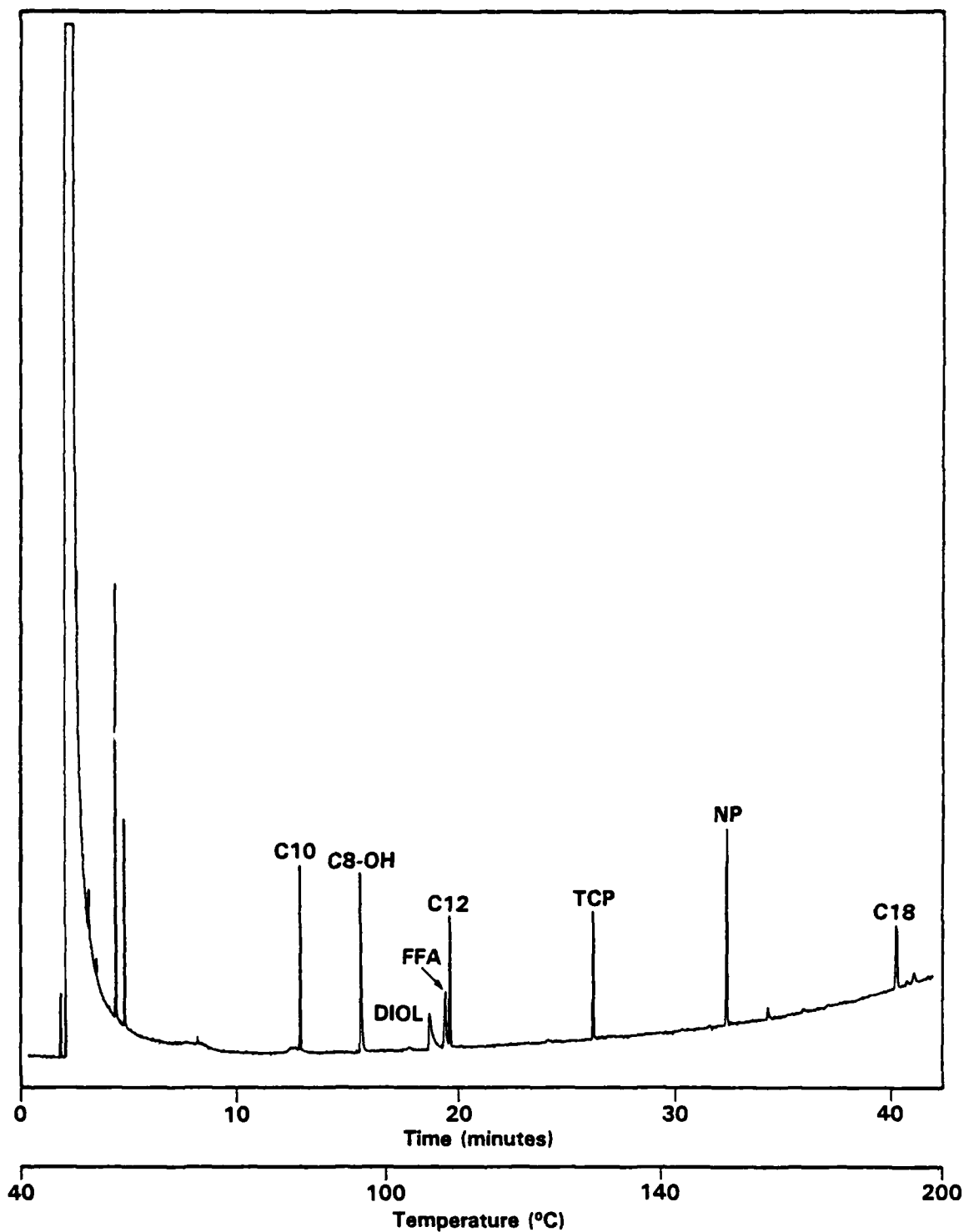
11

Figure 3.   Capillary GC test chromatogram of a polarity mixture
obtained on a column deactivated with a polymeric
siloxane. Chromatographic conditions: 10 m x 50 μm
column coated with SE-54, temperature programmed at
4°C/min from 40°C, 300 psi He carrier gas. Peak
identifications the same as in Figure 2.

polymethylhydrosiloxane deactivation. A test chromatogram of a different polarity mixture obtained on a column deactivated in this manner is shown in Figure 4. This chromatogram was also obtained by gas chromatography under temperature programmed conditions. The polar components in this mixture were all eluted with as sharp of peak shapes as the alkanes. Although this mixture does not contain as polar of components as the one shown in the previous figures, the excellent peaks shapes confirm that good deactivation was obtained.

Stationary Phase Stability

The general approach taken to achieve maximum stationary phase stability is to crosslink and bond the polymer to the silica surface. This process involves internal crosslinking of the phase (e.g. one chain to another through methylene bridges) and crosslinking of the phase to the deactivation layer. Thus, if the deactivation layer is effectively bonded to the silica, the stationary phase is also surface bonded. For this reason, the polymeric surface deactivation layers also provide maximum attachment sites for crosslinking to the stationary phase. By increasing the concentration of silica surface hydroxyl groups, more attachment sites exist for bonding the deactivation layer to the silica which ultimately provides greater stationary phase stability. The methanol treatment appears to be most effective for creating an optimum hydroxyl density. Excessive hydroxylation creates a surface that cannot be totally deactivated, and in some instances, can render the surface somewhat porous which prevents efficient coating of the stationary phase. The wet nitrogen treatment at 350°C created such a situation. A test chromatogram of a polarity mixture obtained by gas chromatography with a column that had a methanol treatment to slightly increase the surface hydroxyl concentration followed by a similar deactivation as described for Figure 4 is shown in Figure 5. Very sharp peak shapes were obtained indicating good deactivation and efficient coating.

Wash-out studies, in which the capacity ratios for several alkanes were measured by gas chromatography before and after various solvent and supercritical fluid conditioning treatments, were used to determine the stability of the crosslinked phases. If no crosslinking was done, a solvent wash with pentane would plug (and ruin) the column. Normal crosslinking pro-
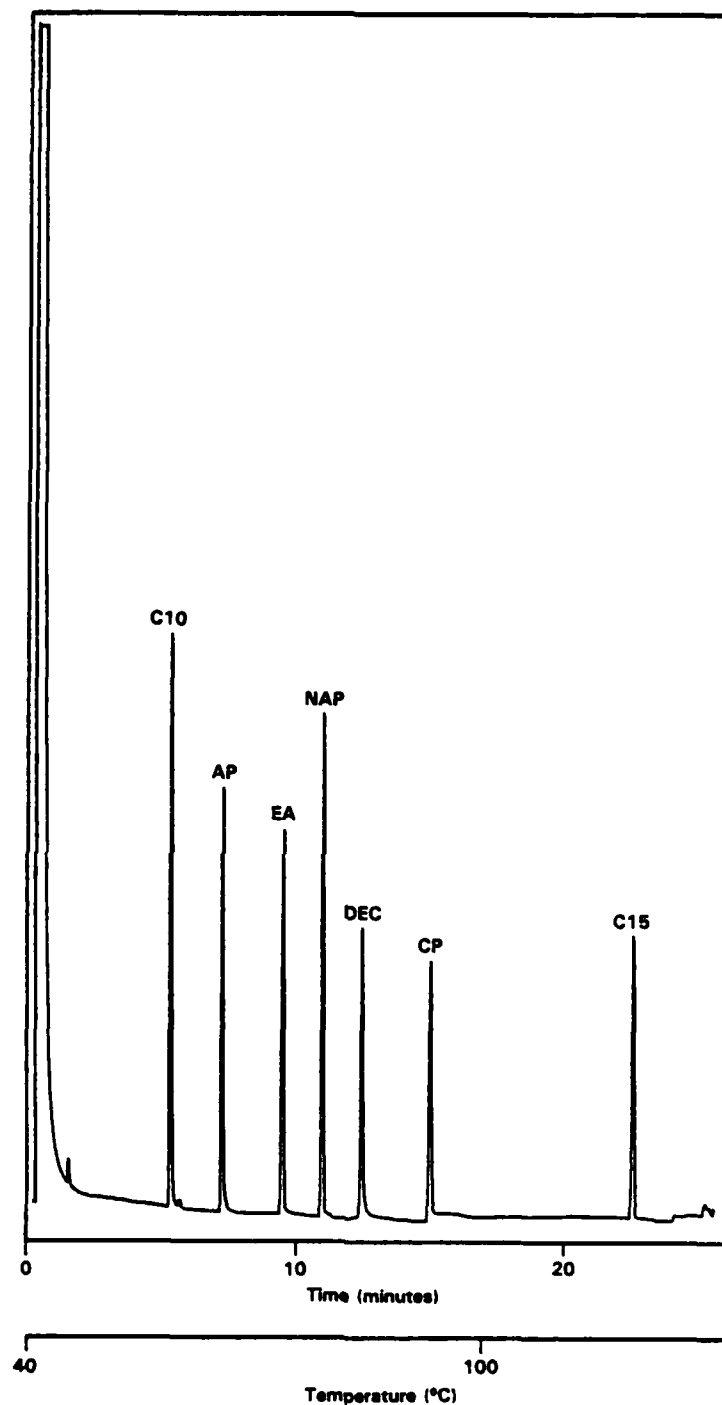
13

Figure 4.   Capillary GC test chromatogram of a polarity mixture obtained on a column deactivated with a polymeric siloxane. Chromatographic conditions: 6 m x 50 μm column coated with SE-54, temperature programmed at 4°C/min from 40°C, 300 psi He carrier gas. Peak identifications: C10 = n-decane, AP = acetophenone, EA = n-ethylaniline, NAP = naphthalene, DEC = 1-decanol, CP = p-chlorophenol, and C15 = n-pentadecane.
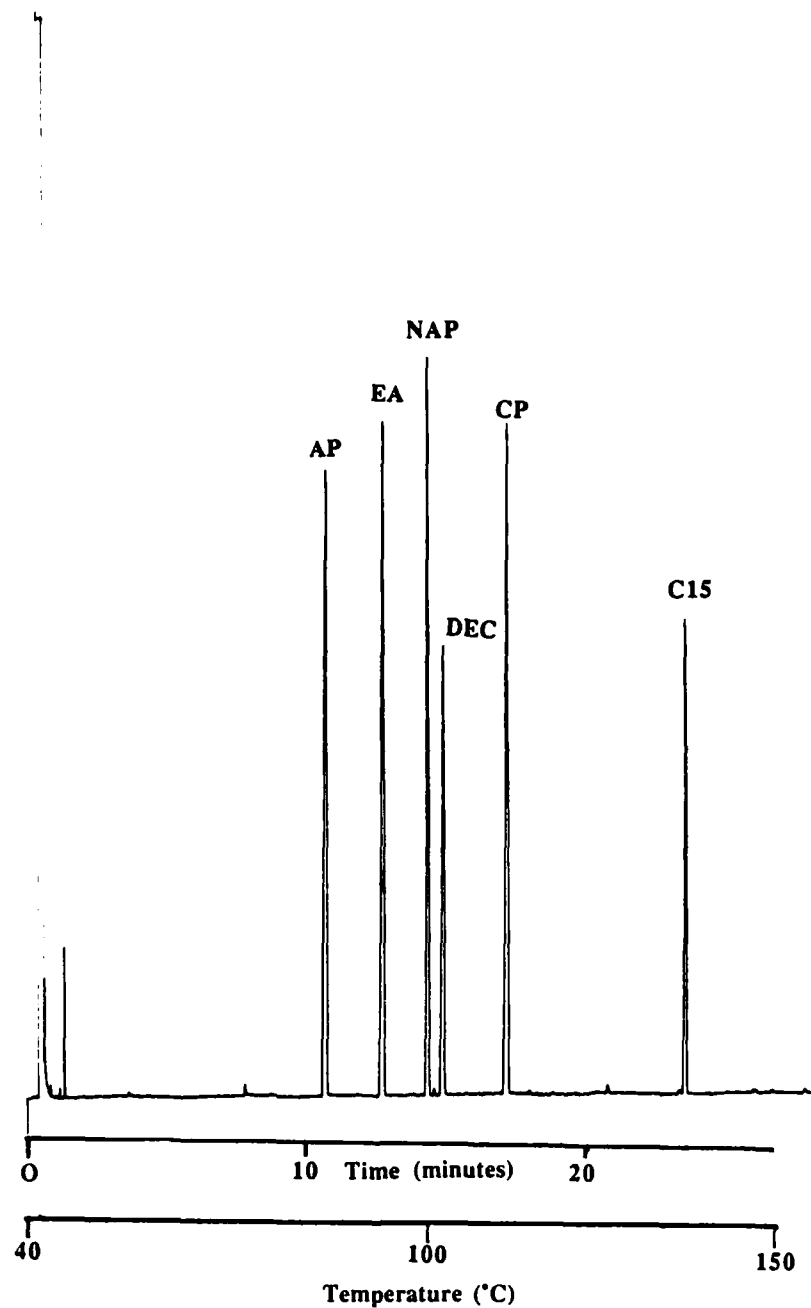
14

Figure 5. Capillary GC test chromatogram of a polarity mixture obtained on a 9 m column treated with methanol to increase the surface hydroxyl concentration followed by deactivation with a polymeric siloxane. Chromatographic conditions and peak identifications the same as in Figure 4.

cedures on a column that was not deactivated, and thus without surface bonding, would withstand solvent rinses with pentane with only a small decrease (~5%) in capacity ratio. However, use with supercritical carbon dioxide for any extended time period (> 10 hours) would lead to greater than a twenty-five percent loss in capacity ratio. In general, a loss of greater than twenty-five percent of the stationary phase leads to very poor column quality. To further enhance stationary phase stability, two replicate crosslinking procedures using azo-t-butane were applied. Columns prepared in this manner did not suffer any significant loss of stationary phase even after extended use (> 100 hours) with supercritical carbon dioxide. Use with supercritical pentane or carbon dioxide-methanol mixtures, however, quickly lead to significant deterioration.

By incorporating surface bonding with internal stationary phase cross-linking, improved stability was achieved. Higher degrees of surface bonding were obtained (inferred from better stability) when using the polymeric deactivation reagents. These reagents not only form a thicker layer to shield the silica surface, but also provide more attachment sites for the stationary phase. Wash-out studies have shown that columns deactivated with a polymeric layer and crosslinked with replicate azo-t-butane treatments are stable to supercritical pentane and up to 20% polar modifier-carbon dioxide mixtures. Usually, no more than 5-10% loss in capacity ratio occurs. Methanol appears to be most destructive modifier examined. Deactivation from monomeric silylation that provides fewer attachment sites also enhanced stability as compared to no deactivation, but not to the same extent as polymeric deactivation. Examples of typical capacity ratio measurments obtained before and after exposure to various supercritical fluid systems for columns prepared using a polymeric deactivation and duplicate crosslinking treatments are listed in Table 1.

Conclusions

Deactivation procedures have been evaluated and optimized for the types of fused silica being used to prepare columns for polar diesel fuel component analysis. The necessary treatments have been defined to provide reproducible and very inert surfaces which allow efficient chromatographic elution of

16

TABLE 1

Stationary Phase Stability Summary

Capacity Ratio (k)

Column	Fluid Exposure	A Before	A After	B Before	B After	C Before	C After	D Before	D After	E Before	E After
OV-17	CO_2-CH_3OH[a,b]	0.96	0.99	4.87	4.86	5.19	4.79				
OV-17	CO_2-CH_3CN[a,c]	0.99	0.94	4.87	5.02	4.79	5.83				
OV-17	CO_2-IPA[a,d]	0.94	1.04	5.02	4.97	5.83	5.89				
SE-54	C_5,C_5-IPA[e]							17.5	15.7	38.3	39.1
SE-54	C_3-IPA[f],CO_2-CH_3OH[a,b]							14.3	14.1	30.1	28.8
SE-54	CO_2-IPA[g]							11.5	12.1	24.2	25.6

(Compound)
A: n-decylbenzene
B: phenanthrene
C: myristophenone
D: n-decane
E: n-undecane

a 120°C and 170 atmospheres

b 15.4 wt. % CH_3OH

c 18.9 wt. % CH_3CN

d 25.4 wt. % IPA (isopropanol)

e 210-230°C, 27-68 atmospheres, 5 vol % IPA

f 130-160°C, 51-204 atmospheres, 5 vol. % IPA

g 150°C-170°C, 88-238 atmospheres, 10 vol. % IPA

17

polar analytes. The best deactivation methods also improve stationary phase stability by enhancing surface bonding through <u>in-situ</u> crosslinking methods. Sufficient stationary phase stability has been achieved for use with polar binary fluid mixtures in SFC. Mixtures of carbon dioxide with up to at least twenty mole percent polar modifier do not adversely affect stationary phase integrity.

TASK B. BINARY FLUID SYSTEM DEVELOPMENT

Introduction

As in liquid chromatography there are a number of possible fluids avail-
able for mobile phases in SFC that offer a range of polarity and selec-
tivity. However, current SFC practice and technology have been limited to
a relatively few, and usually nonpolar fluids. Carbon dioxide has undoubtedly
been used most extensively and has seen wide-spread use in both packed column
(13-16) and capillary column (17-21) applications. The popularity of carbon
dioxide can be accounted for by its mild critical parameters, low cost,
chemical inertness, and compatibility with flame ionization and optical
HPLC detection methods. Although carbon dioxide is nonpolar (e.g. no dipole
moment) and doesn't form any specific interactions (e.g. hydrogen bonding),
it does have a quadrupole moment and is somewhat polarizable which imparts
better solvating properties than might be expected. Experience has shown
that compounds which are soluble in methylene chloride have a higher probability
of being sufficiently soluble in supercritical carbon dioxide to allow suc-
cessful chromatographic elution. However, in many cases the solubility of
many polar compounds in carbon dioxide is so low that they are infinitely
retained and cannot be successfully chromatographed. Other nonpolar fluids
such as ethane (22), nitrous oxide (22), and pentane (23-24) have also been
used in capillary SFC with pentane being used most extensively. The more
general use of pentane has been limited by its higher critical temperature
(197°C) and incompatibility with flame ionization detection.

The use of very polar fluids such as ammonia or sulfur dioxide has
also been explored, but their applicability is limited due to high reactivity
with polar sample components. The very polar fluids also present problems
for the actual instrumentation and the chromatographic columns. The polar
solvents generally used in liquid chromatography that exhibit high solvating
power (e.g. specific interactions) generally have restrictively high critical
temperatures (> 200°C) for convenient operation. The critical parameters
for several polar solvents are listed in Table 2. High operating temperatures
are undesirable due to increased stress to the chromatographic stationary
phase and the greater probability for thermal degradation of sample

19

TABLE 2

Critical Parameters for Selected Polar Solvents

Compound	Critical Temperature (°C)	Critical Pressure (atm)
Benzene	288.9	48.3
Methanol	240.5	78.9
Ethanol	243.0	63.0
Isopropanol	235.3	47.0
Acetone	235.0	47.0
Ethyl Ether	193.8	35.5
Acetonitrile	274.7	47.7
Methylene Chloride	237.0	60.0
Ammonia	132.4	113.3
Sulfur Dioxide	157.2	77.7

compounds during analysis. Higher operating temperatures also decreases
selectivity and can lead to reduced retention and poor separations when
analyzing compounds exhibiting appreciable volatility.

By using mixed fluid systems incorporating a nonpolar fluid with a low
critical temperature and a polar modifier with a high critical temperature,
modified fluid mixtures that have reasonable critical temperatures and higher
solvating powers with specific selectivity can be obtained. A nonpolar
fluid such as carbon dioxide with a critical temperature of ~ 31°C can be
mixed with 20% methanol to provide specific solvating interactions for polar
compounds and still maintain a critical temperature of less than a 130°C.
The determination of the exact critical parameters for a fluid mixture is
not trivial and can require careful phase equilibria measurements. In fact,
very confusing and misleading behavior can be obtained if subcritical two-
phase fluid mixtures are utilized rather than single-phase supercritical
systems. However, approximations of critical parameters can be made using
theoretical considerations (25,26), and in a practical sense, operating
conditions well above the projected critical point can often be used to
obtain a single phase system. This section summarizes the most relevant
studies conducted using various binary fluid mixtures for mobile phases in
capillary supercritical fluid chromatography.

Experimental

In general, high purity carbon dioxide (Scott, SFC grade) that was
dried and further purified by passing through an alumina and activated charcoal
adsorbent trap was used as the nonpolar component for the binary fluid mixtures.
Some studies also utilized propane or pentane as the nonpolar component.
The polar modifiers included high purity (Burdick and Jacson) methanol,
acetonitrile, isopropanol, ethanol and ethyl ether. Binary fluid mixtures
of carbon dioxide and a polar modifier were prepared gravimetrically in a
250 mL high-pressure transfer cylinder. After known amounts of polar modifier
and carbon dioxide were introduced into the cylinder, the resulting mixture
was transfered to the SFC syringe pump. Mixtures ranging from approximately
one to twenty mole percent of modifier in carbon dioxide were prepared.

21

Similar procedures were applied for the preparation of propane-polar modifier mixtures. With pentane, the liquids (pentane and modifier) were premixed volumetrically and transferred to the syringe pump.

Mobile phase solvating power was monitored by comparing chromatographic retention times of selected polar test components in the various binary fluid mixtures to those obtained in pure carbon dioxide (or other nonpolar fluid components). Test mixtures included alkylbenzenes, alkylphenones, netural PAH, a mixture containing n-decylbenzene, phenanthrene, myristophenone, phenanthridine, and peri-naphthenone and a mixture containing n-decane, acetophenone, N-ethylaniline, naphthalene, 1-decanol, and p-chlorophenol. Capacity ratio (k) and relative selectivity (α) were calculated from the chromatographic retention times using the following relationships:

$$k = \frac{t_R - t_o}{t_R} \qquad (1)$$

where t_R is the retention time of the component of interest and t_o is the void or dead time; and

$$\alpha = \frac{k_2}{k_1} \qquad (2)$$

where k_2 is the capacity ratio for the component of interest and k_1 is capacity ratio of the component to which the selectivity is being compared.

Both capillary supercritical fluid chromatography (SFC) with ultraviolet absorption detection and capillary supercritical fluid chromatography-mass spectrometry (SFC-MS) were used to monitor the effects of the various fluid mixtures. The instrumentation for both SFC (23,27) and SFC-MS (21,28) has been described previously. Essentially, the SFC portion of the instruments utilized a modified Varian 8500 syringe pump under microcomputer control to generate high pressure and pulse-free supplies of mobile phase. A modified Hewlett-Packard 5700 gas chromatograph oven provided constant temperature operating conditions. Various chromatographic capillary columns were employed. In general, lengths ranging from 2-15 meters of 50 μm fused silica tubing

22

were deactivated and coated with ~ 0.25 µm films of either a 5% phenyl or 50% phenyl polymethylphenylsiloxane stationary phase that was rendered nonextractable by extensive *in-situ* free radical crosslinking (See Task A). Sample introduction was accomplished using a Valco 0.06 µl C14W injection valve at ambient temperature and with a flow splitter adjusted to allow approximately a 1:10 to 1:50 flow into the chromatographic column.

Ultraviolet absorption detection was accomplished using an Isco V-4 variable wavelength UV detector with an on-column high-pressure flow cell. This flow cell was constructed using a short length of 250 µm i.d. fused silica tubing with 2-3 millimeters of polyimide removed to form a window. The analytical 50 µm i.d. column was threaded through the larger tubing with its end terminating immediately below the window. The analytical column and the window tubing were connected using a butt-connector. Control of the mobile phase flow rate and decompression of the column effluent after detection was accomplished by connecting a short length of small-bore tubing (5-10 µm i.d.) to the 250 µm i.d. window tubing. The detection wavelength was 254 nm. A schematic diagram of the UV detection SFC instrument is shown in Figure 6.

For SFC-MS, mobile phase decompression and regulation of the linear velocity was achieved by connecting the end of the analytical column to a short length of 5 µm i.d. or tapered 25 µm i.d. fused silica. The SFC effluent was injected axially into the chemical ionization source of a quadrupole mass spectrometer. Methane was used as the chemical ionization reagent. The mass spectrometer was scanned from approximately 90 to 300 a.m.u. at approximately two seconds per scan. A schematic diagram of the SFC-MS instrumentation is shown in Figure 7.

Estimation of the critical loci of the binary fluid mixtures was accomplished by computer modeling methods using established techniques (25,26). The modeling utilized a BASIC program run on a Hewlett-Packard 9845T desktop computer.
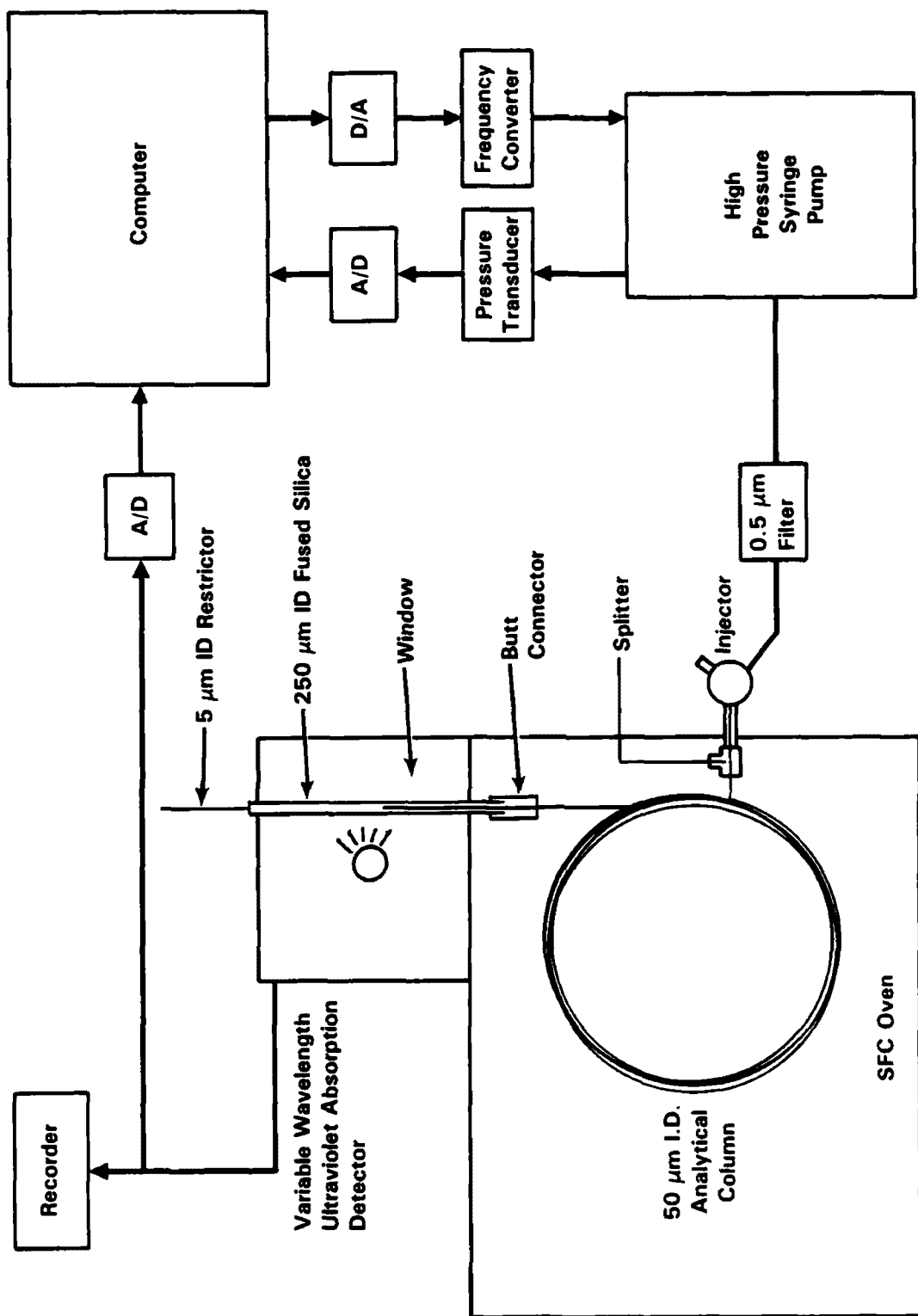
23

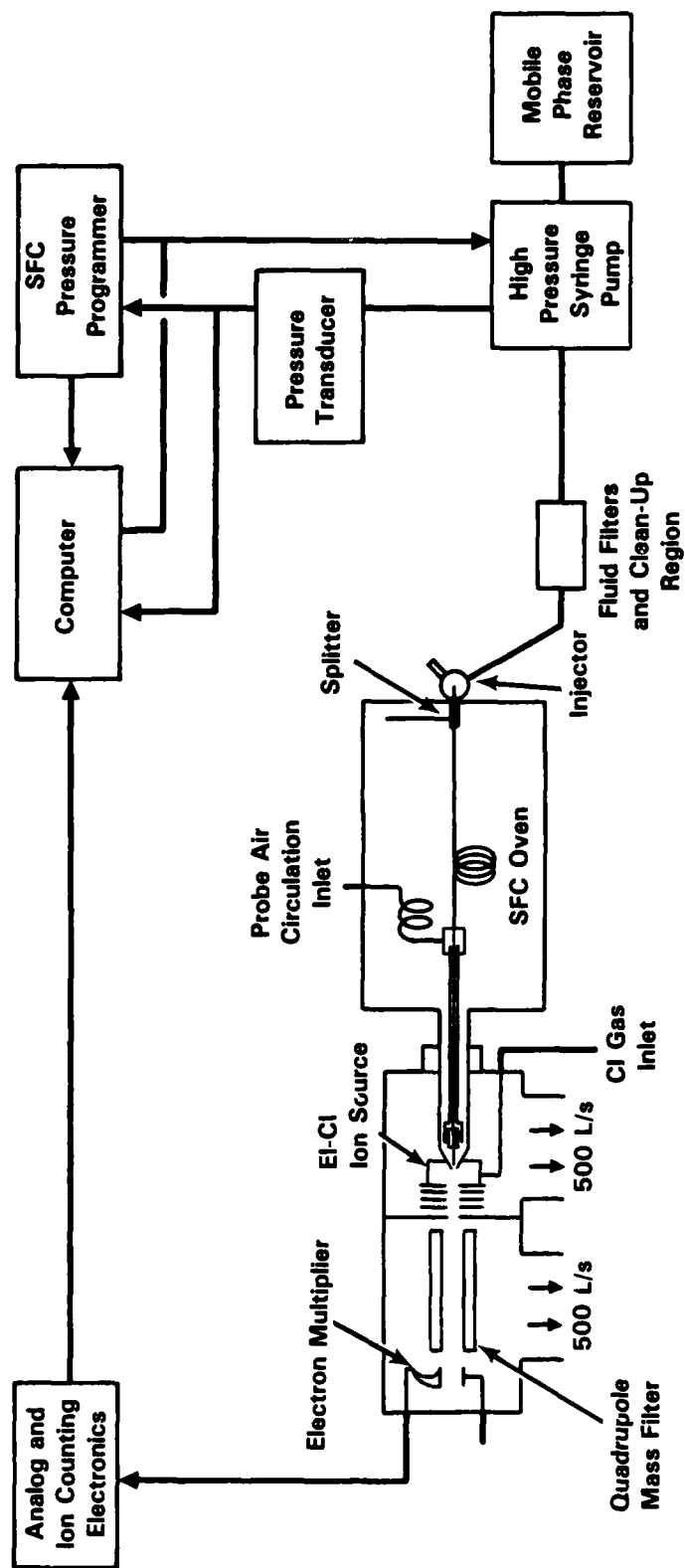Figure 6. Schematic diagram of UV detection SFC instrumentation.

Figure 7. Schematic diagram of SFC-MS instrumentation.

Low (<3%) Modifier Concentration Studies

To probe the effects of low modifier concentrations, a 2.5% (w/w) methanol in carbon dioxide mixture was evaluated using SFC-MS. A less polar stationary phase (5% phenyl polymethylphenylsiloxane) was utilized to make any selectivity changes more pronounced. The polarity test mixture compounds offered a variety of possible chemical interactions that could be influenced by the methanol modifier.

Capacity ratio and selectivity data for a polarity mixture using pure carbon dioxide and a 2.5% (w/w) methanol in carbon dioxide mixture are listed in Table 3. Equivalent chromatographic operating conditions were used to compensate for temperature and density effects of the modified fluid. Equivalent conditions were obtained by using the same reduced pressure and reduced temperature for both the pure carbon dioxide and the carbon dioxide/methanol mixture. Reduced pressure and temperature are defined as the pressure and temperature divided by their respective critical parameters. Reliable critical parameters have recently become available for carbon dioxide-methanol mixtures (29) to allow accurate calculation of reduced parameters. Very similar retention and selectivity behavior were observed for both fluids. The most notable (and only significant) selectivity difference was obtained for the 1-decanol probe. The chromatographic elution of the alcohol would be expected to be most sensitive to the methanol modifier. These data sharply contrast those obtained in packed column SFC binary mixture studies (30,31), in which very low concentrations of modifiers (< 1%) caused dramatic retention changes. This suggests that observations made for packed column SFC result from modification of the stationary phase, possibly by adsorption of the polar modifier on active column sites. The relatively minor impact of low methanol modifier concentrations is reasonable if only fluid properties impact retention since the solvating power of the fluid is increased proportionally as the fluid composition is changed.

SFC-MS chromatograms of a different polarity mixture obtained under pressure ramped conditions using carbon dioxide and a 2.5% (w/w) mixture of methanol in carbon dioxide are shown in Figure 8. (See Table 4 for compound

26

TABLE 3

Capacity Ratio(k) and Selectivity Comparison(α)
of a Polarity Mixture Using Carbon Dioxide and Methanol
Modified Carbon Dioxide (Tr = 1.23 and Pr = 1.27)

Compound	CO_2[a]		CO_2-MeOH(2.5% w/w)[b]	
	k	α	k	α
C_{10}	0.57		0.57	
acetophenone	0.98	1.7	0.99	1.7
N-ethylaniline	1.28	2.3	1.29	2.3
naphthalene	1.84	3.2	1.86	3.3
1-decanol	2.13	3.7	2.21	3.9
p-chlorophenol	2.10	3.7	2.11	3.7

[a] 92 atmospheres and 100°C

[b] 93 atmospheres and 108°C

α Relative to the first eluting component.
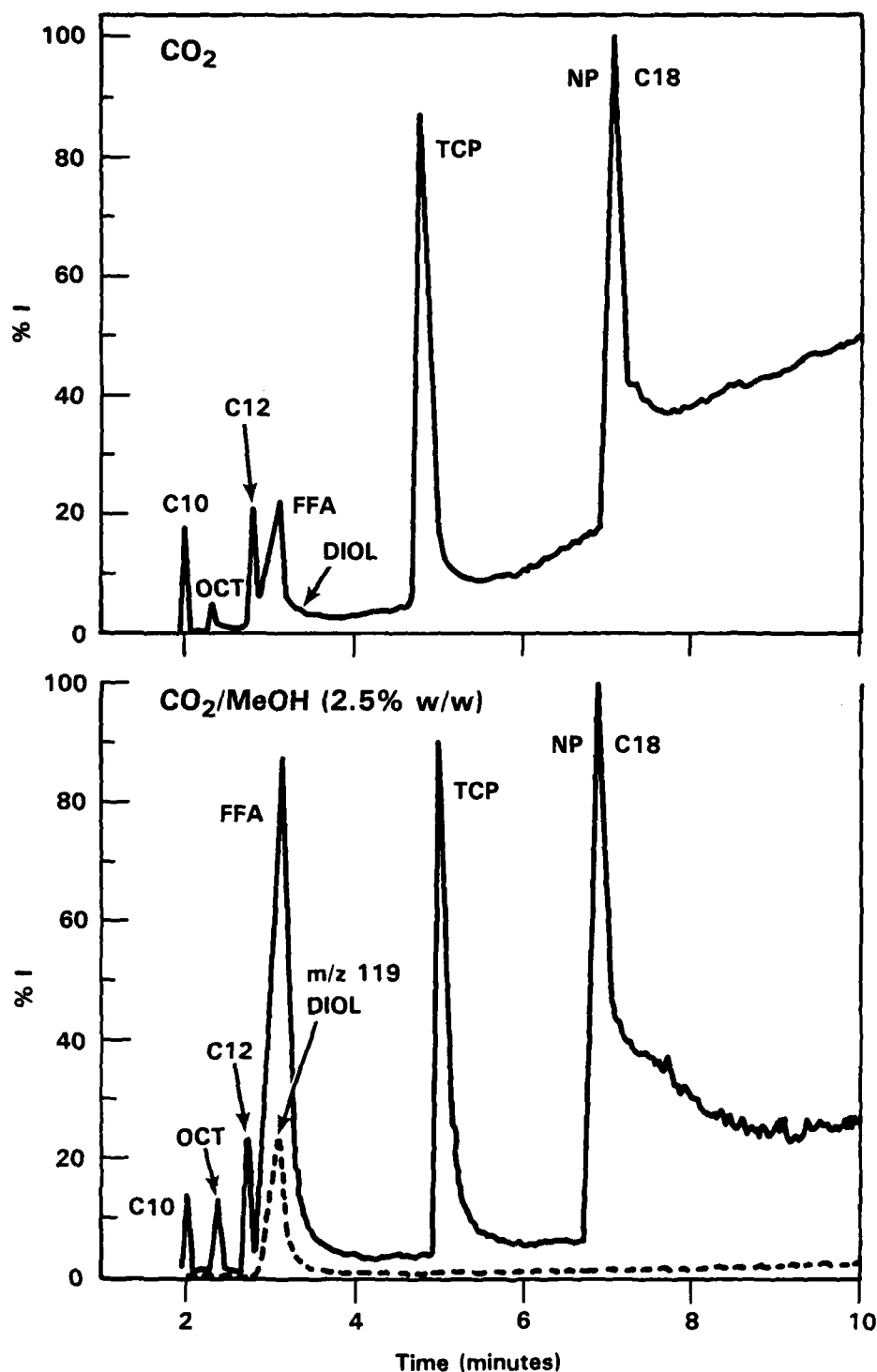
Figure 8. SFC-MS chromatograms of a polarity mixture obtained with
carbon dioxide and methanol modified (2.5% w/w) carbon
dioxide mobile phases. Conditions: 100°C; pressure ramped
from 100 atm at 10 atm/min; 3 m x 50 µm column coated with
5% phenyl polymethylphenylsiloxane. See Table 4 for
compound identifications.

28

identifications). A 10 atm/min pressure ramp starting at 100 atmospheres was used at an operating temperature of 100°C. A short and poorly deactivated 2-3 meter long column coated with 5% phenyl polymethylphenysiloxane was utilized in these separations and hence, the components were not all completely resolved. However, with MS detection it was possible to verify the elution of each component. Although the earlier studies showed nearly insignificant retention and selectivity changes with low modifier concentrations, these chromatograms displayed minor differences. Since capacity ratio data can not be calculated under programmed conditions, actual retention times for the various components from the two mobile phase are listed in Table 4. The two chromatograms were obtained sequentially and no physical changes in the instrumentation were made so a direct comparison of the retention times could be made. The hexanediol was eluted significantly earlier with the methanol modified fluid while no significant difference was obtained for the alcohol. The higher polarity and hydrogen bonding interactions of the diol with the methanol modifier were evidently sufficient to cause this decrease in retention. It is interesting that the trichlorophenol was eluted later and the nitrophenol was eluted earlier with the modified fluid as compared to the pure fluid. While both components are acidic, the nitrophenol is more polar.

In addition to retention differences, there are noticeable changes in the peak shapes between the two fluids. With the more polar fluid mixture, the octanoic acid is more symmetrical (less fronting) indicating higher solubility in the stationary phase. This infers that fluid modifiers can modify the stationary phase surface and enhance partitioning. In the pure carbon dioxide chromatogram, the diol was essentially lost in the baseline; whereas in the modified carbon dioxide chromatogram a symmetrical peak was obtained for the diol from the single ion chromatogram at m/z 119 (super-imposed with dotted lines in the figure). The intensity of the decanol was also greater with the modified fluid. The above observations suggest that polar components which are experiencing adsorption can be more effectively eluted with a more polar mobile phase. The same reasoning also suggests that the deleterious effects of a poorly deactivated column can be compen-sated by using a modified fluid mixture.

TABLE 4

Retention Comparison for Carbon Dioxide and a
Carbon Dioxide-Methanol (2.5% w/w) Mixture

| Compound | Retention Time (min) | |
	CO_2	CO_2-MeOH (2.5% w/w)
decane (C_{10})	2.04	2.01
1-octanol (OCT)	2.35	2.37
dodecane (C_{12})	2.84	2.73
1-octanoic acid (FFA)	3.15	3.06
1,6-hexanediol (DIOL)	3.33	3.09
2,4,5-trichlorphenol (TCP)	4.85	5.02
p-nitrophenol (NP)	7.04	6.77
octadecane (C_{18})	7.14	6.84

Conditions: $100^{\circ}C$ and pressure ramp of 10 atm/min from 100 atm.

Higher (>3%) Modifier Concentration Studies

Since low concentrations of modifier did not significantly affect the solvating power of the chromatographic mobile phase, SFC studies utilizing higher modifier concentrations were also conducted. Since these studies were done using UV absorption detection, it was necessary to use molecules with appropriate chromophores as test probes. The test mixture included both relatively nonpolar molecules and more polar molecules that would be expected to experience selective interactions with the polar modifiers. For instance, the nitrogen lone pair electrons in phenanthridine (a component in the test mixture) are good hydrogen bonding acceptor sites and should interact strongly with hydrogen bonding donor modifiers.

Capacity ratio data and relative selectivities for a polarity test mixture using 20 mole percent mixtures of methanol, acetonitrile, and isopropanol in carbon dioxide compared to pure carbon dioxide mobile phases are summarized in Tables 5 - 7, respectively. In all cases, chromatographic retention was drastically reduced with the modified fluid systems, indicating that higher solvating power conditions were achieved. In general, the isopropanol modifier decreased retention the greatest, followed by acetonitrile and methanol.

Modifiers can also increase the mobile phase solvating power so that compounds which were not eluted with the pure fluid can be successfully eluted. For example, the data in Table 7 indicates that both peri-naphthenone and phenanthridine were not eluted with pure carbon dioxide, but were both eluted when an isopropanol modifier was used. The stationary phase had evidently been modified to prevent elution of these polar compounds with carbon dioxide since in earlier analyses they were successfully eluted with pure carbon dioxide. Interestingly, the methanol modifier (most polar) displayed the greatest selectivity effect for the phenanthridine and eluted it prior to phenanthrene, whereas phenanthridine eluted after phenanthrene with the other modifiers. Identical operating conditions, chosen to be above the estimated critical points, were used for all three fluid mixtures and the pure carbon dioxide. Since accurate critical point data was not available for isopropanol and acetonitrile modified carbon dioxide mixtures, exact reduced temperatures and pressures could not be calculated.

31

TABLE 5

Capacity Ratio and Selectivity Comparison of a Polarity
Mixture using Carbon Dioxide and a Twenty Mole
Percent Methanol in Carbon Dioxide Mixture[a]

Compound	CO_2		CO_2-MeOH	
	k	α	k	α
<u>n</u>-decylbenzene	0.97		0.13	
myristophenone	4.99	5.1	0.21	1.6
phenanthrene	4.86	5.0	0.57	4.4
phenanthridine	6.09	6.3	0.44	3.4
<u>peri</u>-naphthenone	8.65	8.9	0.51	3.9

[a]   120°C and 168 atmospheres.

α   Calculated relative to decylbenzene.

TABLE 6

Capacity Ratio and Selectivity Comparison of a Polarity
Mixture Using Carbon Dioxide and a Twenty Mole Percent
Acetonitrile in Carbon Dioxide Mixture[a]

Compound	CO_2		CO_2-CH_3CN	
	k	α	k	α
<u>n</u>-decylbenzene	0.97		0.09	
myristophenone	4.79	4.9	0.15	1.7
phenanthrene	4.87	5.0	0.32	3.6
phenanthridine	6.09	6.3	0.33	3.7
<u>peri</u>-naphthenone	8.65	8.9	0.35	3.9

[a]   120°C and 168 atmospheres.

α   Calculated relative to decylbenzene.

TABLE 7

Capacity Ratio and Selectivity Comparison of a Polarity
Mixture Using Carbon Dioxide and a Twenty Mole Percent
Isopropanol in Carbon Dioxide Mixture[a]

Compound	CO_2		CO_2-IPA	
	k	α	k	α
n-decylbenzene	0.97		0.05	
myristophenone	5.86	6.0	0.13	2.6
phenanthrene	5.00	5.2	0.25	5.0
phenanthridine	>10	---	0.26	5.2
peri-naphthenone	>10	---	0.29	5.8

a   120°C and 168 atmospheres.

α Calculated relative to decylbenzene.

TABLE 8

Capacity Ratio Comparison of a Polarity Mixture Using
Various Concentrations of Isopropanol in Carbon Dioxide[a]

Compound	Capacity Ratio, % Isopropanol (mole %)					
	0	1.6	5.5	9.8	12.3	20
n-decylbenzene	0.94	0.75	0.42	0.22	0.17	0.05
myristophenone	5.83	3.49	1.50	0.61	0.46	0.13
phenanthrene	5.02	3.68	1.94	0.98	0.77	0.25
phenanthridine	>10	4.44	2.23	1.02	0.78	0.26
peri-naphthenone	>10	6.44	3.01	1.30	1.03	0.29

a   120°C and 168 atmospheres

To examine the effects of modifier concentration, several fluid mixtures with increasing isopropanol concentration in carbon dioxide were evaluated. Capacity ratio data as a function of fluid modifier concentration are listed in Table 8. As expected, increasing modifier concentrations decreased the retention of the polarity mixture compounds. Even concentrations (of isopropanol) as low was 1.6 mole percent (2.1 wt.%) significantly reduced the chromatographic retention of the compounds. These data suggest that isopropanol has a more profound influence on the solvating power of the fluid than similar concentrations of methanol since the data obtained in Table 3 indicated only slight retention changes were achieved with a similar concentration of methanol.

Relative selectivity of the test probes as a function of isopropanol modifier concentration is plotted in Figure 9. The selectivities were calculated relative to the nonpolar decybenzene to better discern the specific interactions occurring between the fluid modifier and the test probes. The less polar phenanthrene would not be expected to experience any specific interactions with isopropanol and indeed, the selectivity did not substantially change with increased modifier concentration. However, the other components would be expected to experience interactions with the alcohol moiety, and for these compounds selectivity changed significantly with modifier concentration.

Propane was also used as the nonpolar component in fluid mixtures due to its low critical temperature (~96°C). An SFC-MS chromatogram of the polarity mixture used in the previously described studies utilizing a 5 vol. % isopropanol in propane fluid mixture is shown in Figure 10. Interestingly, the myristophenone was eluted last in the series rather than second as was observed for the isopropanel-carbon dioxide mixtures. This further illustrates the wide range of fluid selectivity that can be achieved in SFC by controlling the mobile phase composition.

Pentane was also used as the nonpolar component for binary fluid mixtures. Modifiers including ethanol, isopropanol, and ethyl ether were evaluated. However, due to the high critical temperature of pentane (~196°C), the resulting binary fluid systems had excessively high operating temperatures (>200°C) for efficient separation of the polarity test mixture and the polar fuel
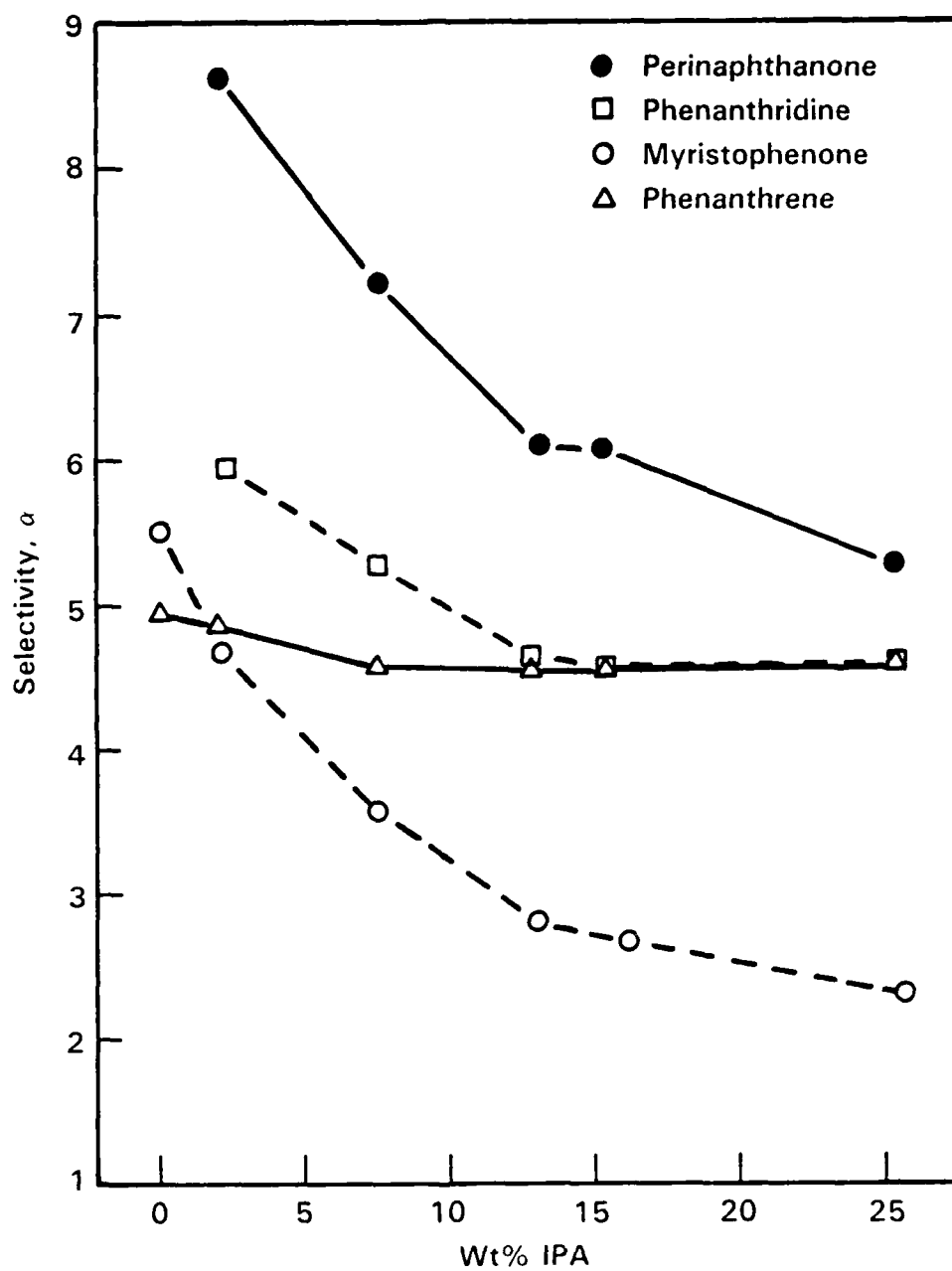
Figure 9.   Plot of selectivity as a function of isopropanol (IPA) modifier concentration for selected test probes.
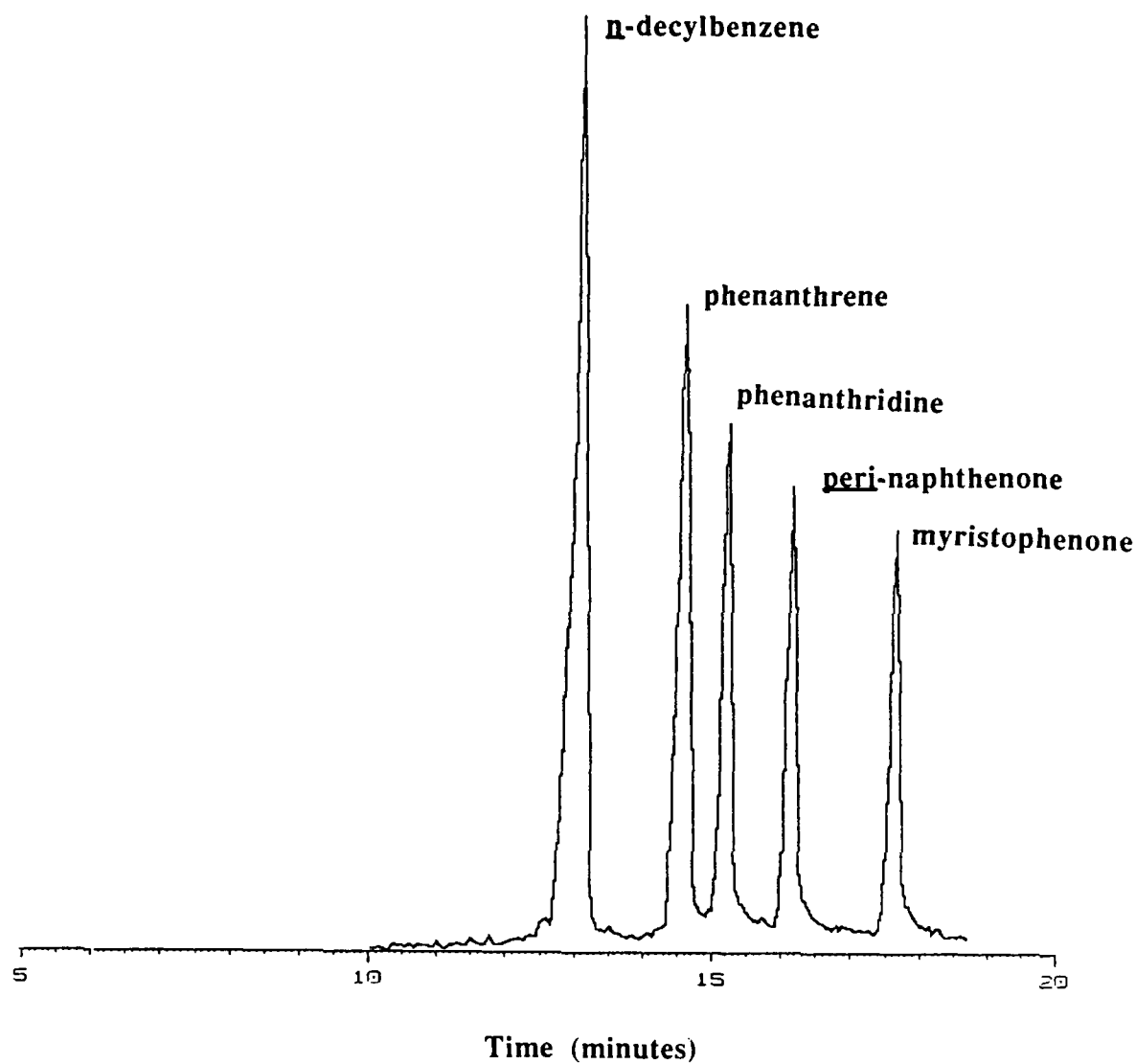
n-decylbenzene

phenanthrene

phenanthridine

peri-naphthenone

myristophenone

Time (minutes)

Figure 10.   SFC-MS chromatogram at a polarity test mixture obtained with a
5% (v/v) isoporpanol in propane fluid system. Conditions: 8 m x
50 μm column coated with 5% phenyl polymethylphenylsiloxane,
140°C operating temperature and pressure ramped from 60 atm
after 5 minutes at 2.5 atm/min.

fractions. At high temperatures these compounds have sufficient volatility to have low chromatographic retention which prevents efficient separation.

A very important consideration for utilizing binary fluid mixtures in capillary SFC is an understanding of the critical conditions and the phase behavior of the mixture. With two component mixtures, it is possible that non-homogeneous two-phase systems can exist below certain pressures and temperatures. Utilization of this gas-liquid phase can lead to spurious results and misleading conclusions. For instance, the capacity ratio data listed in Table 9 were originally unknowingly obtained under subcritical two-phase conditions. The retention actually increased for two of the test probes rather than decreasing as would be expected when using the higher solvating mixed fluid system. The decrease in retention for the other two test probes was much less than expected. This anomalous behavior probably occurred due to the use of a lower solvating gas-phase mixture as the mobile phase rather than the expected supercritical binary fluid mixture. Thus, caution must be applied to choosing the proper operating conditions when using a binary fluid mixture.

This problem is further emphasized by the SFC-MS chromatograms shown in Figure 11. In these separations, a 10 volume percent isopropanol modifier in propane was utilized at three different temperatures. At the lower temperature of 120°C, the PAH components present in the coal tar sample were eluted close together and with very poor resolution. As the temperature was increased to 130°C, the retention times of the components were increased and the components were separated over a wider pressure range as the fluid pressure was increased. Increasing the temperature an additional 20° to 150°C, slightly improved the chromatographic resolution, but not to the same extent as increasing the temperature from 120° to 130°C. This behavior is probably explained by the lower temperature mixture existing as a liquid with strong solvating properties which eluted the component together. Under such conditions pressure programming is of reliatvely little value since density does not change greatly. At the slightly higher temperature, a single-phase supercritical fluid state was probably achieved and the expected high chromatographic efficiency and the solvatig power increase with pressure was then observed.

TABLE 9

Capacity Ratio Comparison of Alkylphenone Using Carbon
Dioxide and a Twenty Mole Percent Methanol in Carbon
Dioxide Mixture at Subcritical Conditions[a]

Compound	k	
	CO_2	CO_2-MeOH
n-octanophenone	0.19	0.33
n-decanophenone	0.32	0.39
n-laurophenone	0.54	0.45
n-myristophenone	0.88	0.53

[a] 100°C and 150 atm.

Coal Tar
Propane-Isopropanol (10% v/v)
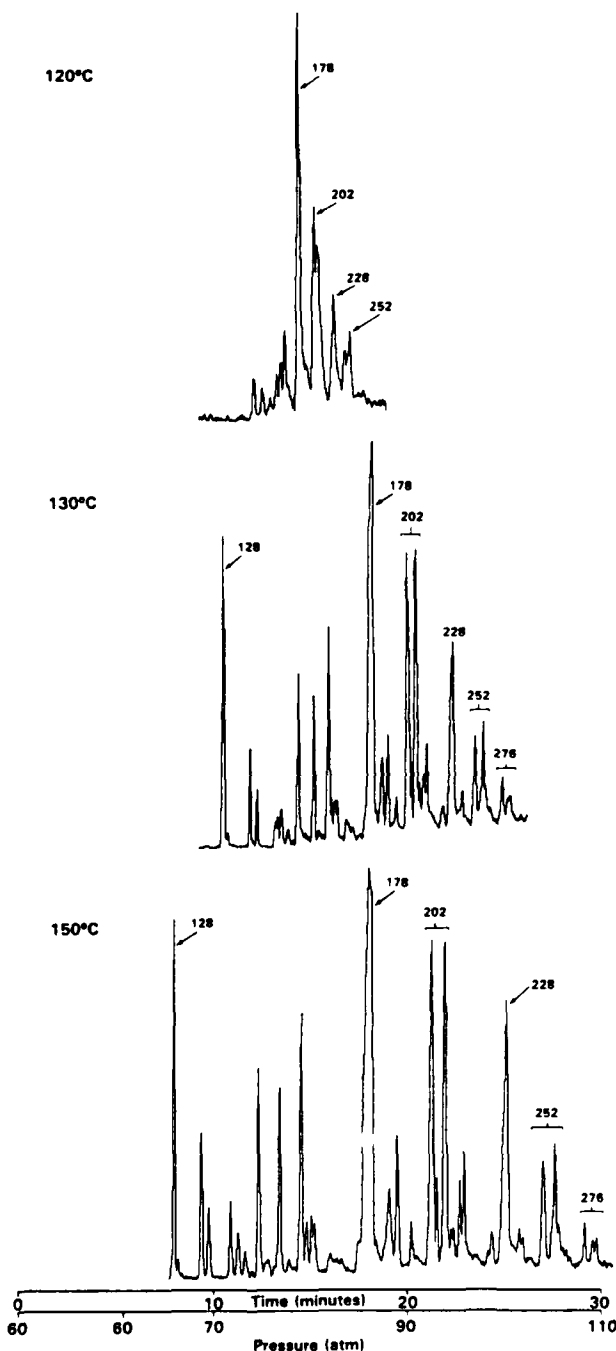
Figure 11.   SFC-MS chromatograms of coal tar obtained with a 10 volume %
isopropanol in propane fluid system at various temperatures. Peak
labels refer to molecular weight of PAH components. Conditions:
pressure ramped from 60 atm at 2 atm/min; 8 m x 50 μm column
coated with 5% phenyl polymethylphenylsiloxane.

39

The critical phase behavior of two-component mixtures can be predicted using thermodynamic approximations. Although these approximations include an adjustable parameter, valuable guidance in estimating appropriate critical conditions can be obtained. For example, the critical pressures and temperatures as a function of modifier mole fraction for a carbon dioxide-isopropanol fluid mixture are plotted in Figure 12. This type of data is very useful for choosing chromatographic operating conditions when using a specific modifier concentration.

Conclusions

The use of polar modifiers in carbon dioxide or other nonpolar fluids can significantly change the solvating power and selectivity of a fluid. Low modifier concentrations (1 - 2%) have a minor impact on the fluid properties and decrease chromatographic retention slightly. This contrasts the behavior observed for packed column SFC in which modifier concentrations less than one percent can alter chromatographic retention more than an order of magnitude. Such changes suggest the modifier is deactivating the packed column stationary phase rather than significantly altering the fluid solvating properties. Increased concentrations of modifier in capillary SFC have proportionally greater effects on chromatographic retention, with twenty mole percent mixtures decreasing the retention of the polarity mixture compounds studied over an order of magnitude. Such effects can be attributed almost entirely to the altered solvating characteristics of the fluid. Isopropanol appears to provide greater solvating power increases than either acetonitrile or methanol fluid modifiers. In addition to decreasing retention, modifiers can also render more polar compounds sufficiently soluble to be successfully eluted. Very polar compounds with low fluid phase solubilities may be infinitely retained on a column unless sufficiently strong solvating conditions are obtained. The use of modifiers also affects chromatographic selectivity, with the more polar compounds experiencing stronger interactions (with greater retention shifts) with the modifiers. Both the polarity of the compound and the fluid determine the magnitude of the selectivity effects. This
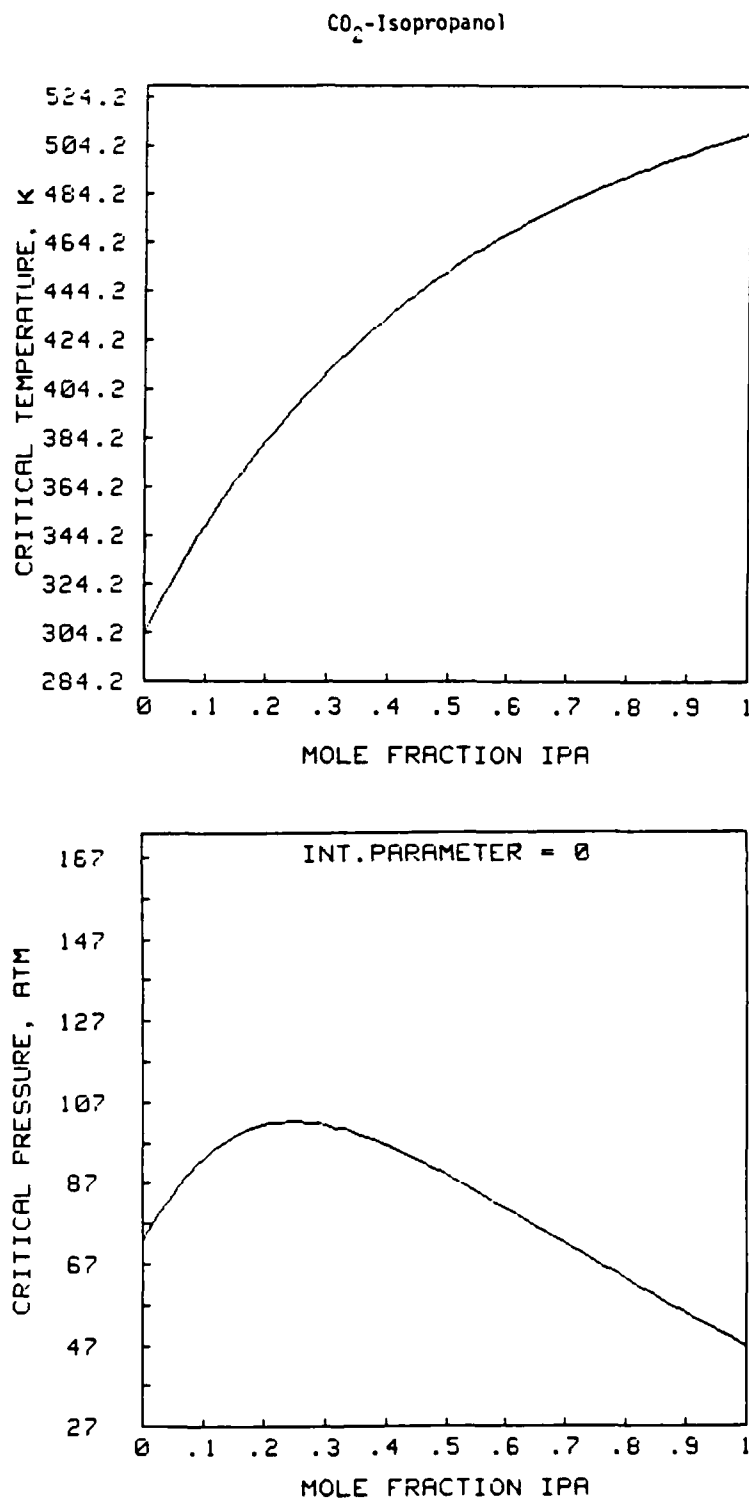
CO$_2$-Isopropanol

Figure 12.   Calculated phase behavior of carbon dioxide-isopropanol
fluid mixtures.

behavior provides a wide range of solvent control for tailoring a specific analysis to specific compound types.

TASK C. POLAR FUEL FRACTION ANALYSIS

Introduction

The formation of gums and sediments in fuels during storage is a very
serious problem. Several studies relating chemical properties and fuel
stability have been conducted (32-42). In general, lower stability (e.g.,
increased sediment formation) has been attributed to, and can be correlated
with, higher concentrations of heteroatomic species, particularly nitrogen
containing compounds.

Capillary supercritical fluid chromatography (SFC) and capillary super-
critical fluid chromatography-mass spectrometry (SFC-MS) offer potential
advantages for the characterization of complex fuel matrices. These advantages
accrue from the nature of a supercritical fluid. At elevated pressure this
single phase will have properties which are intermediate between those of
the gas and liquid phases. The density of a supercritical fluid is typically
$10^2 - 10^3$ times greater than of the gas, yet solute diffusivities are up to
two orders of magnitude greater and viscosities significantly less than of
the liquid (42). The liquid-like densities result in favorable solvation
properties which allow the separation of less volatile compounds than is
possible with gas chromatography. Furthermore, the lower viscosities and
higher diffusion coefficients result in enhanced chromatographic efficiency
and shorter analysis times compared to liquid chromatography.

The compressibility of supercritical fluids is large just above the
critical temperature and small changes in pressure result in large changes
in density. This allows the solvating power of the fluid to be easily
controlled as a function of pressure and can be used in an analogous manner
to temperature programming in gas chromatography or gradient elution in
liquid chromatography. In addition, the critical temperature of many
fluids or fluid mixtures is low which allows application to the analysis of
thermally sensitive or labile compounds. The use of small diameter
capillary columns (<75 μm i.d.) allows high separation efficiencies of
greater than 3,000 plates/meter to be obtained and "capillary gas
chromatography-like" high resolution separations can be achieved.

SFC and SFC-MS are ideally suited to the separation problems encountered in the characterization of polar fuel components. Many of these compounds could be thermally sensitive and unstable at the higher temperatures required for gas chromatographic analysis. The complexity of the fuel matrix can also limit the usefulness of lower resolution liquid chromatographic methods. Optimized capillary SFC methods that allow the successful analysis of polar compounds have now been developed (Tasks A and B). The application of these methods to the analysis of the polar fuel components in diesel fuel marine (DFM) samples is described in this section.

Experimental

An unstable diesel fuel marine sample, 81-6 (Good Hope), and a more stable diesel fuel marine sample, 81-5, provided by NRL were utilized in these studies. The samples were stored in glass vials at 4°C until analyzed.

The polar components were fractionated from the fuels using alumina adsorption column chromatography. These separations were obtained in the following manner. Neutral aluminum oxide (Brockman Activity 1, 80 - 200 mesh, Fisher No. A950) was standardized to an activity level ~1.2% H_2O-AL_2O_3 by calcining at 145°C for 12 hours. Approximately 0.2 g of fuel sample was dissolved in chloroform and adsorbed to 3 g of alumina. After evaporation of the chloroform, the alumina was packed in an 11 mm i.d. column that had been previously packed with 6 g of the alumina. The column was then eluted with 20 ml of hexane followed by 50 ml of benzene. These fractions contained the aliphatic and neutral polycyclic aromatic compounds and were discarded. The first fraction of interest (A-3), containing the more polar nitrogen heterocyclic compounds, was obtained by elution with 70 ml of chloroform (containing an 0.75% ethanol). A final fraction (A-4) containing the most polar hydroxylated polycyclic aromatics was obtained by elution of the column with 50 ml of methanol.

SFC and SFC-MS analyses were performed on the A-3 and A-4 fractions of the fuels utilizing the chromatographic columns and mobile phase systems developed in Tasks A and B. In addition, carbon dioxide and pentane fluid systems were used to provide comparative analyses. Since polar binary

44

fluid mixtures were utilized as chromatographic mobile phases, flame ionization detection was not possible (i.e., the modifiers give a flame ionization response). Consequently, fluorescence detection was utilized for the SFC studies. The instrumentation (except for the detector) was very similar to that described in Task B for the UV absorption detection instrumentation (see Figure 6). Fluorescence detection was accomplished using a modified Schoeffel Instrument FS 970 HPLC fluorescence detector. The flow cell was removed and replaced with a length of 250 μm i.d. fused silica with a small window formed by burning off 3-4 mm of the polymide coating. The analytical column (210 μm o.d.) was threaded through the larger tubing and extended to a point immediately below the window. The larger window tubing and the analytical column were connected with a Supelco butt-connector. Decompression of the mobile phase and flow rate regulation were accomplished by connecting a short length of restrictor tubing to the exit end of the window tubing. Consequently, detection was accomplished prior to decompression, but since the detector was unheated, the fluid may return to the liquid phase prior to detection. The small window on the 250 μm i.d. tubing was carefully aligned in the light path of the tungsten lamp. Appropriate slits were used to illuminate only the interior of the cell to minimize the background created by diffracted light. A schematic diagram detailing the modified 2π steradian fluorescence collection system and on-column flow cell is shown in Figure 13. An excitation wavelength of 254 nm and collection of all radiation greater than 275 nm were used for the analyses conducted in these studies. The SFC-MS instrumentation was described previously in Task B (see Figure 7).

Results and Discussion

SFC Studies

The polar fuel fractions (A-3 and A-4) obtained from the alumina separation effectively concentrated the polar components of the fuels. Each of these fractions from DFM 81-6 comprised only approximately 1.5% (by weight) of the total fuel. Analyses of the polar fuel fractions using highly deactivated columns and pure carbon dioxide mobile phases were attempted. A typical chromatogram obtained with flame ionization detection SFC of the A-3 fraction

45

250 μm Tubing

Tubing Holder

Hemispherical
Quartz Reflector

Front View

Restrictor

250 μm Tubing

Photomultiplier
Tube

Window in
Polyimide

Tubing Holder

Analytical Column

Side View

Monochromatic
Excitation
Energy

Hemispherical
Quartz Reflector
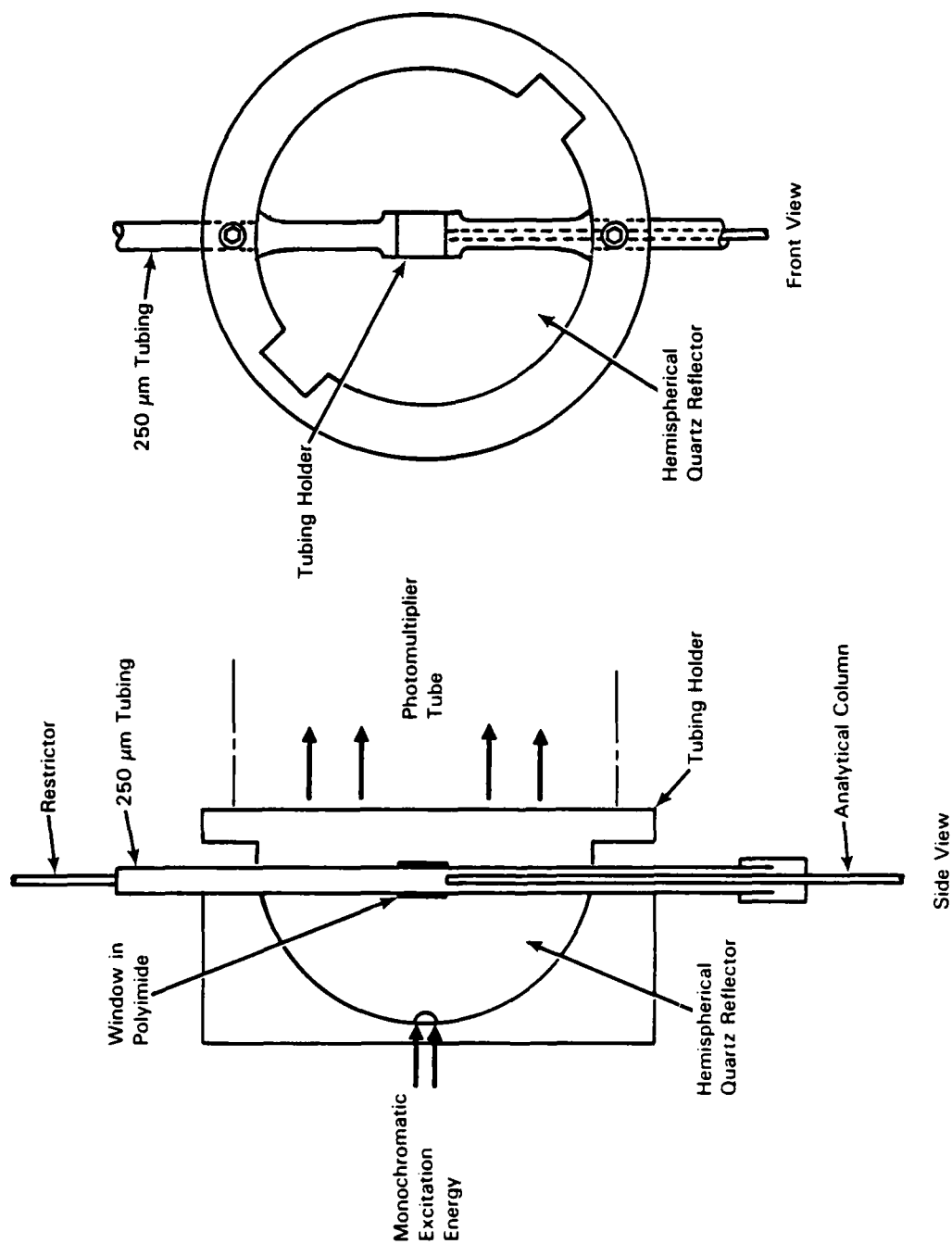
Figure 13. Schematic diagram of on-column fluorescence detection system.

of DFM 81-6 is shown in Figure 14. A very concentrated sample was injected, and only a few small peaks were eluted. This suggests the majority of the sample components were quite polar and not sufficiently soluble in the carbon dioxide mobile phase to be eluted from the SFC column. Similar behavior was also observed for the A-4 fraction. It was this evidence that directed the need for mobile phases with higher solvating power for polar heteroatomic polycyclic aromatic compounds.

Although pentane is nonpolar, it is a good solvent for aromatic hydrocarbon material. Thus, it was evaluated as a potential fluid. SFC chromatograms obtained with fluorescence detection of the A-3 and A-4 fractions of DFM 81-6 are shown in Figure 15. More dilute samples (50 times) were used for these analyses than were used when using carbon dioxide as the mobile phase and significantly greater quantities of material were eluted. The components were poorly resolved, however, and were eluted early in the analyses. The mobile phase liner velocity was more rapid than optimal, but this alone would not account for the poor chromatographic resolution. The reduced chromatographic retention and resolution can likely be attributed to high sample volatility at the relatively high operating temperature ($210^{o}C$) needed for pentane. This clearly indicates the necessity of utilizing a fluid with a lower operating temperature but also appropriate for more polar fuel components. Although pentane did not provide highly useful chromatographic separations, it did demonstrate that significant quantitites of material existed in these polar fuel fractions which should be amenable to SFC.

The studies conducted in Task B suggested that isopropanol-carbon dioxide binary fluid mixtures provided higher solvating power mobile phases with lower operating temperatures than several other potential binary mixtures. The impact of isopropanol on the chemical ionization behavior of the sample components during mass spectrometry (formation of complex spectra) is also lower than for other modifiers. Consequently, isopropanol-carbon dioxide mixtures were chosen as the fluid system of choice for these studies.

An SFC chromatogram of the A-3 fraction of DFM 81-6 utilizing fluorescence detection and a 10 mole percent isopropanol carbon dioxide fluid system is shown in Figure 16. This high resolution separation was obtained at $110^{o}C$ and with a slow pressure ramp of 0.1 atm/min beginning 10

47
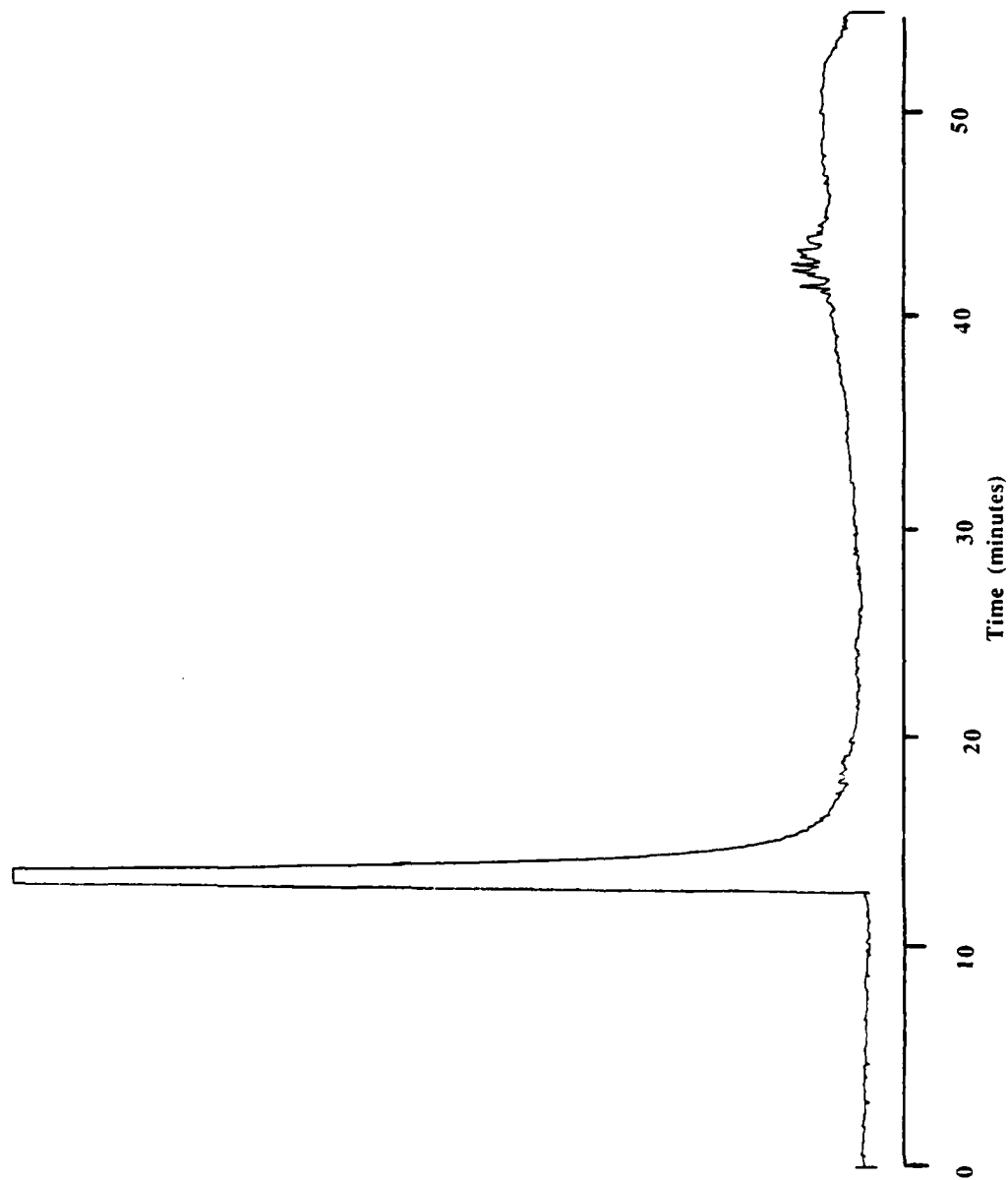
Figure 14. Capillary SFC chromatogram of the A-3 fraction of DFM 81-6 obtained using pure carbon dioxide as the mobile phase and flame ionization detection. Conditions: deactivated 10 m x 50 μm i.d. capillary column coated with 5% phenyl polymethylphenylsiloxane, 100°C operating temperature and density programmed from 0.14 g/mL at 0.01 g/mL after elution of the solvent peak.

48
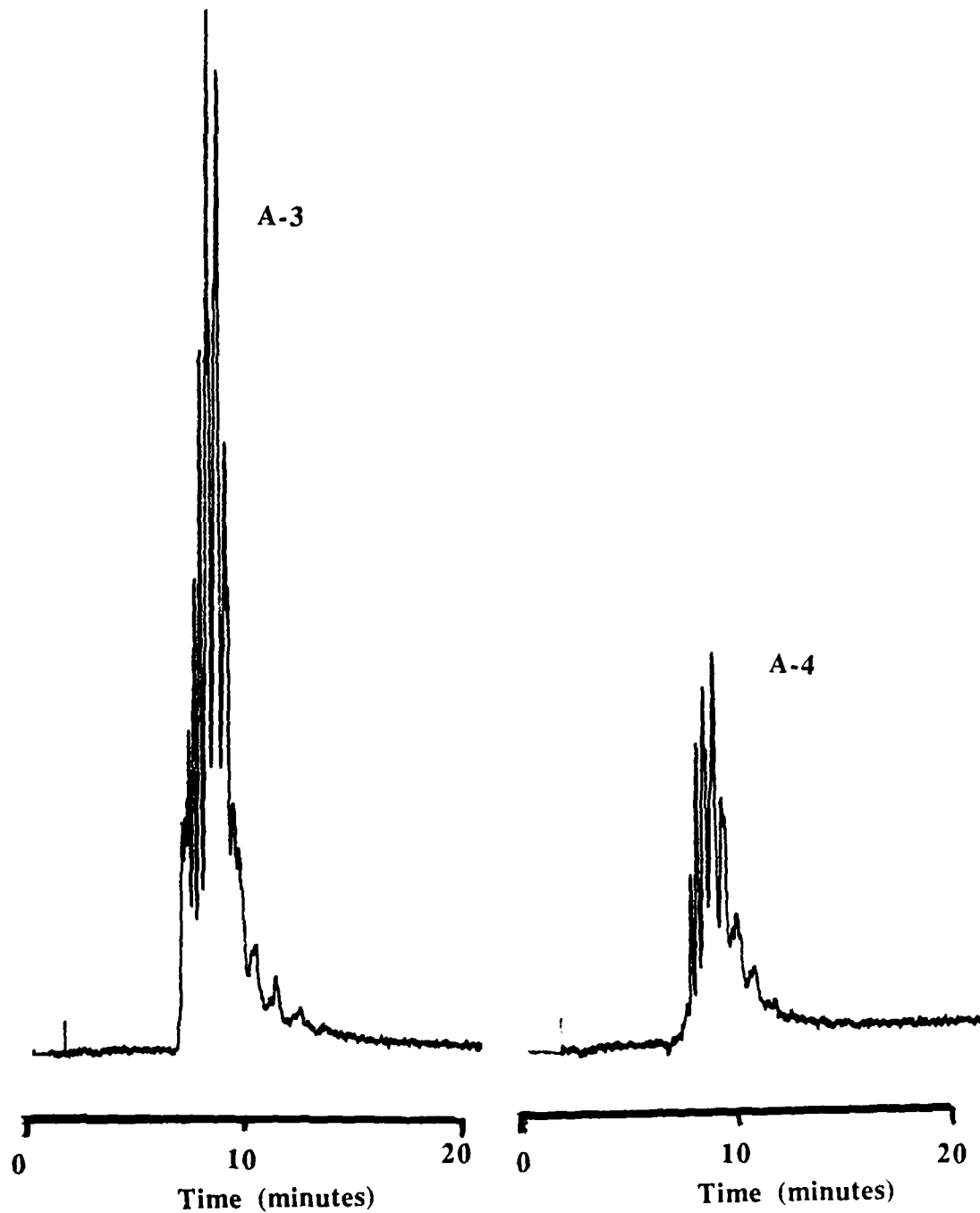
Figure 15.   Capillary SFC chromatograms of the A-3 and A-4 fractions of DFM 81-6 obtained with a pentane mobile phase and fluorescence detection. Conditions: deactivated 15 m x 50 μm i.d. capillary column coated with 5% phenyl polymethylphenylsiloxane, 210°C operating temperature and pressure programmed from 24 to 27 atmospheres.
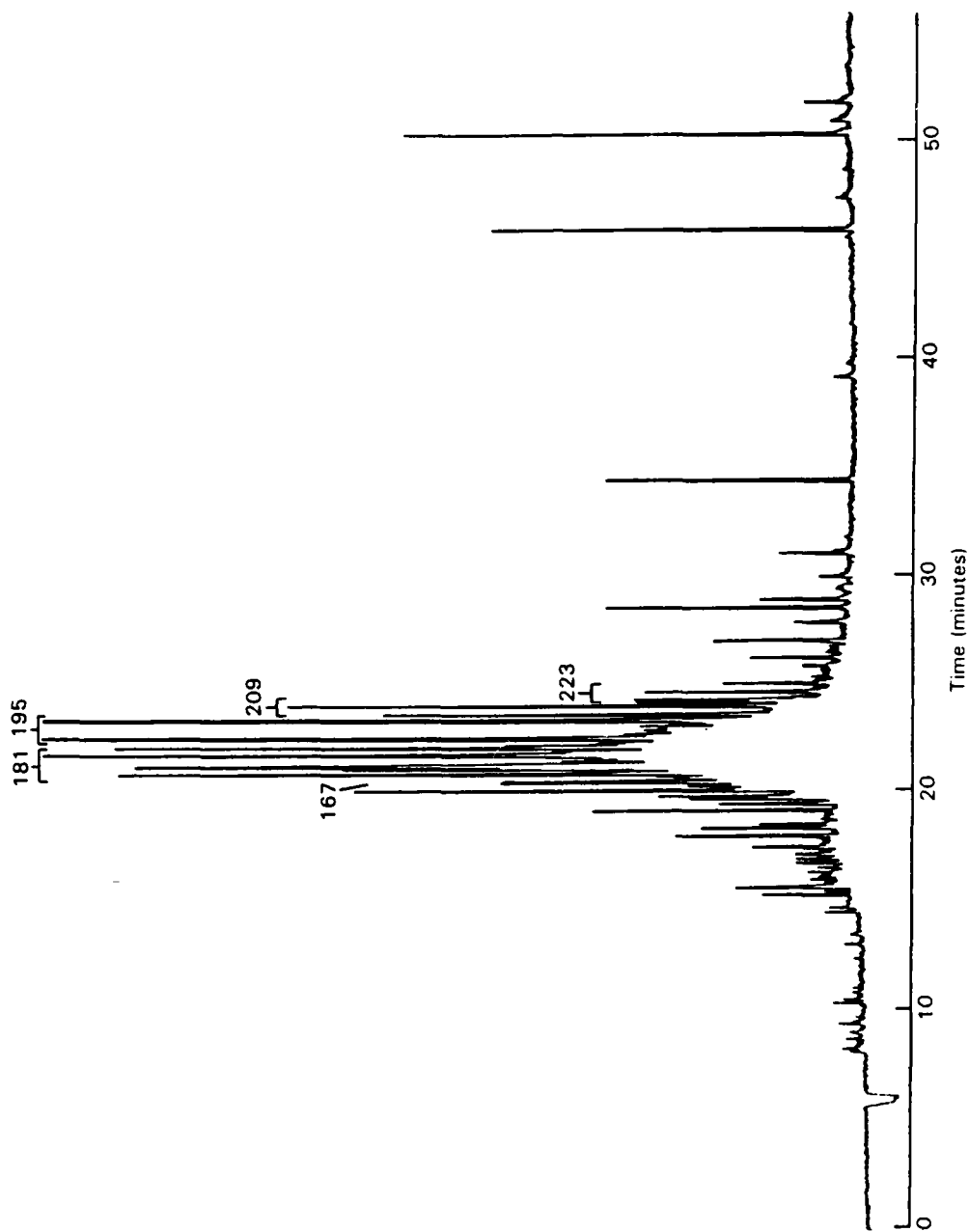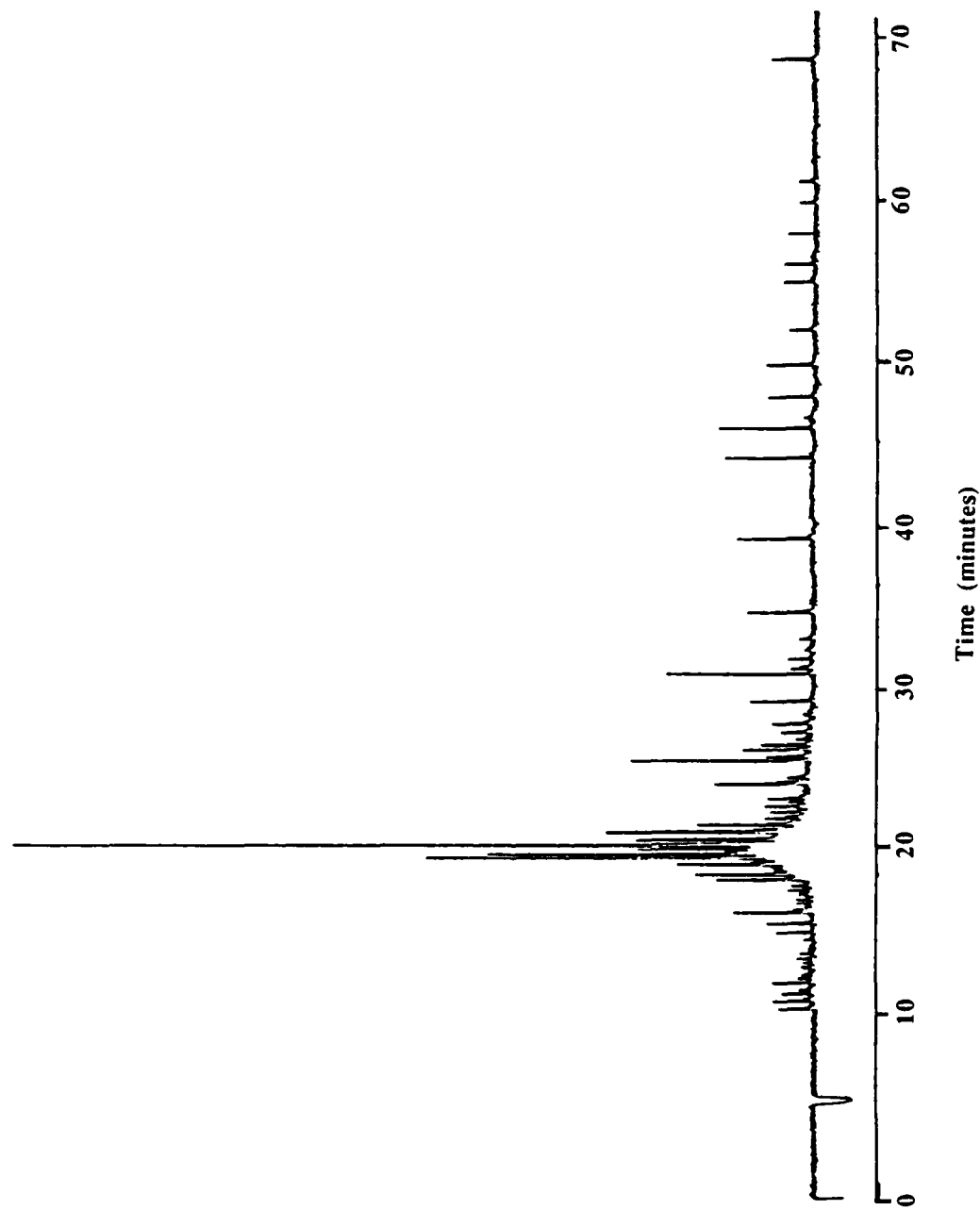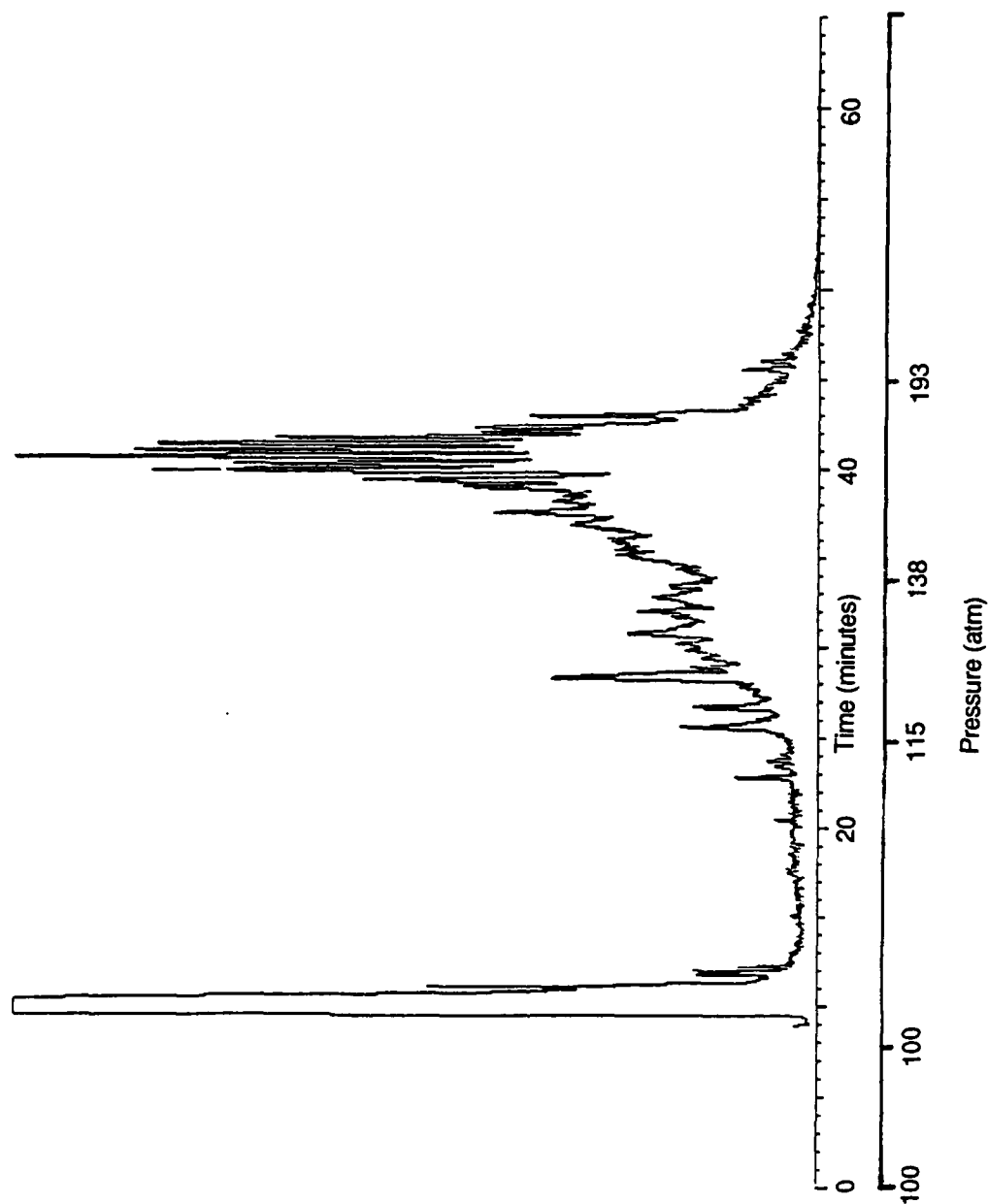
Figure 16. Capillary SFC chromatogram of the A-3 fraction of DFM 81-6 obtained using a 10 mole percent isopropanol-carbon dioxide fluid system and fluorescence detection. Conditions: deactivated 10 x 50 μm i.d. fused silica capillary column coated with 5% phenyl polymethylphenylsiloxane, 110°C operating temperature and pressure programmed at 0.1 atm/min from 110 atmospheres starting ten minutes after injection. Peak labels refer to molecular weight of marked components.

minutes after injection at 110 atmospheres. Numerous components were resolved, but many other additional compounds remained unresolved as evidenced by the "hump" in the chromatogram. Both lower pressure and lower temperature operating conditions were evaluated to decrease mobile phase solvating power and solute volatility, respectively, in an effort to better resolve the components. However, decreasing either resulted in drastic deterioration of the separation suggesting that a subcritical two-phase mixture was being utilized as the mobile phase. Interestingly, a greater number of components was evident in this SFC separation of the A-3 fraction of DFM 81-6 than were observed in the GC chromatogram of the same fraction (43). This suggests that a number of very polar or thermally labile compounds was not successfully eluted by GC analysis.

An SFC chromatogram of the A-4 fraction of DFM 81-6 utilizing fluorescence detection and a 10 mole percent isopropanol-carbon dioxide fluid system is shown in Figure 17. Other chromatographic parameters were the same as used for the separation shown in Figure 16. Numerous components were also resolved in the separation of this complex mixture. Qualitatively, it appears that this fraction was somewhat less complex than the A-3 fraction. SFC analyses of the A-3 and A-4 fractions of DFM 81-5 revealed essentially the same profiles as were obtained for DFM 81-6. Identical chromatographic conditions were utilized and only minor differences could be observed between the two fuels. As with the A-3 fraction, the results show additional components not eluted by GC. Consequently, differences in chemical composition between the fuels must arise from the very low level components.

SFC-MS Studies

SFC-MS was also utilized to analyze the polar fractions from DFM 81-6. A slightly less polar 6.5 mole percent isopropanol-carbon dioxide fluid mixture was utilized for these separations. The SFC-MS total ion chromatogram of the A-3 fraction is shown in Figure 18. This separation was obtained at 100°C and the pressure was ramped from 100 atmospheres at 1.25 atmospheres/min beginning 13 minutes after injection, then at 2.5 atmospheres/min at 25 minutes, at 5 atmospheres/min at 34 minutes, and finally at 10 atmospheres/min at 45 minutes. Since this fluid mixture contained less isopropanol than was used for the SFC separations, a slightly lower operating temperature

Figure 17. Capillary SFC chromatogram of the A-4 fraction of DFM 81-6 obtained using a 10 mole percent isopropanol-carbon dioxide fluid system and fluorescence detection. Conditions the same as in Figure 16.

Figure 18. Capillary SFC-MS total ion chromatogram of the A-3 fraction of DFM 81-6 obtained using a 6.5 mole percent isopropanol-carbon dioxide fluid mixture. Conditions: deactivated 15 m X 50 µm i.d. fused silica capillary column coated with 5% phenyl polymethylphenylsiloxane, 100°C operating temperature and pressure progammed at various rates from 100 atm starting 13 minutes after injection.

and lower initial pressure could be used and still maintain a single-phase critical mixture. The slightly lower solvating power of this fliud also provided increased retention. As would be anticipated, this SFC-MS profile is very similar to the fluorescence detection SFC profile shown in Figure 16. Although several distinct peaks were apparently resolved, numerous other unresolved components are evident from the "humps" in the chromatographic profile.

However, by utilization of the mass selective detection capabilities available with mass spectrometric analysis, numerous ion series could be resolved from the overlapping and coeluting chromatographic peaks. Preliminary evaluation of the mass spectral data suggested that many of the components were alkylated homologs. Consequently, several series of selected ion plots, increasing in mass by 14 dalton (a methylene unit), were generated. These series of selected ion plots are shown in Figures 19-30. In some instances, a compound series could be tentatively identified on the basis of molecular weight and relative chromatographic retention time. Unfortunately, however, in the absence of additional studies using appropriate standards or MS/MS capabilities, the information was often insufficient to make definite assumptions regarding the identity of many of the compound series. It should be noted that no carbon-13 corrections were applied, and thus, significant contributions from high intensity ions could be observed in selected ion plots of one dalton higher mass. The more significant carbon-13 contributions are marked with an asterisk (*) in the Figures.

The ion series shown in Figure 19 probably correspond to a parent at m/z 130 and its C_1 through C_4 alkyl homologs at m/z 144, 158, 172, and 186, respectively. Methane was used as the CI reagent gas and $[M+1]^+$ ions predominate. Consequently, the parent at m/z 130 has a molecular weight of 129 and probably corresponds to quinoline, isoquinoline, or both. In addition to C_1-quinolines, the m/z 144 grouping could also include aminonaphthalenes. Alkylated C_1 through C_3 aminonaphthalenes could also contribute to the m/z 158, 172, and 186 ion plots.

Another series of ions beginning with m/z 145 is shown in Figure 20. An intense m/z 145 peak was observed at approximately 25.5 minutes and could correspond to an aminoquinoline. A grouping of peaks was also observed at
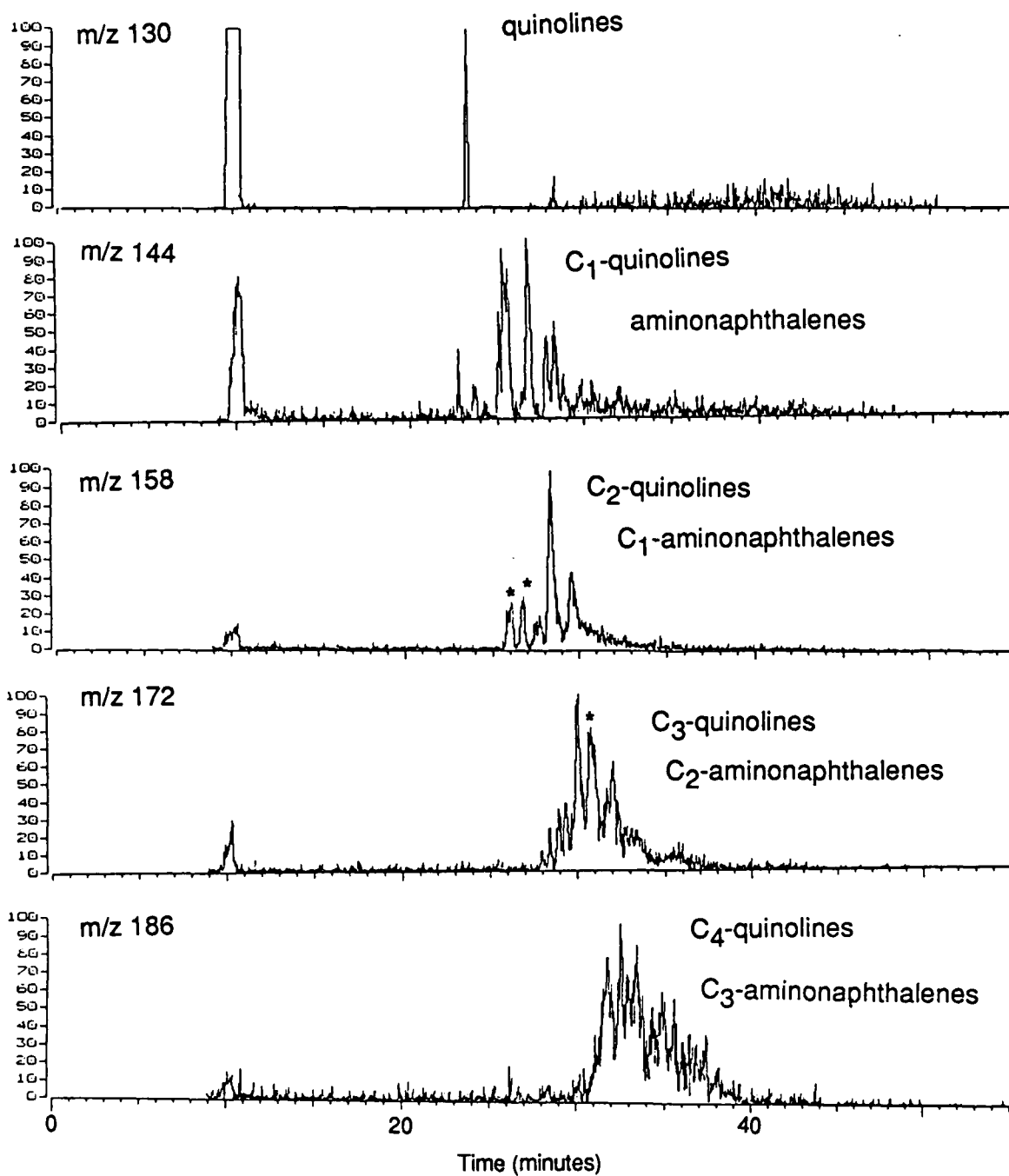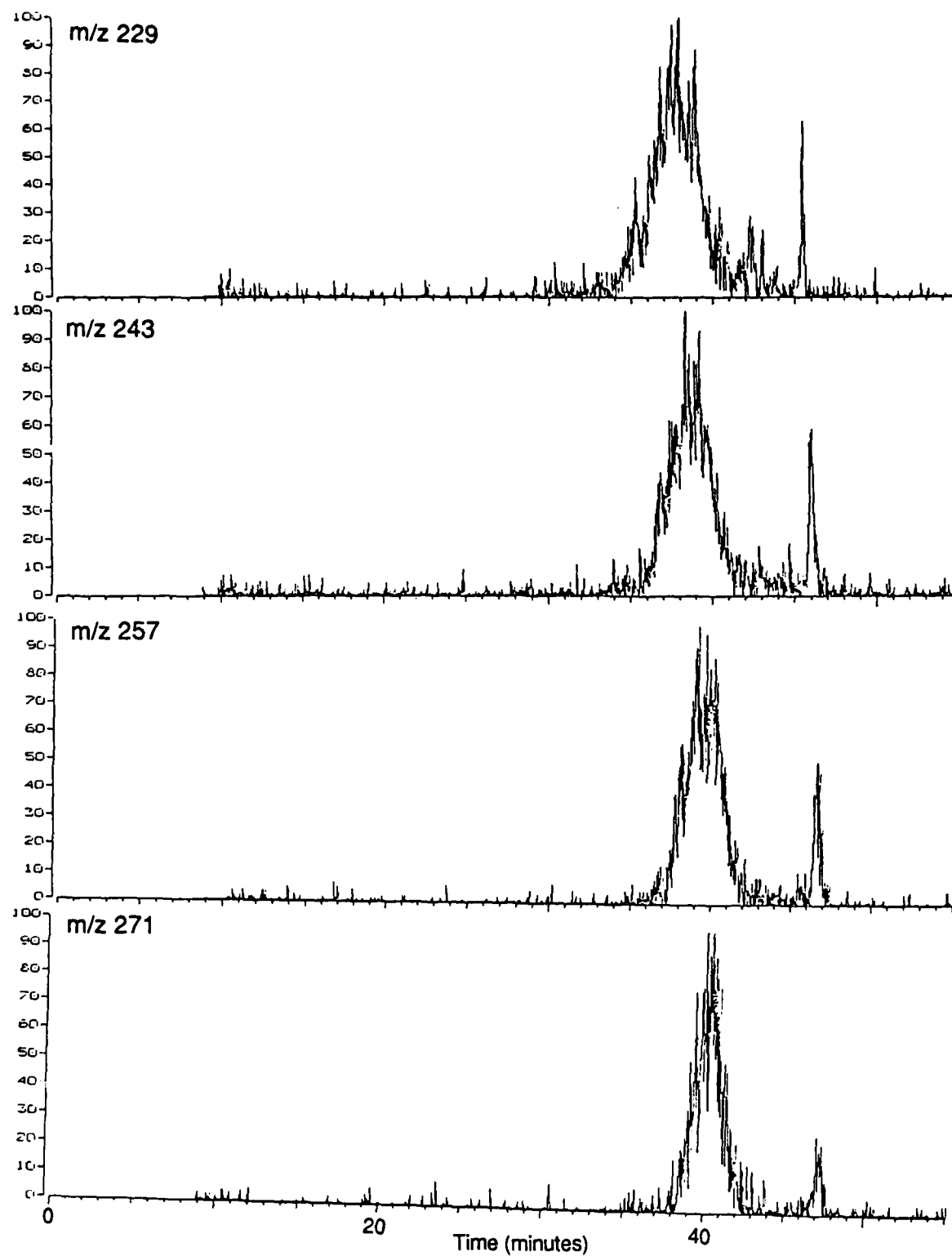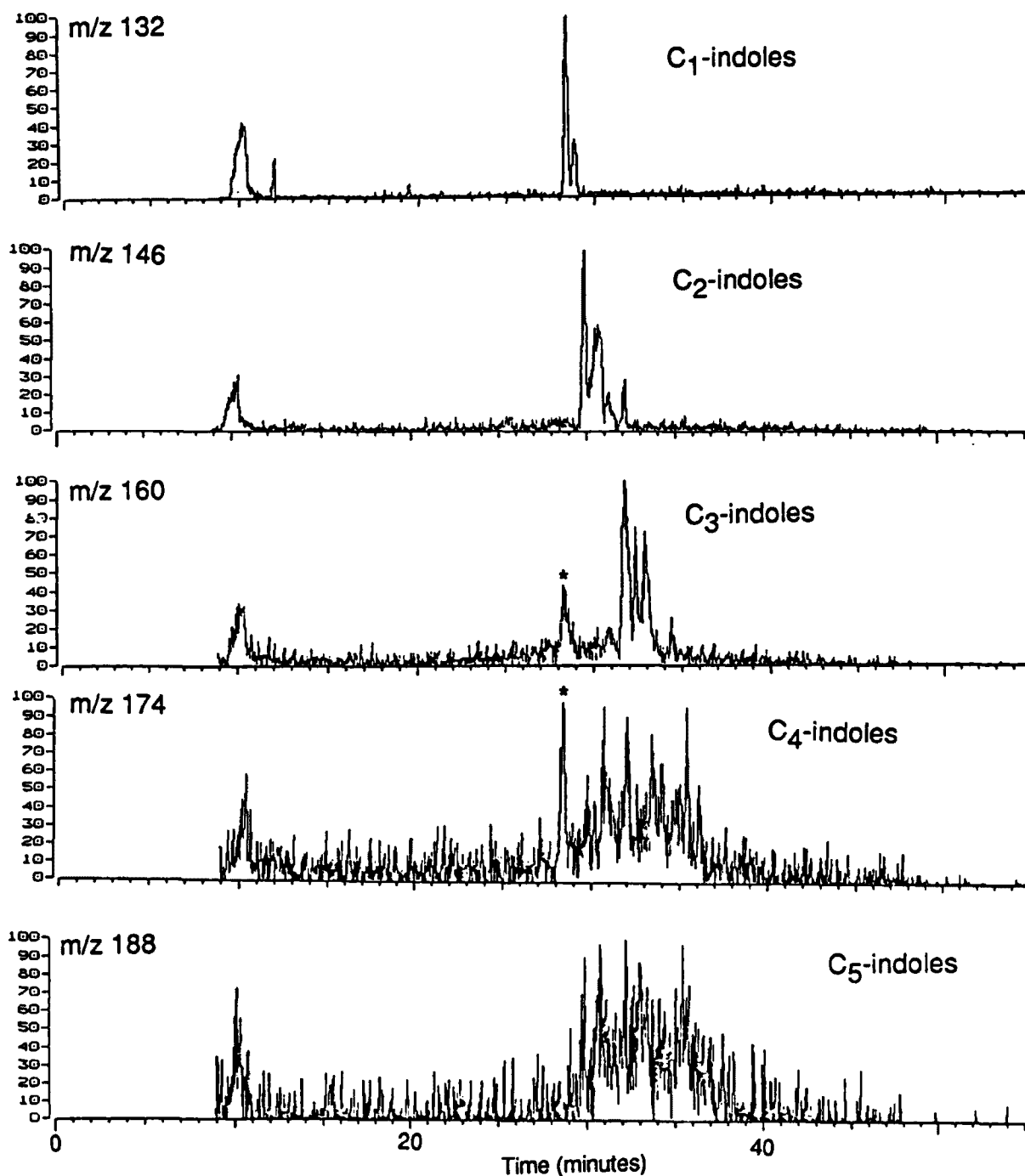
Figure 19.   Single ion plots obtained by SFC-MS of the A-3 fraction of DFM 81-6. The m/z values correspond to [M+1]+ ions.
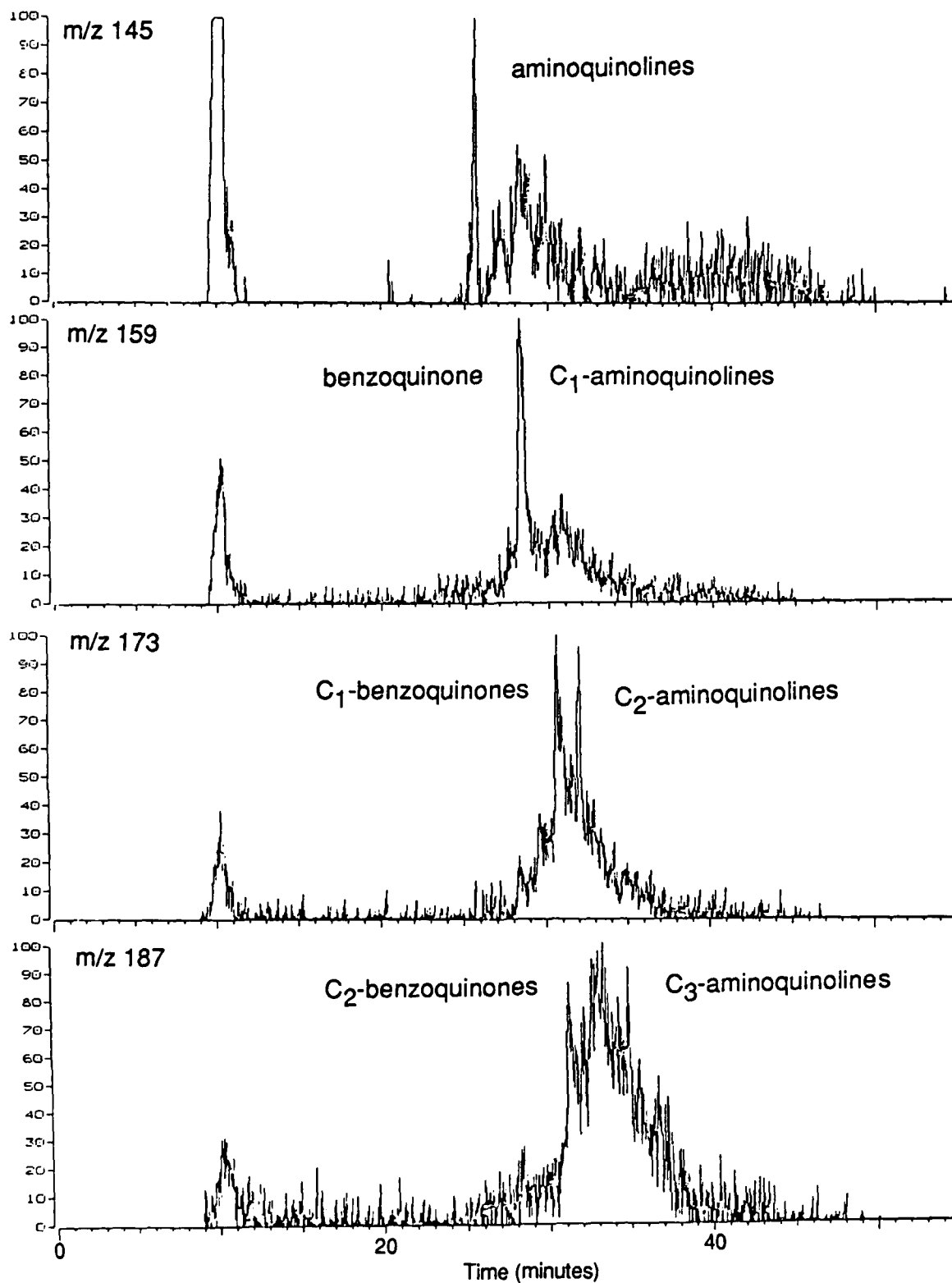
Figure 20.   Single ion plots obtained by SFC-MS of the A-3 fraction of
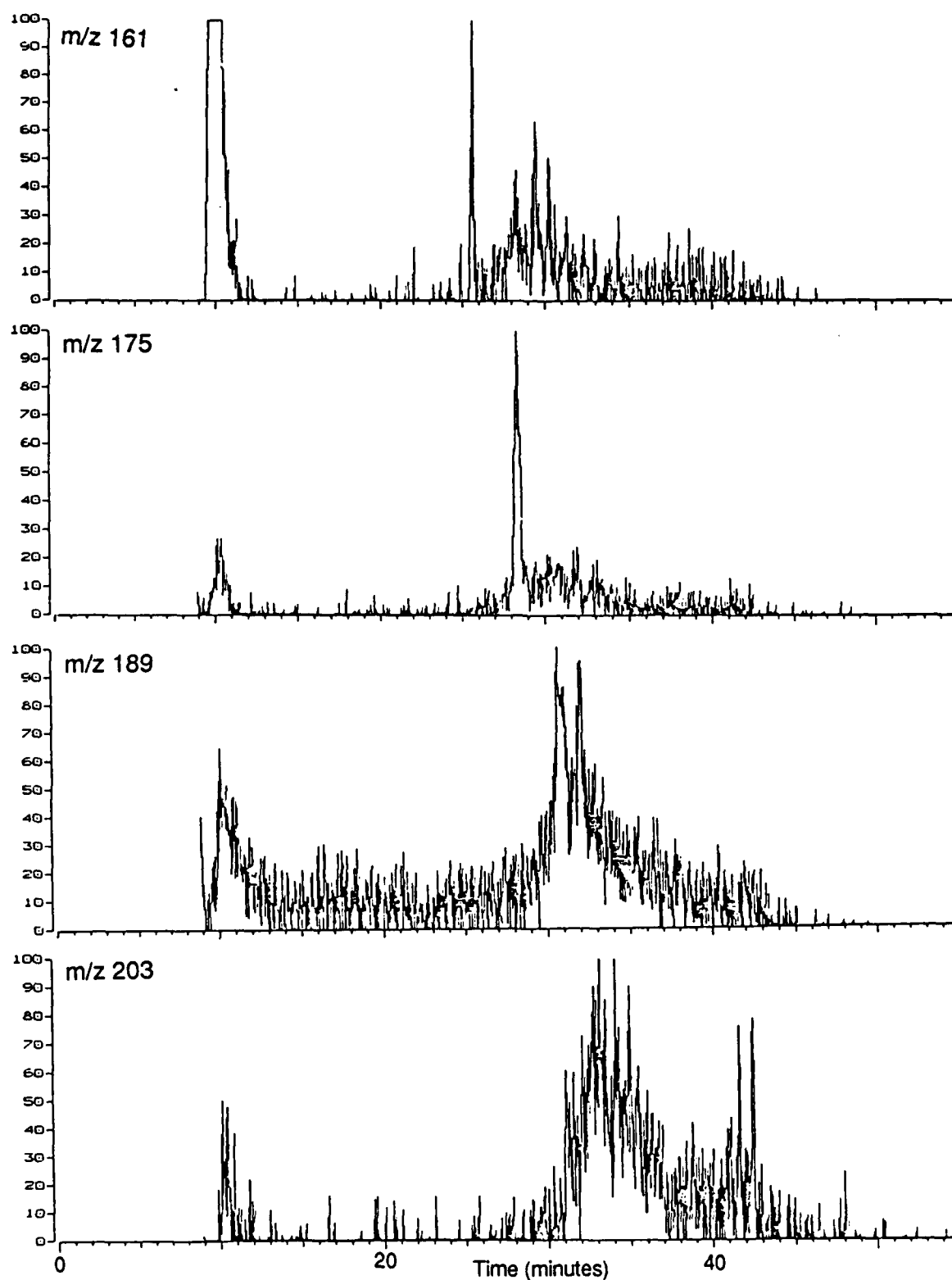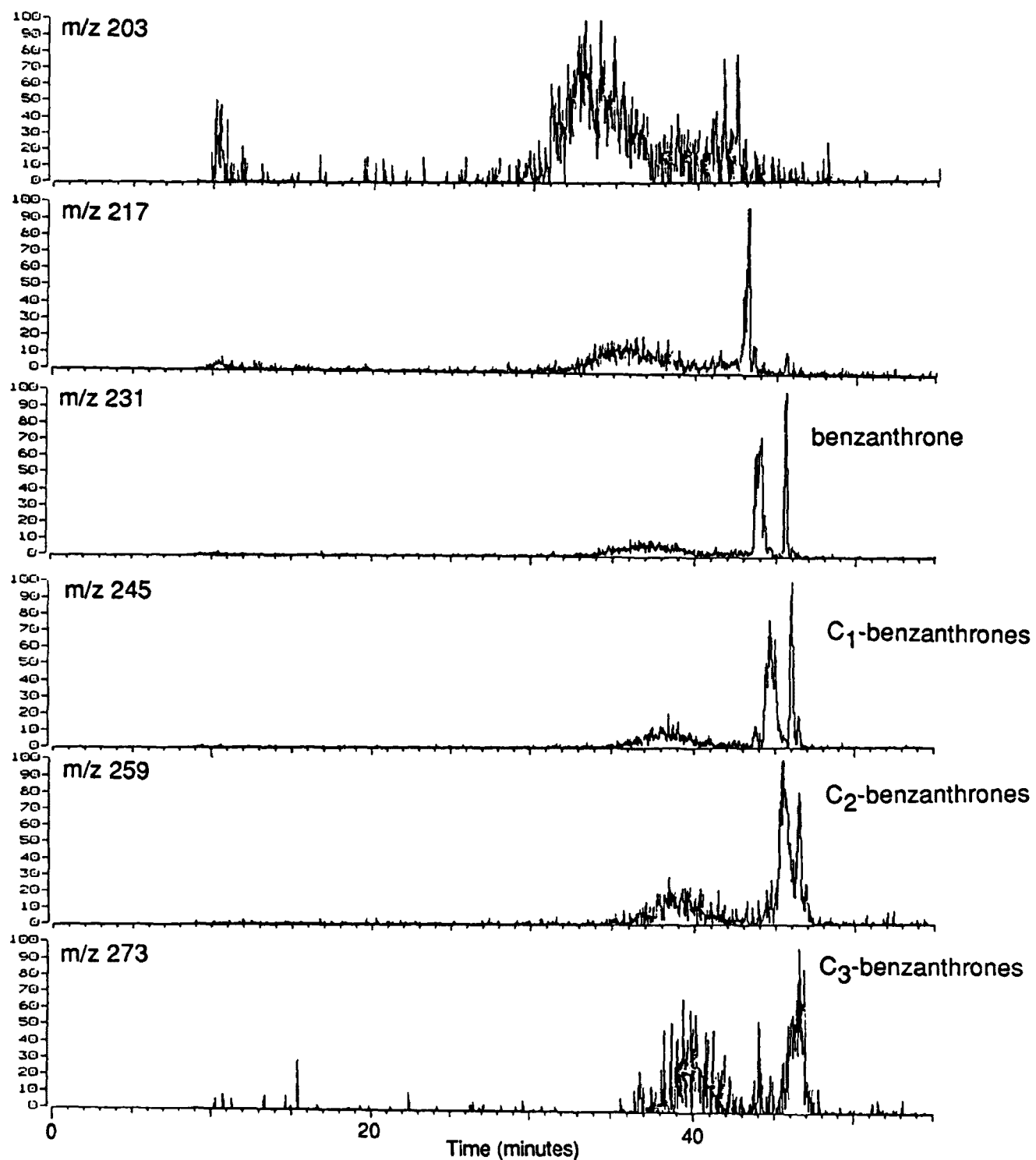   DFM 81-6. The m/z values correspond to $[M+1]^+$ ions.

m/z 145 which would be expected to correspond to the alkyl homologs of a parent. However, no significant ions at the correct retention time for a parent (m/z 131) were detected. Alkylated species of the m/z 145 parent could account for the m/z 159, 173, and 187 ions, although the major m/z 159 contribution was from a single component which could correspond to a benzoquinone. Thus, some of the ions at m/z 173 and 187 could also correspond to C_1 and C_2 benzoquinones. The continuation of the same series of m/z values, after skipping two increments which did not contain any significant contributions, is shown in Figure 21. At m/z 229 two major groupings can be observed with the first group centering around a retention time of 37 minutes and corresponding to numerous peaks, and the second at a retention time of 45.5 minutes consisting of a single component. Each C_1 increment in the m/z values of these groupings shift to slightly higher retention times which is consistent with increasing alkylation.

The series of ions shown in Figure 22 probably correspond to alkyl indoles. The first plot of m/z 132 indicates at least two components are present between retention times of 28 and 29 minutes, which is consistent with C_1-indole isomers. The parent indole at m/z 118 may have been present, but the spectrometer was not scanned to a sufficiently low mass for it to be detected. The remaining ions at m/z 146, 160, 174, and 188 probably correspond to the C_2 through C_5 aklyl indoles, respectively. As can be observed by the background, the compounds giving the m/z 174 and 188 ions were at significantly lower concentration levels. Some of the m/z 174 contributions could arise from nitronaphthalenes.

Another series of ions beginning with the m/z 161 is shown in Figure 23. Although several peaks were apparent at m/z 161, suggesting alkyl isomers of a parent, no significant ions were detected at m/z 147, where the parent would be expected. Since m/z 175 consists essentially of one main peak, it could also correspond to a parent structure and the numerous m/z 189 and 203 contributions could be its alkylated homologs.

The same ion series, beginning with m/z 203, are continued in Figure 24. The m/z 203 could correspond to the neutral PAH, pyrene or fluoranthene, although only very low concentrations would be expected to be found in the A-3 fraction. The m/z 203 profile shows two main groupings with numerous

57

Figure 21.   Single ion plots obtained by SFC-MS of the A-3 fraction of
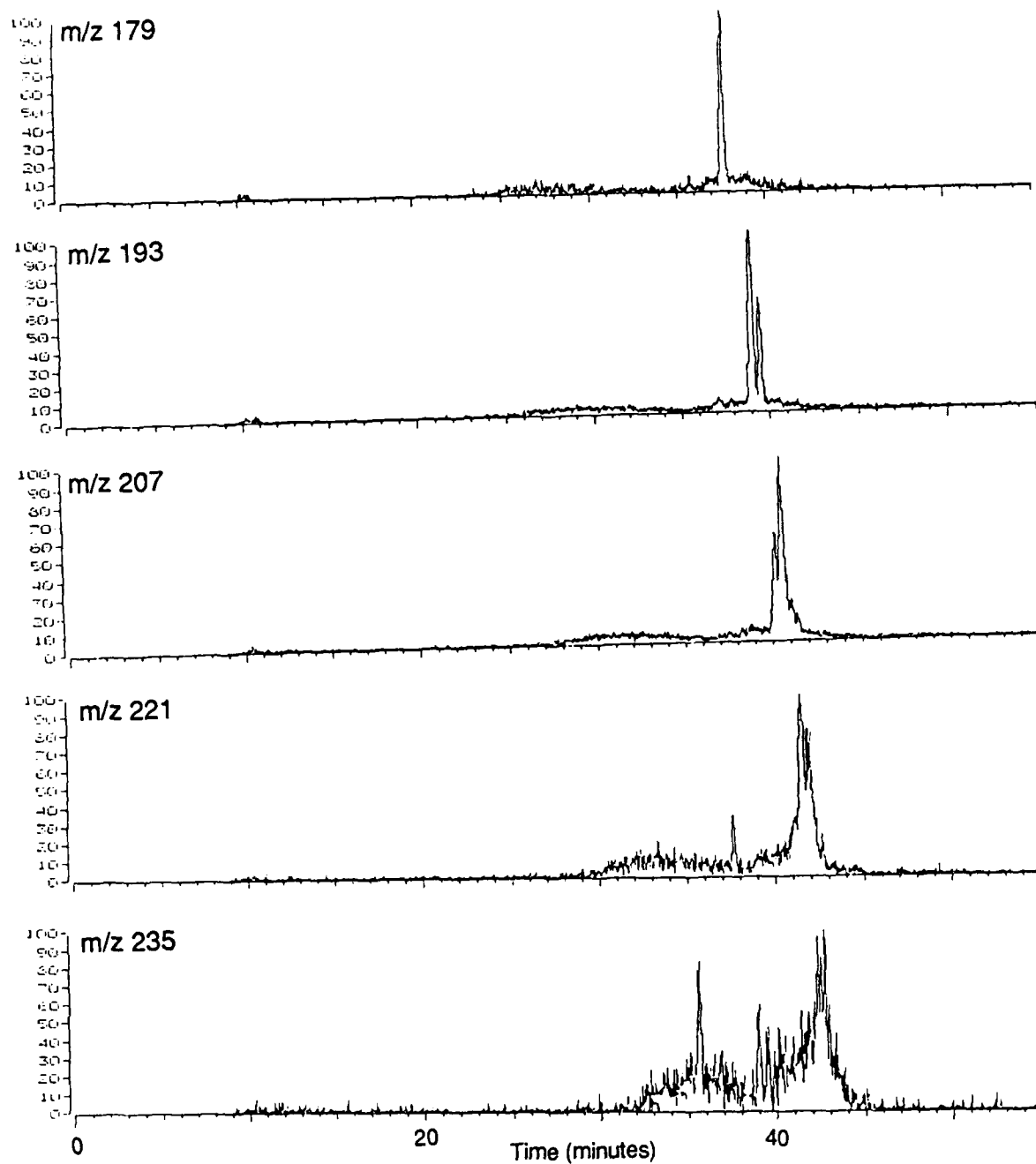DFM 81-6.   The m/z values correspond to [M+1]$^+$ ions.
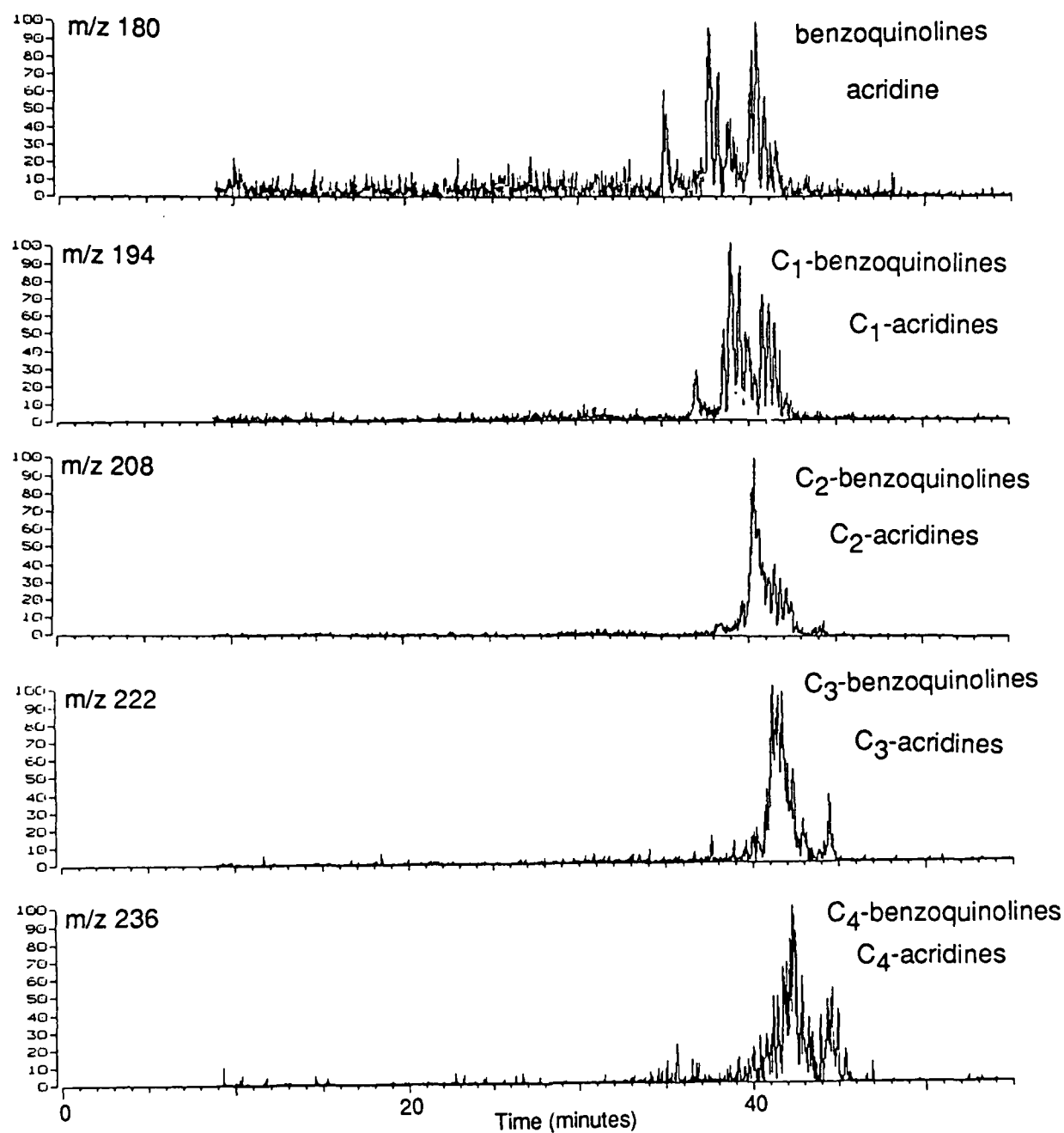
58

Figure 22.   Single ion plots obtained by SFC-MS of the A-3 fraction of DFM 81-6.   The m/z values correspond to $[M+1]^+$ ions.

Figure 23.   Single ion plots obtained by SFC-MS of the A-3 fraction of DFM 81-6. The m/z values correspond to [M+1]+ ions.

Figure 24.   Single ion plots obtained by SFC-MS of the A-3 fraction of DFM 81-6.   The m/z values correspond to [M+1]$^+$ ions.

ions centering around a retention time of 33 minutes which could be the alkylated homologs discussed in the preceeding paragraph. Two other separate peaks occured near a retention time of 42 minutes and could correspond to fluoranthene and pyrene, and the m/z 217, 231, 245, 259 and 273 ions could be their C_1 through C_5 alkyl homologs. However, a second major peak at a retention time of 45.5 minutes can be observed on the m/z 231 plot which does not appear to belong to the alkylated pyrene or fluoranthene series, and it likely corresponds to a benzanthrone. A probable sequence of alkylated benzanthrones is also observable at m/z 245, 259, and 273.

Another series of ions beginning with m/z 179 is in Figure 25. The m/z 179 ion could correspond to phenanthrene or anthracene, but only very low concentrations of neutral PAH would be expected in this fraction, and this ion was at a relatively high concentration level. Thus, it might correspond to some other more polar unidentified compound. Alkylated homologs are also evident at m/z 193, 207, 221, and 235. Other compounds eluting earlier than the alkyl homologs can be observed in the m/z 221 and 235 ion plots.

The series of ions beginning with m/z 180 shown in Figure 26, probably correspond to benzoquinolines and acridine. Several isomers are possible and numerous peaks are observable. The C_1 through C_4 alkyl homologs are also evident at m/z 194, 208, 222, and 236, respectively. The complexity of the m/z 180 ion plot might suggest that additional components are also present, such as highly alkylated pyrroles (C_8-pyrroles), especially since the alkylated homolog series do not increase in complexity. It is unlikely that any lower alkylated species of different parents are present in the m/z 180 ion plot, since no significant contributions were found at m/z 166.

Another series of ion plots beginning with m/z 167 is shown in Figure 27. The earlier eluting peak at 32.5 minutes could correspond to either fluorene or phenalene (neutral PAH), but the remaining components must arise from more polar components. Two groups of peaks can be observed at m/z 181 with the second group possibly corresponding to C_1 alkyl homologs of the potential parent with m/z 167. The m/z 181 ions could also correspond to phenanthrolines or fluorenone. The alkyl homologs of both groups of m/z 181

Figure 25.   Single ion plots obtained by SFC-MS of the A-3 fraction of DFM 81-6. The m/z values correspond to [M+1]+ ions.

Figure 26. Single ion plots obtained by SFC-MS of the A-3 fraction of DFM 81-6. The m/z values correspond to $[M+1]^+$ ions.
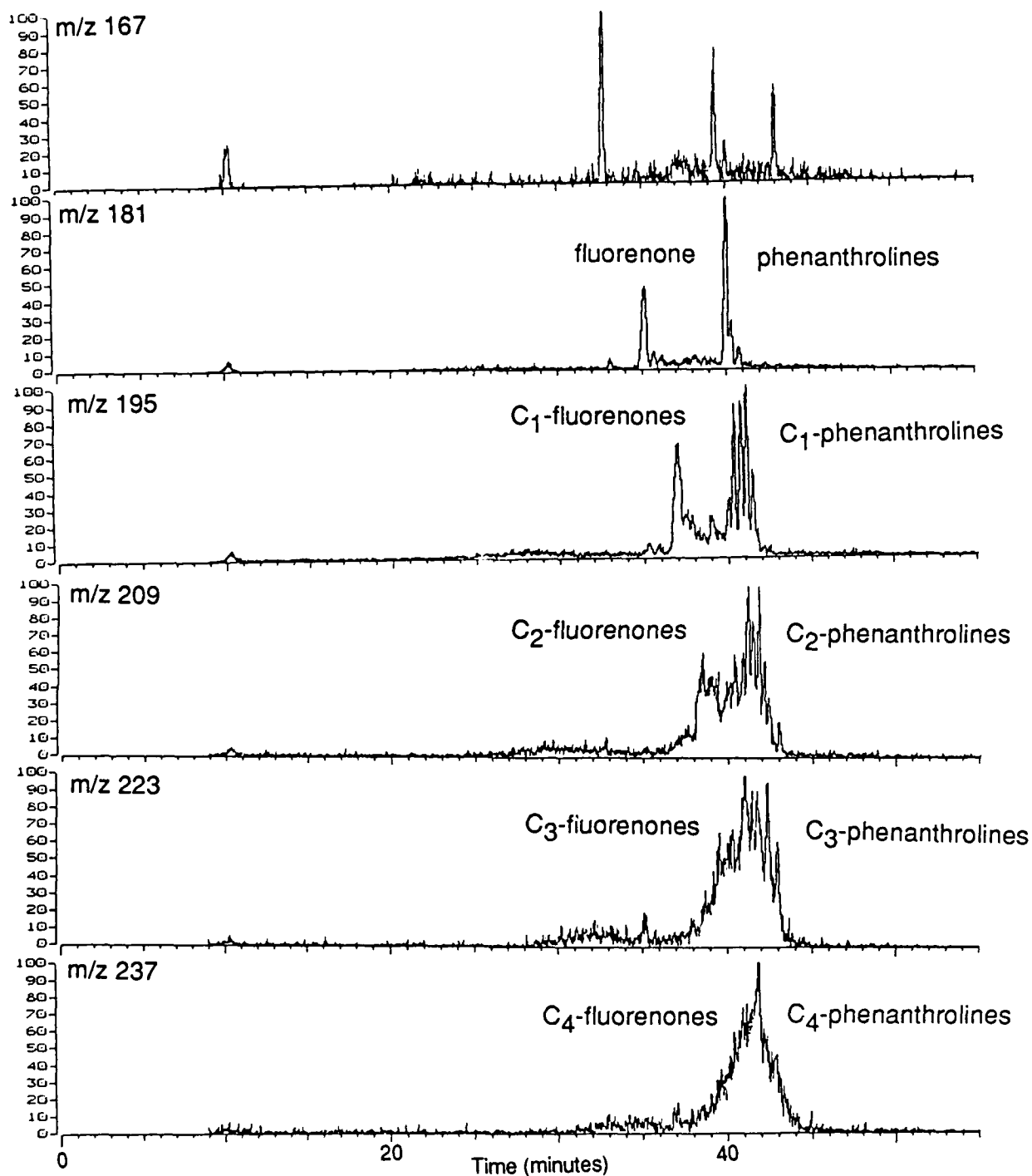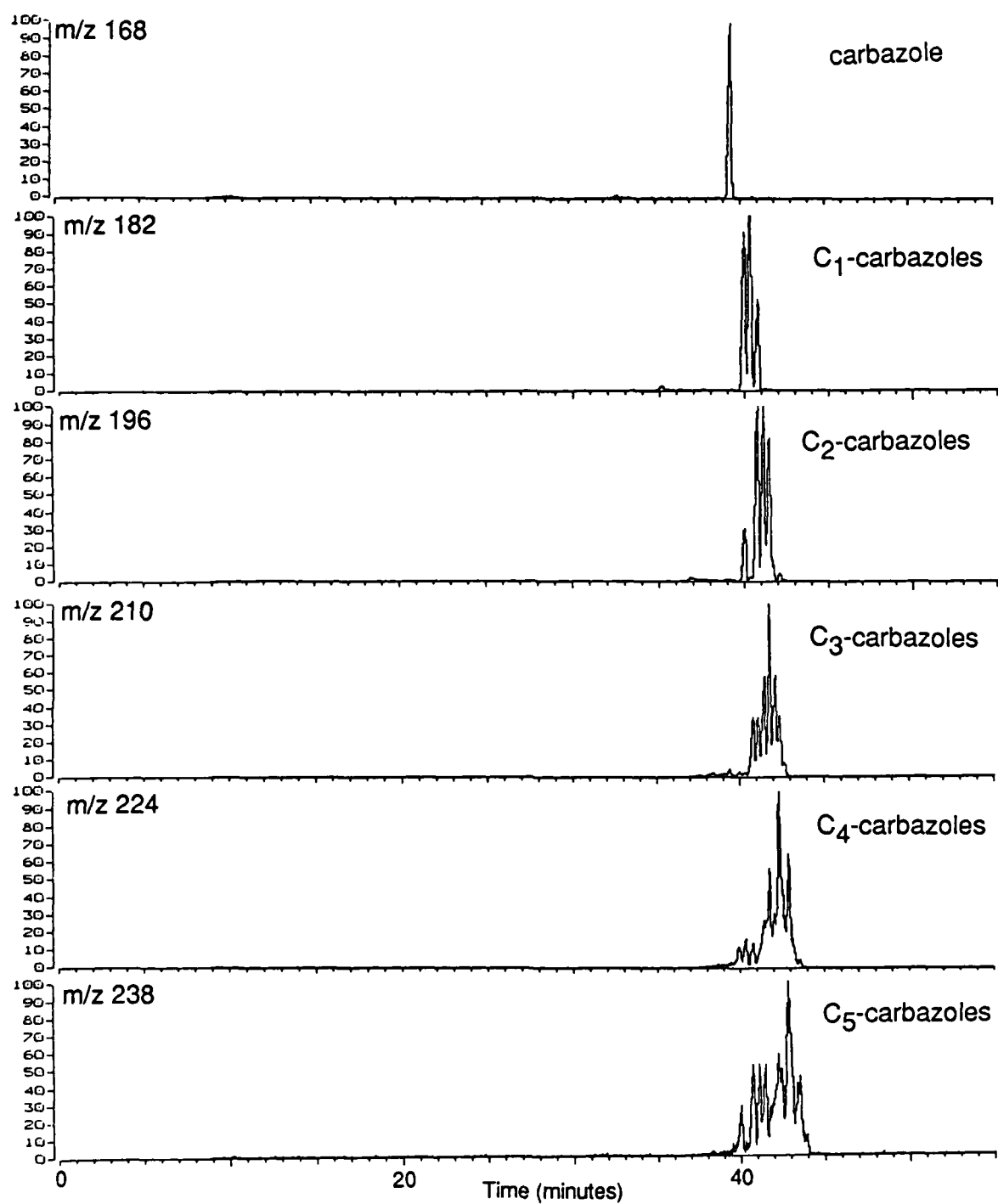
Figure 27.   Single ion plots obtained by SFC-MS of the A-3 fraction of
DFM 81-6.   The m/z values correspond to [M+1]$^+$ ions.

are clearly present at m/z 195, 209, 223, and 237 as progressively higher retention times are observed with increased alkylation.

The most intense signals in the analysis arise from the ion series shown in Figure 28. The parent structure at m/z 168 is undoubtedly carbazole and its C_1 through C_5 alkyl homologs are clearly present at m/z 182, 190, 210, 224 and 238, respectively. As would be expected, the retention times increase slightly with increased alkylation. The C_1 through C_3 species were present at similar concentration levels slightly greater than carbazole. Lower levels of the C_4 and C_5 species were present.

Another series of ion plots, beginning with m/z 169, is shown in Figure 29. Although numerous components are evident, no significant contributions were found at 14 dalton lower mass at m/z 155, which suggests that the m/z 169 ions are not aklylated species. Azacarbazoles and dibenzofuran could be possible components in this sequence. The m/z 183, 197, 211, 225 and 239 ion groupings proably arise from increased alkylation since the retention times progressively increase. As noted earlier, carbon-13 contributions were not subtracted and a significant number of ions in this series arise from the carbon-13 contributions from the carbazoles.

The final series of ion plots from the SFC-MS analysis of the A-3 fraction of DMF 81-6 are shown in Figure 30. The first sequence at m/z 143 could correspond to neutral C_1-naphthalenes, but since only two isomers exist and three peaks are present, another unknown component is also present. Significant contributions for potential alkylated species at m/z 157, 171, 185, 199, and 213 are also present.

These mass spectral data illustrate the extreme complexity of this fuel fraction. Although much information has been gained, a tremendous amount of additional characterization would be required to completely understand the fuel composition. Standard compounds of potential components would need to be analyzed under similar conditions to obtain exact retention times and comparison mass spectra. Other ionization methods (i.e., electron impact) and other CI reagents could also provide additional spectral information. This work, however, forms the basis for the development of a more complete characterization of the polar compounds in this fuel and demonstrates that

Figure 28.   Single ion plots obtained by SFC-MS of the A-3 fraction of
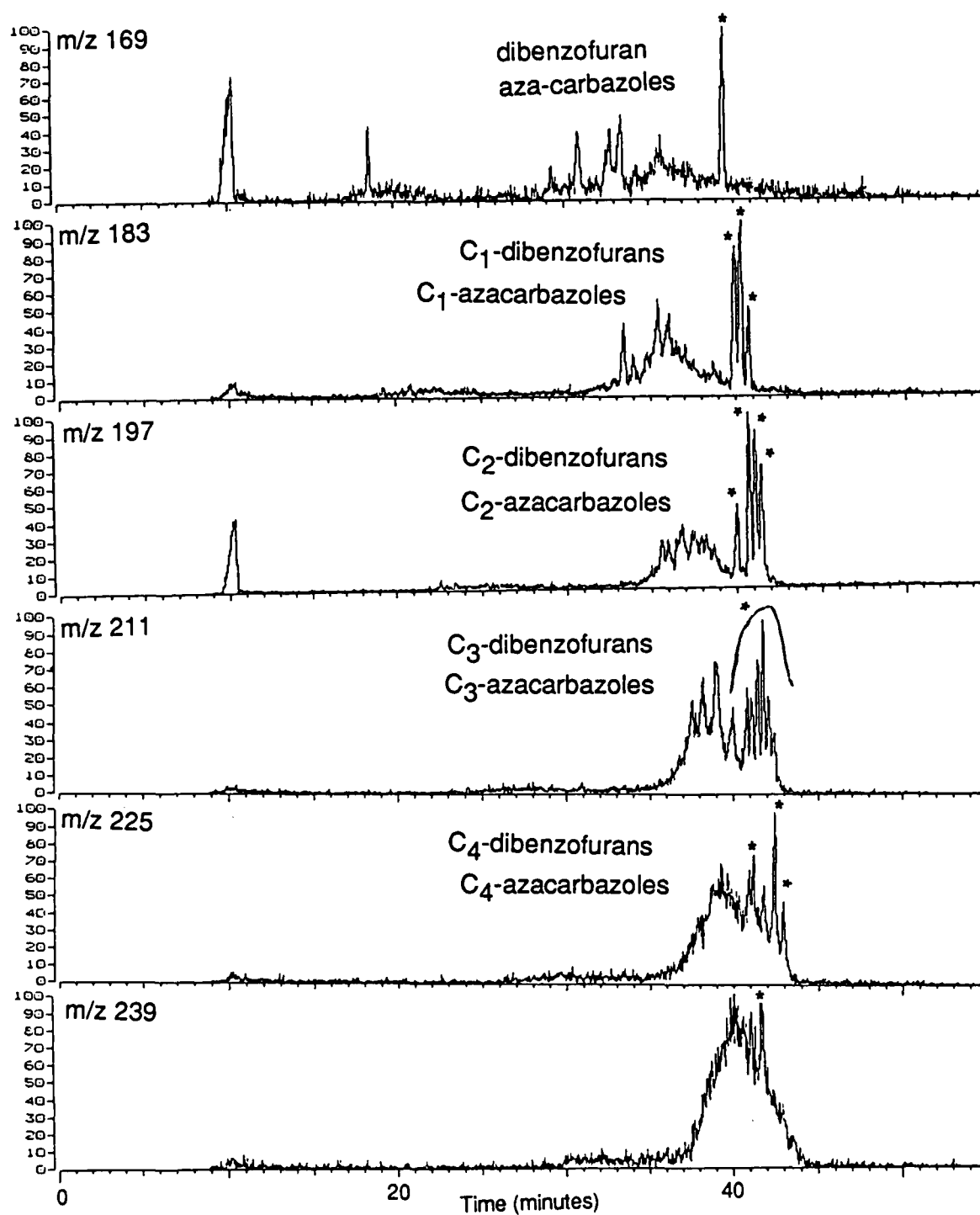   DFM 81-6.   The m/z values correspond to [M+1]$^+$ ions.

Figure 29.   Single ion plots obtained by SFC-MS of the A-3 fraction of DFM 81-6. The m/z values correspond to [M+1]$^+$ ions.
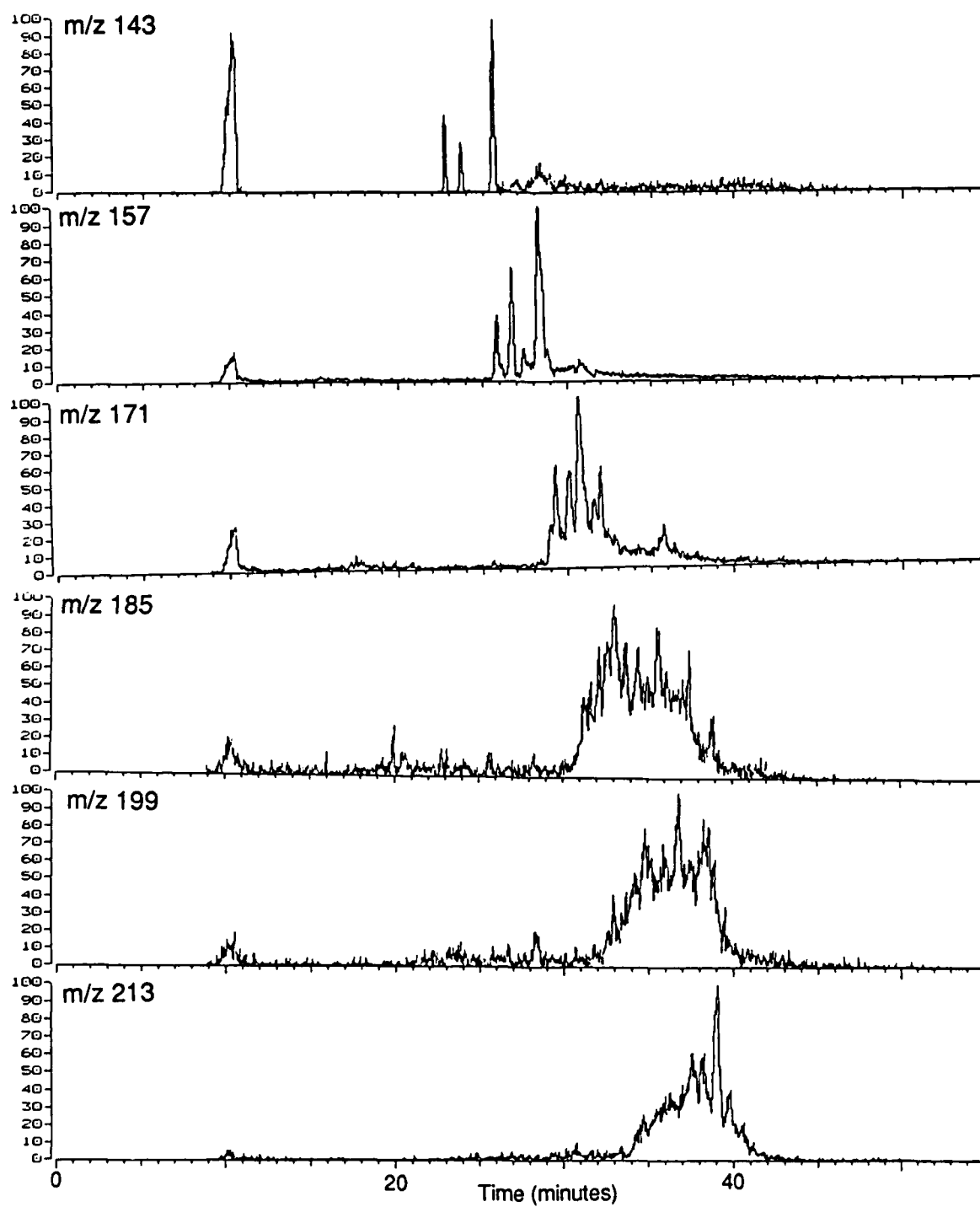
Figure 30.   Single ion plots obtained by SFC-MS of the A-3 fraction of
               DFM 81-6. The m/z values correspond to [M+1]$^+$ ions.

SFC-MS can be used to successfully characterize very complex matrices of polar and potentially labile components.

SFC-MS was also utilized to analyze the A-4 fraction of DFM 81-6. The total ion chromatogram is shown in Figure 31. The same chromatographic column and mobile phase fluid mixture were used in this separation as were used for the A-3 separation shown in Figure 18. The separation was obtained at 150°C and the pressure was ramped from 130 atmospheres at 1 atmospheres/min beginning 13 minutes after injection. Since a higher temperature and higher initial starting presure were used than for the A-3 fraction analysis, the components in this mixture were eluted relatively early in the analysis. As evident from the total ion chromatogram, this fraction is also very complex and numerous resolved and unresolved peaks can be observed.

Selected ion plots (Figures 32-40) of this SFC-MS analysis were made to obtain specific information regarding the chemical composition. Ion series increasing by 14 dalton increments were utilized to distinguish the alkylated species of particular parent structures. The compounds in this fraction all appear to be hydroxylated species, and several hydroxylated species of the components found in the A-3 fraction were detected.

The ion plots shown in Figure 32 correspond to at least three different alkylated series of compounds. The m/z 145 ions at a retention time of approximately 19 minutes probably correspond to hydroxynaphthalenes. The C_1 through C_4 hydroxynaphthalenes can be observed at m/z 159, 173, 187 and 201, respectively, at progressively higher retention times. A second compound series can be observed in the m/z 159 ion plot at a retention time of approximately 30 minutes. This series is likely the hydroxylated moieties of the unidentified m/z 143 compound observed in the A-3 fraction. The C_1 homologs of these compounds can also be observed at m/z 173. The third compound series can be observed in the m/z 173 ion plot at a retention time of approximately 43 minutes. This component(s) is probably the hydroxylated analog of the unidentified m/z 157 compound also observed in the A-3 fraction. The C_1 and C_2 alkyl homologs can be observed at appropriately higher retention times in the m/z 187 and 201 ion plots.
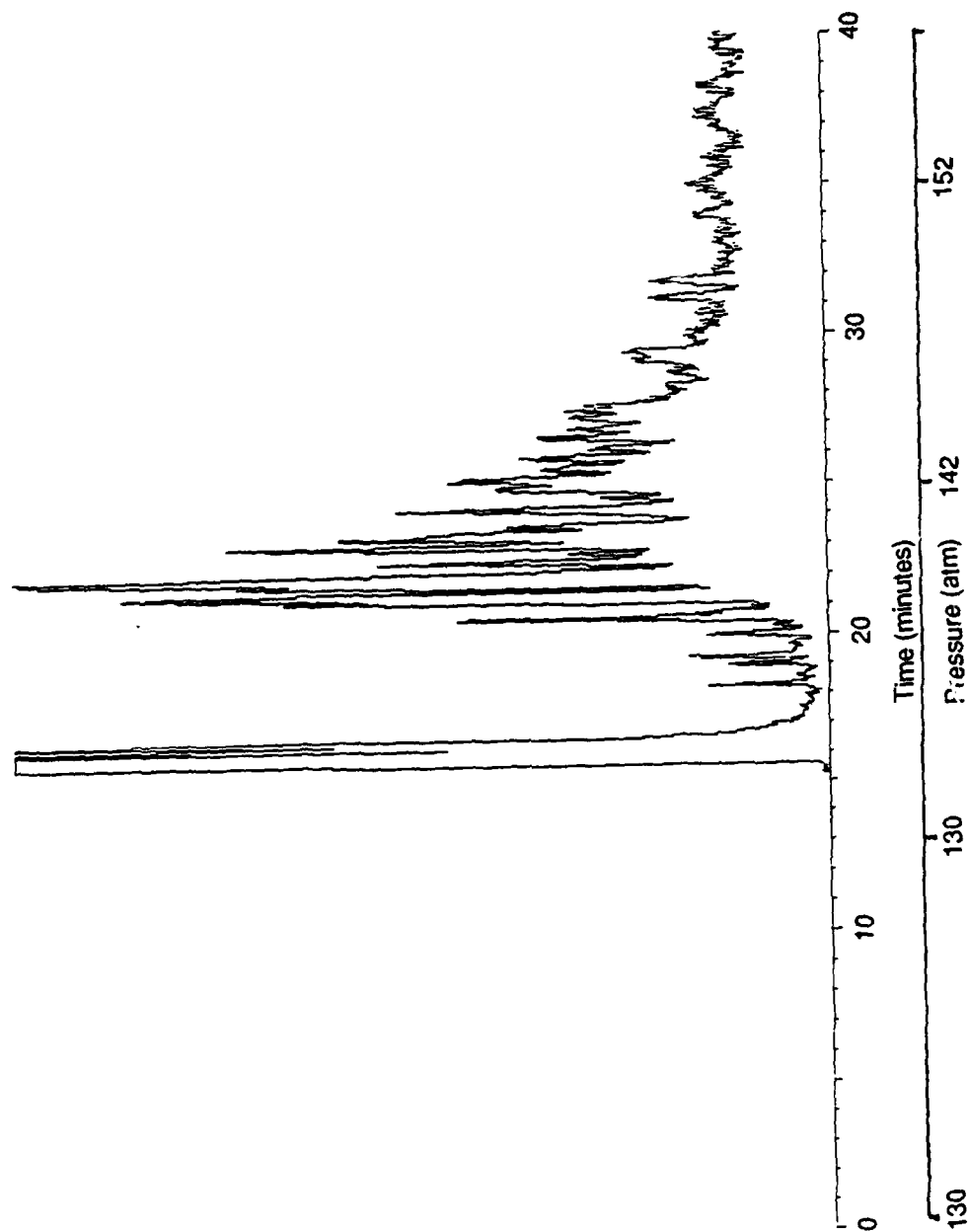
Figure 31. Capillary SFC-MS total ion chromatogram of the A-4 fraction of DFM 81-6 obtained using a 6.5 mole percent isopropanol-carbon dioxide fluid mixture. Conditions: deactivated 15 m x 50 μm i.d. fused silica column coated with 5% phenyl polymethylphenylsiloxane, 150°C operating temperature and pressure programmed at 1 atm/min from 130 atm starting 13 minutes after injection.
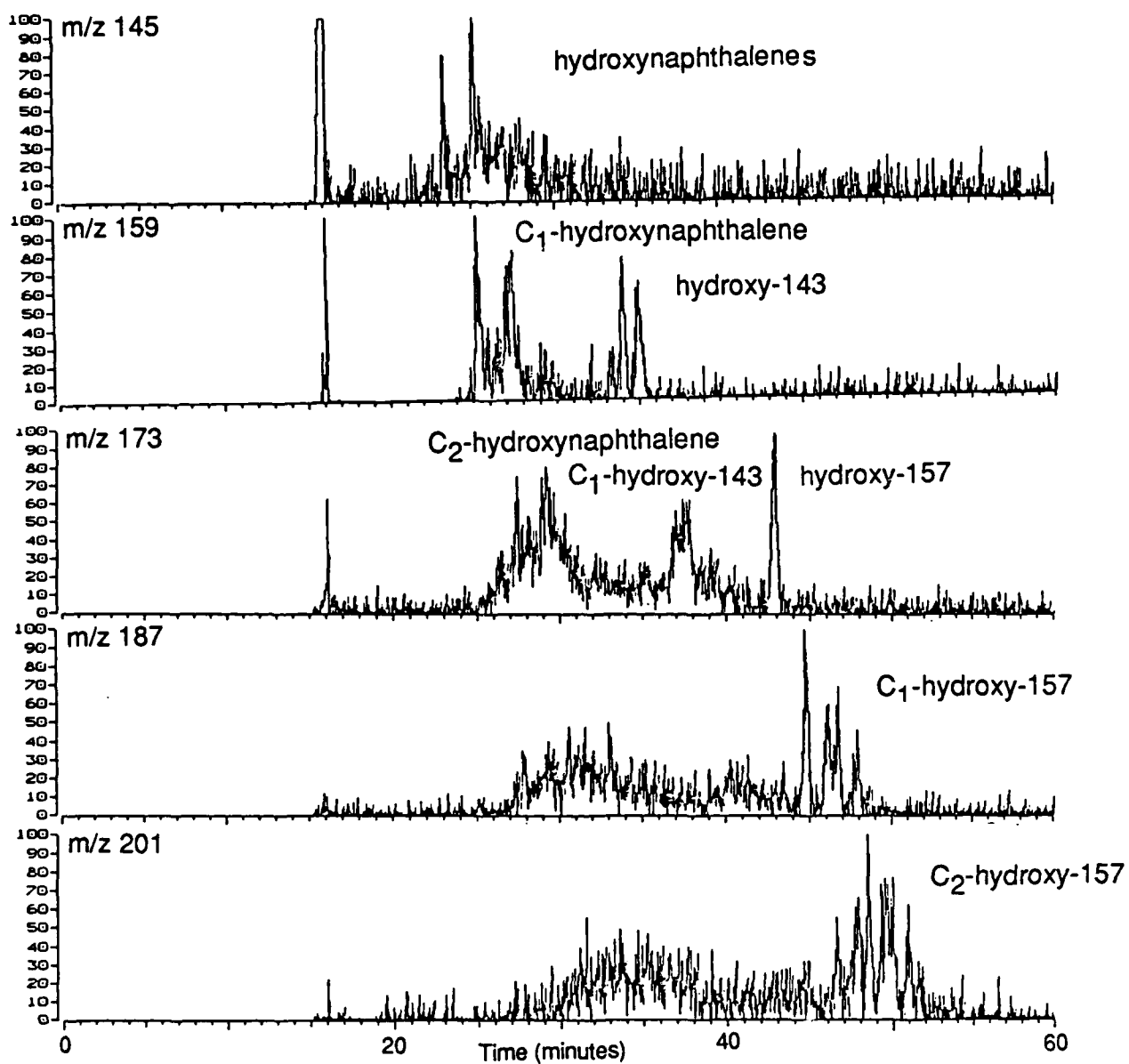
Figure 32.   Single ion plots obtained by SFC-MS of the A-4 fraction of DFM 81-6. The m/z values correspond to $[M+1]^+$ ions.

Two selected ion plots of a parent and a C_1 alkyl homolog are shown in Figure 33. The m/z 132 ions probably arise from a hydroxylated compound, but the information available was insufficient to offer a probable identification.

The ion series shown in Figure 34 beginning with m/z 133, probably arise from hydroxyindenes and their C_1 through C_4 alkyl homologs. Several hydroxyindene isomers exist, which is consistent with the cluster centering around a retention time of approximately 24 minutes. The alkyl homologs at m/z 147, 161, 175, and 189 progressively shift to higher retention times and increase in complexity, which is also consistent with the postulated structural assignments.

Another series of ions beginning with m/z 135 is shown in Figure 35. The m/z 135 ions could arise from either hydroxybenzofurans or hydroxyindans. Two groupings at retention times of approximately 21.5 and 24.5 minutes appear to be present, which could account for both compound series. Peak groupings at m/z 149, 163, 177 and 191 probably correspond to the C_1 through C_4 alkyl substituted parents. The groupings shift to slightly higher retention times and the m/z 149 and 163 clusters show evidence of two envelopes suggesting the alkyl homologs of both parents were present. The m/z 149 ions at higher retention times are from phthalate contaminants.

Another ion series with two potential parent molecules is shown in Figure 36. The m/z 136 ions could correspond to either hydroxyazaindans or hydroxyazabenzofurans. Two envelopes of peaks appear to be present centering around retention times of approximately 21.5 and 24.5 minutes, which suggests both compound types could be present. The m/z 150, 169 and 178 ions probably correspond to the C_1 through C_3 alkyl homologs. Two distinct envelopes can be observed for the C_1 substituted compounds at m/z 150, but the complexity of the C_2 and C_3 ion plots obscure any distinction between potential groupings. The m/z 136 ions could also arise from C_4-pyridines.

The most intense signals detected in the A-4 fraction arise from the ion series shown in Figure 37. The m/z 137 ions undoubtedly arise from C_3 alkyl phenols and the remaining m/z 151, 165, 179, 193, and 207 ions from progressively higher alkylated phenols. The parent phenol and the C_1 and C_2 alkylated phenols were also undoubtedly present, but were not detected because the mass spectrometer was not scanned to low enough masses. A second series
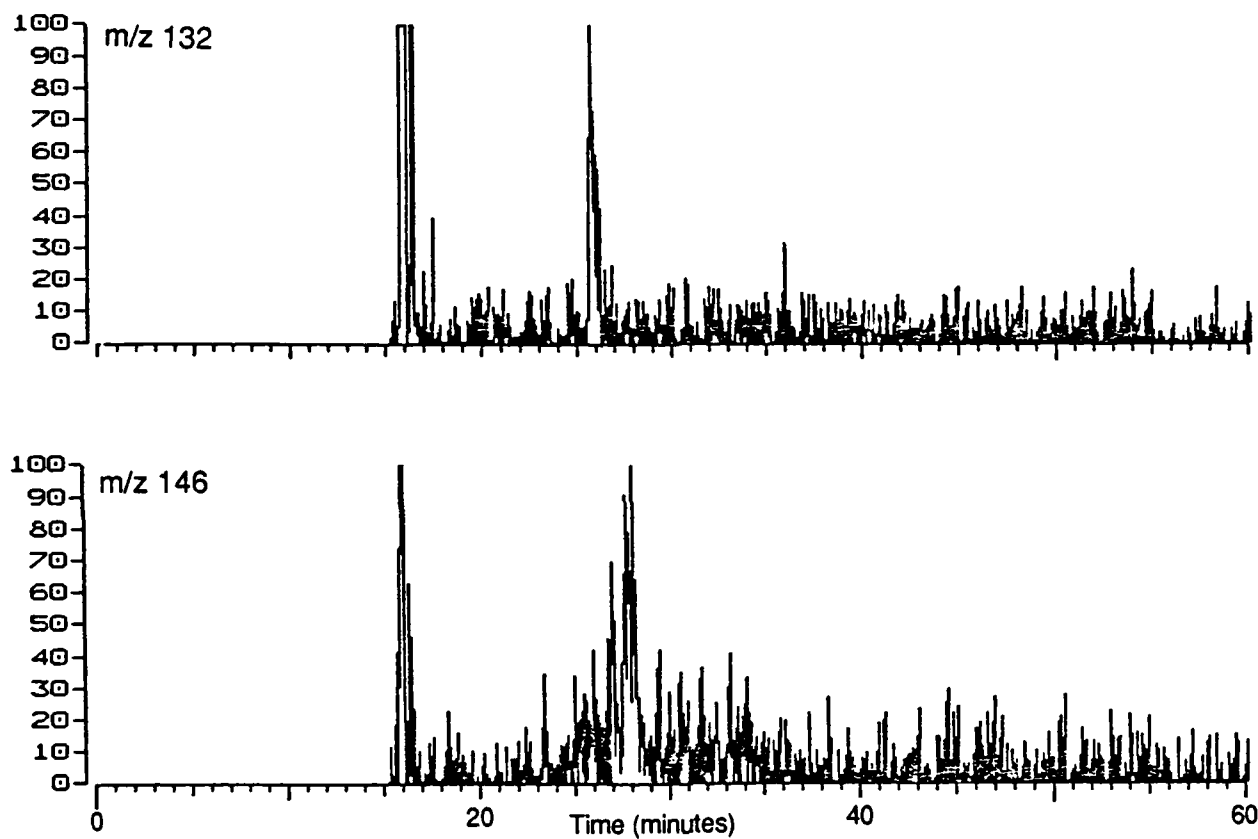
73

Figure 33.   Single ion plots obtained by SFC-MS of the A-4 fraction of DFM 81-6. The m/z values correspond to $[M+1]^+$ ions.
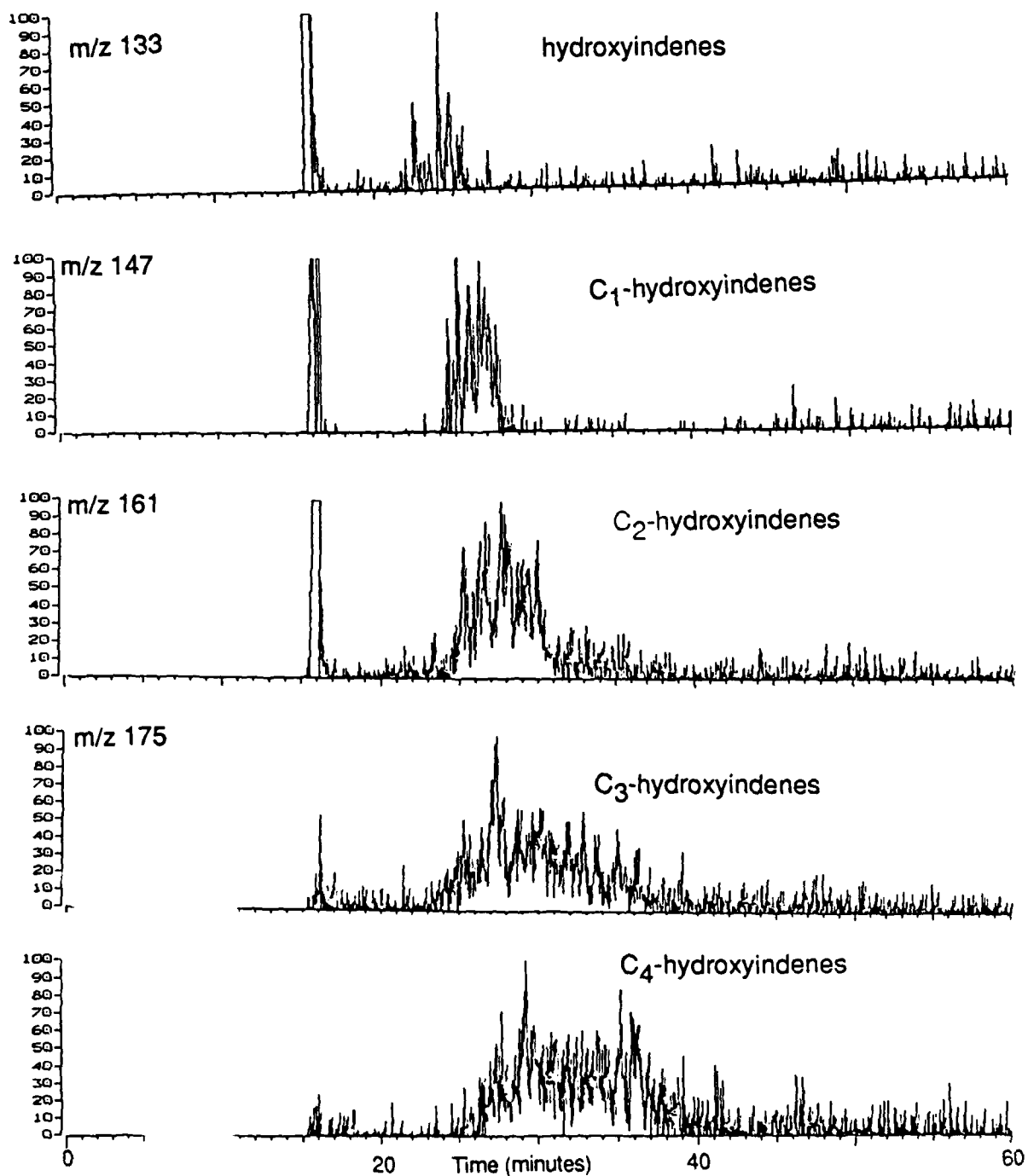
Figure 34. single ion plots obtained by SFC-MS of the A-4 fraction of DFM 81-6. The m/z values correspond to $[M+1]^+$ ions.
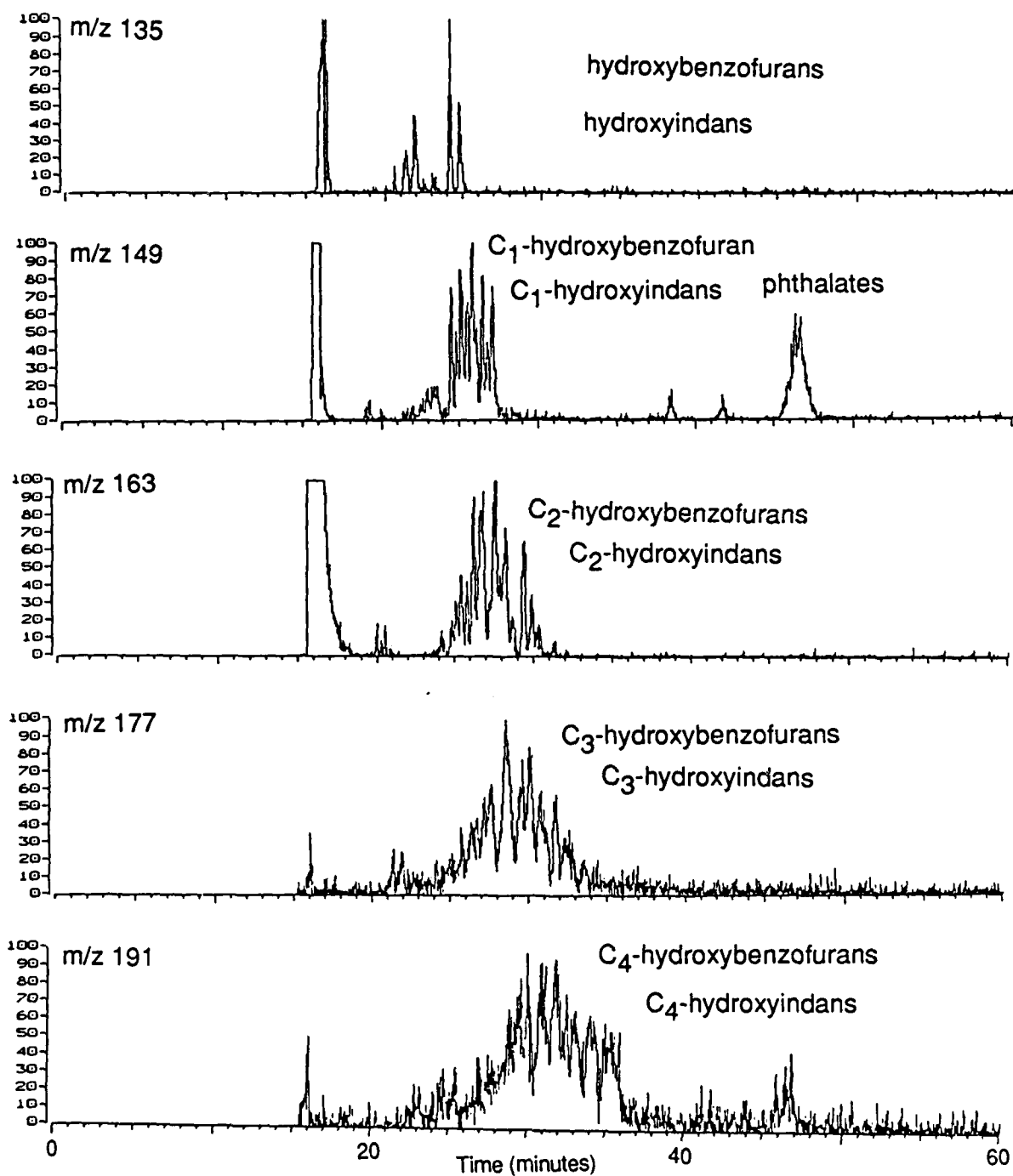
Figure 35.   Single ion plots obtained by SFC-MS of the A-4 fraction of DFM 81-6.   The m/z values correspond to $[M+1]^+$ ions.
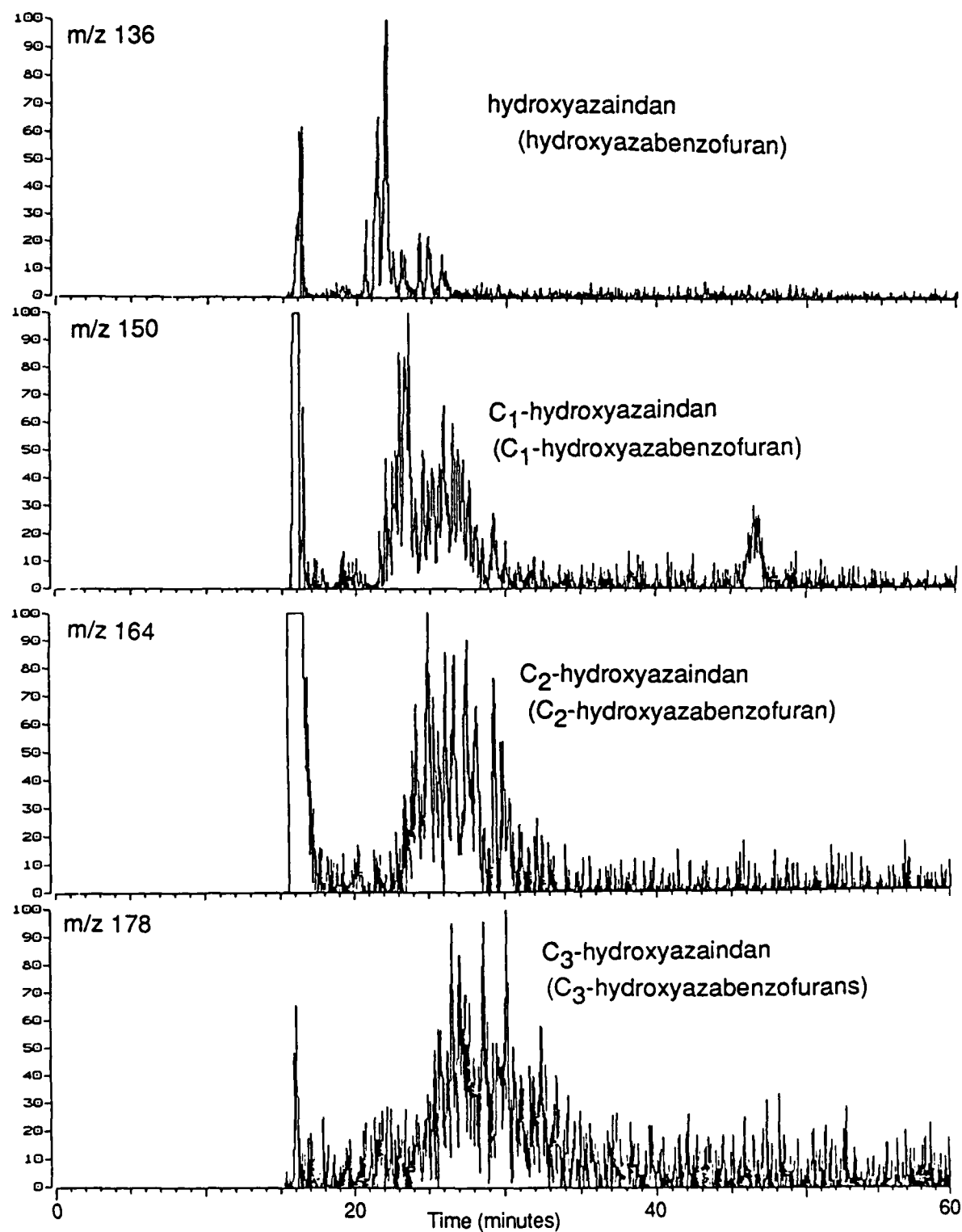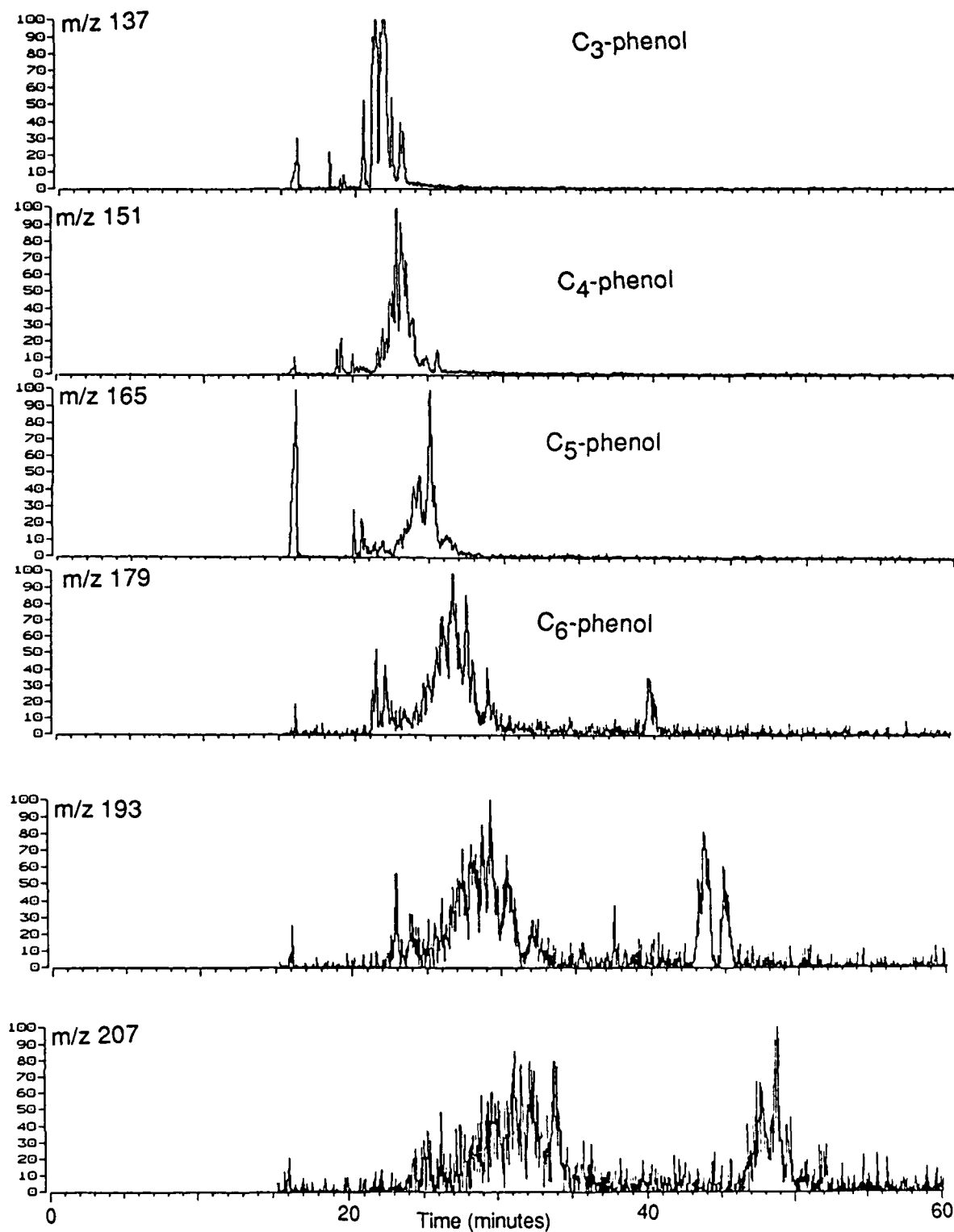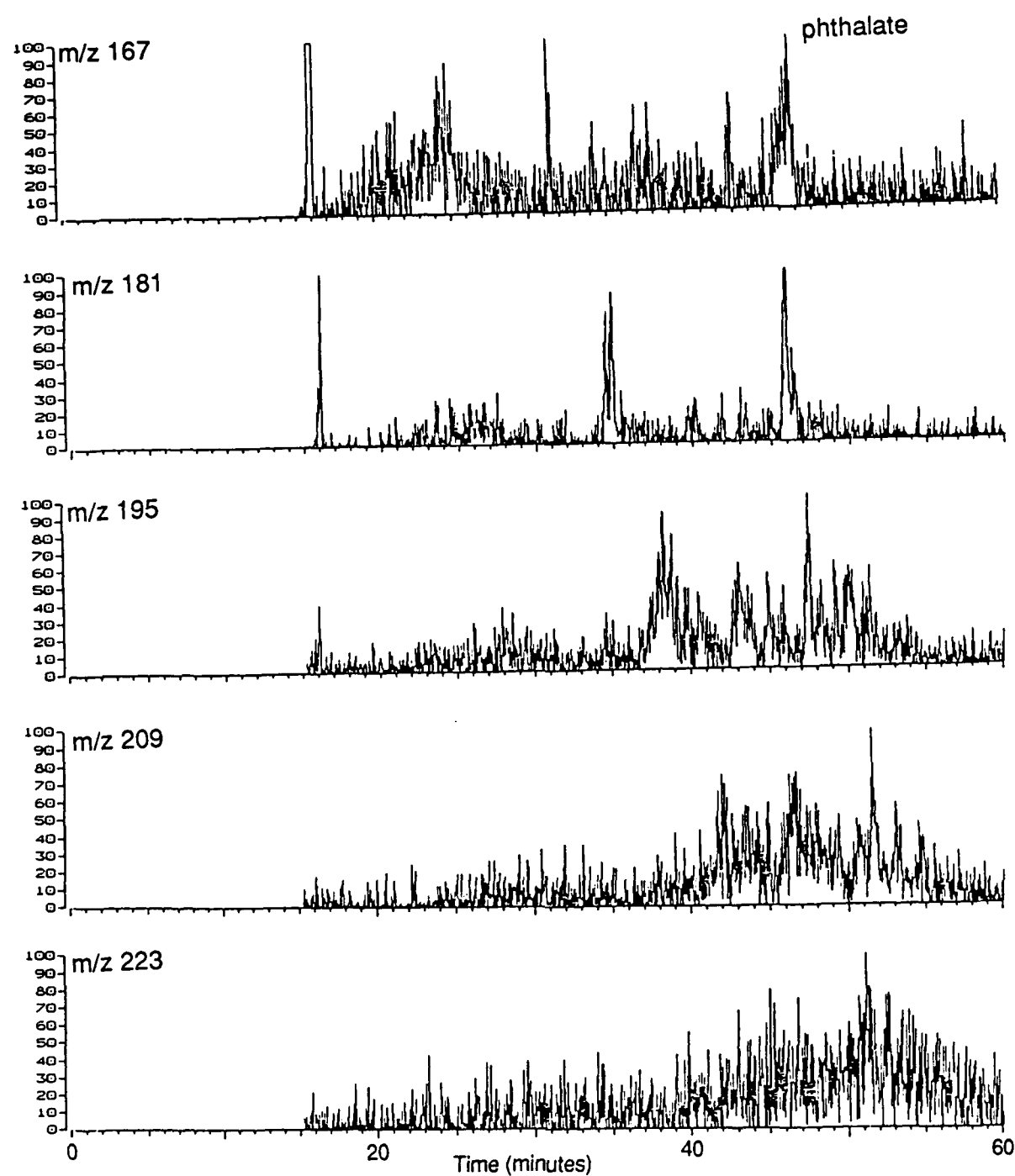
Figure 36.   Single ion plots obtained by SFC-MS of the A-4 fraction of
DFM 81-6. The m/z values correspond to [M+1]$^{+}$ ions.

Figure 37.   Single ion plots obtained by SFC-MS of the A-4 fraction of
DFM 81-6. The m/z values correspond to [M+1]+ ions.

78

of compounds can also be observed beginning at m/z 179 with potential C_1 and C_2 alkyl species evident at m/z 193 and 207, respectively. These compounds could be low levels of neutral PAH (phenanthrene or anthracene) and their alkylated homologs.

Another series of compounds beginning with m/z 167 is shown in Figure 38. The later eluting components in the m/z 167 plot are due to phthalate contaminants, but several peaks and peak clusters are observable at earlier retention times. At m/z 181 two main ion groups can be observed, and it is not clear if they are alkyl homlogs of an m/z 167 parent or if they are parent molecules. The remaining ions (m/z 195, 209, 223) in this series, however, appear to be alkyl homologs of the m/z 181 ions.

A series of ions corresponding to hydroxycarbazoles and alkylated hydroxycarbazoles is shown in Figure 39. The peaks at a retention time of approximately 46 minutes in the m/z 183 plot likely corresponds to hydroxycarbazoles. The C_1 and C_2 hydroxycarbazoles can be observed at slightly higher retention times in the m/z 197 and 211 ion plots, respectively. The alkyl homologs of the unidentified m/z 183 components observed at a retention time of approximately 35 minutes can also be observed in the m/z 197 and 211 ion plots.

The final series of selected ion plots for the A-4 fraction is shown in Figure 40. At least three different compound series can be observed. The first and second series begin with m/z 143 at retention times of approximately 23.5 and 25.5 minutes, respectively. The alkylated homologs for each of these series can be observed at progressively higher retention times at m/z 157, 171, 185, and 199. However, the complexity of the groupings at m/z 157 and 171 do not significantly increase, which could infer that the ions at m/z 143, 157, and 171 are not alkylated homologs. If that were the case, then m/z 171 would be the parent and the C_1 and C_2 alkylatd homologs would be at m/z 185 and 199, respectively. The third ion series begins with m/z 171 at a retention time of approximately 37.5 minutes. The C_1 through C_3 alkylated homologs can be observed at m/z 185, 199, and 213 respectively. These ion series probably corespond to hydroxybiphenyls (m/z 171) and their alkylated homologs.

79

Figure 38.   Single ion plots obtained by SFC-MS of the A-4 fraction of DFM 81-6. The m/z values correspond to [M+1]$^+$ ions.
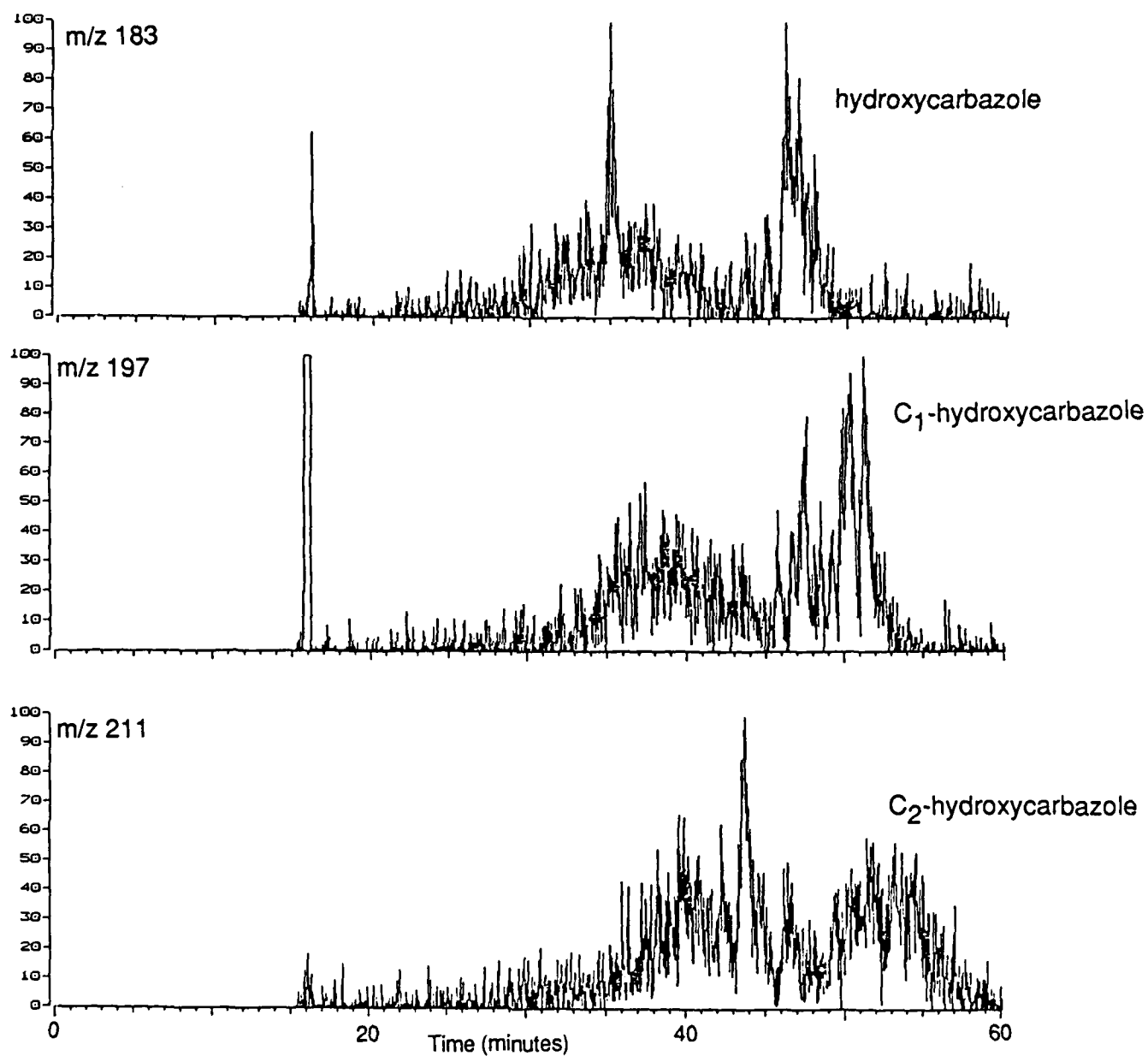
Figure 39. Single ion plots obtained by SFC-MS of the A-4 fraction of DFM 81-6. The m/z values correspond to [M+1]$^+$ ions.
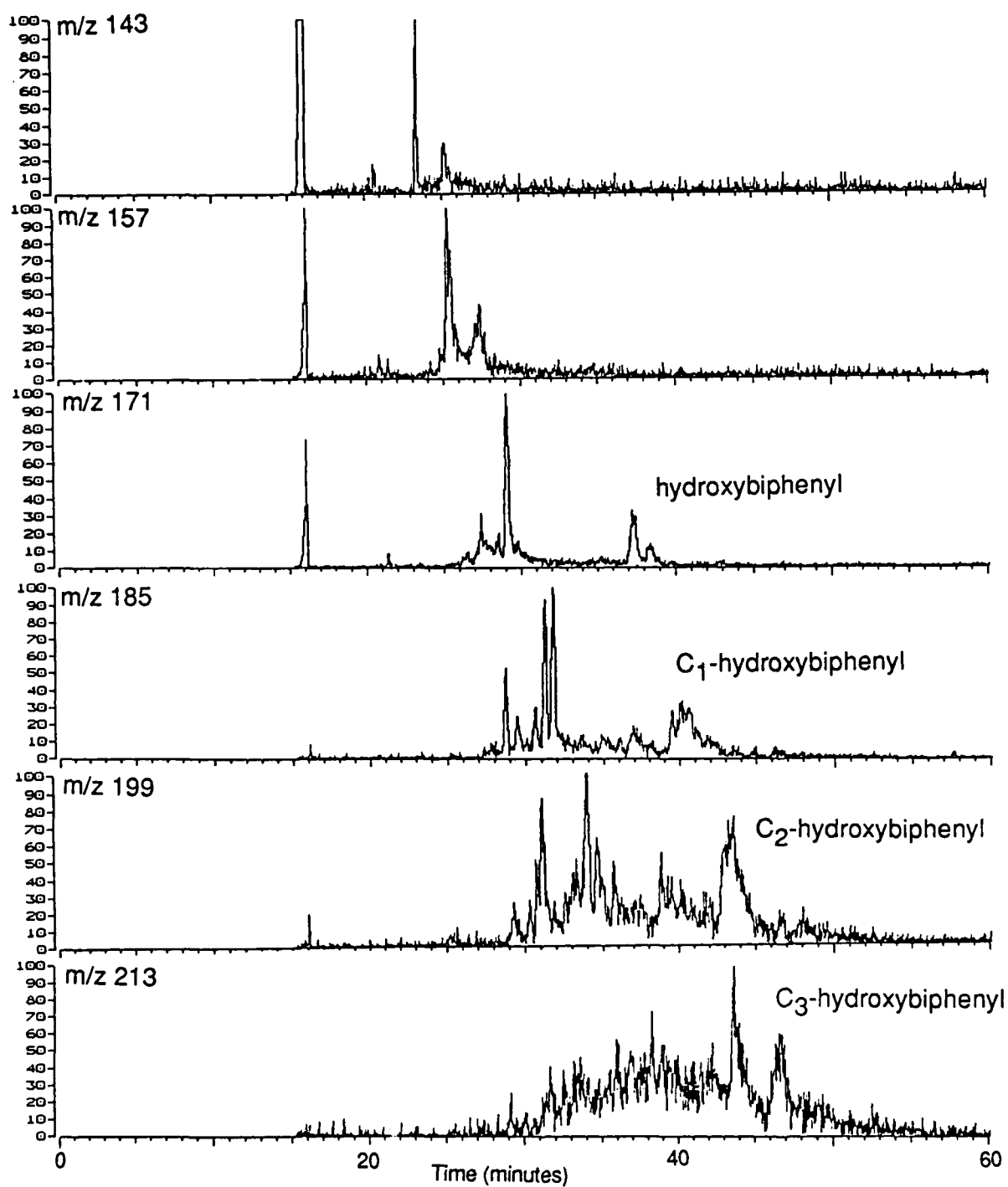
Figure 40.   Single ion plots obtained by SFC-MS of the A-4 fraction of DFM 81-6.   The m/z values correspond to [M+1]$^+$ ions.

Conclusions

Capillary supercritical fluid chromatography and capillary supercritical
fluid chromatography-mass spectrometry were utilized to analyze the polar
fractions from DFM 81-6. Successful SFC required the use of a polar modified
fluid for the chromatographic mobile phase and highly inert capillary columns.
An isopropanol modified carbon dioxide fluid mixture was utilized to provide
sufficient solvating power to elute the polar compounds. Polar fuel fractions
were obtained by alumina adsorption chromatography using chloroform-ethanol
and methanol as eluents to generate two polar fractions.

The SFC and SFC-MS analyses illustrate the complexity of these fuel
fractions in which hundreds of resolved and partially resolved chromatographic
peaks were observed. Hundreds of additional components were resolved from
the complex chromatographic profiles by utilization of the mass selective
detection capabilities of SFC-MS. In addition, probable molecular weight
assignments were possible by SFC-MS. The major components in the A-3 fraction
were alkylated carbazoles. Dozens of other nitrogen and oxygen-containing
heterocycles were also tentatively identified and included parent compounds
such as quinoline, aminanaphthalenes, animoquinolines, benzoquinones,
nitronaphthalenes, indoles, benzanthrones, benzoquinolines, fluorenone,
phenanthrolines, dibenzofuran and azacarbazoles. The matrix was highly
alkylated with all parent molecules showing evidence of up to five alkyl
carbons. Alkylated phenols were the major component identified in the A-4
fraction. Essentially all of the compounds in this fraction were hydroxylated
and many of these were hydroxylated species of the A-3 fraction compounds.
The A-4 compounds were also highly alkylated with evidence of over six alkyl
carbons for certain parent compounds.

To obtain more complete characterization, it would be necessary to
analyze numerous standard compounds to obtain specific retention times and
comparison mass spectra. Additional ionization methods to provide complementary
structural information or the use of tandem mass spectral methods would
also provide helpful information. This work demonstrates the powerful potential
of SFC-MS for the characterization of complex matrices of polar and potentially
labile components. Further gains in the information obtainable from such
studies are anticipated as improvements in sensitivity are obtained (which

would assist in many cases where limited signal-to-noise ratios existed) and as improved fluid and column technologies allow better separations for the more polar fuel components.

TASK D. SUPERCRITICAL FLUID EXTRACTION-MASS SPECTROMETRY OF FUEL SEDIMENTS

Introduction

The storage stability of middle distillate fuels is an important concern. A manifestation of fuel instability is the formation of gums and insoluble sediment material upon aging. These materials can lead to deleterious consequences prior to and during combustion. Extensive work relating chemical properties and fuel instability has been conducted (32-41,44). However, due to the generally intractable nature of the sediment, little success has been achieved in the characterization of this material. An improved understanding of the chemical composition of the sediment matrix may provide valuable insight into better understanding the mechanisms involved in deposit formation and fuel instability.

New analytical methods that exploit the properties of supercritical fluids offer potential advantages for the analysis of intractable fuel sediments. Direct supercritical fluid extraction-mass spectrometry (SFE-MS) allows a sample matrix to be selectively extracted using a high solvating power solvent and directly introducing the extraction effluent into the chemical ionization source of a quadrupole mass spectrometer for continuous on-line analysis (45,46). Tandem mass spectrometry (MS/MS) methods can also be applied to gain additional structural information (47). The advantages of SFE-MS result from the properties of supercritical fluids. These properties were discussed previously in Section C.

This study describes the application of SFE-MS to the analysis of the sediment from an unstable diesel fuel and to sediments formed by stressing fuels doped with additives believed to promote sediment formation.

Experimental

The samples utilized in this investigation included a sediment sample obtained from an unstable diesel fuel and four "model" sediments prepared by adding compounds believed to induce sediment formation (48). Octaethyl-porphyrin was used to verify proper instrument operation and numerous C_1 to C_3 alkyl indoles and alkyl carbazoles, and amino and diaminofluorenes were
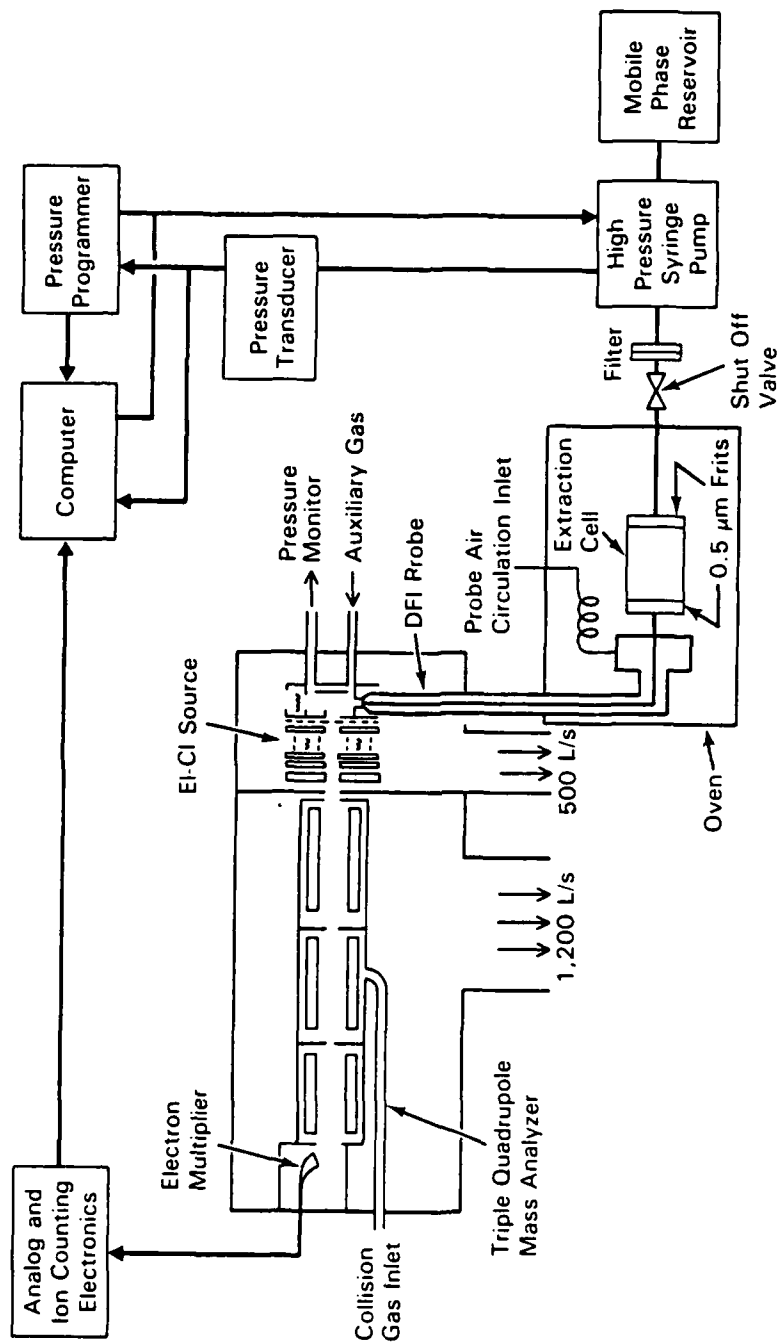
85

Figure 41.   Schematic diagram of the supercritical fluid extraction - mass spectrometry (SFE-MS) instrumentation.

used as standards for the collision-induced dissociation (CID) mass spectrometry studies. Sediment samples were obtained from DFM 81-6 that had been stressed at 80°C for 14 days to accelerate aging (49). Sediment formed during storage at 4°C was also utilized. The model sediments were generated by adding various pyrrole compounds to shale-derived middle distillate fuels followed by stressing at 80°C for 14 days to induce sediment formation. The sediments were designated NRL-1 through NRL-4, and 2,4-dimethyl-3-ethyl-pyrrole, 2,5-dimethylpyrrole and t-butylhydroperoxide, 2,3,4,5-tetramethy-pyrrole, and dimethylpyrrole were doped into separate fuel samples, respectively, to induce sedimentation.

Several fluids were utilized for supercritical fluid extraction-mass spectrometry of the sediment materials. Pure fluids included high-purity pentane (Burdick and Jackson) and nitride grade anhydrous ammonia (Airco). Mixed fluid systems were also utilized and included a 5% (v/v) (13 mole %) methanol in pentane mixture and a 5% (v/v) (7 mole %) isopropanol in pentane mixture. The ammonia was filtered and redistilled during transfer to the syringe pump.

The instrumentation for supercritical fluid extraction-mass spectrometry (SFE-MS) has been described previously (45,46,50). A schematic diagram of the system is shown in Figure 41. The system included a modified syringe pump (Varian, Model 8500) for a pulse-free flow of high pressure fluid and a gas chromatograph oven to maintain the extraction cell at the desired temperature. The extraction cell design was based on a 1/4" to 1/16" reducing LC column end fitting (Swagelok SS-400-6-1ZV) containing two stainless steel frits (0.5 μm) and a stainless steel spacer ring to define the cell volume (approximately 50 μL). The cell volume could be reduced by inserting a stainless steel slug into the spacer ring. High pressure fluids were supplied to the cell through 1/16" stainless steel tubing with an in-line 0.2 μm filter. Connection to the sample cell was made by silver soldering the 1/16" tube inside a length of 1/4" o.d. high pressure tubing. This design allowed the fluid supply connection to be changed between samples or fluids to avoid cross-contamination. Transfer lines to connect the extraction cell to the mass spectrometer were either one meter lengths of 50 μm i.d. fused silica capillary tubing (deactivated using hexamethyldisilazane and chlorotrimethylsilane) for pentane and modified pentane fluids, or 100 μm

87

i d. platinum-iridium tubing for ammonia. For the fused silica transfer
lines, a short (35 - 50 mm) length of 8 μm i.d. fused silica capillary wa
used as a pressure restrictor to regulate fluid flow rate. For ammonia
extractions the exit end of the platinum-iridium transfer tubing was crimped
to obtain the desired flow rate. In an effort to aid heat transfer when
using fused silica restrictors (51), the polyimide coating of the capillary
was removed and the fused silica etched with hydrofluoric acid to decrease
the thickness of the capillary walls. A similar approach using restrictors
reproducibly drawn (tapered) from lengths of larger diameter (25 μm) fused
silica tubing (52) was also utilized. Constant temperature ($\pm$0.5°C) condi-
tions were maintained along the transfer line to the point of injection
using an air heated direct fluid injection (DFI) probe assisted by an auxil-
iary electrical heater.

The DFI probe tip allowed heating of the pressure restrictor independent
of the oven DFI probe, and ion source (51) to aid in transport of nonvolatile,
higher molecular weight species. This was accomplished by inserting the
restrictor into a short length of resistively heated stainless steel hypo-
dermic tubing with a slightly larger i.d. than the o.d. of the fused silica
capillary restrictor. The length of the heated region was <10 mm and the
flow restrictor was positioned slightly back from the exit of the steel
tube to insure location in the heated region. Thermal insulation of the
restrictor from the transfer line was provided by a void space and a ceramic
cement plug. The hypodermic tubing could be heated to greater than 600°C.
The optimum temperature of this region might be anticipated to increase for
less volatile compounds with exact conditions depending upon the design of
the restrictor and the amount of cooling produced during expansion of the
supercritical fluid (51). The temperature of this region was varied between
source temperature (approximately 125°C) and the maximum. Generally, best
results are obtained at moderately high restrictor heater temperatures where
pyrolysis is negligible (due to fluid cooling) and discrimination effects
are minimized.

The entire effluent from the DFI transfer line was injected into the
CI region of an Extranuclear Laboratories (Pittsburgh, PA) "simultaneous"
dual EI-CI source and mass spectra obtained using an Extranuclear triple
quadrupole mass analyzer. The instrument was operated under "typical" chem-

ical ionization (CI) source operating conditions (low repeller fields, 0.2-1 torr pressure). CI reagent gases were methane, isobutane, n-pentane and ammonia. To obtain collision-induced dissociation (CID) spectra (47), the second quadrupole was enclosed and operated in the RF only mode to act as a collision cell, with argon employed as the target gas. A collision energy of 40 eV was used with ~60-70% attenuation of the parent ion signal. The mass spectrometer was controlled and the data collected with a Teknivent Corp. (St. Louis, MO) data system.

Supercritical extractions were performed on small amounts (<100 μg) of each sediment material. Chemical ionization mass spectra were continuously recorded as the pressure of the supercritical fluid was increased. Analyses were preceded by "blank" experiments which also served to condition the sample cell and transfer line. The pressure of the supercritical fluid solvents was ramped during extraction to gradually increase the solvating power and achieve selective solvation of the solutes. For pentane and modi-fied pentane extractions, pressure ramp rates of 0.5, 1.0 and 2.0 bar/min, from approximately 30 bar to 90 bar were generally used. Pressure ramp rates of 1 and 5 bar/min from 100 or 150 bar to 415 bar were used for ammonia extractions. Collision-induced dissociation (CID) studies of model compounds were performed following isobaric transport using liquid ammonia at 100 bar. Temperatures for the extractions were 205°C (T_r = 1.02), 210°C (T_r=1.03) and 230°C (T_r=1.04) for pentane; 150°C (T_r=1.04) and 175°C (T_r=1.10) for ammonia, and 215°C for pentane-methanol fluids and 230°C for pentane-isopropanol mixtures.

Results and Discussion

DFM 81-6 Sediment

Several supercritical fluid systems were utilized to extract the DFM 81-6 sediment. Initially, a methanol and isopropanol modified pentane mix-tures were evaluated due to their expected high solvating properties, but due to the formation of significant chemical ionization artifacts (complex adduct ions, etc. and significant background across an extended mass range), these fluid mixtures were discontinued. Pure pentane was next evaluated for extraction of the sediment material. Although, only small amounts (~

25%) of the sediment appeared to be soluble in supercritical pentane, meaningful mass spectra could be acquired. Examples of typical spectra obtained during supercritical pentane extraction of the sediment are shown in Figure 42. An extraction temperature of 230°C and methane chemical ionization were utilized. The spectrum shown in Figure 42A was acquired early in the analysis when the fluid pressure was 31 atmospheres and the spectrum shown in Figure 42B was acquired later in the analysis when the pressure was at 53 atmospheres. Two envelopes of major ions are observable in both spectra with the first envelope (m/z 132, 146, 160, and 174) more intense at the lower pressure, and the second envelope (m/z 182, 196, 210, and 224) more intense at the higher pressure. The first envelope of ions probably correspond to $(M+1)^+$ ions of alkylated indoles and the second envelope of ions to $(M+1)^+$ ions of alkylated carbazoles (e.g., m/z 132 = C_1 -indole and m/z 182 = C_1-carbazole). The alkyl indoles were more soluble at lower pressures than the carbazoles and generated a more intense signal. Later in the analysis when the pressure was higher and the carbazoles were more soluble, the alkyl indoles were partially exhausted from the sample as evidenced by their lower intensity ions. In addition to the alkyl indoles and alkyl carbazoles, an envelope of low intensity ions extending to a mass of approximately 350 dalton was observable. No specific compound identifications could be made from these ions in the absence of an additional dimension of selectivity (such as obtained by SFC-MS or MS/MS).

Since alkyl indoles and carbazoles are soluble in typical organic solvents, it is somewhat surprising that supercritical fluid extraction was necessary to remove them from the sediment matrix. (The sediment had been extensively washed with methylene chloride prior to extracton). This suggests that these components were trapped within or were highly associated with the sediment matrix. Supercritical pentane extraction of sediment material that had only been rinsed with methylene chloride yielded extensive contributions from the residual fuel as evidenced from the mass spectrum shown in Figure 43. This spectrum was acquired later in the extraction after many of the more soluble fuel components had been partially exhausted. The m/z 157, 171, 185, and 199 ions can probably be attributed to either aliphatic hydrocarbons or alkylated naphthalenes. Only low intensity ions were observed that could be attributed to the sediment material.
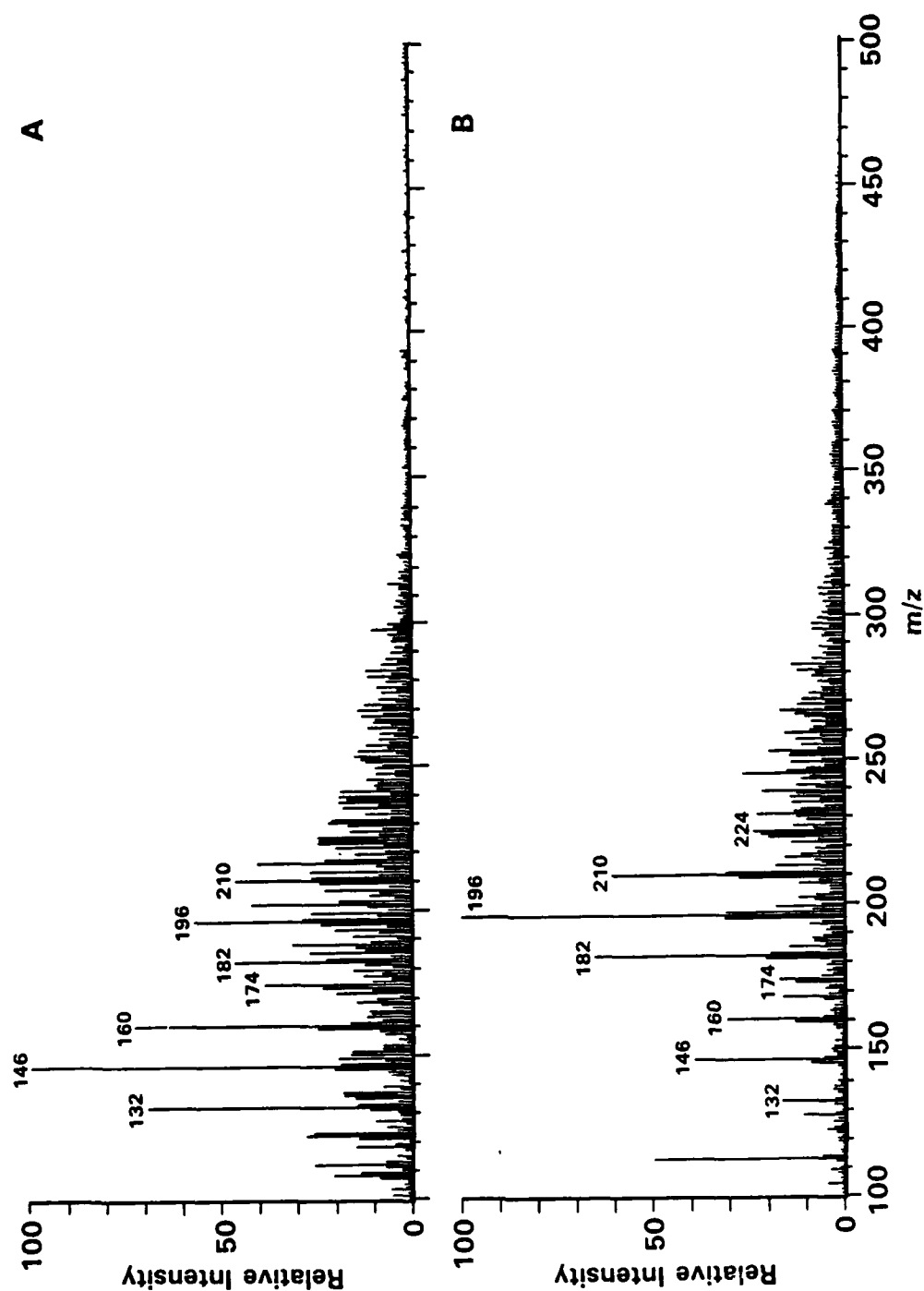
Figure 42. Methane chemical ionization mass spectra of DFM 81-6 sediment obtained during supercritical pentane extraction at 230°C and progressively higher pressures of 31 atmospheres (A) and 53 atmospheres (B) utilizing a 350°C restrictor.
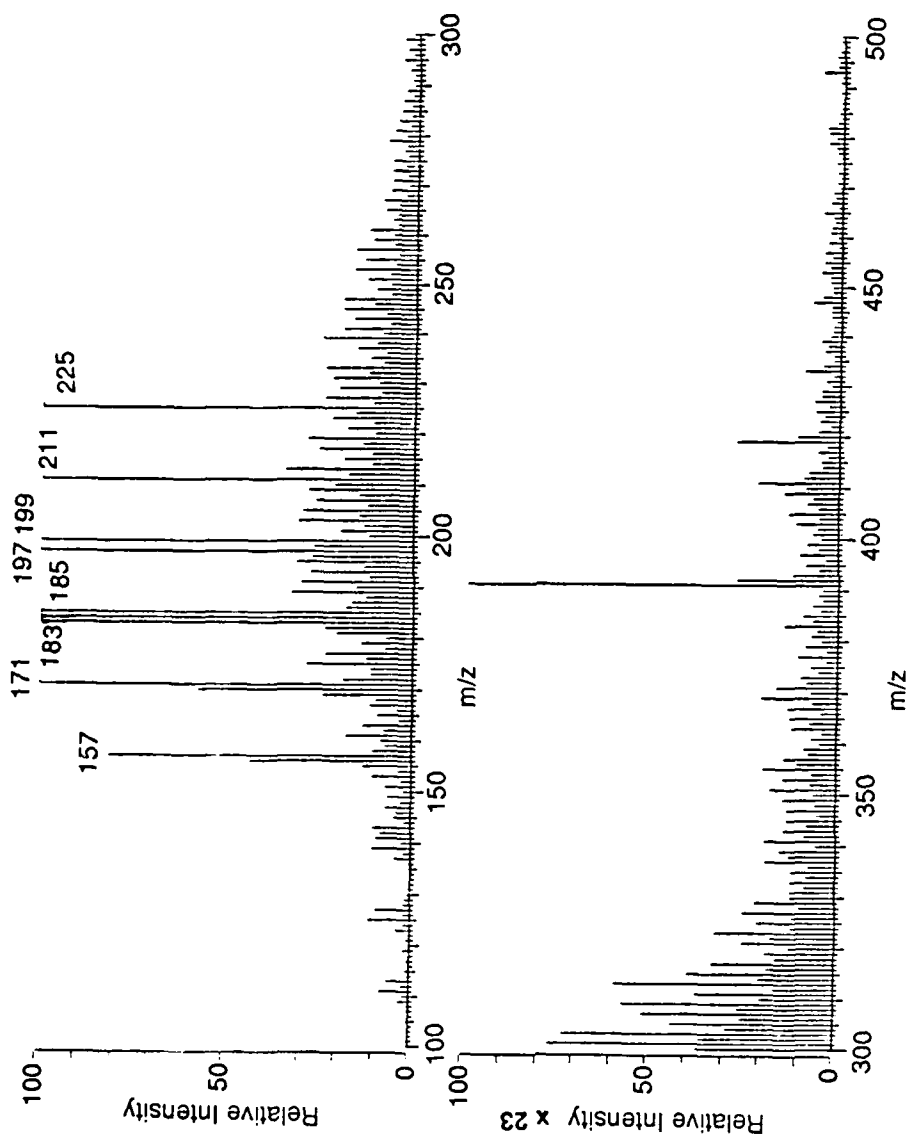
Figure 43. Methane chemical ionization mass spectrum of DFM 81-6 sediment containing residual fuel obtained during supercritical pentane extraction at 210°C and 35 atmospheres utilizing a 350°C restrictor.

Since only ions of any significant abundance up to masses of approximately 350 dalton were observed, and only a small fraction of the sediment was depleted after several hours of extraction with pentane, supercritical ammonia extraction was also utilized. Much higher solvating powers and higher extractability for polar components would be expected to be achieved with supercritical ammonia. As anticipated, much greater material was extracted with essentially 95% (or greater) of the sediment depleted after extraction for less than an hour. A mass spectrum obtained during supercritical ammonia extraction of the sediment is shown in Figure 44. Similar ion envelopes corresponding to the alkyl indoles and aklyl carbazoles were also observed in this extraction spectrum. Since the proton affinities of these compounds are similar to that of ammonia, protonated molecules $(M+1)^+$, were formed with ammonia chemical ionization. A major concern of using ammonia as an extraction fluid was the possibility for reaction with the matrix. However, since essentially the same spectrum was obtained with supercritical ammonia extraction as was obtained with supercritical pentane extraction, it is unlikely that any significant reactions occurred with the sediment matrix. Unfortunately, however, only the same limited mass range of ions were obtained with ammonia extraction. This was surprising considering the much higher solubility of the sediment matrix in supercritical ammonia. Although the spectrum shown in Figure 44 was obtained with an extraction pressure of only 166 atmospheres, extraction at higher pressures (up to 420 atmospheres) did not significantly change the molecular weight range of the extracted components.

One explanation of this behavior (only low molecular weight components detected) could be that only low molecular weight materials were present in the sediment, but highly associated and tightly bound to create an intractable matrix. Another explanation could be that the higher molecular weight components were thermally decomposed during transport of the extraction effluent to the ion source. The restrictor in the MS interface is typically heated to 350°C or greater to aid the transport of molecules of lower volatility to the gas phase for subsequent ionization. This possibility was tested by extracting a higher molecular weight compound and changing the restrictor temperature during the extraction. A relatively labile compound, octaethylporphyrin, molecular weight 534, was utilized for this experiment. Examples
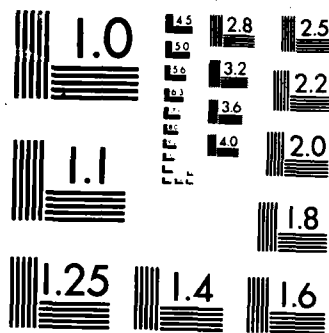
MICROCOPY RESOLUTION TEST CHART
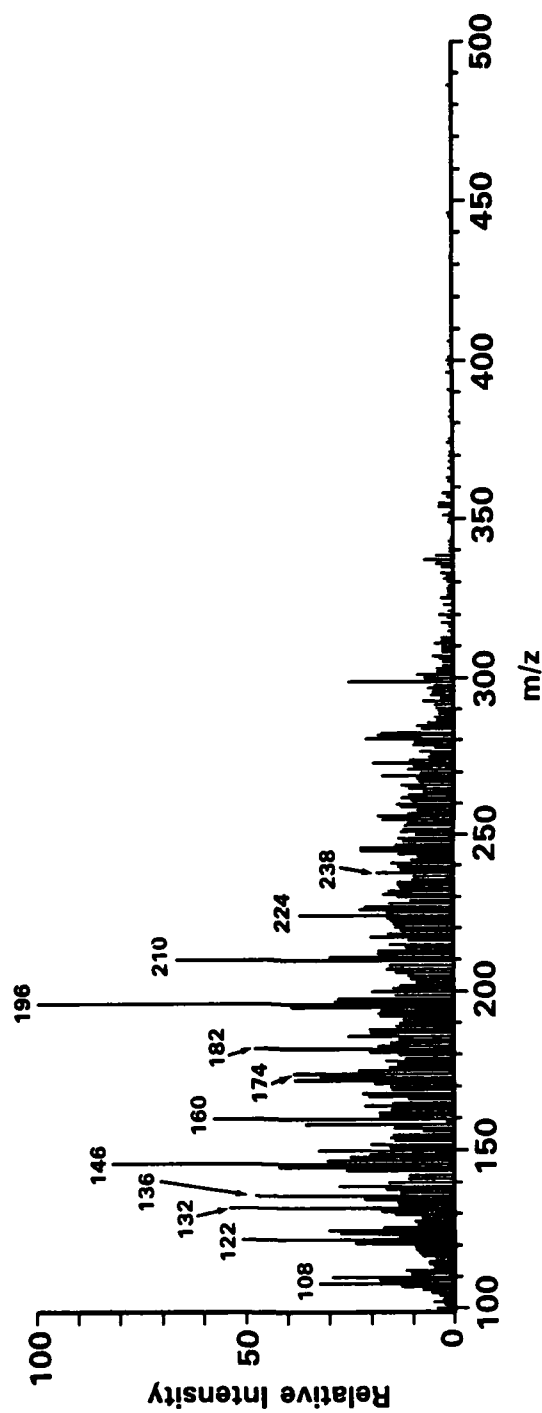
NATIONAL BUREAU OF STANDARDS-1963-A

Figure 44. Ammonia chemical ionization mass spectrum of DFM 81-6 sediment obtained during supercritical ammonia extraction at a 150°C and 166 atmospheres utilizing a 350°C restrictor.

94

of spectra obtained during supercritical ammonia extraction are shown in Figure 45. The upper spectrum, obtained with a cooler 300°C restrictor, shows an intense protonated molecular ion, $(M+1)^+$, and low relative abundances of fragment ions of low mass. In the lower spectrum, obtained at a higher restrictor temperature of 350°C, the protonated molecular ion could no longer be detected and greater relative abundances of low mass ions were obtained suggesting that thermal degradation of the compound occurred. This behavior was reproducible and the different characteristic spectra could be obtained repeatedly by changing the temperature.

Consequently, the sediment was again subjected to supercritical ammonia extraction, but with a cooler restrictor. Averaged mass spectra obtained under these conditions are shown in Figure 46. For the lower spectrum the mass spectrometer ion source had been retuned and the resolution decreased slightly (to ~400) to give more sensitive detection at higher m/z. Again, the ion envelopes corresponding to the alkyl indoles and alkyl carbazoles were observable, but, in addition, significant ion contributions up to a mass of 850 dalton were also present. The upper mass limit for the quadrupole mass analyzer was approximately 900 dalton, otherwise, higher molecular weight material would undoubtedly have been detected. The major ion clusters occurred at 14 dalton intervals indicating a highly alkylated matrix. Evidently, the higher molecular weight components (greater than 350 dalton) were very thermally sensitive, since they were essentially totally decomposed by the sub-second contact with the higher temperature restrictor.

Another set of spectra obtained during supercritical ammonia extraction of the sediment are shown in Figure 47. These spectra were obtained at progressively higher ammonia pressures and illustrate the increasing molecular weight range of components that were solvated at higher solvating power fluid conditions. At a pressure of 350 atmospheres only components up to mass 550 were extracted. At 400 atmospheres the mass range extended to over 600 dalton and at 415 atmospheres components up to the upper mass limit of the mass spectrometer were observed. Essentially, the same spectral profile was obtained for the sediment in this extraction as was obtained for the extraction shown in Figure 46.
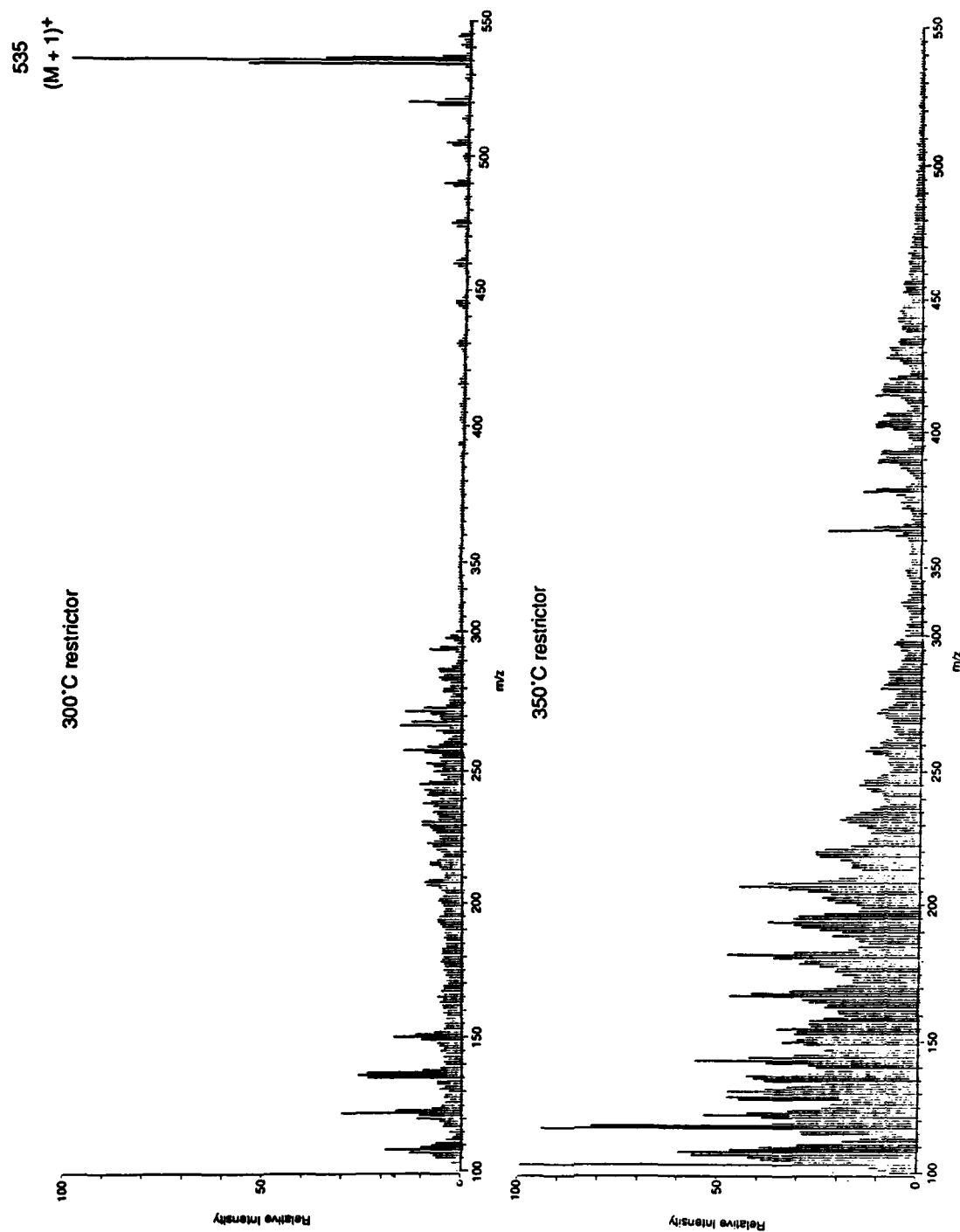
95

Figure 45. Ammonia chemical ionization mass spectra of octaethylporphyrin obtained during supercritical ammonia extraction at 150°C and 250 atmospheres with a 300°C restrictor (top) and a 350°C restrictor (bottom).
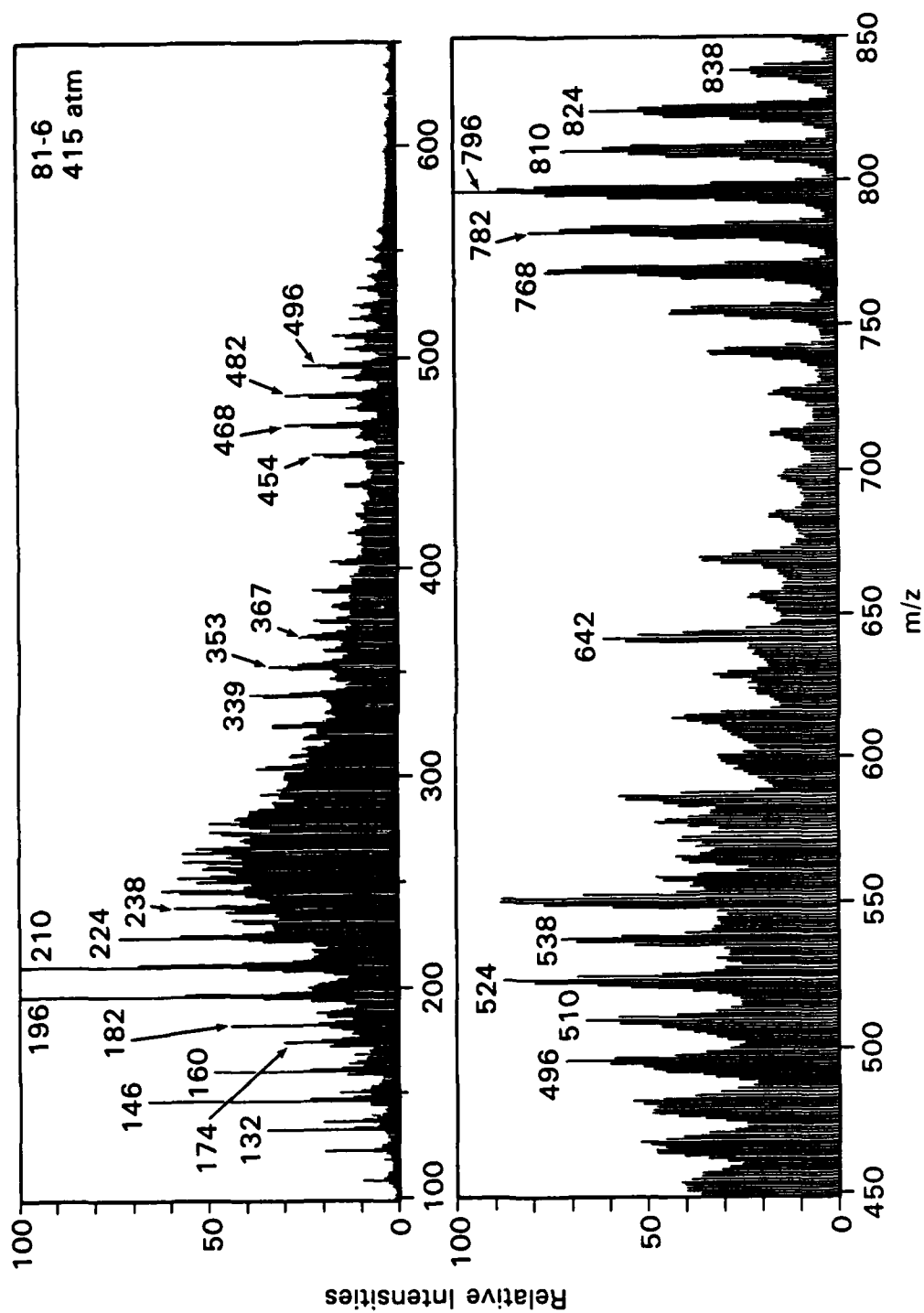
Figure 46. Ammonia chemical ionization mass spectra of DFM 81-6 sediment obtained during supercritical ammonia extraction at 150°C and 415 atmospheres with a 300°C restrictor. Lower spectrum obtained at lower resolution to achieve higher sensitivity at higher m/z.
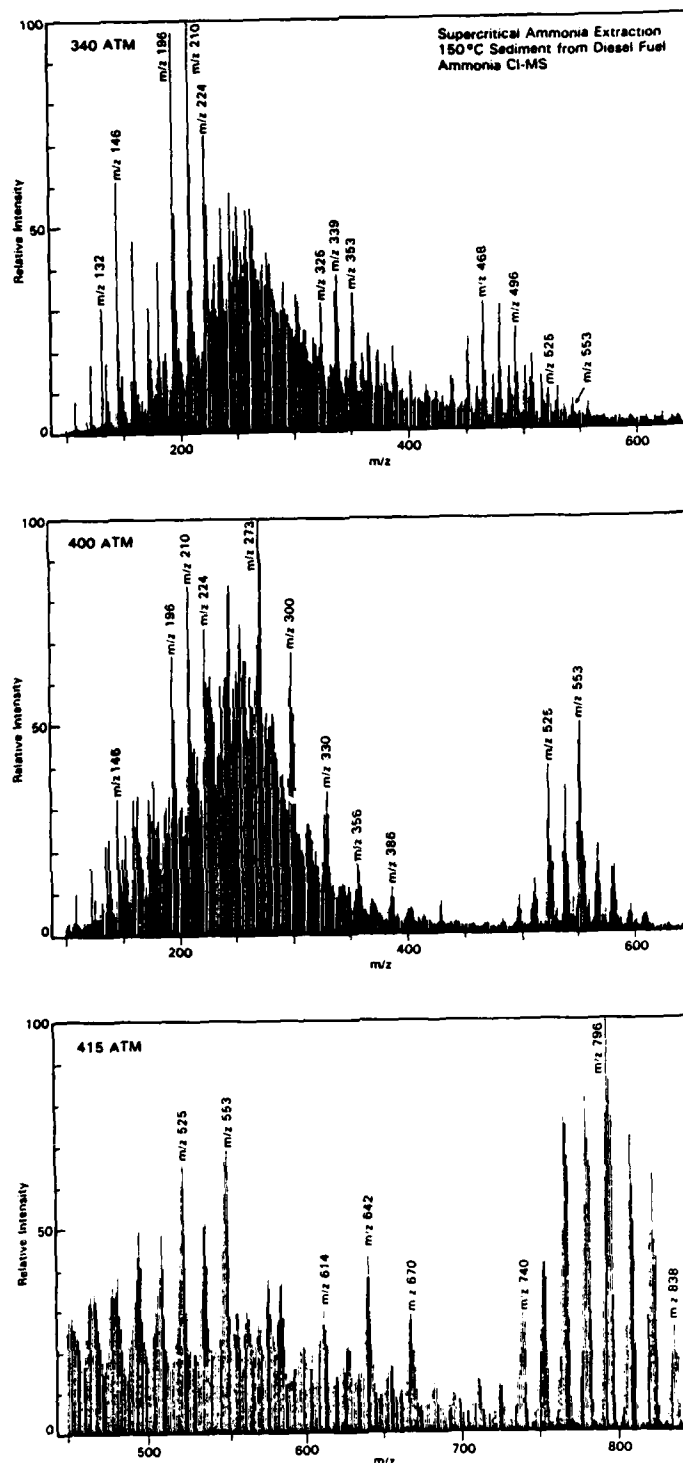
Figure 47.   Ammonia chemical ionization mass spectra of DFM 81-6
              sediment obtained during supercritical ammonia extraction at
              150°C and three progressively higher pressures of 340
              atmospheres (top), 400 atmospheres (middle), and 415
              atmospheres (bottom) with a 300°C restrictor.

98

Since much higher molecular weight material could be observed in the supercritical ammonia extractions when using a cooler restrictor temperature, the sediment was re-examined by supercritical pentane extraction using the milder restrictor temperature. The resulting methane chemical ionization mass spectrum is shown in Figure 48. The alkyl indole and alkyl carbazole ions were again the major ions, but the other lower intensity ions only extended to an upper mass of approximately 400 dalton. In fact, this extraction spectrum is nearly identical to that obtained when the higher temperature restrictor was used (see Figure 42). Consequently, it can be concluded that only the lower molecular weight (up to approximately mass 350) components of the sediment were soluble in supercritical pentane and that very few of these components were as thermally sensitive as the higher molecular weight components extracted by supercritical ammonia. The higher molecular weight components, however, could have increased thermally sensitivity in supercritical ammonia.

An interesting observation can be made about the ammonia chemical ionization mass spectra from the DFM 81-6 sediment extract. In the region between about m/z 440 and m/z 600, along with the 30-50% relative intensity (Figure 46) ions, there is a second series of ions at (10-15% relative intensity), that are also spaced at 14 dalton increments. Ions in this lower intensity series occur 6 dalton lower than the higher intensity ions. These series of ions are more readily apparent in Figure 49. The difference of 6 dalton coincides with chemical ionization of naturally occurring porphyrins (macrocyclic tetrapyrroles), using ammonia, hydrogen and methane as chemical ionization reagents (53-57). In the case of the porphyrins, the 6 dalton difference corresponds to reduction of the porphyrin ring to the related porphyrinogen with incorporation of 6 hydrogen atoms. The porphyrinogens fragment more readily than the parent porphyrins to yield mono-, di- and tripyrroles. This reaction is found to occur for both metallated and nonmetalled porphyrins (56). Whether the structure of these undetermined components of the diesel fuel sediment resembles substituted porphyrins or an oligomeric chain of pyrroles, and if a similar hydrogenation mechanism is operable during ionization of the extracts remains unknown. It should be noted that some of the lower molecular weight ions in the mass spectra from the sediment extract have the same nominal molecular weight as monopyrrolic fragments of
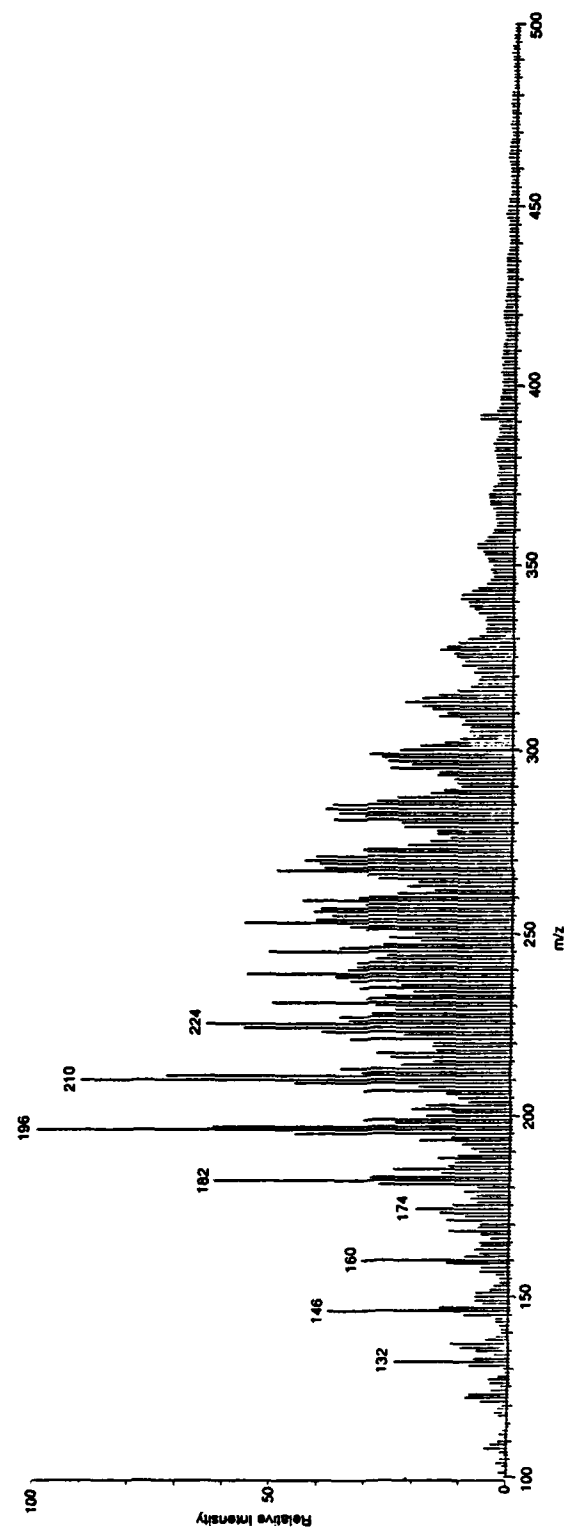
99

Figure 48.   Methane chemical ionization mass spectrum of DFM 81-6 sediment obtained during supercritical pentane extraction at 210ºC and 50 atmospheres with a 300ºC restrictor.
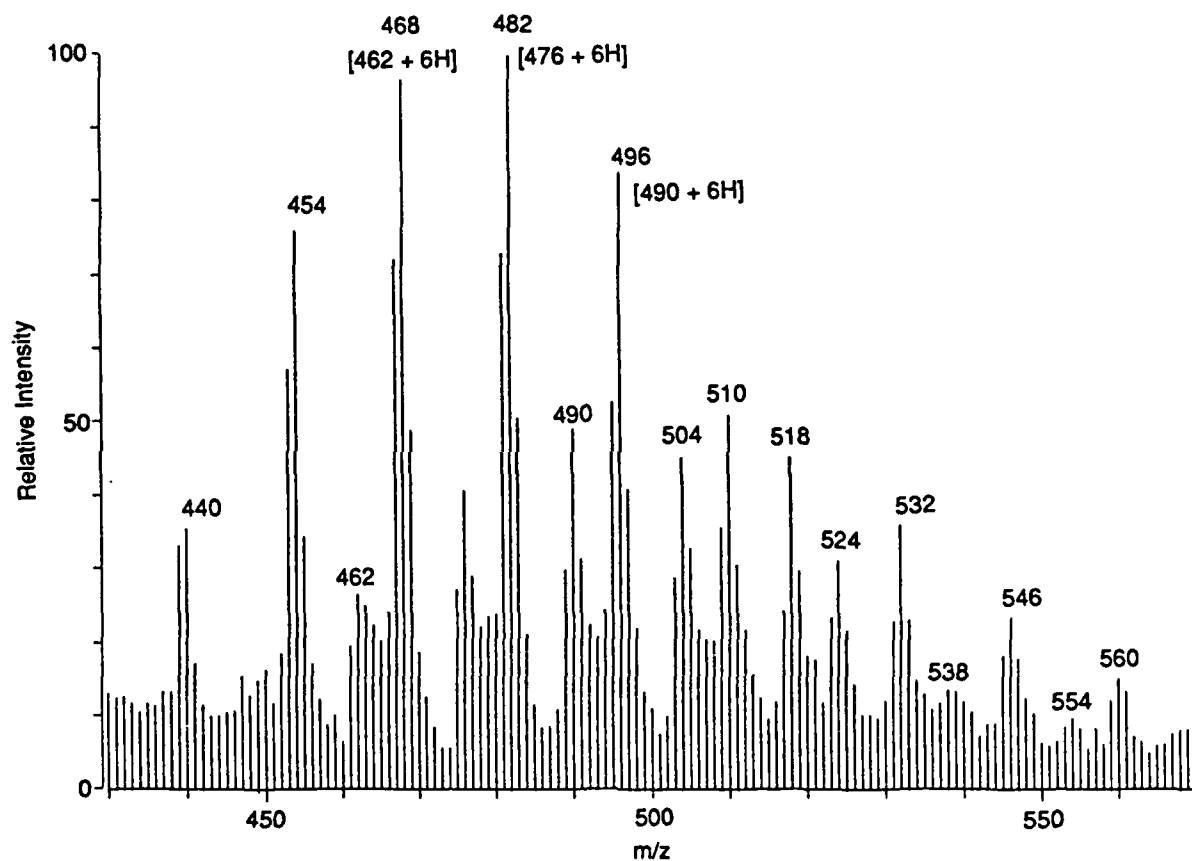
100

Figure 49.   Portion of ammonia chemical ionization mass spectrum of DFM
             81-6 sediment obtained during supercritical ammonia
             extraction at 150°C and 415 atmospheres with a 300°C
             restrictor.

porphyrins. Porphyrin and porphyrinogen-like and pyrrole polymer structures can be postulated with molecular weights corresponding to those found in the mass spectra of the sediment extract. Since the sediment material (and residual fuel) contained only approximately 0.5% (by weight) (non fuel containing sediment could contain up to 1-1.5%) elemental nitrogen, the sediment matrix could not consist entirely of pyrrole-like structures, but would also have to contain numerous alkyl groups and other non-nitrogen containing molecules. It is also interesting that octaethylporphyrin exhibited a similar restrictor temperature sensitivity, (e.g., no high molecular weight or parent ion production at high restrictor temperatures) as was observed for the sediment extract during SFE-MS.

Collision Induced Dissociation (CID) Tandem Mass Spectrometry

In an effort to further identify the more abundant components in the DFM sediments, collision induced dissociation (CID) (47) experiments were conducted during supercritical fluid extraction. The SFE-MS instrumentation, when coupled with a triple quadrupole analyzer mass spectrometer, allows this type of experiment to be performed on-line, while recording a mass specrtrum of the entire extract effluent. The information obtained in CID studies is also useful in determining the relationship of ions in the complex extract mass spectra (e.g., parent-daughter, homologous ion series, etc.). CID mass spectra can also be used to distinguish types of substitution on larger molecules (alkyl, amino, hydroxyl, etc.), degree of alkyl substitution, and type of bond broken during the CID process (strong, covalent bond yielding low intensity fragments versus weak, associative bond, such as found in an ammonium or alkyl adduct ion). This latter type of information is useful in determining if species found during supercritical fluid extractions, particularly when using ammonia as the extraction solvent, arise from reaction of the supercritical fluid with the sediment material.

CID mass spectra for ions found in the supercritical ammonia extracts of DFM 81-6 sediment and from standard compounds are shown in Figure 50. The upper spectra for the parent ions m/z 132 (A) and m/z 146 (B) were obtained during extraction of the sediment and the lower pair (C and D) are CID spectra of standard alkyl indole compounds extracted under the same instrumental conditions. The m/z 132 ion in Figure 50C corresponds to the protonated
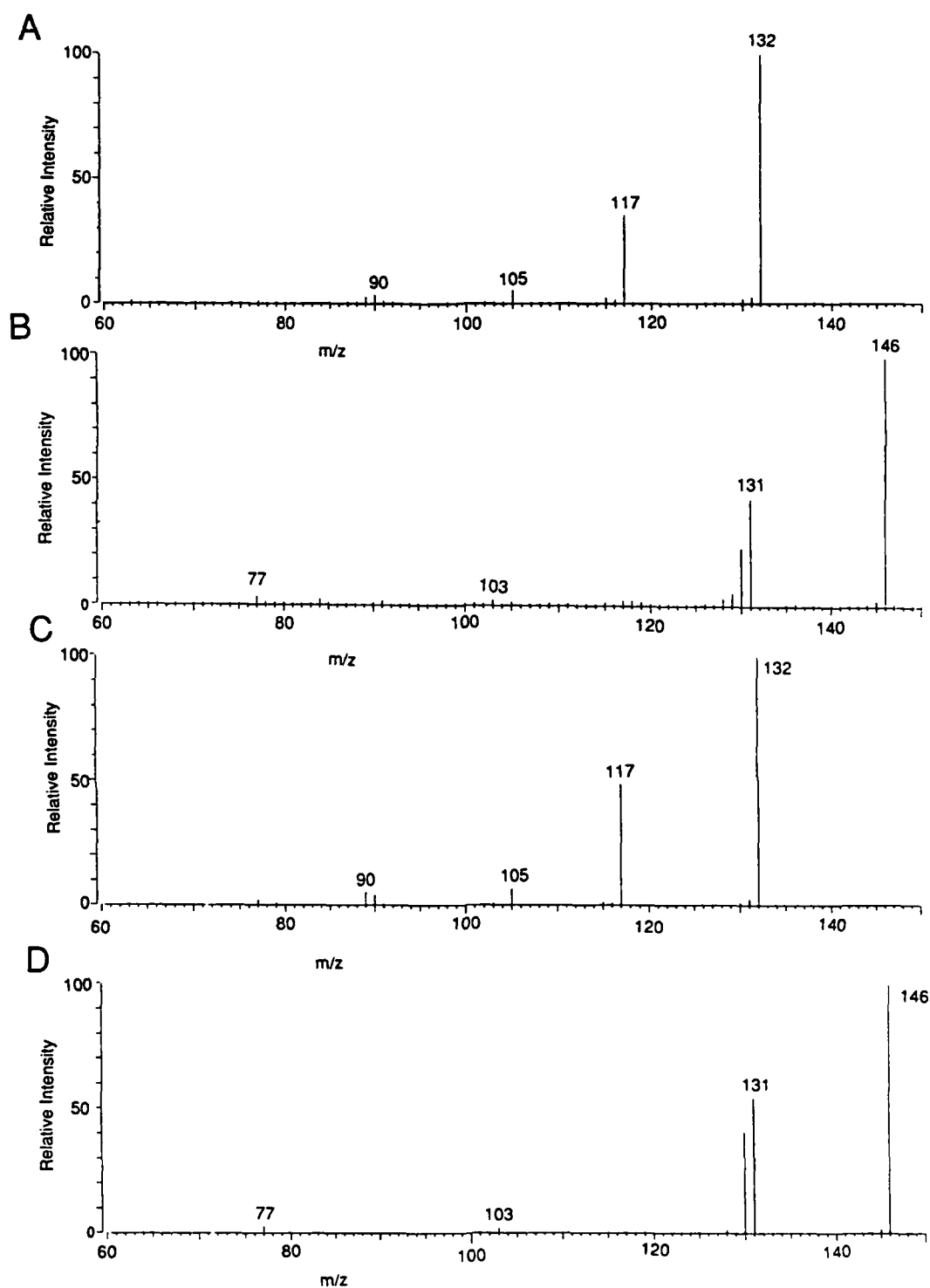
Figure 50. CID mass spectra of m/z 132 and 146 parent ions obtained during supercritical ammonia extractin of DFM 81-6 sediment (A and B) and standard alkyl indole compounds (C and D).

molecule $(M+H)^+$ for 3-methylindole, and shows loss of a methyl group to form the $(MH-15)^+$ ion at m/z 117 following collision with 40 eV argon atoms. The CID mass spectra of the m/z 132 parent from the sediment extract (Figure 50A) is very similar in appearance to the standard (Figure 50C) so that assignment of the ion as a protonated methyl indole is plausible. CID mass spectra of other isomeric methylindoles (2-and 7-methyl) were similar in appearance to that of the 3-methyl isomer. Consequently, the position of the alkyl substitution for the unknown could not be determined.

Results for the m/z 146 parent ions are similar to those for the m/z 132 ions leading to the assignment of the unknown as a C_2-indole. Since the loss of 29 dalton (C_2H_5) was not seen in the CID spectrum of the unknown, it is unlikely the compound was an ethyl indole, but was more likely a dimethyl species. As with the C_1 indoles, the alkyl substitution position was indeterminate and the extract mass spectra can most likely be attributed to a mixture of alkyl indole isomers.

The CID mass spectra for m/z 160 and m/z 174 obtained from the ammonia extraction of the sediment indicate these species are also due to alkyl substituted indoles. The predominance of alkyl losses in these CID spectra, as opposed to the loss of ammonia, 17 dalton, indicates that amines are not the principle source of nitrogen containing species in this series of ions. Furthermore, these ions are not ammonium adduct ions, $(M+NH_4)^+$, as the loss of ammonia under CID conditions would be a facile process leading to an intense daughter ion corresponding to the protonated molecule and a low relative abundance of parent ion.

These points are clearly illustrated with the pair of CID mass spectra shown in Figure 51. The upper spectrum, Figure 51A, is the CID spectrum of the m/z 199 ion found in the ammonia CID spectrum of 2-aminofluorene of molecular weight 181. This compound was chosen as a standard since it yields a protonated molecule with nominal mass (m/z 181) coincident with a probable constituent of the DFM sediment, methyl carbazole. Furthermore, the CID spectrum of this compound would be clearly distinct from an alkyl carbazole, as loss of ammonia would be the principle fragmentation pathway. The m/z 199 ion in the mass spectrum of 2-aminofluorene is the ammonium adduct ion, $(M+NH_4)^+$, and the CID mass spectrum of this ion clearly shows a facile loss
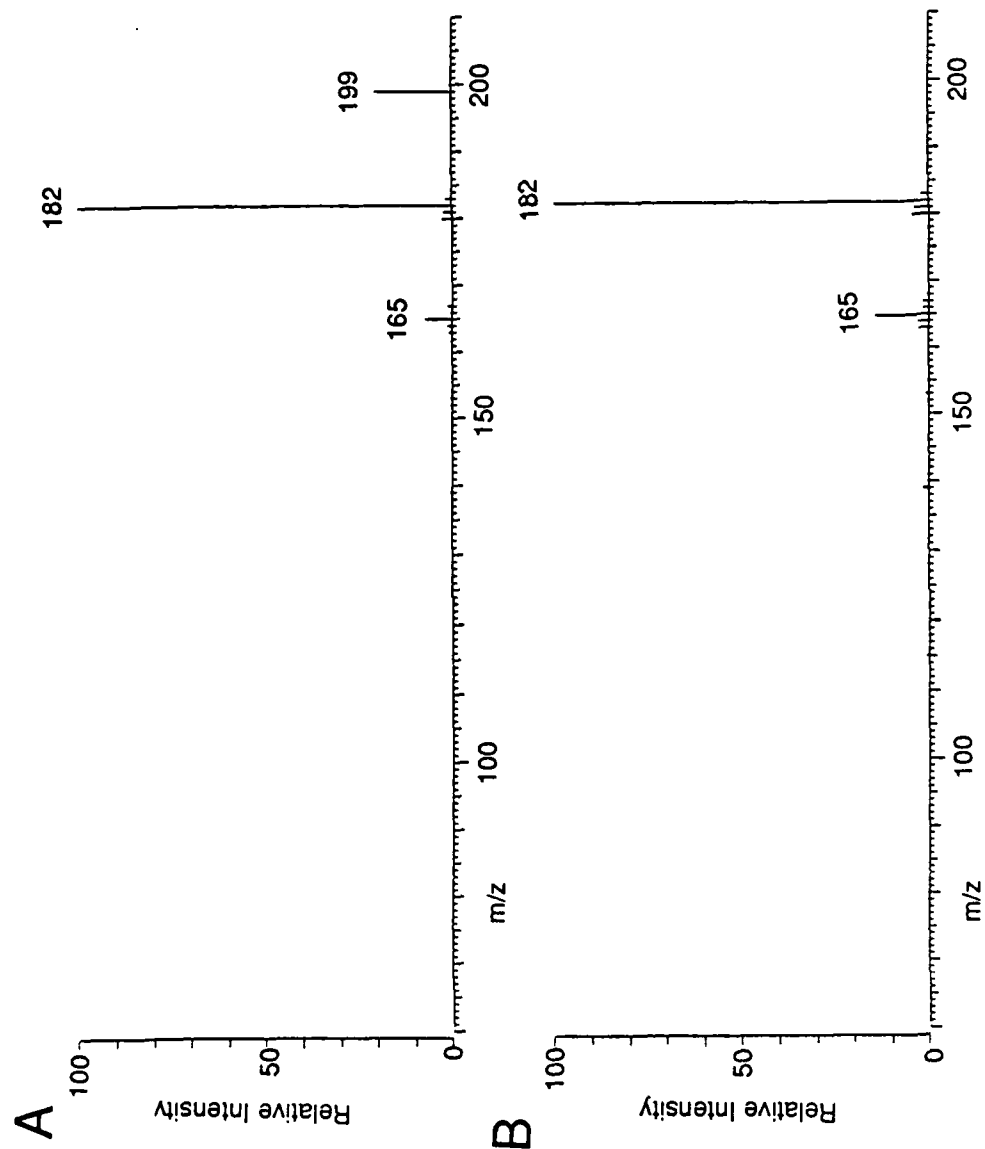
Figure 51. CID mass spectra of the m/z 199 and 182 parent ions found in the ammonia chemical ionization mass spectrum of 2-amino-fluorene.

of ammonia (17 dalton) to the daughter ion at m/z 182. A further loss of 17 dalton, loss of the amine substituent, yields the ion at m/z 165. No fragmentation of aromatic hydrocarbon rings was found under the conditions used in this study. The CID spectrum (Figure 51B) of m/z 182, $(M+H)^+$, from 2-aminofluorene shows a loss of the amine group to yield the ion at m/z 165. These spectra (Figure 51) illustrate the difference between loss of ammonia found as an adduct and a covalently bonded amine group.

The CID daughter ion spectrum of the $(M+H)^+$ ion of 2-aminofluorene (Figure 51B) can also be compared with an isobaric ion found in the spectrum (Figure 52A) obtained from the ammonia extraction of the sediment. For this species, the principle loss was to m/z 167 which can be accounted for as the loss of a methyl group. The CID spectrum shown in Figure 52A qualitatively matches the CID spectrum of a methylcarbazole standard (m.wt. 181), and it is most likely that methyl carbazole isomers are the source of these ions in the sediment extract. A clear distinction can be made between amino-PAH and alkyl substituted nitrogen-containing PAH using CID tandem mass spectrometry.

It should be noted that the CID daughter ion mass spectrum of the m/z 182 parent ion is not constant during supercritical fluid extraction of the DFM 81-6 sediment. Daughter ion spectra obtained early in the extraction, at lower (<300 bar) fluid pressures, exhibit the loss of an amine functionality (17 dalton) as opposed to the loss of a methyl group (15 dalton) found in daughter ion spectra obtained later (at higher pressures) in the extraction. This would indicate that a portion of the m/z 182 ion signal found in the extract spectra could be due to aminofluorenes as well as methylcarbazoles.

The remaining spectra shown in Figure 52 with parent ions at m/z 196 and m/z 210 correspond to C_2- and C_3- substituted carbazoles extracted from the fuel sediment. The principle loss in these spectra was that of a methyl group (15 dalton), but further losses of alkyl groups leading to low intensity fragments in the CID spectra of the more highly substituted alkyl carbazole were also observed. The parent ions are most likely due to a mixture of alkyl carbazole isomers.

A series of ions was also found at m/z 108, 122, 136 and 150 in the ammonia extract of the DFM sediment. Figure 53 shows CID daughter ion spectra
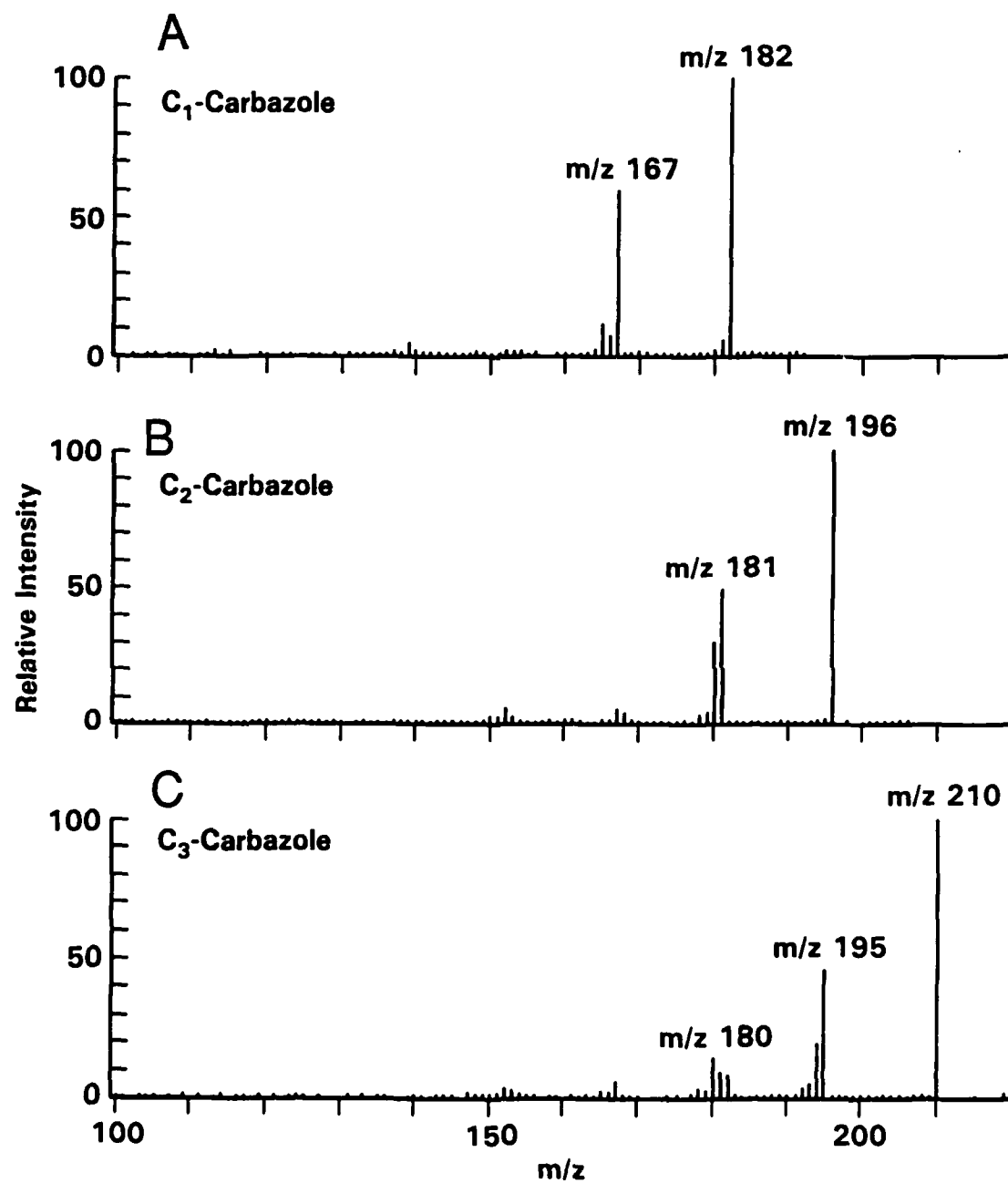
106

Figure 52. CID mass spectra obtained during supercritical ammonia extraction of DFM 81-6 sediment of m/z 182 (A), m/z 196 (B), and m/z 210 (C) ions.
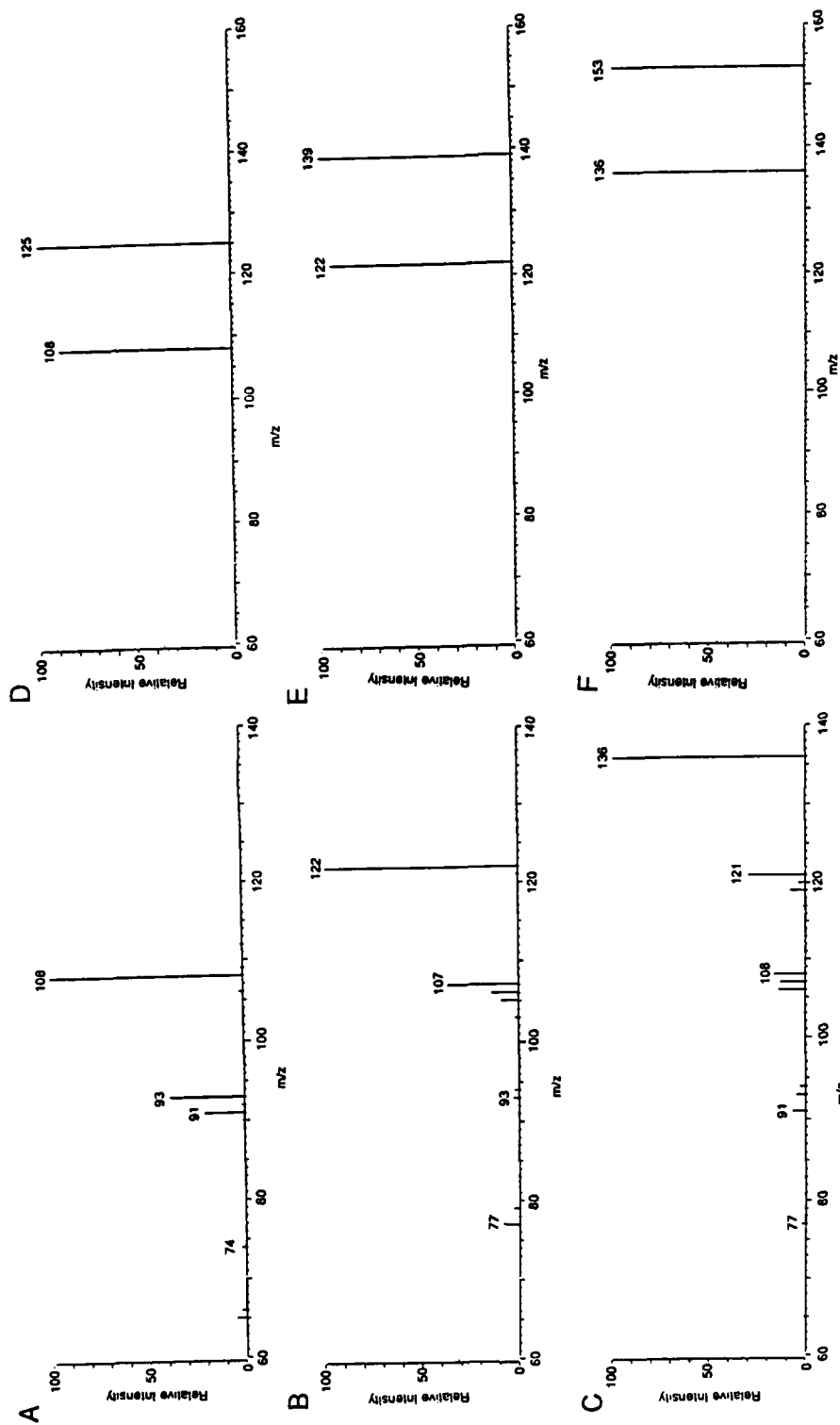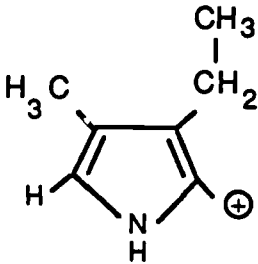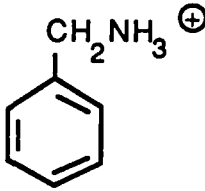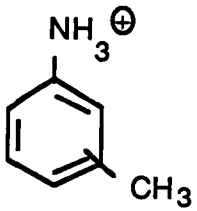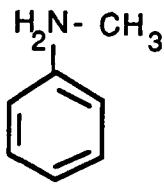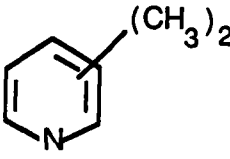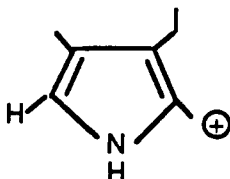
Figure 53. CID mass spectra obtained during supercritical ammonia extraction of DFM 81-6 sediment of the m/z 108 (A), 122 (B), 136 (C), 125 (D), 139 (E) and 153 (F) ions.

for the m/z 108, 122 and 136 ions, as well as the related ions at m/z 125, 139 and 153. This second set of ions (Figure 53D, E,F) corresponds to ammonia adducts for the species yielding the m/z 108, 122 and 136 ions, as is clearly indicated by the facile loss of ammonia (NH_3, 17 dalton). It is not certain, however, what species are responsible for the ions at m/z 108, 122 and 136. One possible molecular formula for the lowest mass member of this series is $(C_7H_{10}N)^+$. The daughter ion spectra (Figure 53B and C) indicate that m/z 122 and 136 ions are likely more highly alkylated members of this series of compounds.

The CID mass spectrum of the m/z 108 ion indicates an alkyl substituted (loss of 15 dalton, CH_3) species that was otherwise relatively stable. The loss of 17 dalton, which may arise from a single loss of ammonia (NH_3) or sequential loss of hydrogen (H_2) and a methyl group (CH_3) from the parent ion, was also observed. A small contribution from the loss of H_2 is observed at m/z 106. The interpretation of these spectra is further complicated by the lack of a pre-separation step so that a number of isobaric compounds could be contributing to the ion signal at m/z 108 (as well as the more highly alkylated compounds at m/z 122 and m/z 136). Possible structures for this series of ions are methyl and ethyl pyrroles (Table 10). Ions of this type are found as fragments of porphyrin molecules under ammonia CI conditions (53-57). They may also be present as parent ions or fragments of other monopyrroles. The relative abundance of these ions in the mass spectrum of the sediment extract roughly correlates with the abundance of these ions found as fragments from porphyrinogens (55). These observations alone, of course, are insufficient to indicate that porphyrin-like molecules are the source of this series of ions.

Table 10 includes other possible (and equally likely) structures corresponding to the formula $(C_7H_{10}N)^+$ which would yield very similar CID daughter ion spectra. Approximate values for the proton affinities (PA) for the general classes of compounds represented by the structures are also listed in Table 10. These values are all higher than that of ammonia (PA=205 Kcal/mole), which would indicate why both ammonium adduct ions and protonated molecules are formed for this series of ions. As the mass range below m/z 100 was not routinely scanned during extraction of sediments, the presence of less alkylated species, specifically the pyridines, could not be verified.

109

TABLE 10

Possible Structures for the Ion at m/z 108

Possible Structures	Compound Type	Proton Affinity (Pa, Kcal/mole)[58]
	alkyl pyrrole	~210
	benzylamine	214 - 220
	methylaniline	214
	N-methylaniline	218.2 (N-Me) 223.8 (N-Me$_2$)
	alkyl pyridines	227 (2,4-Me$_2$)
	oligomeric pyrrole fragment	

Without obtaining daughter ion mass spectra of authentic samples of these compound types, it is not possible to make an absolute assignment of the source of these ions. It is apparent, especially from this last example, that further study, both by tandem mass spectrometry alone and following some form of separation of the extract, could be beneficial in obtaining further information on the species present in ammonia extracts of fuel sediments.

Model Sediment Studies

SFE-MS was also performed on a series of sediments that had been produced by accelerated aging of fuels doped with compounds believed to induce sedimentation (41,44,48,59,60). Chemical ionization mass spectrometry was used to monitor the extract effluent for these materials in the same manner as for the naturally occurring sediment samples. General observations on the results of these experiments indicate: (1) the chemical ionization mass spectra of extracts of model sediments do not, in general, resemble the mass spectra of natural sediment extracts; (2) the majority of the signal in the mass spectra obtained following supercritical fluid extractions can be accounted for by compounds formed by oxidation of the additive materials; and (3) the extracts of naturally occurring sediments were found to contain many significant components with molecular weights in excess of 1000 dalton, whereas, the extracts of the model sediments were found to contain very little material in excess of 500 dalton. The results of these experiments indicate the structures of the model sediments are different than those of naturally occurring sediments, even though the alkylpyrroles used to promote sedimentation may contribute to natural sediment formation. The mechanism(s) of natural sediment formation was not fully modelled by these tests.

The methane CI mass spectrum shown in Figure 54 was obtained during the supercritical pentane extraction (205°C, 85 atm) of sediment NRL-2. Dimethylpyrrole and t-butyl-hydroperoxide were used to promote sedimentation in this sample. This mass spectrum is characterized by the presence of two intense ions at m/z 110 and m/z 124 that correspond to protonated molecules of oxidation products of the pyrrole additive. Possible structures for these compounds are given in Figure 55. Structures for other compounds yielding ions under these conditions, m/z 175 and m/z 189, are also shown in Figure 52 and are likely dimeric forms of the additive. Although not
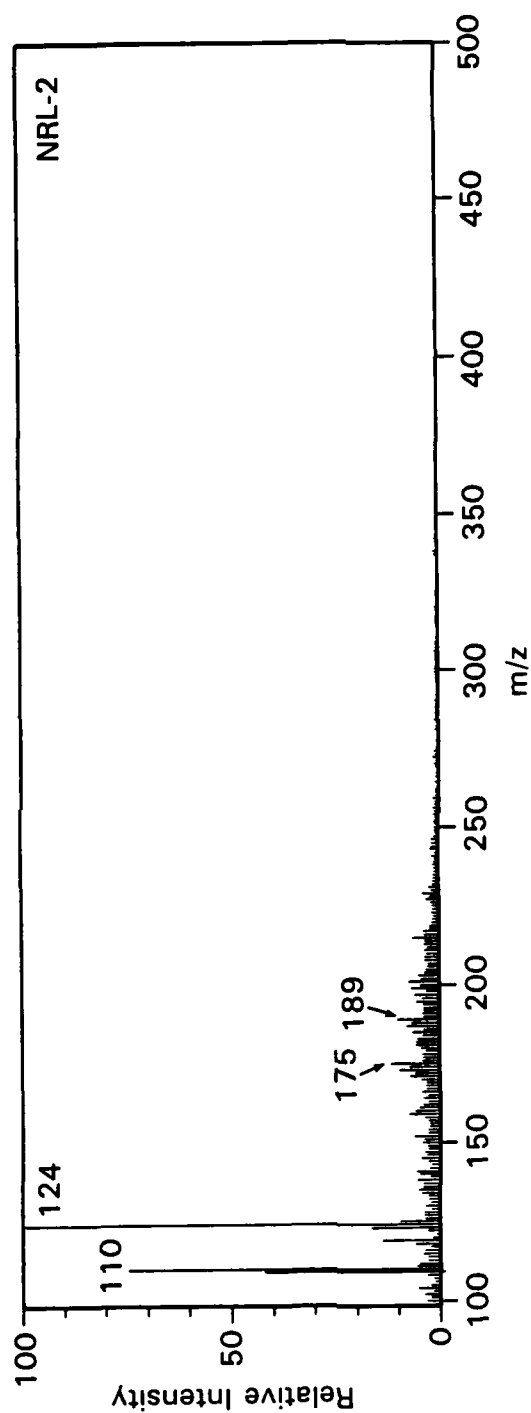
111

Figure 54.   Methane chemical ionization mass spectrum of NRL-2 sediment obtained during supercritical pentane extraction at 205°C and 85 atmospheres.
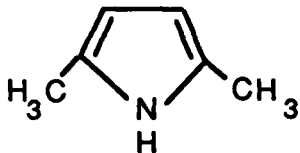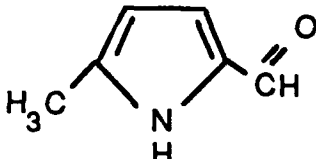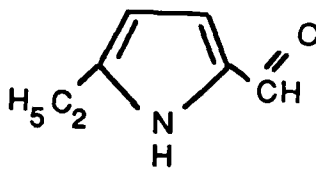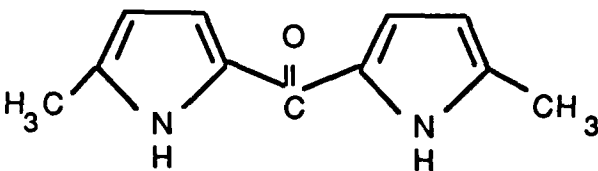
112
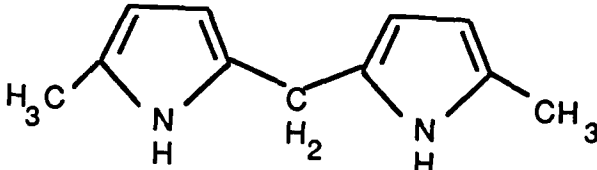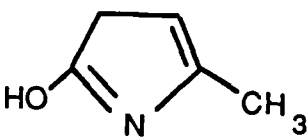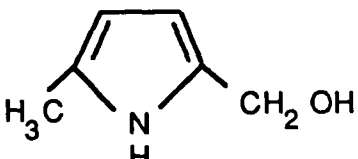
	M/Z PROTONATED MOLECULE
A.	96
B.	110
C.	124
D.	189
E.	175
F.	98
G.	112

Figure 55.   Possible structures for oxidation products of 2,5-dimethylpyrrole.

113

present in the mass spectrum shown in Figure 54, ions corresponding to the protonated molecule of dimethylpyrrole, m/z 96, and another oxidation product, Figure 55F, with an ion at m/z 98, were also found in this extract.

The results obtained for the NRL-2 sediment are similar to those obtained for the NRL-4 sediment in which only dimethylpyrrole was used as the additive. The principle distinction between the extract mass spectra of these sediments was the presence of an ion at m/z 112, which probably corresponds to 5-methylpyrrole-2-methanol (Figure 55G), an oxidation product of the additive, in the NRL-4 extraction spectrum. The m/z 112 ion was present at about 70% relative abundance (m/z 124 was still the base peak) while m/z 110 ion (Figure 55B) was present at about 25% relative abundance. These differences may reflect that greater oxidation occurred in the NRL-2 sediment in which $\underline{t}$-butylhydroperoxide was also used as an additive. The mass spectral results of NRL-2 and NRL-4 are similar to results obtained by low voltage electron impact ionization with high resolution mass spectrometry for model sediments formed in accelerated aging tests (41). The predominance of additive oxidation products and lack of higher molecular weight components were also observed in the previous mass spectral studies.

The NRL-1 sediment was induced using 2-4-dimethyl-3-ethylpyrrole. Mass spectra of the pentane and pentane-methanol extracts of this sediment are shown in Figure 56. Methane was used as the CI reagent for this extraction and yielded primarily protonated molecules. If similar sediment forming mechanisms were functional for this more alkylated pyrrole, as experienced for dimethylpyrrole, similar oxidation products might be postulated. These structures are given in Figure 57 and as can be seen, the oxidation products of the additive account for the principle ions found in the mass spectrum. Without additional information, however, the sites of oxidation are indeterminate and could be any of the alkyl sites. The m/z 138 and 140 ions are protonated molecules for pyrrole-aldehydes and pyrrole-alcohols (Figure 57B and C), respectively, and m/z 126 corresponds to a protonated molecule of the hydroxypyrrole (Figure 57D). The additive was detected as the protonated molecule at m/z 124 and possibly as a methanol adduct ion, $(M+CH_3OH_2)^+$, at m/z 156. The m/z 156 ion could be a hydronium adduct ion, $(M+H_3O)^+$, of the pyrrole-aldehyde. Methanol (and likely water) were available in the ion source due to the supercritical solvent. Alkyl adduct ions, due to either
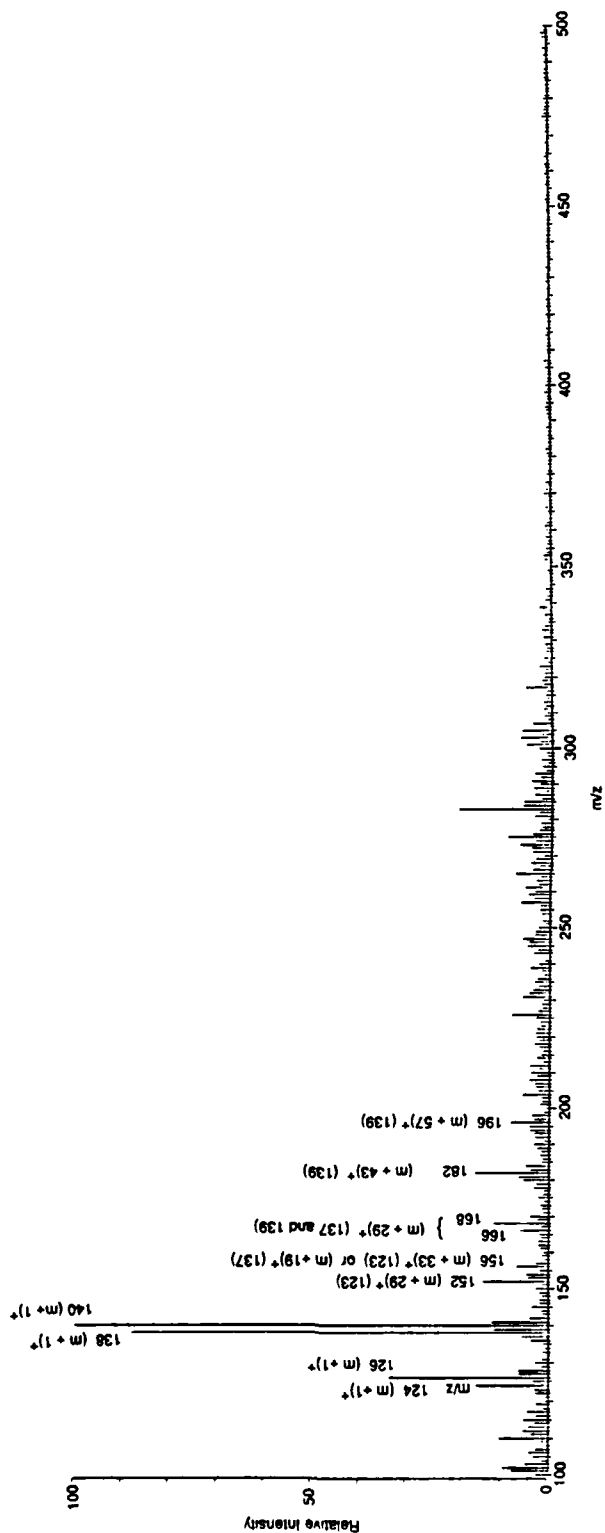
Figure 56. Methane chemical ionization mass spectrum of NRL-1 sediment obtained during supercritical pentane-methanol (95:5 v:v) extraction at 230°C and 85 atmospheres.
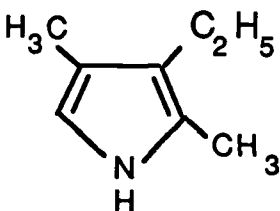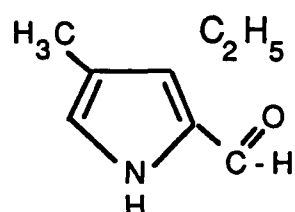
115
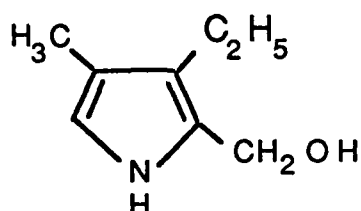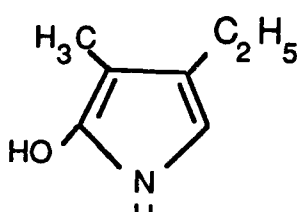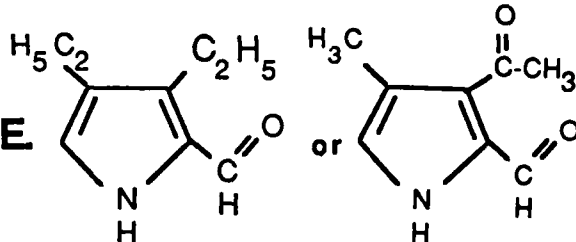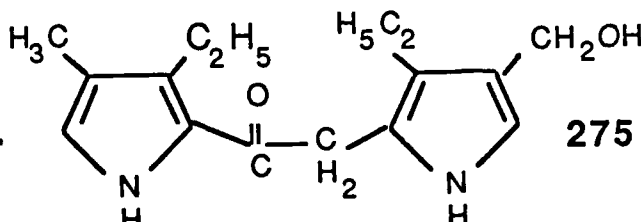
	$(M+1)^+$	$(M+18)^+$	OTHER ADDUCTS
A.	124	141	156 $(M+CH_3OH_2)^+$ 152 $(M+29)^+$
B.	138	155	156 $(M+H_3O)^+$ 172 $(M+NH_4NH_3)^+$ 166 $(M+29)^+$
C.	140	157	168 $(M+29)^+$ 182 $(M+43)^+$ 196 $(M+57)^+$
D.	126	143	
E.	152	169	
F.	275	292	

Figure 57.   Possible structures for ions related to oxidation products of 2,5-dimethyl-3-ethylpyrrole.

116
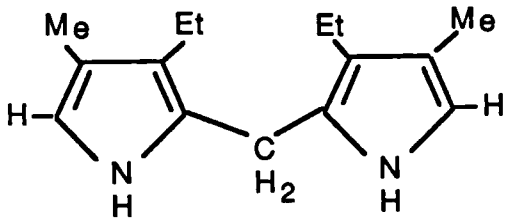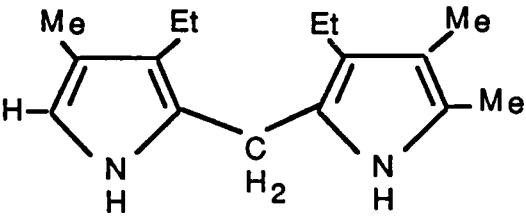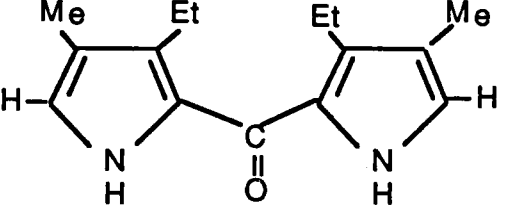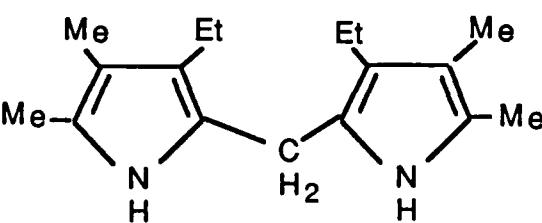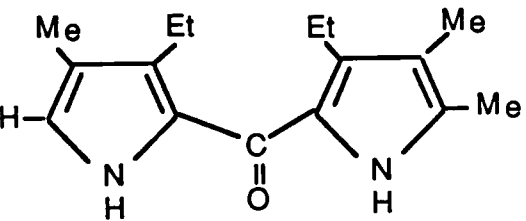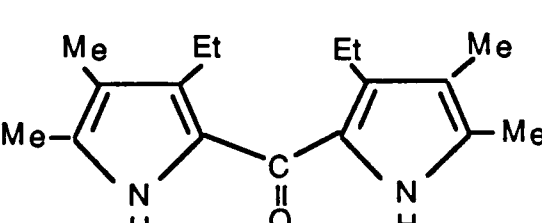
(M+1)+   (M-1)+

231

245   **243**

245   **243**

259   **257**

259   **257**

273   **271**

Figure 57.   (Continued)

	(M+1)+	(M-1)+
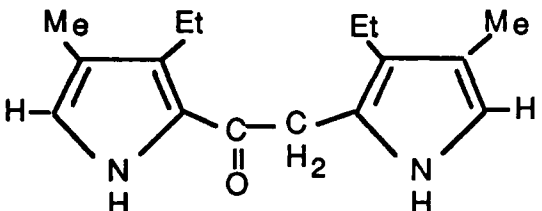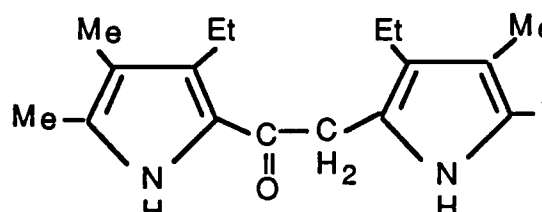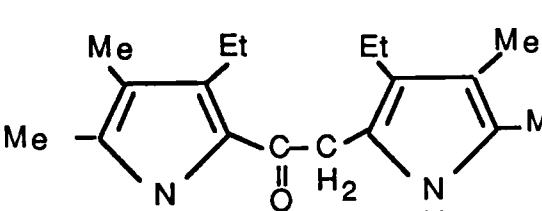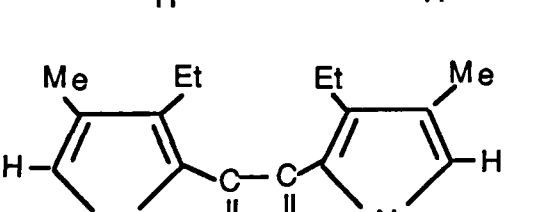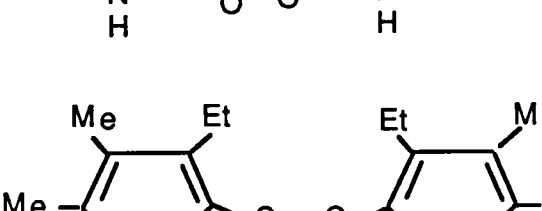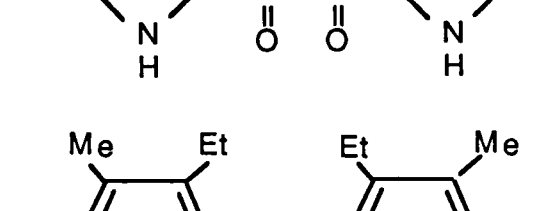
	(M+1)+	(M-1)+
Structure 1	259	257
Structure 2	273	271
Structure 3	287	285
Structure 4	273	271
Structure 5	287	285
Structure 6	301	299

Figure 57.   (Continued)

118

the CI reagent or supercritical solvent, at $(M+29)^+$, $(M+43)^+$ and $(M+57)^+$ are present at m/z 152, 166, 168, 182 and 196. Another source of the m/z 152 ion is the protonated molecule of the diethylpyrrole-aldehyde, Figure 57E, oxidation product. Higher mass ions (m/z 245, 259, 273 and 275) may also be due to further oxidation-dimerization products of the pyrrole additive.

Comparable to data from other mass spectral techniques (41), little contribution above mass 300 was found in the pentane and modified pentane extracts of the model sediments. However, it was clear from the large amount of material remaining in the extraction cell and physical form of the residue, at times indistinguishable from non-extracted sediment, that less than 25% of the sediment was extracted using pentane or the more polar alcohol-modified pentane fluids. The change to a more polar fluid, supercritical ammonia, led to significantly greater quantitites (in some cases >95%) of the sediment being removed from the sample cell, but did not always lead to significantly more complex mass spectra or spectra with additional higher molecular weight components.

The mass spectrum in Figure 58 was obtained during supercritical ammonia extraction of the NRL-1 sediment using ammonia as the CI reagent. The presence of the oxidation products of the pyrrole additive described earlier is confirmed by their ammonium adduct ions, in similar relative abundances, at m/z 155, 157, 143, 292, etc., as found for the protonated molecules in the super-critical pentane spectrum (Figure 56). The ions at m/z 139 and 108 may result from fragmentation of some of the oxidation product ions. The likelihood that these ions were due to reaction of the sediment with super-critical ammonia is negated by detection of the protonated molecules for the same parents obtained using a different supercritical solvent and chemical ionization reagent. The highest molecular weight ions in this mass spectrum are found between m/z 390 and m/z 450, and are of very low relative abund-ance and can probably be attributed to trimers of the pyrrole additive.

Extraction mass spectra of the NRL-3 sediment obtained with super-critical ammonia at 150°C and three progressively higher pressures are shown in Figure 59. Interestingly, these spectra are more complex than the spectra obtained from the other "model" sediments and have significant contributions

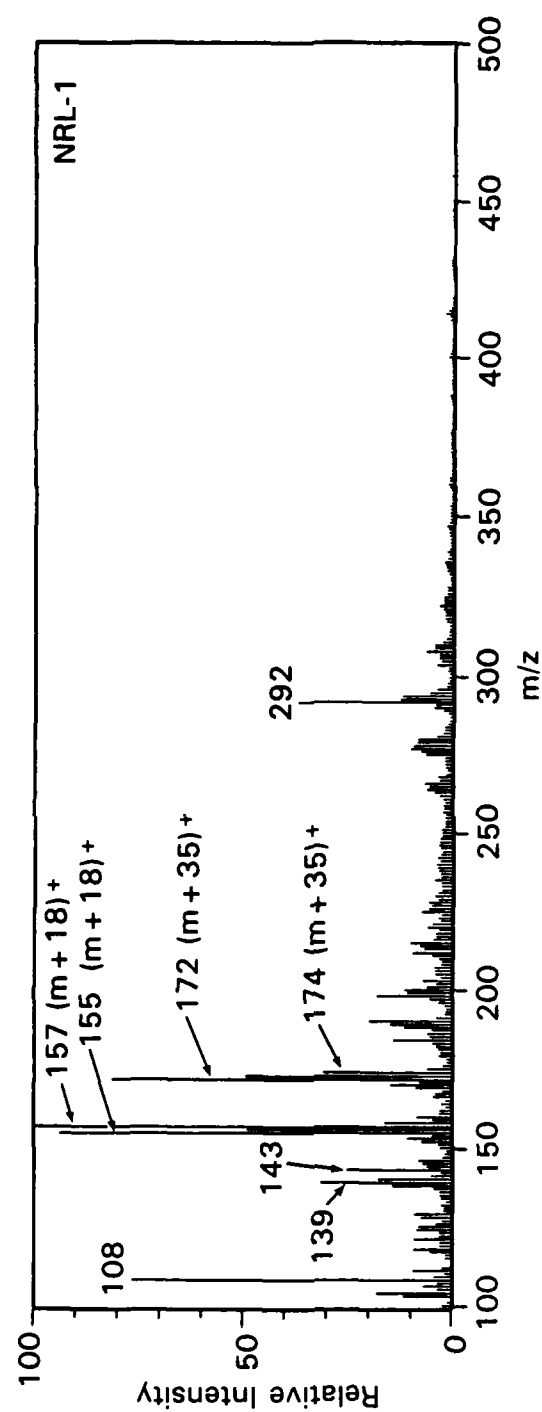Figure 58.   Ammonia chemical ionization mass spectrum of NRL-1 sediment obtained during supercritical ammonia extraction at 150°C and 200 atmospheres.
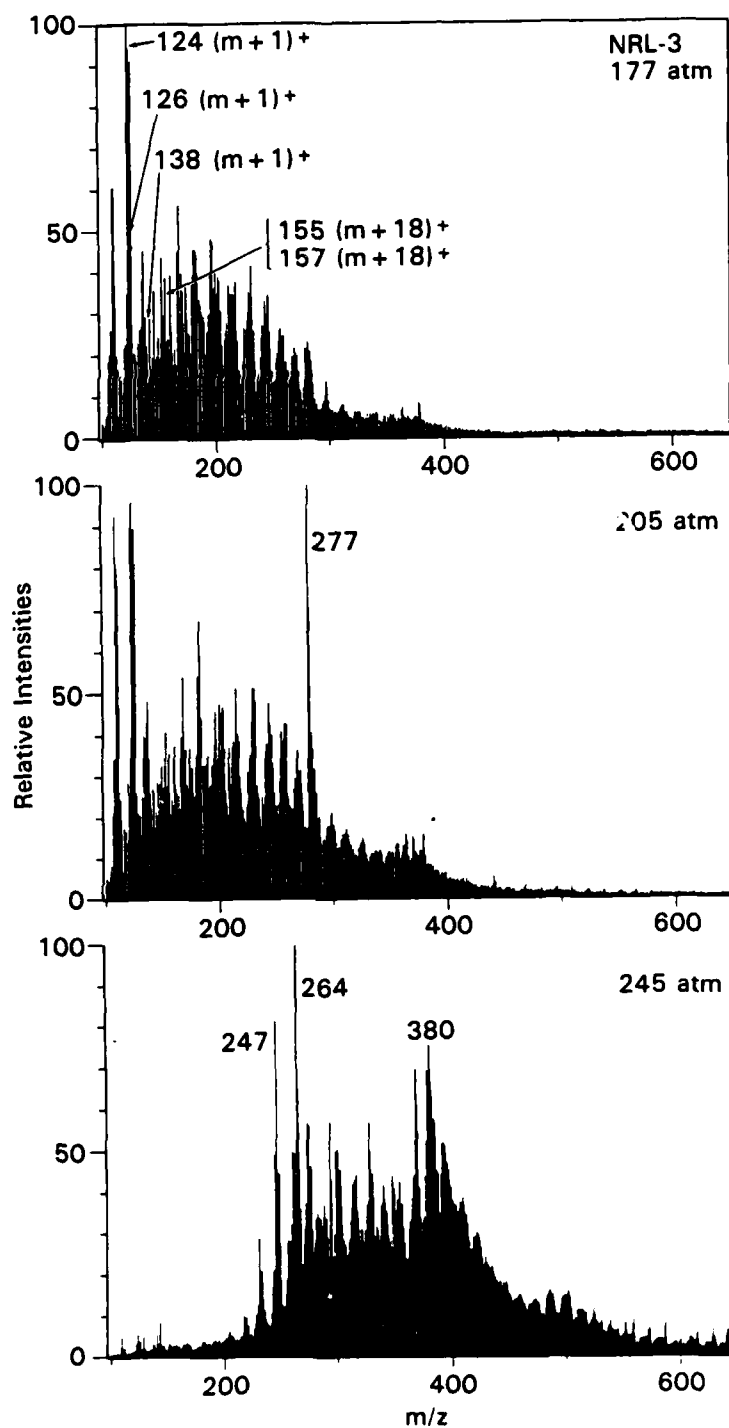
Figure 59.   Ammonia chemical ionization mass spectra of NRL-3 sediment obtained during supercritical ammonia extraction at 150°C and at three progressively higher pressures of 177 atmospheres (top), 205 atmospheres (center), and 245 atmospheres (bottom).

121

up to masses over 500 dalton. As evident from the spectra, progressively higher molecular weight material was extracted at higher pressures. However, increasing the pressure above 245 atmospheres did not significantly change the mass spectrum. An additive isobaric to that used for the NRL-1 sediment, tetramethylpyrrole, was used to induce sedimentation in this sample. Consequently, ions of the same nominal masses were found in these spectra as were obtained for the NRL-1 sediment and similar oxidation products can be postulated. The m/z 124 ion corresponds to the protonated molecular ion of the additive and the m/z 126 and 138 ions correspond to protonated molecular ions of oxidation products, a trimethypyrrole-aldehyde and a hydroxytrimethylpyrrole, respectively. Many of the higher molecular weight contributions in the spectra from this sediment are likely due to oxidation product dimers and trimers.

The elemental composition of the model sediment materials is consistent with their being composed of oxidation products of the pyrrole additives and oxidation product dimers and trimers. The elemental composition for NRL-2, NRL-3, and NRL-4 sediments is listed in Table 11. High nitrogen contents (~ 10%) easily allow pyrrole rings to form the base structures. High oxygen contents are also available for keto and hydroxyl functionalities. Oxygen composition was by difference for the NRL-2 and NRL-4 sediments and these values are enclosed in parentheses in the Table.

Conclusions

The sediment material from DFM 81-6 was successfully analyzed using supercritical fluid extraction-mass spectrometry. Supercritical ammonia and the proper thermal conditions provided essentially complete solvation of the material with characteristic mass spectra obtained to molecular weights over 850 dalton. Alkyl indoles and alkyl carbazoles were found to be major constituents of the sediment matrix. The matrix itself appeared to be highly alkylated and some evidence exists that it could partially consist of oligomeric pyrrole or macrocyclic pyrrole structures. Tandem MS/MS methods were also utilized to obtain additional structural information and verify the identity of the alkyl indoles and alkyl carbazoles.

TABLE 11

Elemental Composition of Model Sediment Materials

Sample	% Elemental Composition				
	C	H	N	O	Total
NRL -2	60.1	5.6	10.7	(23.6)	76.4 (100)
NRL -3	73.5	6.8	8.5	10.8	99.6
NRL -4	61.8	4.2	12.1	(21.9)	78.1 (100)

In addition to the natural sediment, model sediments formed by doping fuels with additives believed to induce sedimentation were also analyzed by SFE-MS. These studies indicated the nature of these model sediments was significantly different than the natural sediments and that their mechanisms of formation were undoubtedly different. In general, the chemical ionizaion mass spectra of these model sediments were relatively simple with the majority of the ions accounted for as oxidation products of the additive materials. The model sediments also consisted of much lower molecular weight structures than the natural sediment.

Additional studies utilizing high resolution mass spectrometry and additional tandem MS/MS methods are needed to more adequately characterize the natural sediment matrix. High resolution mass spectrometry could help establish the molecular formulae for many of the components in the sediment and MS/MS could be applied to additional ions to obtain possible structural assignments. The use of a higher mass analyzer (>1000 dalton) would also prove instructive. SFE-MS has been demonstrated to be a potentially valuable tool for the characterization of intractable sediment materials; valuable contributions arising from future application can be anticipated.

TASK E. CHEMICAL CLASS FRACTIONATION DEVELOPMENT

Introduction

An important aspect of fuel characterization is the rapid quantitative determination of hydrocarbon types or chemical classes (e.g. saturates, olefins, monocyclics, dicyclics). Compositional effects on fuel performance have been well documented (62,63) and considerable interest exists for these comparisons. The fluorescent indicator adsorption (FIA) method (64) has been used extensively for these chemical class determinations. However, the FIA method has several drawbacks and a faster, more reliable method would be desirable. Several alternative approaches utilizing HPLC and various off-line and on-line detection approaches have been developed (65-67).

However, quantitation is complicated by the lack of a sensitive and universal detector for HPLC. Recently, supercritical fluid chromatography (68) was demonstrated for the chemical class fractionation of various fuels. Use of the flame ionization detector (FID) provided reliable and straight-forward quantitation. However, this initial work (68) utilized a packed HPLC column with a mobile phase flow rate too large for direct interfacing to the detector. Thus, the column effluent was split with only a fraction going to the detector. The effluent split occurred in the heated portion of the detector which could lead to mass discrimination and spurious quantitative results.

Alternative approaches to allow improved quantitation would include use of a more optimized splitting arrangement or use of microbore or capillary columns with lower flow rates so that direct interfacing to the detector would be possible. The objectives of this research task were to develop the necessary instrumentation for SFC chemical class fractionation and evaluate the applicability of various HPLC and specialized capillary columns to provide efficient chemical class fractionation (saturates, monocyclics, and dicyclics) of various diesel fuels. Instrumentation development and various column evaluations efforts are reported in this section.

Experimental

Instrumentation similar to that used in capillary column SFC (27) was modified to operate with packed HPLC columns. This mainly consisted of changing the injection system and the detector interface. A generalized schematic diagram of the SFC/FID instrumentation used for chemical class fractionation is shown in Figure 60. Essentially a high pressure syringe pump (Varian 8500) under computer control was used to generate a high-pressure and pulse-free flow of carbon dioxide. A Hewlett-Packard 5700 GC with a flame ionization detector was used to provide constant temperature conditions and detection. Injection was accomplished with a Valco C14W injection valve with either a 0.06 µl or 0.10 µl sample volume rotor. Connections from the injector to the column, and from the column to the detector were made with low volume tubing and zero-dead volume connections to minimize any extra-column band broadening.

Several types of HPLC columns were used. As an initial step in the instrumentation development, a 25 cm x 4.5 mm (i.d.) silica column (5 µm particles) (Alltech) was utilized. This column required the column effluent to be split prior to detection. This was accomplished using a 1/16" Swagelock tee and appropriate lengths of small diameter (5-10 µm) fused silica restrictor tubing. The split ratio was adjusted by controlling the degree of restriction on the detector and vent lines. The split was made at mild oven temperatures and discrimination effects would be expected to be negligible. A 10 cm (Brownlee) and two 25 cm silica (Brownlee and Alltech) (5 µm particle) microbore columns (1 mm i.d.) were also evaluated. These columns were connected directly to the detector through a short length of small diameter fused silica restrictor tubing. Microbore guard columns and regular guard columns were also examined.

Silica wall-coated capillary columns were also prepared and evaluated. These columns were prepared using 250 µm i.d. thick-walled fused silica tubing. The tubing was rinsed with deionized water to remove any impurities and to hydroxylate the surface. A diluted mixture (1:1) of sodium silicate (water glass) in deionized water was pushed slowly through the column to form a thin "hydro-gel" layer. This layer was dehydrated and rendered porous
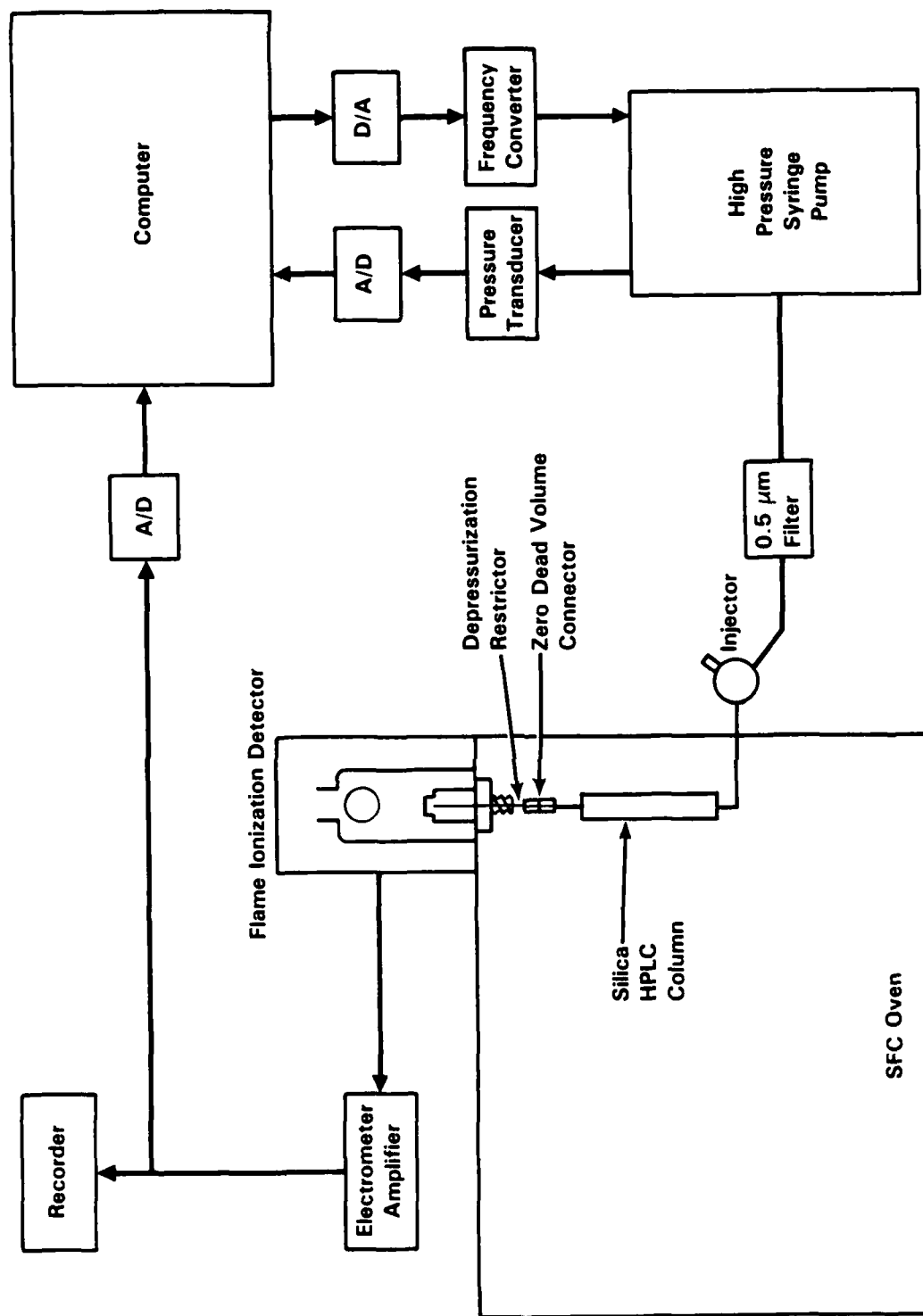
126

Figure 60. Schematic Diagram of SFC/FID Chemical Class Fractionation Instrumentation.

by slowly evaporating the water by purging with nitrogen at 110°C. This porous silica layer was further cured and activated by treatment with HCl gas at 200°C. To remove any remaining traces of HCl gas or water, the columns were purged with nitrogen at 200°C for several hours.

High purity carbon dioxide (Airco) was further dried and purified by distilling it from the cylinder to the syringe pump through activated charcoal and alumina. A 1% (v/v) formic acid-carbon dioxide fluid mixture was also utilized as the mobile phase in selected experiments. Various constant pressure and temperature operating parameters ranging between 100 and 250 atmospheres and 40° to 60°C were examined. Diesel fuels DFM 81-5 and 81-6 were used for evaluation of the methodology.

Results and Discussion

Packed Column Evaluation

Preliminary instrumentation development was accomplished using a similar design as reported in the literature (68). This design incorporated a 25 cm x 4.6 mm silica packed column and which splitting of the column effluent prior to detection. In order to achieve reasonable linear velocities (and analysis times), a relatively high split ratio (> 10:1) was necessary. The split, however, was done at oven temperature rather than detector temperature (>200°C) to minimize any discrimination effects. Although the column provided a reasonable pressure drop, it was still necessary to use an additional restrictor to maintain proper flow and pressure conditions across the column. Examples of chemical class fractionation chromatograms using this approach are shown in Figure 61. These chromatograms were obtained at 125 atmospheres and 40°C where resolution was found to be maximized. Higher pressures (up to 250 atmospheres) provided similar, but slightly poorer, separations between the chemical classes. Chemical class assignments were made by chromatographing standards representative of each chemical class and defining retention windows in which they eluted. All aliphatics (and olefins) eluted in a very narrow band while the various aromatic molecules displayed slightly wider retention windows. In fact, the tailing components
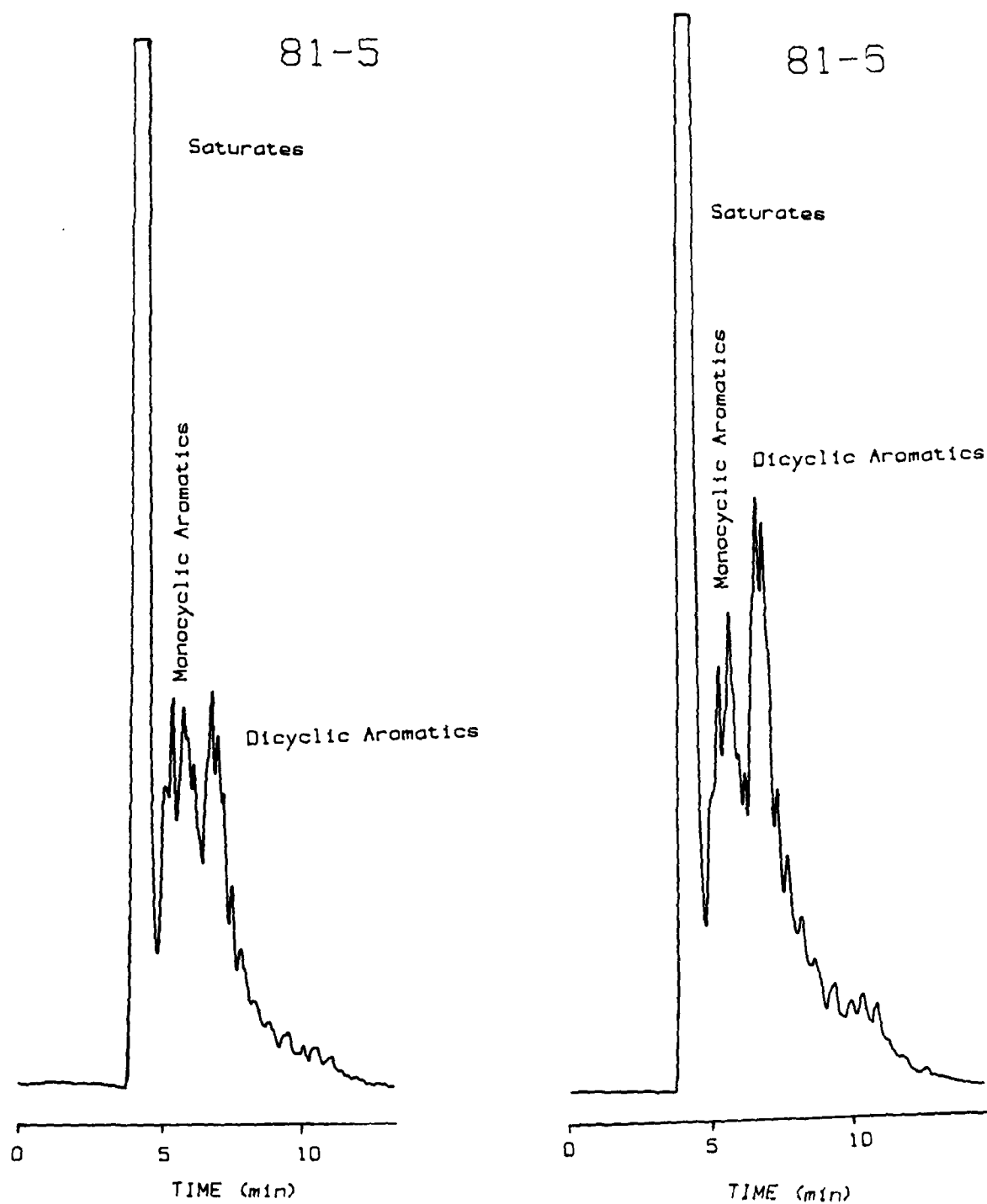
Figure 61. SFC Chemical Class Fractionation of DFM 81-5 and 81-6. Conditions: CO_2 at 125 atm and 40°C. Column: 25 cm x 4.5 mm silica (5 µm).

eluting after the sharper dicyclic band can be attributed to polycyclic aromatic compounds.

The silica column was activated at various higher temperatures (up to 200°C) in an effort to obtain improved selectivity and separation between the compound classes, but no significant improvements occurred. Smaller sample sizes (<0.06 µl) were injected by splitting the inlet flow by creating a small "leak" at the column inlet to determine if smaller sample loadings would improve the resolution between chemical classes. However, no significant effects were observable and inlet splitting was discontinued. The use of a formic-acid modifier fluid system was also evaluated to determine if improved selectivity could be obtained. A formic acid modifier may possibly activate the silica surface and provide better selectivity between the saturates and various aromatics. Formic acid has essentially no flame ionization response and did not interfere with detection. However, even after equilibration of the column overnight with the modified fluid, no improvements in selectivity were obtained.

Guard Column Evaluations

After reasonable success was achieved using the packed column mode with effluent splitting, approaches designed to eliminate splitting were examined. The first approach was to use guard columns; both a standard 4.6 mm x 3 cm cartridge and a microbore 2.1 mm x 3 cm cartridge. In these modes the volumetric flow rates through the columns could be maintained sufficiently low that the total effluent could be interfaced to the detector through an appropriate restrictor and still give reasonable retention times. However, very low resolution between compound classes was obtained as illustrated by the example chromatograms of DFM 81-5 shown in Figure 62. Chromatogram A was obtained with a standard guard column at optimized conditions and only minimal separation between the aliphatics and aromatics was obtained. Chromatogram B was obtained using a microbore guard column (also at optimized conditions, e.g., conditions that gave best performance) and its performance was even poorer. Essentially no resolution was obtained between the aliphatics and aromatics. These later results are not surprising since a microbore guard column has limited efficiency and capacity.

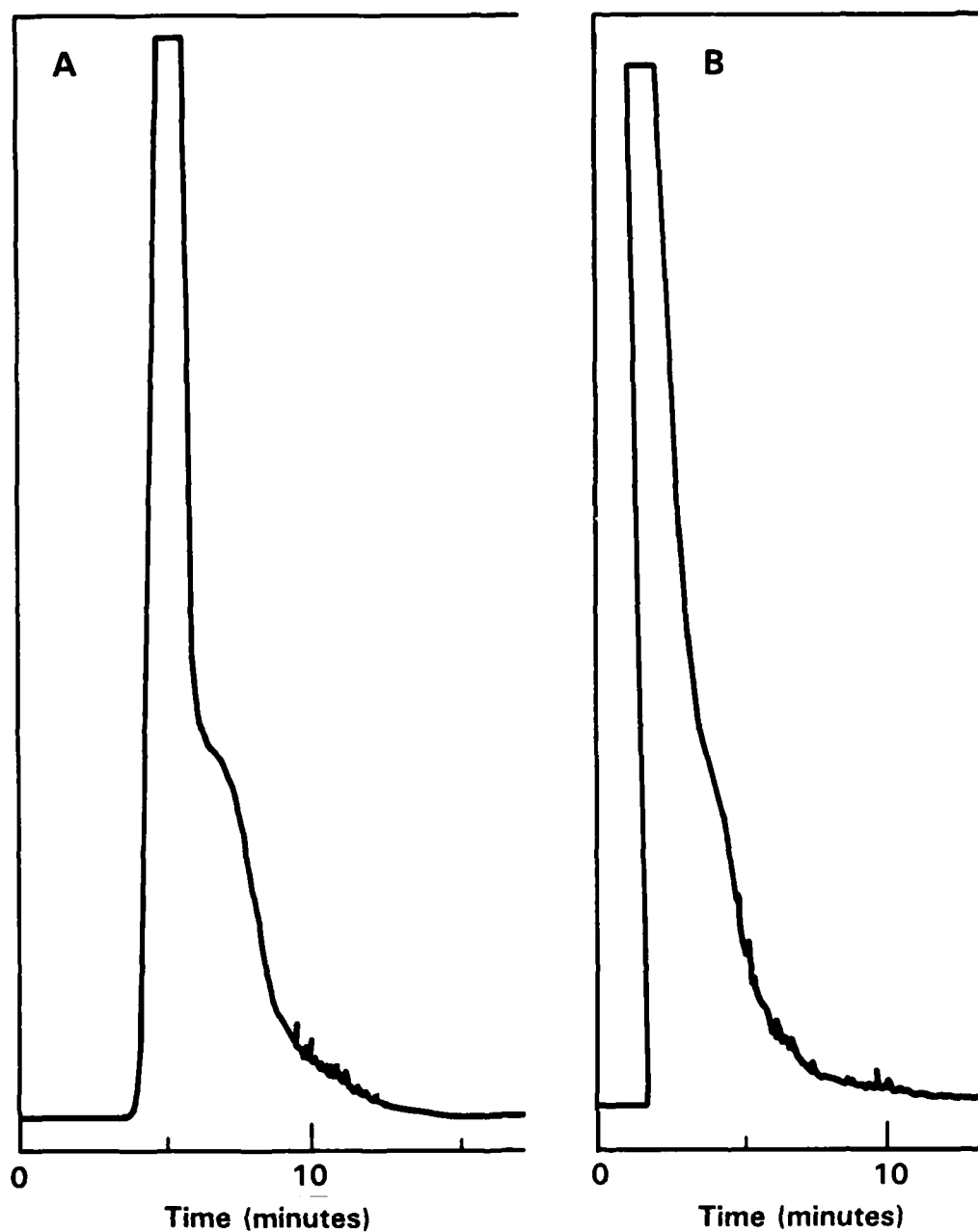130

Figure 62. SFC/FID Chemical Class Fractionation Chromatograms of DFM
81-5 obtained with (A) 4.6 mm x 3 cm silica (5 μm)
standard guard column at 40°C and 125 atm, and (B) a 2.1
mm x 3 cm silica (5 μm) microbore guard column at 40°C and
90 atm.

Microbore Column Evaluations

To increase the separation capacity and still maintain appropriate flow rates, a 10 cm microbore (1 mm i.d.) column was evaluated. A chromatogram of DFM 81-5 obtained at optimized conditions is shown in Figure 63. The resolution obtained with this column was much better, as evidenced by the appearance of two shoulders off the main peak. Although the monocyclic and dicyclic aromatic compounds were partially resolved, the quality at the separation was not sufficient to provide quantitative data for the discrete fractions.

To obtain increased resolution and separation efficiency, a longer microbore column was chosen for the next evaluation. Again, flow rates compatible with direct interfacing to the detector were achieved. Chromatograms of DFM 81-5 obtained with a 25 cm x 1 mm silica column (5 μm) at 40°C and at carbon dioxide pressures of 122 and 102 atmospheres are shown in Figure 64. Better separations were obtained with this column as evidenced by the numerous peaks. .However, the rising and tailing baseline makes integration somewhat arbitrary and complicates accurate quantitation. The differences in elution behavior at the two pressures are not surprising. The higher pressure analysis with the more solvating mobile phase eluted the components more quickly with little overall change in selectivity. However, more drastic differences in pressure would have made significant differences in the elution profile (e.g. at high pressures the components would have essentially coeluted as one peak and at low pressures only the first few components would have eluted in the time-frame of a normal analysis).

The most striking feature of these chromatograms, however, is the lack of any discernible compound-class groupings. To obtain elution windows for the chemical classes, standards containing representative compounds were chromatographed. These chromatograms were obtained at 40°C and 102 atmospheres and are shown in Figure 65. Surprisingly, the aliphatic components (alkanes, cyclohexane, etc) were individually resolved and eluted over a fairly wide range which overlapped into the monocyclic aromatics. The same aliphatics were eluted as a single large peak in a similar analysis using the packed column (discussed earlier). The monocyclics (trimethylbenzene, tetrahydronaphthalene, and cumene) and the dicyclics (methyl naphthalene
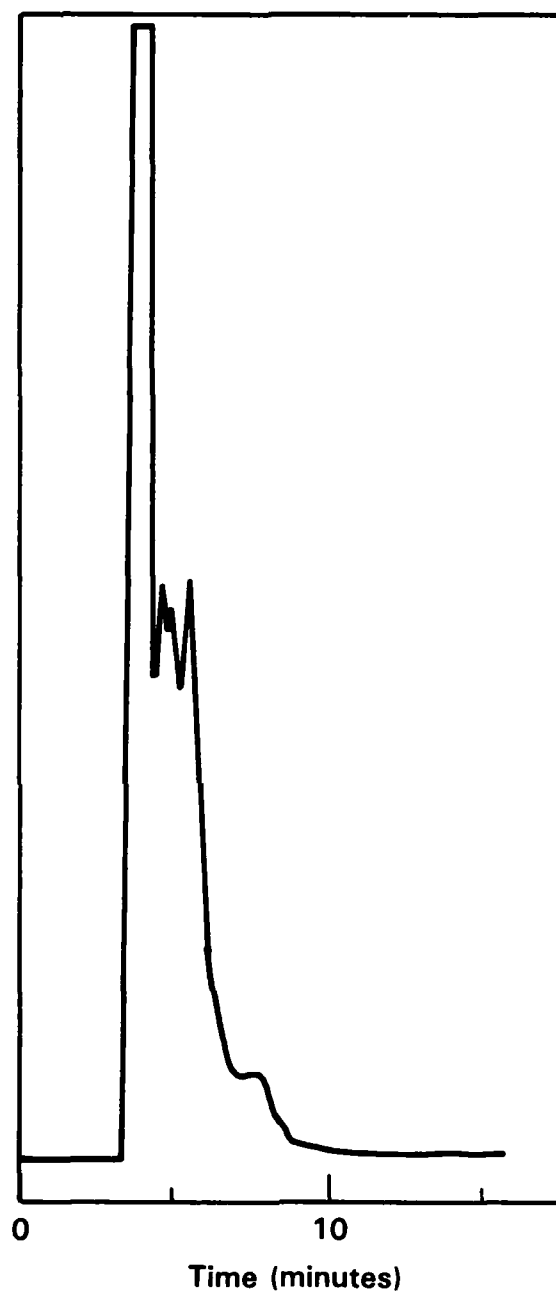
Figure 63.   SFC/FID Chemical Class Fractionation Chromatogram of DFM
            81-5 obtained with a 10 cm microbore silica column (5 µm)
            at 40°C and 125 atm.

133

Figure 64. SFC/FID Chemical Class Fractionation Chromatograms of DFM 81-5 at two pressures. Conditions: 25 cm x 1 mm silica column (5 μm), 40°C, and 122 and 102 atm CO_2.

Figure 65. SFC/FID Chemical Class Fractionation Chromatograms of Aliphatic, Monocyclic Aromatic, and Dicyclic Aromatic Standards. Conditions: 25 cm x 1 mm Silica Column (5 μm), 40°C, and 102 atm CO_2.

135

and biphenyl) eluted in separate windows as expected. (Traces of iso-octane
were also in the mono and dicyclic chromatograms since it was used to clean
the syringe). Operation at higher pressures decreased the retention for
all the compounds but did not significantly improve the selectivity. Elution
of the aliphatic compounds still overlapped with the monocyclic aromatics.
It is not clear why the various aliphatics were separated since no specific
selectivity should exist for them on a silica column. However, this behavior
was reproducible using similar columns from different manufacturers, and
thus cannot be attributed to a specific column effect. Evidently, the
higher resolution capability intrinsic to the longer microbore columns was
sufficient to individually resolve the specific aliphatic components.
While desireable in most applications, this type of behavior unfortunately
precludes the use of microbore columns under these conditions for chemical
class separations.

Capillary Column Evaluation

One meter and three meter lengths of the porous silica wall-coated
capillary columns were evaluated. They were directly connected to the injec-
tion system and to a short length of restrictor tubing (3-5 cm of 5-10 μm
i.d.) to form the interface to the detector. Appropriate detector flow
rates (< 30 mL/min) and mobile phase linear velocities were achieved with
this configuration. An example of a typical chemical class fractionation
is shown in Figure 66. This separation was obtained at 40°C and 110 atmos-
pheres using the three meter column length. Although some separation of
the aromatics from the aliphatics was achieved, the overall quality of the
fractionation was very poor. Utilization of other operating parameters
including split injection to decrease sample loading, use of formic acid
modified carbon dioxide for the mobile phase, and various temperature and
pressure combinations did not significantly improve the resolution between
chemical classes. Evidently, the porous silica layer provided insufficient
surface area for effective separation to occur. Other options with capillary
columns utilizing a crosslinked "honeycomb" network or silica packings may
provide sufficient selectivity to achieve high-quality chemical class frac-
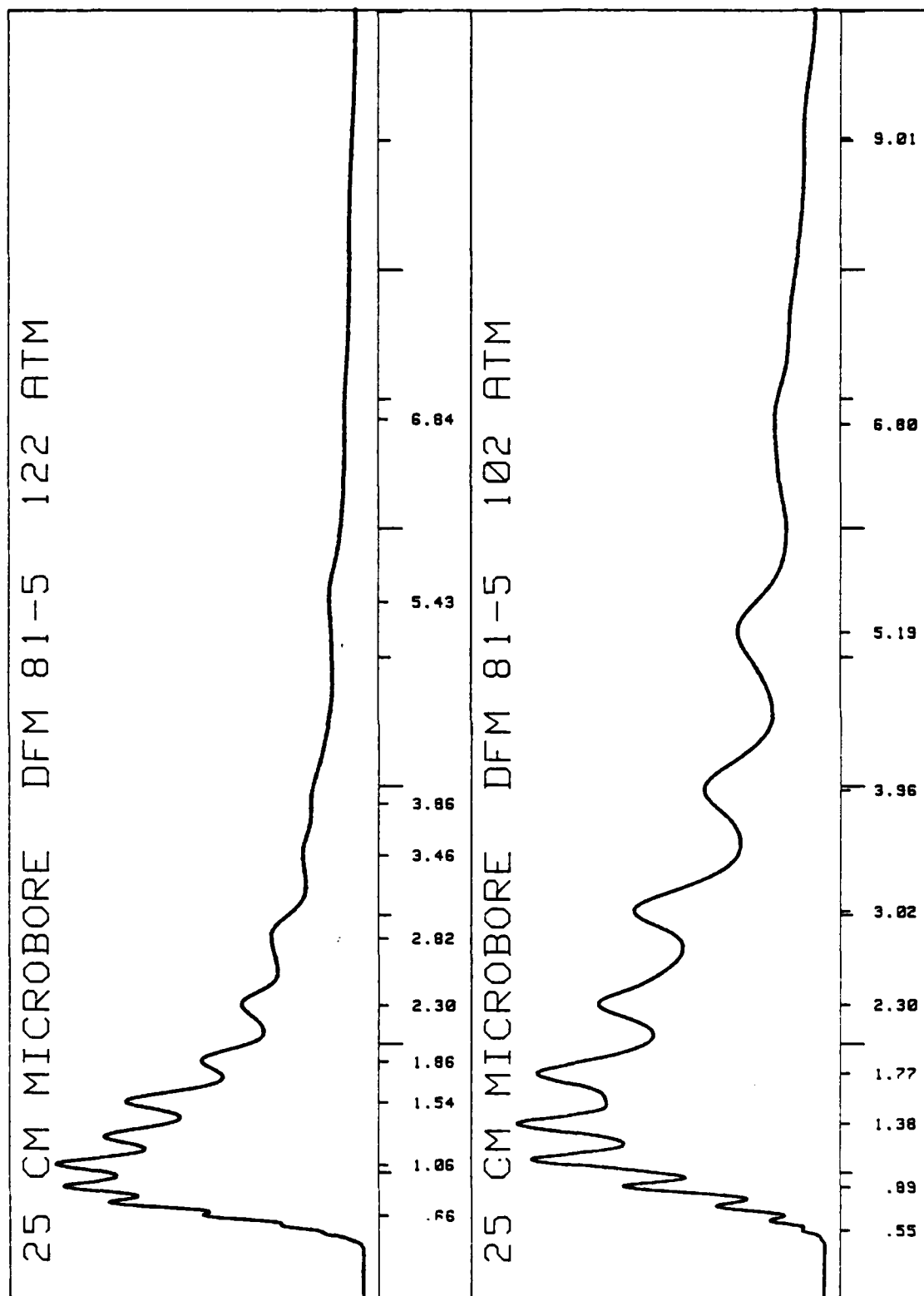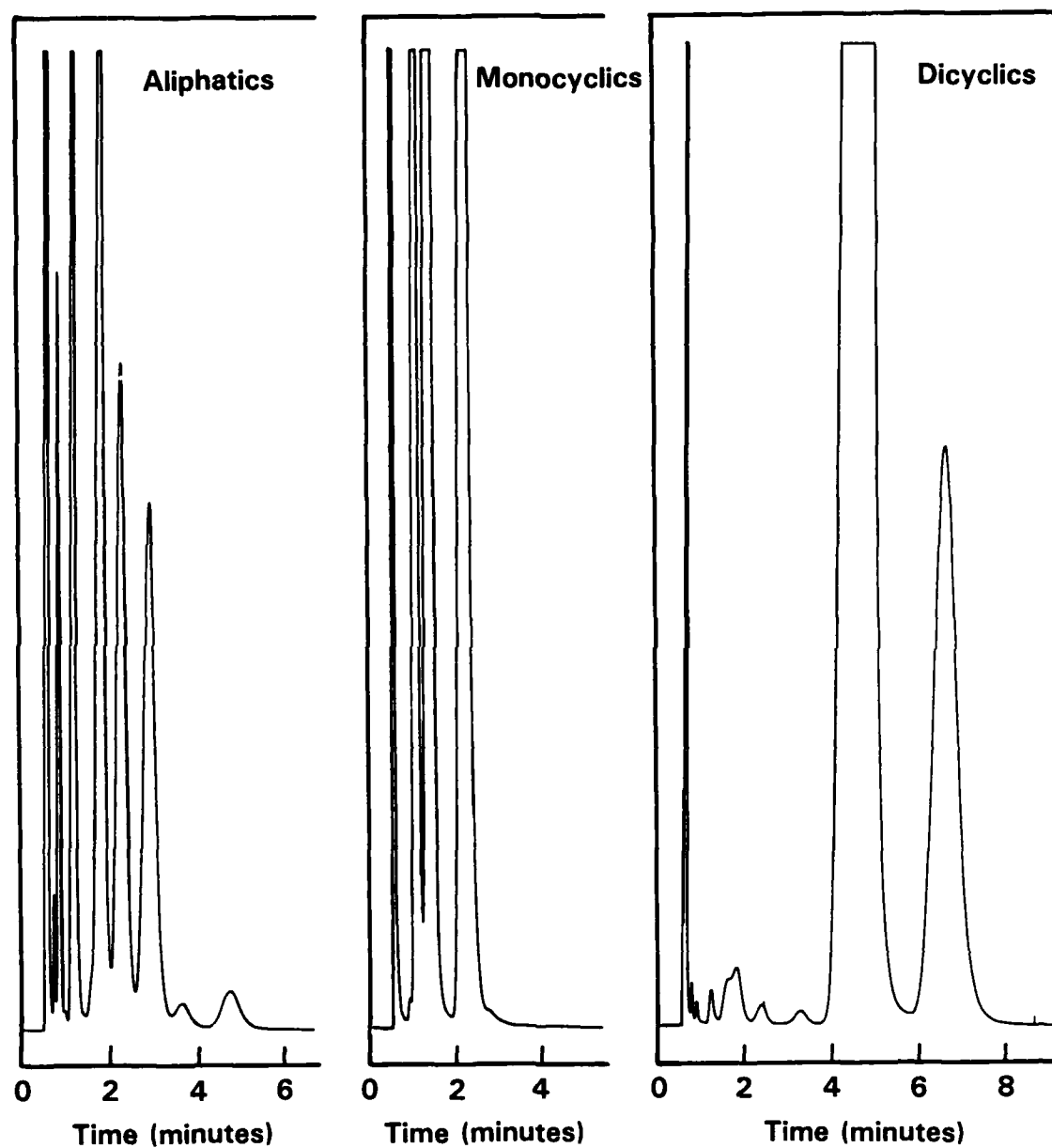tionation.
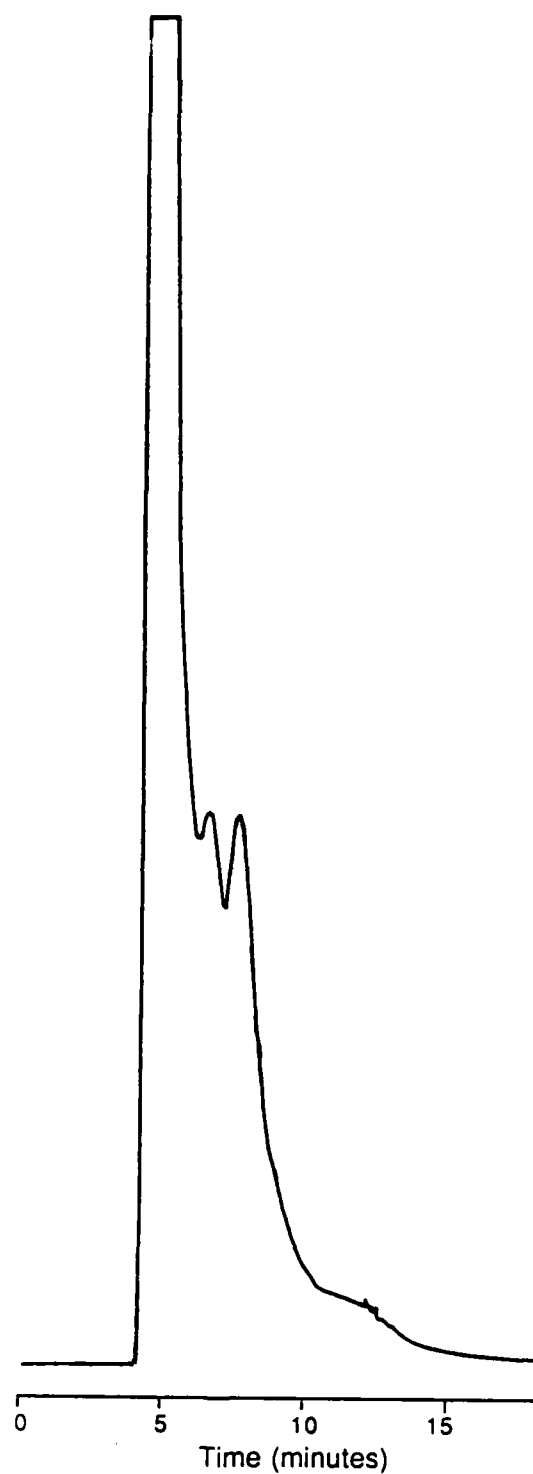
Figure 66.   SFC/FID chemical class fractionation chromatogram of DFM 81-5
obtained using a porous silica wall-coated capillary column
at 40°C and 110 atmospheres carbon dioxide.

Conclusions

Chemical class fractionation using supercritical fluid chromatography and flame ionization detection was shown to be marginally feasible. The best chromatographic results were obtained using a standard packed HPLC column and the most compatible detector flow rates were achieved using microbore or capillary columns. Shorter guard columns and 10 cm microbore columns did not provide adequate separation efficiency and the chemical classes were not sufficiently resolved. The utilization of 25 cm microbore columns also proved unfeasible due to the individual separation of the aliphatic components which overlapped with the monocyclic components. The porous silica wall-coated capillary columns also failed to provide adequate separation or selectivity between the various chemical classes. Thus, the best overall results in these studies were obtained using a standard packed HPLC column with effluent splitting. These results clearly suggest that more appropriate microbore columns to achieve such separations are feasible, but further development will be required to determine the correct combination of stationary phase, column parameters, and fluid conditions. Such a development would eliminate any effluent splitting and provide the desired quantitative capability. The utilization of a PAC (polyaminocyano) column might provide satisfactory performance since this column type has been successfully used for aliphatic, monocylic, and dicyclic chemical class fractionations in HPLC (66-67).

Task F. CHEMICAL CLASS FRACTIONATION ANALYSES

Introduction

The development and evaluation of various SFC chemical class fractiona-
tion methodologies were described in Task E. The most successful method
utilized a standard 4.6 mm i.d. x 25 cm silica packed HPLC column, a carbon
dioxide mobile phase, and effluent splitting prior to flame ionization detection.
The application of the methodology to obtain quantitative chemical class
fractionation data for twelve middle distillate fuels is described in this
section.

Experimental

The middle distillate fuels utilized in this investigation included
NRL 81-5 (DFM), NRL 81-6 (DFM), NRL 83-2 (DFM), NRL 83-4 (No. 2 heating
oil), NRL 82-10B (DFM), NRL 83-6 (light cycle oil (LCO)), NRL 1773 (30% LCO
in straight run (SR)), NRL 2059 (SR), NRL 1770 (SR), NRL 1771 (LCO), NRL 2060
(LCO), and NRL 2065 (30% LCO in SR).

The instrumentation for packed column SFC/FID chemical class fractiona-
tion was described in detail in the previous section. Slightly different
operating parameters of 45°C and 200 atmospheres carbon dioxide pressure
were found to provide the best resolution between chemical classes (e.g.,
aliphatics and olefins, monocyclic aromatics, dicyclic aromatics, and poly-
cyclic aromatics). The FID response for various chemical classes was cal-
ibrated by analyzing neat standards of hexane, iso-octane, benzene, and
toluene. Solutions of representative dicyclic and polycyclic aromatic com-
pounds were also analyzed to define retention time windows for their elution.
The FID signal was digitized and the chromatographic profiles integrated
with a Nelson Analytical 4416 chromatographic data system.

Results and Discussion

The chromatograms obtained from the chemical class fractionation analyses
of the twelve middle distillate fuels are shown in Figures 67-72. In general,

139

Figure 67.   SFC/FID chemical class fractionation chromatograms of middle
               distillate fuels obtained with a 25 cm x 4.5 mm silica
               column (5 μm) and carbon dioxide at 45°C and 200
               atmospheres.

140
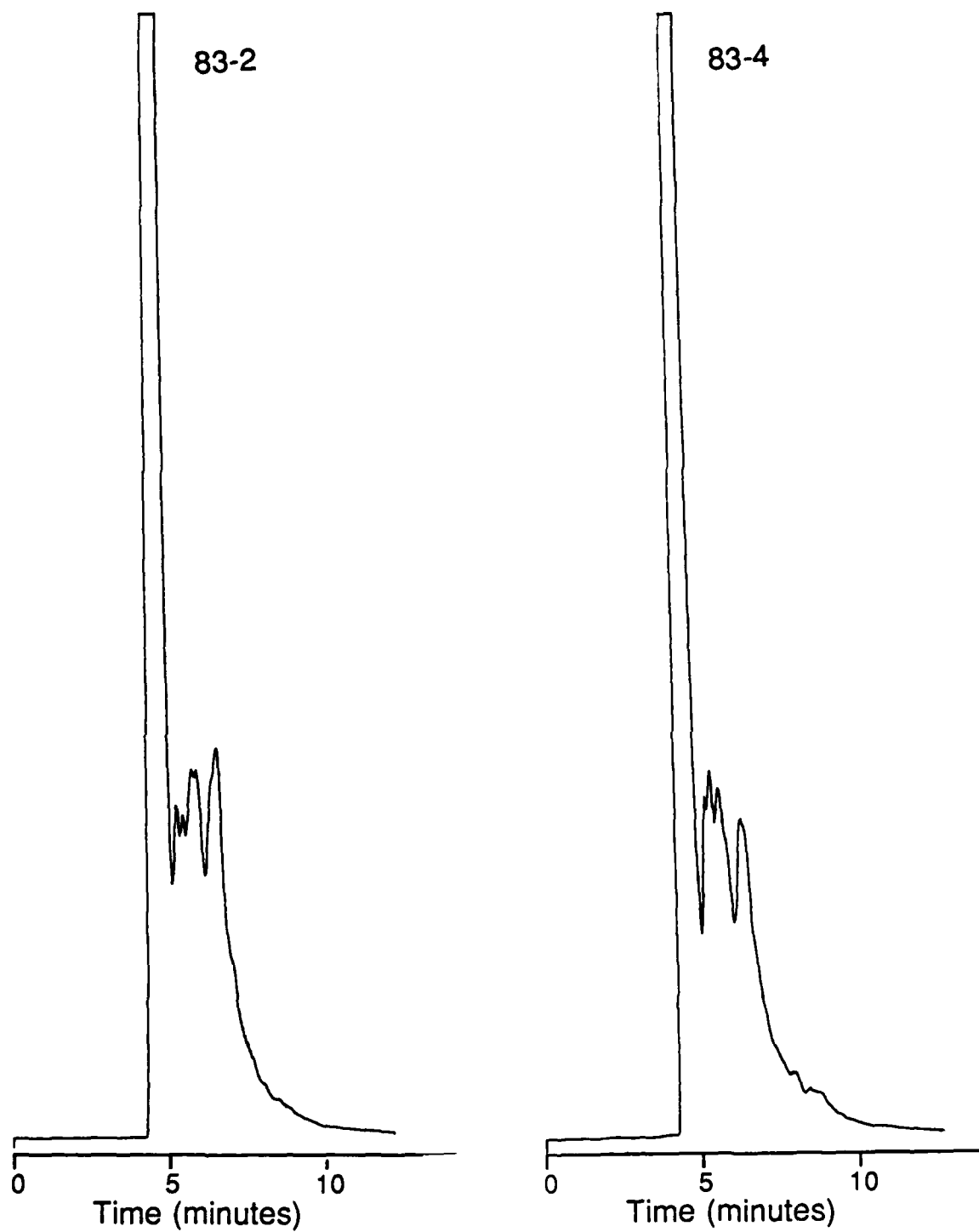
Figure 68.   SFC/FID chemical class fractionation chromatograms of middle distillate fuels obtained with a 25 cm x 4.5 mm silica column (5 μm) and carbon dioxide at 45°C and 200 atmospheres.
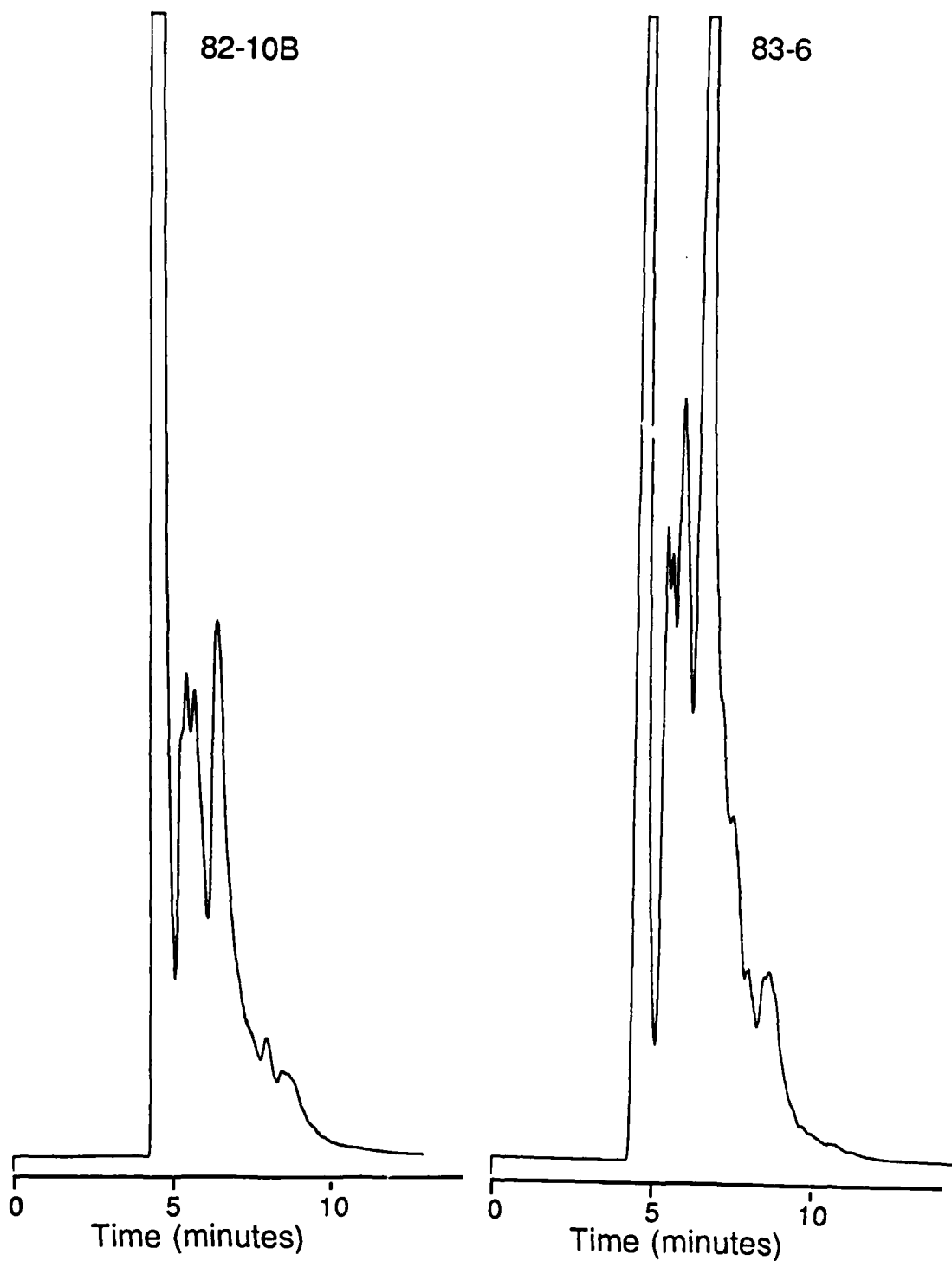
Figure 69.   SFC/FID chemical class fractionation chromatograms of middle
distillate fuels obtained with a 25 cm x 4.5 mm silica
column (5 µm) and carbon dioxide at 45°C and 200
atmospheres.

142

Figure 70.   SFC/FID chemical class fractionation chromatograms of middle
              distillate fuels obtained with a 25 cm x 4.5 mm silica
              column (5 μm) and carbon dioxide at 45°C and 200
              atmospheres.

143

Figure 71.   SFC/FID chemical class fractionation chromatograms of middle
               distillate fuels obtained with a 25 cm x 4.5 mm silica
               column (5 μm) and carbon dioxide at 45°C and 200
               atmospheres.
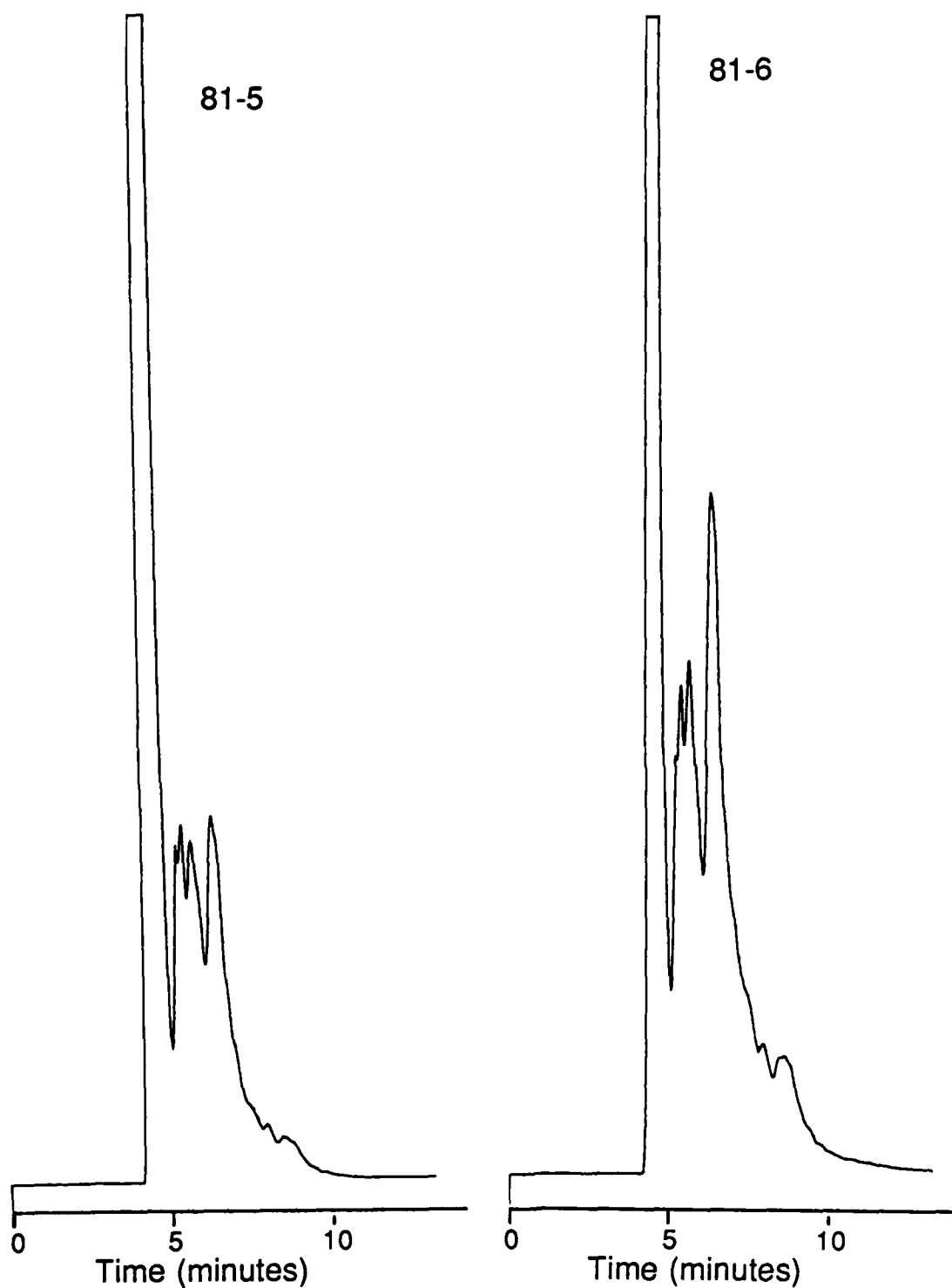
Figure 72.   SFC/FID chemical class fractionation chromatograms of middle distillate fuels obtained with a 25 cm x 4.5 mm silica column (5 μm) and carbon dioxide at 45°C and 200 atmospheres.
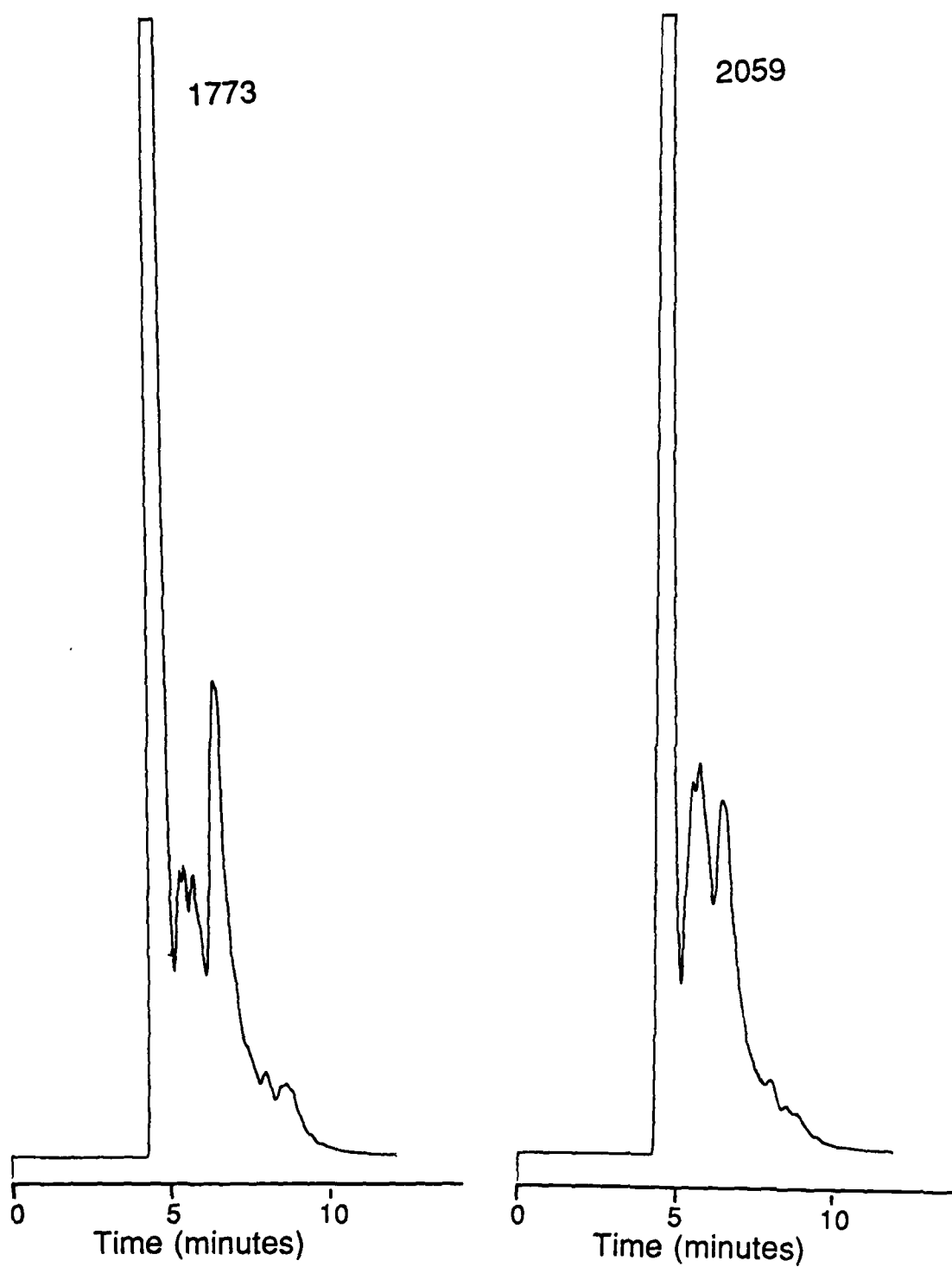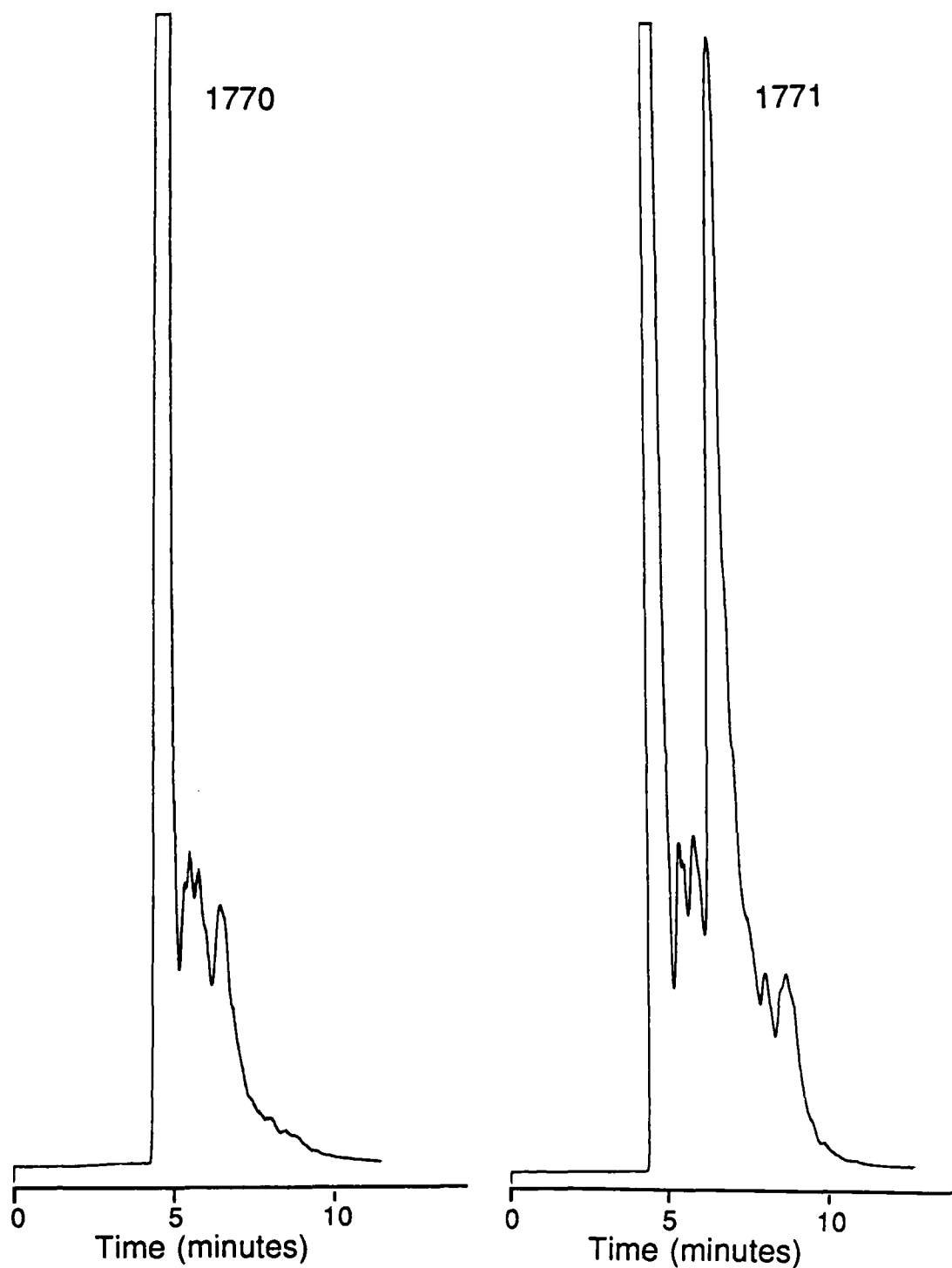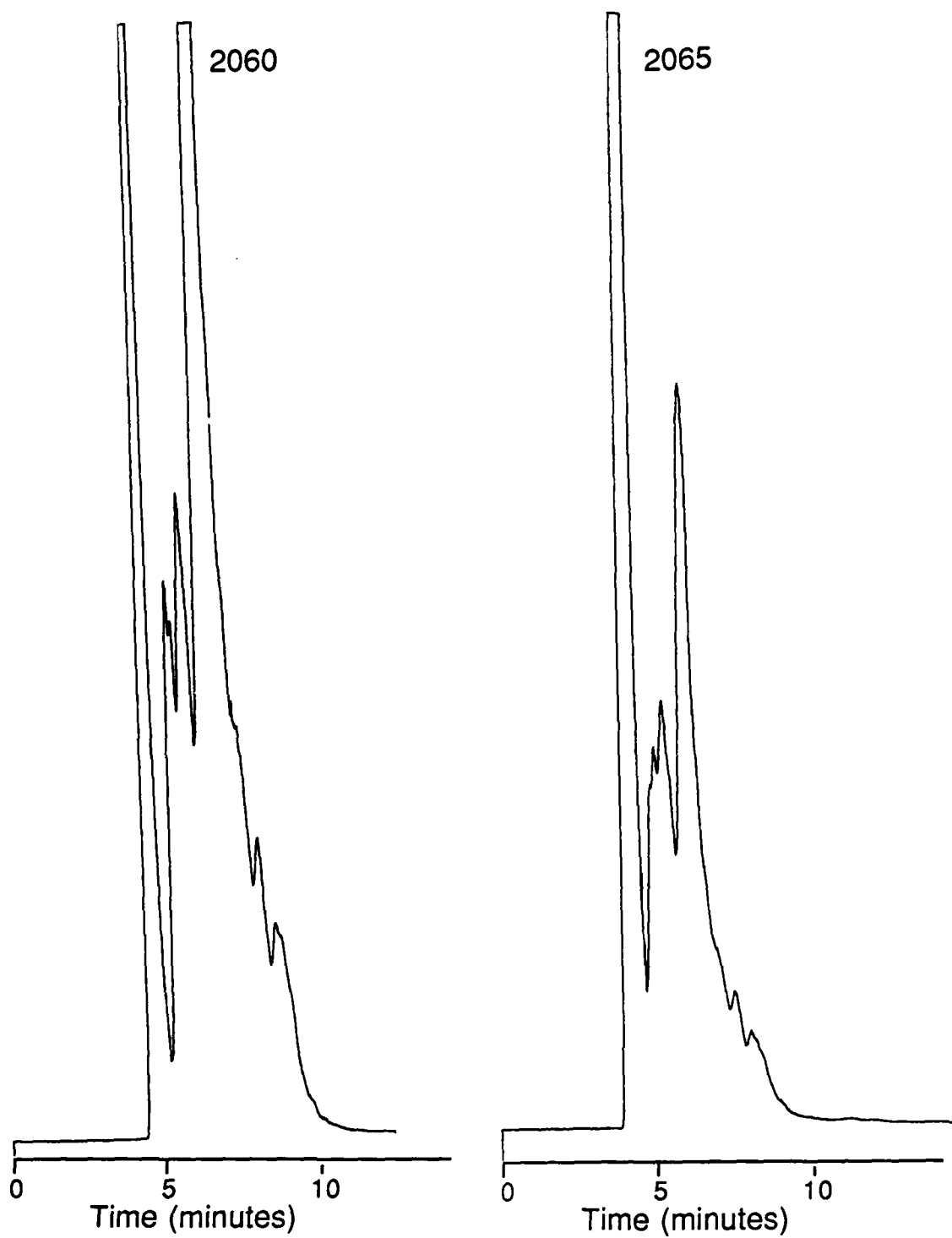
the DFM and SR fuels can be qualitatively characterized by high aliphatic concentrations and lower levels of monocyclic and dicyclic aromatic compounds. The LCO fuels, however, had as high of concentrations of dicyclic aromatic compounds as aliphatic compounds. As would be expected, the blended fuels had lower dicyclic aromatic compound concentrations than the LCO fuels, but higher concentrations than the SR fuels.

An important consideration for quantitative chemical class fractionation analyses is the detector response for compounds from different chemical classes, and to a lesser extent, for compounds within each chemical class. The flame ionization detector, in general, exhibits response proportional to the mass of an organic compound, which is nearly independent of its specific structure. However, since some differences exist, response factors for representative aliphatic and aromatic compounds were evaluated. These response factors are listed in Table 12. Each compound was injected several times and an average area (μv-sec) determined. The variance between injections was relatively low as reflected by the low relative standard deviations (RSD) (0.4-3.8%) listed in parentheses by the average area. The response factors were calculated relative to iso-octane since it gave the lowest response per unit mass injected. Both aliphatic compounds had very similar response factors (within 3%) and both aromatic compounds had very similar response factors (within 2%). The overall difference in response factors between the aliphatic and aromatic compounds was only approximately 10%. The response factors for dicyclic aromatic compounds would be expected to be similar to the monocyclic aromatic compound response factors, and depending on the substitution, could be intermediate between the aliphatic and monocyclic aromatic compound response factors. The overall similarity of response factors greatly simplifies the quantitative aspects of chemical class fractionation analyses.

The area and area percent of each chemical class fraction for the various fuels are listed in Table 13. It should be noted that the olefins were not well resolved from the aliphatic compounds and thus, the aliphatic class also includes the olefins. The weight percent data for each chemical class fraction for the various fuels are listed in Table 14. Weight percent was calculated using an average response factor of 0.98 for the aliphatic compounds, 0.91 for the monocyclic aromatic compounds, 0.93 for the dicyclic aromatic

146

TABLE 12

Response Factor Calculation Summary

Compound	Density	Average Area Count	Relative Response Factor*
h-hexane	0.6603	27,758,118 (3.8% RSD)	1.03
iso-octane	0.7025	28,633,932 (2.9% RSD)	1.00
benzene	0.8765	39,748,076 (0.8% RSD)	1.11
toluene	0.8669	38,317,738 (0.4% RSD)	1.08

*Area/amount (relative to iso-octane)

TABLE 13

Area Percent Data for the Chemical Classes of the Various Fuels

Fuel	Area (µv-sec)				Area Percent			
	Aliphatics	Monocyclics	Dicyclics	Polycyclics	Aliphatics	Monocyclics	Dicyclics	Polycyclics
81-5	24261034	3503616	3908514	780775	74.8	10.8	12.0	2.4
81-6	17797928	4694451	8790005	949024	55.2	14.6	27.3	2.9
83-2	25755236	1766409	1885991	<1000	87.6	6.0	6.4	<0.1
83-4	25446113	3698711	4360979	296712	75.3	10.9	12.9	0.9
82-10B	21283404	4797710	5780736	1599331	63.6	14.3	17.3	4.8
83-6	10105352	6281712	14208912	1655424	31.3	19.5	44.0	5.1
1773	21430072	2745771	4472088	120173	74.5	9.5	15.5	0.5
2059	21820276	3784120	4203661	420946	72.2	12.5	13.9	1.4
1770	25506183	3007715	3136138	234061	80.0	9.4	9.8	0.7
1771	17320451	3116457	5043648	1328374	64.6	11.6	18.8	5.0
2060	8259337	6700703	24047532	3178189	19.6	15.9	57.0	7.5
2065	16726281	4328042	9163188	761675	54.0	14.0	29.6	2.4

TABLE 14

Chemical Class Weight Percent Data for the Various Fuels

Fuel	Weight Percent			
	Aliphatics	Monocyclics	Dicyclics	Polycyclics
81-5	75.9	10.2	11.6	2.3
81-6	56.7	13.9	26.6	2.8
83-2	88.3	5.6	6.1	<0.1
83-4	76.4	10.3	12.4	0.8
82-10B	65.0	13.6	16.8	4.6
83-6	32.6	18.8	43.5	5.0
1773	75.6	9.0	15.0	0.4
2059	73.4	11.8	13.4	1.3
1770	81.0	8.9	9.4	0.7
1771	66.0	11.0	18.2	4.8
2060	20.5	15.4	56.6	7.4
2065	55.5	13.3	28.8	2.4

compounds, and 0.92 for the polycyclic aromatic compounds. The differences between area and weight percent are nearly insignificant as would be expected. The quantitative values for the chemical class fractions vary between 20.5 and 81.0 wt.% for the aliphatic compounds, 5.6 and 18.8 wt.% for the monocyclic aromatic compounds, 6.1 and 56.6 wt.% for the dicyclic aromatic compounds, and 0.0 to 7.4 wt.% for the polycyclic aromatic compounds.

Undoubtedly, the largest quantitative errors result from the integration of the chromatograms. Typical plots acquired with the chromatographic data system are shown in Figure 73. These chromatograms were generated from the same analyses as the chromatograms shown in Figures 67 and 72. The time scales were extended and the signal intensities attenuated to allow the peaks to be on scale. Since the peaks for each chemical class were not totally resolved, integration is more difficult. As can be observed in Figure 73, a combination of projected baselines and vertical cut off points were utilized to define specific peaks. The monocyclic aromatic fraction was usually integrated as two or three peaks which were then summed. Since the chemical class fractions were not totally resolved, integration errors probably limit the overall quantitative accuracy to within ± 10%. Better resolution of the chemical class fractions would allow more accurate integration. Newer chemometric methods for chromatographic data also promise more accurate quantitation based upon such data.

Conclusions

SFC/FID chemical class fractionation methodology was successfully utilized to obtain quantitative class fractionation data for twelve middle distillate fuels. The response factors for various compounds appear to be very similar which simplifies quantification.
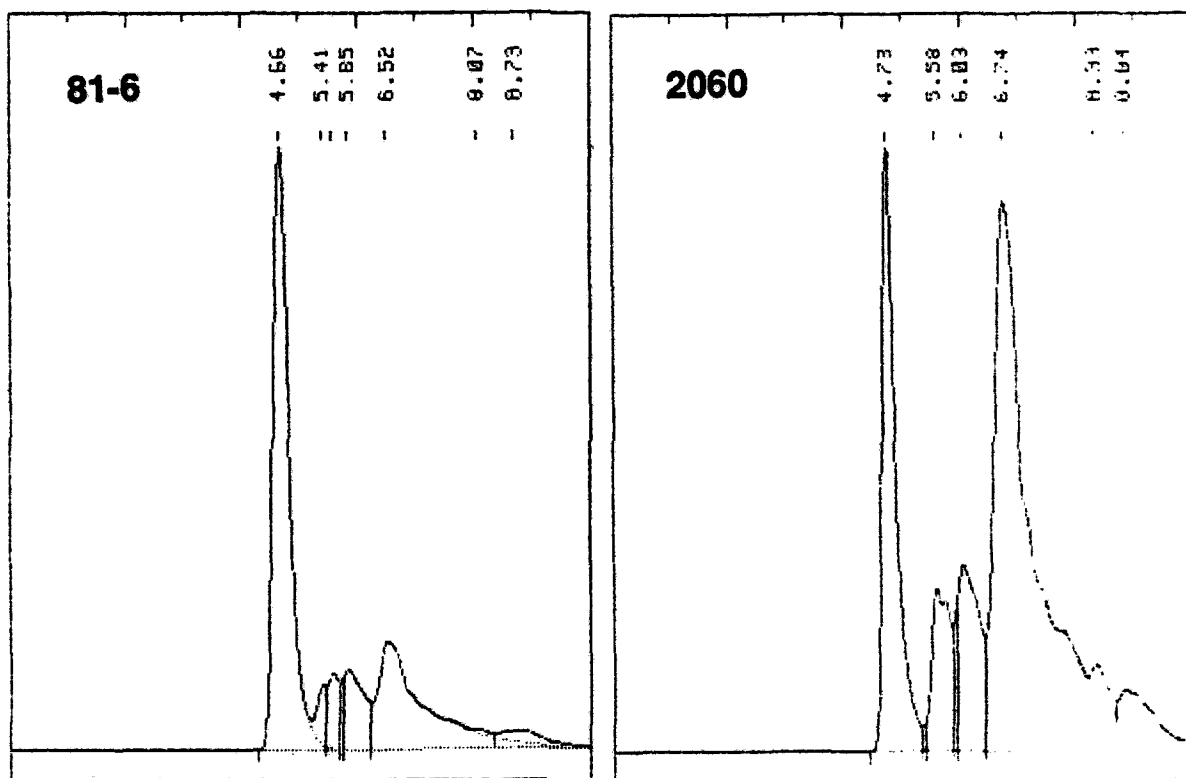
Figure 73.   Typical chemical class fractionation chromatograms obtained
with the chromatographic data system.

TASK G. ANTIOXIDANT ANALYSIS DEVELOPMENT USING SUPERCRITICAL FLUID
EXTRACTION-GAS CHROMATOGRAPHY

Introduction

Various additivies (e.g., stabilizers, antioxidants, etc.) are utilized
to modify specific aspects of fuel behavior and performance. Complicated
and time consuming sample preparation is currently necessary to accurately
determine low levels of these additives. Monitoring depletion at ppm levels
of these additives and developing a correlation of fuel behavior with additive
concentration presents a challenging analytical problem.

On-line supercritical fluid extraction-gas chromatography exploits the
selective solvating power and fractionation capacity of supercritical fluid
extraction to isolate an appropriate fraction (containing the additive(s))
from the fuel and deliver it to the inlet of a capillary gas chromatographic
column for subsequent high resolution chromatographic analysis. The fraction-
ation capability is based upon variation of fluid solvating power by manipu-
lation of pressure and/or temperature. This approach allows trace levels
of an analyte to be concentrated at the column inlet by extracting as large
a fuel volume as necessary for the required sensitivity. The on-line approach
offers intrinsically high sensitivity since all the material which is extracted
is also analyzed and eliminates the need for any manual work-up procedures.
Two-dimensional separation selectivity can be achieved by utilizing different
polarity separation mechanisms for the fractionation and chromatographic
steps. This section describes the initial development and application of
this methodology for the isolation and analysis of two fuel additives from
a diesel fuel.

Experimental

The determination of two fuel additives was explored in this investi-
gation. They were FOA-3 stabilizer, a tertiary alkyl amine used to neutralize
acids and inhibit free radical formation in diesel fuels, and Ionol, a hin-
dered phenol (2,6-di-tert-butyl-4-methylphenol) used as an antioxidant in
JP-5 jet fuel. A blended diesel fuel, Code 2067, containing FOA-3 at 24

152

mg/l (~28 ppm) was used as the fuel matrix for both additives. Higher con-
centration levels of the additives, ranging from 250 ppm to 1 ppt, were
spiked into the fuels to aid method development.

Several supercritical fluid systems were evaluated to find optimum
selectivity for fuel extraction. They included carbon dioxide, Freon-13
(monochlorotorifluoromethene), and ethylene. These fluids have critical
temperatures of 31°, 28.9°, and 9.9°C, respectively, and allow low tem-
perature extraction.

The automated on-line SFE-gas chromatography instrumentation consists
primarily of four sections which includes a high pressure pump and extraction
cell, a switching valve and interface region, a gas chromatograph with a
flame ionization detector, and a minicomputer and its associated interface
circuitry. A schematic diagram of this instrumentation is shown in Figure
74.

A modified Varian 8500 syringe pump provided the high pressure supply
of fluid to the extraction cell. The fluid was generally purified by dis-
tillation through activated charcoal while filling the syringe pump. The
extraction cells were constructed from Swagelok stainless steel zero volume
1/4" to 1/16" column end fittings (SS-400-6-1ZV) containing two 1/4" o.d.
sintered stainless steel frits with 2.0 μm mean pore size separated by a
1/8" long x 3/16" o.d., cup-shaped stainless steel insert. The insert was
positioned with the closed end to the cell exit to prevent the fuel sample
from being entrained in the fluid flow. The 1/4" o.d. inlet to the extraction
cell was made by cutting and silver soldering the smoothed end from standard
1/16" o.d. stainless steel tubing that was inserted through a short length
(1-2") of 1/4" o.d. x 5/64" i.d. stainless steel tubing. This design provided
an entirely stainless steel extraction cell with a total volume of approxi-
mately 25 μl (excluding internal frit volumes). Larger cell volumes could
be obtained by using different inserts. The extraction cell and several
inches of inlet tubing were placed inside a thermostatically regulated heating
block to control the fluid and extraction cell temperature. Extraction
temperatures in the range of 20° to 40°C were generally used. For extrac-
tion temperatures cooler than ambient (e.g., 25°C), the cell was removed
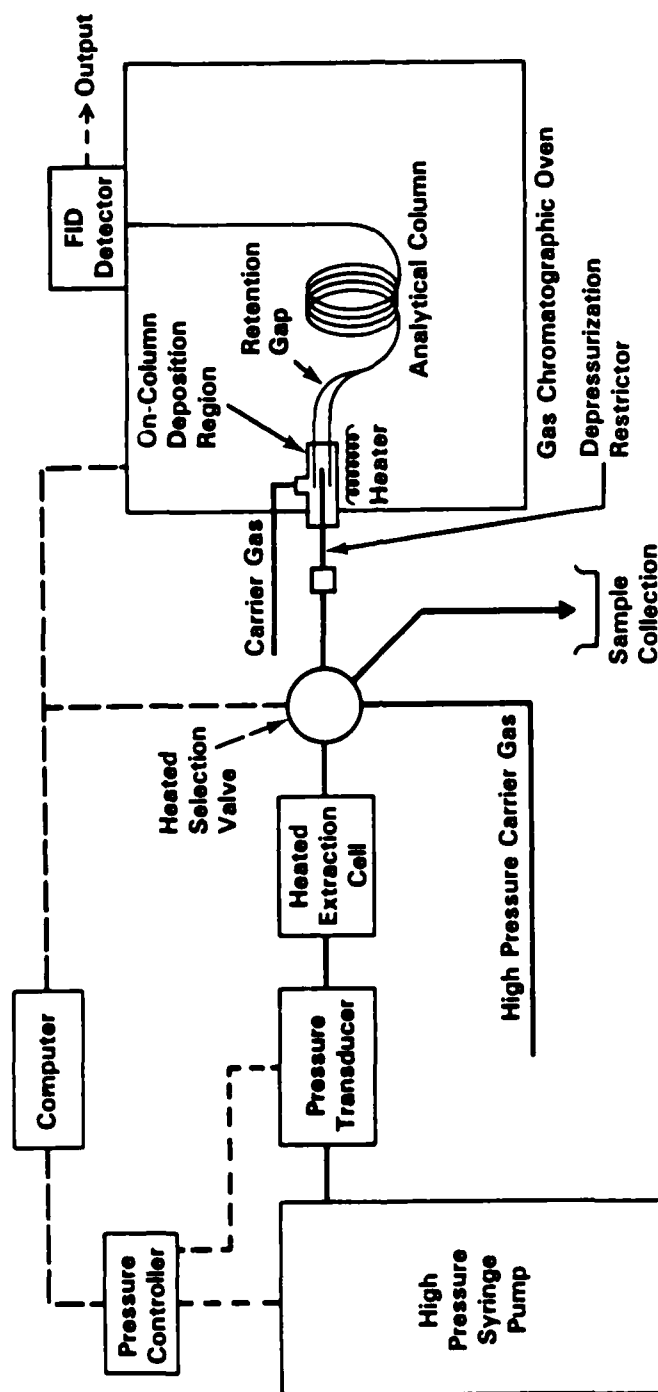from the heating block and wrapped with copper tubing. A water-ethylene

153

Figure 74.   Schematic diagram of the on-line supercritical fluid extraction-gas chromatography instrumentation.

glycol solution at the desired temperature was circulated through the tubing to cool the cell.

An air-actuated Rheodyne 7010 six-port switching valve was used to direct the extraction cell effluent to either an exterior vent or to the gas chromatographic column for on-column deposition and concentration of the extract. Short lengths (2-4 cm) of nominally 5 μm i.d. fused silica were used as depressurization restrictors and to maintain supercritical pressures up to the point of on-column deposition or exterior venting. The restrictor for the on-column deposition was mounted through a 1/16" tee to allow the gas chromatograph carrier gas to enter coaxially along the restrictor. This connection was also mounted in a heated block to control the temperature of the restrictor and expansion region. Typically, this region was maintained near the upper operating temperature of the chromatographic oven which was between 150 and 200°C. High pressure carrier gas (300 psi) was also connected to the six-port valve which was alternately switched with the extraction effluent between the chromatographic column and the collection vent to purge any remaining extract from the system.

A Hewlett-Packard 5890 gas chromatograph equipped with a single flame ionization detector was used to perform the chromatographic analyses. Typically, 15 m x 0.25 mm i.d. fused silica capillary columns coated with a 0.25 μm film thickness of crosslinked 5% phenyl polymethylphenylsiloxane (SE-54) were utilized. A short retention gap of deactivated fused silica tubing (30 cm x 0.53 mm i.d.) was connected to the inlet of the chromatographic column to aid solute focusing and concentration of the extraction effluent. The fused silica retention gap was deactivated by simple silylation with hexamethyldisilazane at 350°C. A polyimide connection was made between the retention gap and the analytical column to prevent thermal drag during temperature programming. The chromatographic oven was cooled to 0°C with liquid carbon dioxide during on-column deposition and concentration of the extraction effluent. Subsequent analyses were performed by termination of the cooling and allowing the oven to warm to 40°C and temperature programming at 3°C/min to ~200°C. Helium was used for the carrier gas at linear velocities of approximately 40 cm/sec. Detector sensitivity was adjusted to give full-scale peak response for approximately 5 ng per component. Signal output

155

was acquired using a stripchart recorder or with a Nelson Analytical 4416 chromatographic data system.

The instrumentation was automated using an Apple IIe minicomputer with an Adalab interface card (Interactive Microware Inc., State College, PA) and other in-house designed control circuitry. System automation included computer operation of the syringe pump to control pressure, switching of the six-port valve, start-up of the gas chromatograph temperature program cycle, and initiation and termination of data acquisition. A Fourth computer program allowed automated operation in which a sample could be subjected to numerous extractions at selected pressures for defined time intervals. In addition, the computer monitored if fluid was still available in the pump, if the correct extraction pressure was reached, and if the oven temperature was ready for another cycle to begin.

Results and Discussion

For the SFE-GC approach to be successful for the analysis of low levels of fuel additives, two important conditions must be met. The additive(s) of interest must be soluble (and extractable) in the supercritical extracting fluid and a sufficiently wide range of solvent power must exist to allow selective extraction of the fuel. It would also be feasible for the additive(s) to exhibit negligible solubility in the fuel extracting fluid and then a second fluid could be utilized to extract the additive(s). However, it is much less likely that this second condition could be met. Successful application of these techniques also requires that sample volatility at the extraction temperature be quite low.

To evaluate the solubility (and extractability) of the two additives of interest in this study in supercritical carbon dioxide, nanogram levels of the additives were separately spiked into the extraction cell and extraction-chromatography analyses subsequently performed. Since identical extraction-analysis conditions were utilized as we assumed would be desirable for actual fuel analyses, accurate chromatographic elution temperatures for each additive were also obtained. A chromatogram obtained by SFE-GC of the Ionol antioxidant is shown in Figure 75. The extraction was done with carbon dioxide at 40°C and 125 atmospheres. The extraction effluent was deposited
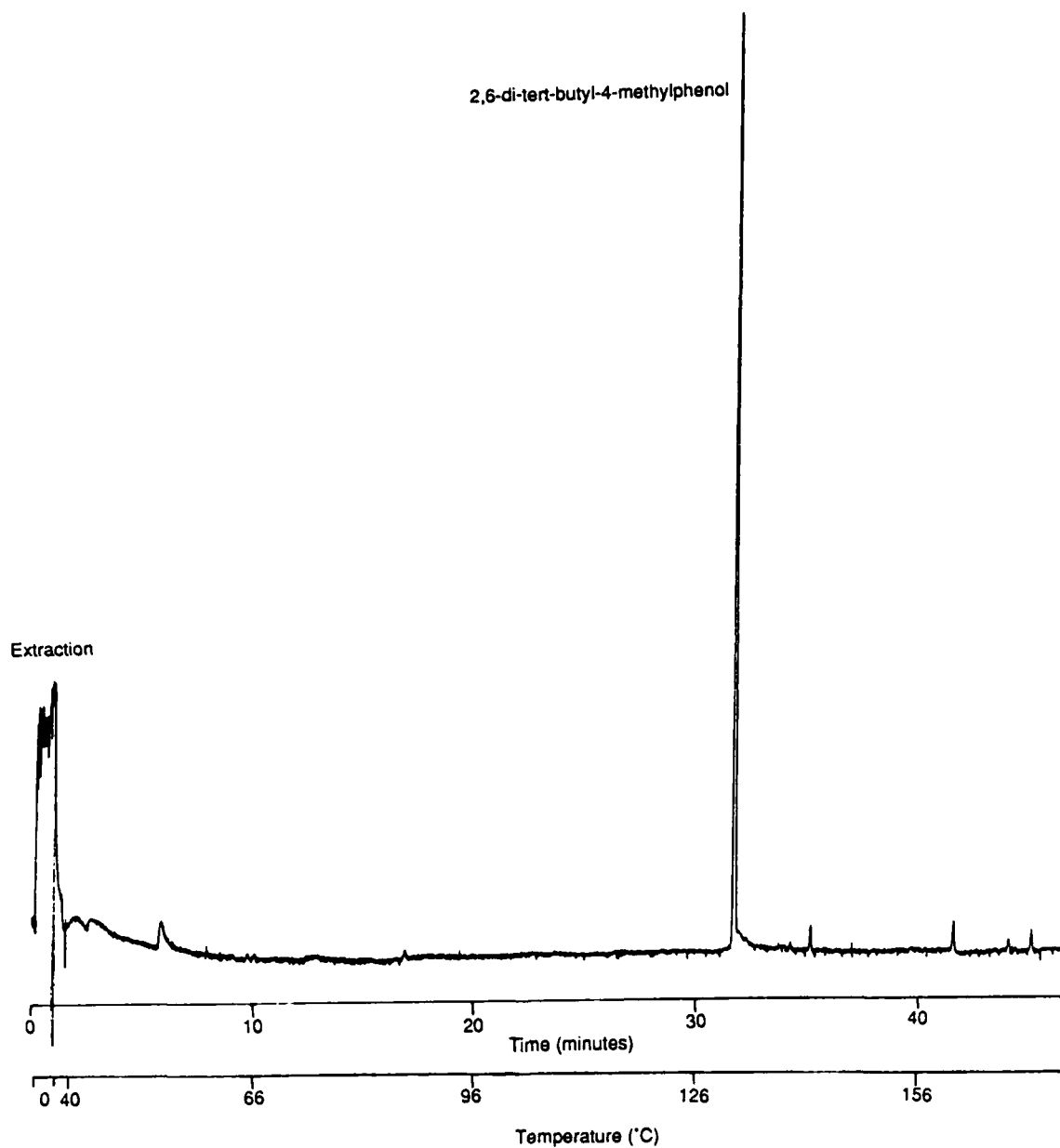
156

Figure 75.   Supercritical fluid extraction - capillary gas chromatogram of Ionol antioxidant additive. Conditions: 1 min CO_2 extraction at $40^{\circ}C$ and 125 atm, on-column collection at $0^{\circ}C$, temperature programmed from $40^{\circ}C$ at $3^{\circ}C/min$, 15 m x 0.25 mm i.d. crosslinked SE-54 column.

157

into the entrance of the chromatographic column that was cooled to 0°C.
After the extraction period (1 minute) was completed, the oven temperature
was ballistically heated to 40°C and a temperature ramp at 3°C/min initiated.
The Ionol eluted at an oven temperature of 130°C under these conditions.
To determine if the Ionol would be extracted at lower solvating powers,
additional extraction-analyses were performed at progressively lower pressures
until the critical pressure of 73 atmospheres was reached. (The lowest
convenient pressure for a fluid with a critical temperature near ambient
conditions is near the critical pressure due to the gas-liquid equilibria;
attaining lower pressures with syringe pumps requires a more complex system
or cooling of the syringe.) Even at 73 atmospheres the Ionol was rapidly
and efficiently extracted. The same experiments were also done for the
FOA-3 additive. A typical chromatogram obtained by SFE-GC is shown in Figure
76. This extraction was also done with carbon dioxide at 40°C and 125
atmospheres, but extraction at 73 atmospheres also proved successful. The
same chromatographic conditions described above were also utilized for these
analyses. The FOA-3 additive eluted at 60°C under these conditions.

Since the first condition (e.g., additives soluble and extractable)
was met, an actual fuel sample spiked with 250 ppm of both Ionol and FOA-3
was subjected to SFE-GC. The chromatogram of this analysis is shown in
Figure 77. Extraction was done very close to the critical point (75
atmospheres) to achieve as low of solvating power as possible, without cooling
the syringe, and hence obtain selective extraction of the additives and the
more soluble portion of the fuel. However, the chromatogram obtained from
this extraction-analysis was very complex and it appears that a significant
portion of the total fuel was extracted. The locations in the chromatogram
of the expected elution points for the additives are marked by an asterisk.
However, due to the complexity of the chromatogram, it would be difficult
to unambiguously identify (on the basis of retention time) and quantify
such low level components. (Mass selective detection would provide additional
selectivity and sensitivity, but a more selective fractionation process
would still be desireable). Extraction of the fuel containing higher levels
of th additives (1 ppt, parts per thousand) yielded essentially the same
chromatographic profile, except relatively large peaks obscured the elution
windows marked by the asterisks.
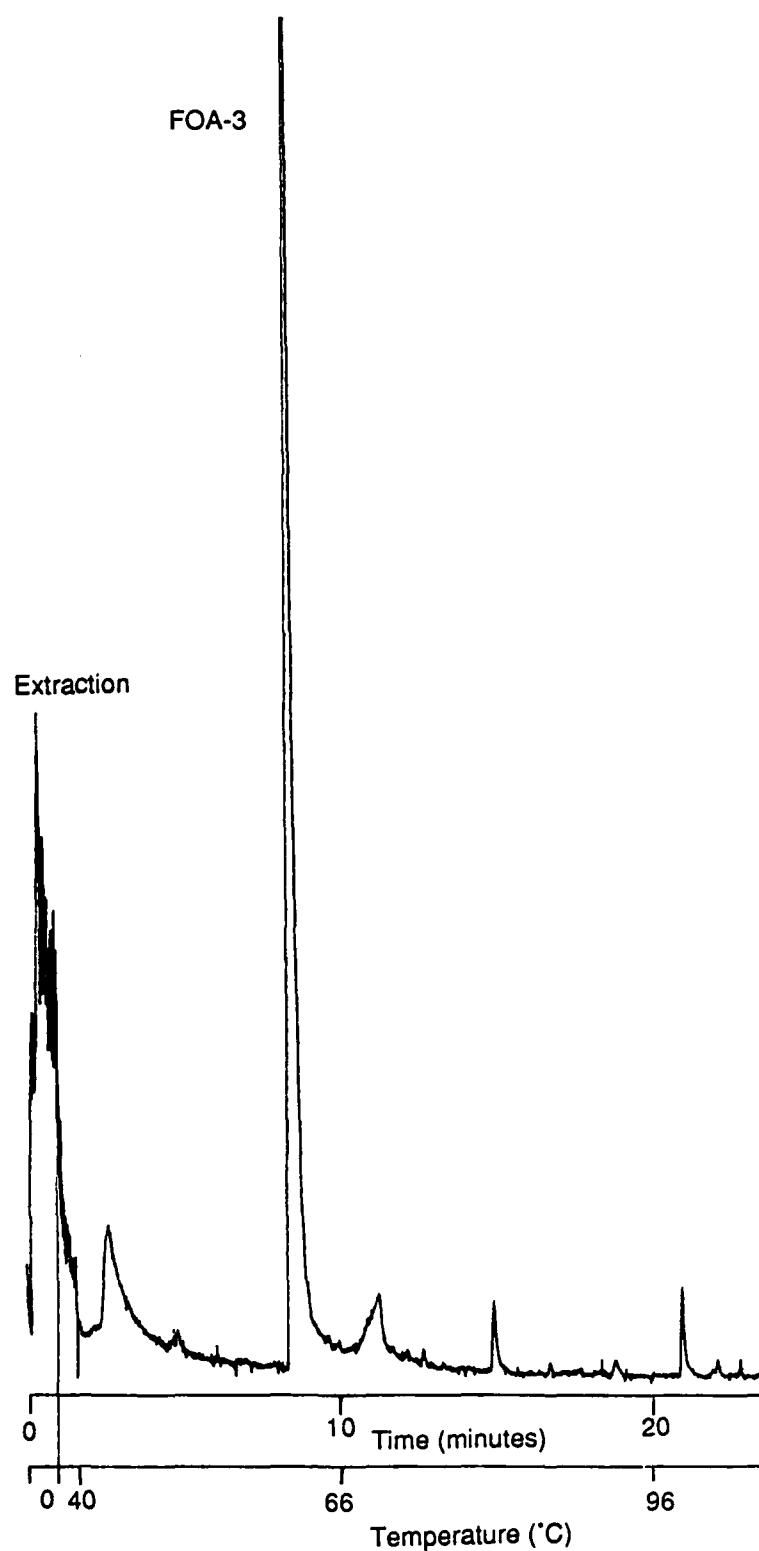
158

Figure 76.   Supercritical fluid extraction - capillary gas chromatogram
of FOA-3 additive. Conditions the same as in Figure 75.
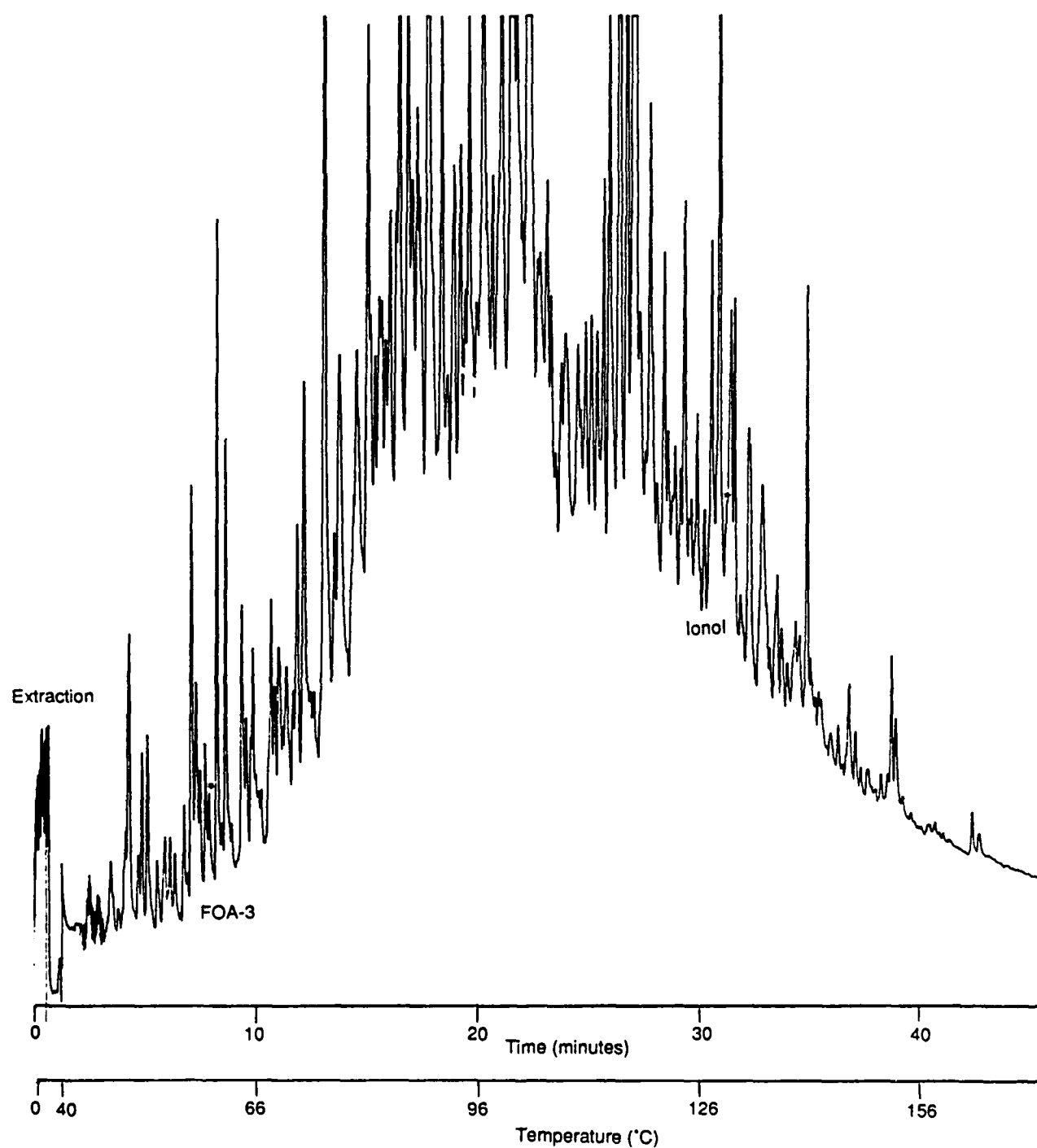
159

Figure 77.   Supercritical fluid extraction - capillary gas chromatogram
of fuel 2067 spiked with an additional 250 ppm FOA-3 and
Ionol. Conditions: 0.5 min CO_2 extraction at 40°C and 75
atm, other conditions the same as in figure 75.

160

The fuel components are quite volatile at 40°C and a competing mechanism of volatility and solubility could be operative for sample transport. Thus, in an attempt to minimize volatility influences, a lower temperature of 35°C and a somewhat lower pressure of 70 atmospheres was used for extraction of the fuel. The chromatogram obtained from this extraction-analysis is shown in Figure 78. A different chromatographic profile was obtained with a higher concentration of lower molecular weight material. This trend indicates more selective extraction conditions for the more soluble components were actually obtained. Again, the expected elution points for the two additives are marked by asterisks in the chromatogram. A higher concentration of FOA-3 (indicated by the potential FOA-3 peak) was obtained in this analysis than observed in the analysis shown in Figure 77. The Ionol, however, (indicated by the potential Ionol peak) was in lower concentration than obtained in the previously described analysis, which is consistent with more selective extraction conditions for lower molecular weight components. It is obvious that extraction conditions must be independently optimized for the two additives.

The above results indicate that although some selectivity could be obtained with supercritical carbon dioxide extraction, it was not possible to achieve sufficiently low solvating power to obtain the necessary selectivity to form highly enriched fuel fractions. Consequently, other supercritical fluids with lower solvating powers and lower critical temperatures were evaluated. Since the fuel is relatively volatile, a lower extraction temperature would increase the possibility of achieving a wider range of selective extraction conditions. Both Freon-13 and ethylene were evaluated as potential extracting fluids. Problems were encountered with the Freon-13, and since ethylene had a lower critical temperature, work with Freon was discontinued. Ethylene, unfortunately, gives a flame ionization response which requires the decompressed fluid to be purged through the capillary column prior to chromatographic analysis. This was not anticipated to be a serious problem, but as the chromatogram obtained from the SFE-GC analysis of the fuel using ethylene extraction shown in Figure 79 indicates, an excessively long time (e.g., 100 minutes) was required for the ethylene to be eliminated from the chromatographic column. This extraction was obtained at 20°C and 95 atmospheres and, even after waiting for 100 minutes, a reasonable chromatographic

161

Figure 78.   Supercritical fluid extraction – capillary gas chromatogram
             of fuel 2067 spiked with an additional 250 ppm FOA-3 and
             Ionol. Conditions: 0.5 min CO_2 extraction at 35°C and 70
             atm, other conditions the same as in Figure 75.
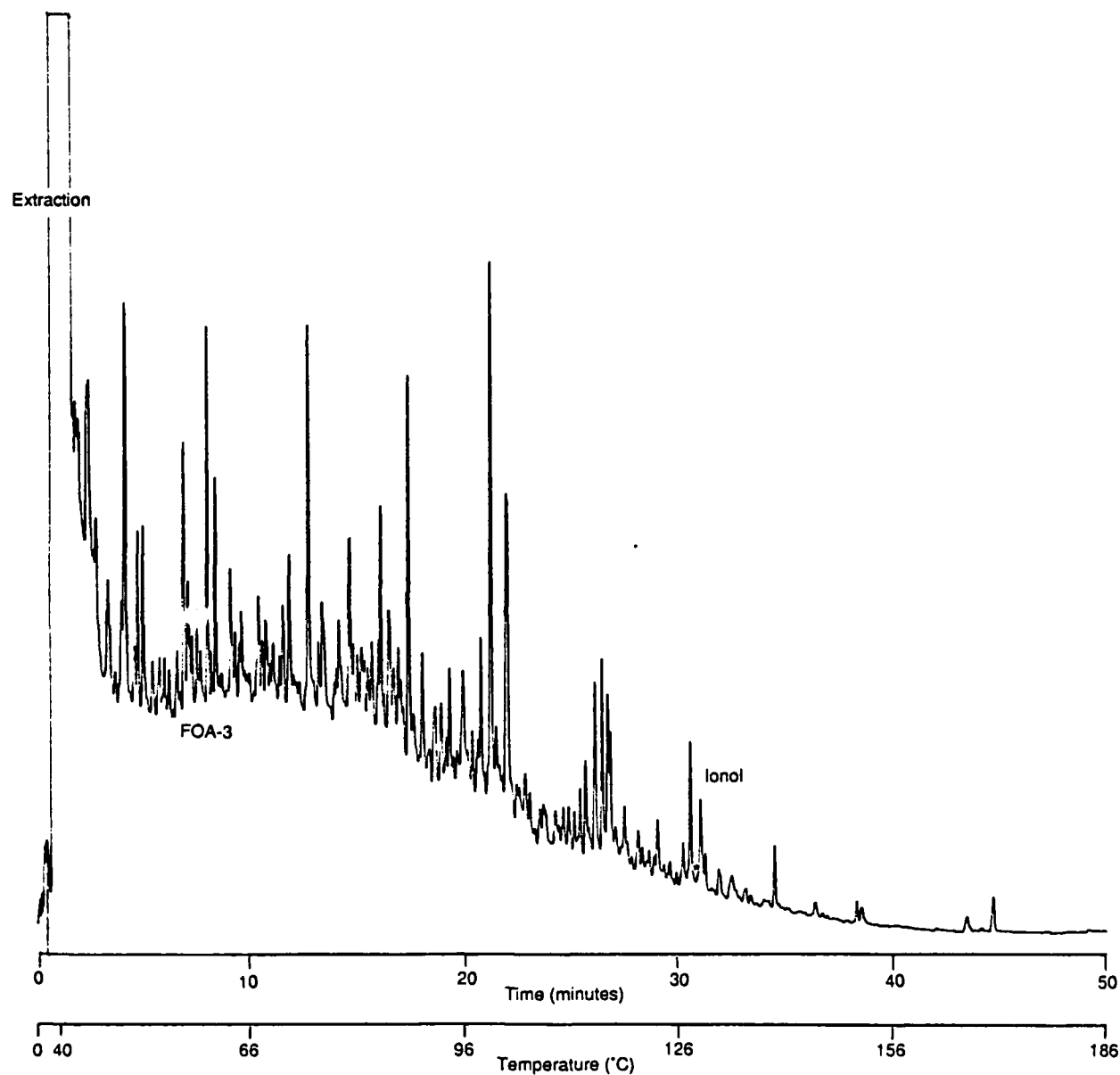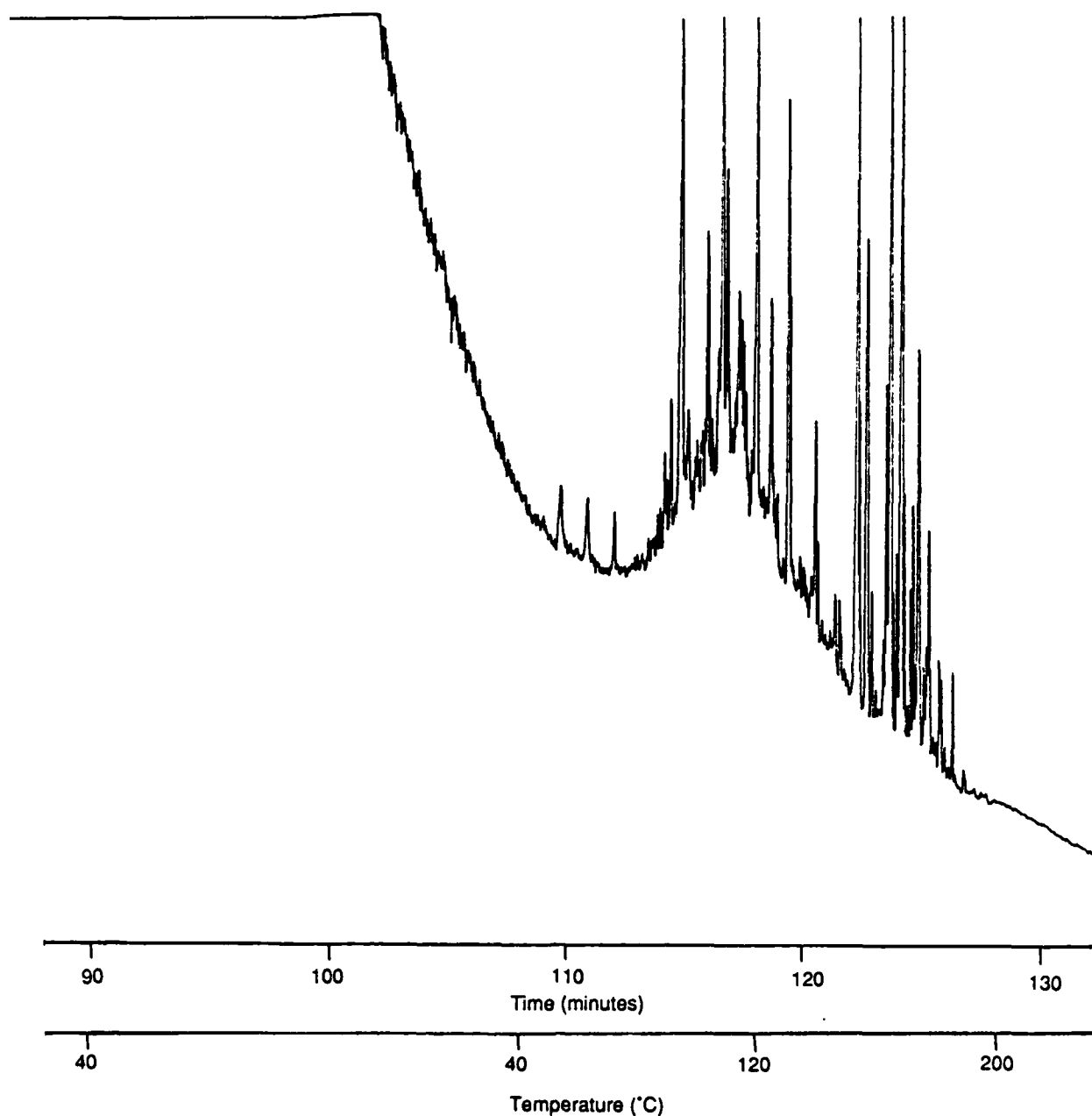
162

Figure 79.   Supercritical fluid extraction - capillary gas chromatogram of fuel 2067 spiked with an additional 250 ppm FOA-3 and Ionol. Conditions: 15 sec ethylene extraction at 20°C and 95 atm, on column collection at 0°C, temperature elevated to 40°C while ethylene purged, temperature programmed at 8°C/min, 15 m x 0.25 mm i.d. crosslinked SE-54 column.

163

separation of the fuel was obtained. Since, the critical pressure of ethylene is approximately 51 atmospheres and the critical temperature is 10°C, lower solvating power conditions (and lower volatility conditions) could be utilized to obtain a wider range of extraction selectivity than was obtained with carbon dioxide.

In order to reduce the amount of ethylene injected into the column, the flow restrictor was modified to limit the flow from the extraction cell. However, this did not make a significant difference. Next, a technique was implemented in which the ethylene was back-flushed out of the column through the carrier gas inlet after the extraction effluent had been deposited on the column. It was found that unless the column was maintained at less than 5°C during backflushing, a significant portion of the fuel was lost. Residual ethylene also remained after backflushing which still required in excess of twenty minutes to purge. The current flow system was not designed for backflushing and for more successful results using this concept, a differently designed system would need to be implemented. This would greatly complicate the instrumentation and a better option would be to find other non-FID responding fluids or fluid mixtures with low critical temperatures and low solvating powers. An unconventional fluid, such as krypton (critical temperature of -63°C), could conceivably provide the necessary properties. This is an important area of further investigation.

Conclusions

The initial evaluation of supercritical fluid extraction-gas chromatography for the analysis of trace levels of fuel additives suggests that with additional development a viable methodology might be developed. The present work demonstrates the concept of SFE-GC and illustrates that fuel additives and fuel components can be successfully extracted and analyzed. Additional work on choosing fluids and optimization of extraction conditions needs to be pursued. Carbon dioxide proved unsuitable as an extraction fluid due to too high of solvating power and/or critical temperature. Ethylene with lower solvating power and a lower critical temperature appeared to have an appropriate selectivity range, but due to its FID response, proved difficult to utilize. A non-FID responding fluid with low solvating power and a low critical temperature would be anticipated to provide the necessary conditions for the selec-

164

tive extraction of a fuel matrix to concentrate and analyze low levels of trace additives. Of the potential fluid systems, krypton seems to offer the most potential. Its low critical temperature (-64°C) would provide the flexibility necessary for subambient operation. In addition, the solubility parameter for Kr at liquid density is ~9.3; actually slightly larger than ethylene (8.8). Such a system would appear to offer general utility for SFE-GC fractionation procedures, but experimental studies are necessary to confirm this.

LITERATURE CITED

1. M. L. Lee and B. W. Wright, J. Chromatogr., 184, 235(1980).

2. B. W. Wright, B. E. Richter and M. L. Lee, in "Modern Aspects of Capillary
    Separations Techniques," M. Novotny (Ed.) Wiley and Sons,New York, NY
    (1985).

3. G. Schomburg, H. Husmann and H. Borwitzky, Chromatographia, 12, 651(1979).

4. T. J. Stark, R. D. Dendeneau and L. Mering, 1980 Pittsburgh Conference,
    Abstract 002, Atlantic City, NJ (1980).

5. L. Blombᵔrg, K. Markides and T. Wannman, J. High Resoln.
    Chromatogr./Chromatogr. Commun., 4, 527(1980).

6. B. W. Wright, Ph.D. Dissertation, Brigham Young University (1982).

7. R. C. Kong, C. L. Woolley, S. M. Fields and M. L. Lee, Chromatographia,
    18, 362(1984).

8. C. L. Woolley, R. C. Kong, B. E. Richter and M. L. Lee, J. High Resoln.
    Chromatogr./Chromatogr. Commun., 7, 329(1984).

9. J. Bouche and M. Verzele, J. Gas Chromatogr., 6, 501(1968).

10. R. C. Kong and M. L. Lee, J. High Resoln. Chromatogr./Chromatogr. Commun.,
    6, 319(1983).

11. B. W. Wright, P. A. Peaden, M. L. Lee and T. J. Stark, J. Chromatogr.,
    248, 17(1982).

12. E. Wilberg and E. Amberger, "Hydrides of Elements of Main Groups I-
    IV," Elsevier, New York, NY (1971).

13. D. R. Gere, R. D. Board and D. McManigill, Anal. Chem., 54, 736(1982).

14. H. H. Lauer, D. McManigill and R. D. Board, Anal. Chem., 55, 1370(1983).

15. M. G. Rawdon, Anal. Chem., 56, 831(1984).

16, T. Takeuchi, D. Ishil, M. Saito and K. Hibi, J. Chromatogr., 295, 323(1984).

17. J. C. Fjeldsted, R. C. Kong and M. L. Lee, J. Chromatogr., 179, 449(1983).

18. J. C. Fjeldsted and M. L. Lee, Anal. Chem., 56, 619A(1984).

19. T. L. Chester, J. Chromatogr., 299, 424(1984).

20. B. W. Wright, H. R. Udseth, R. D. Smith and R. N. Hazlett, J. Chromatogr.,
    314, 253(1984).

21. R. D. Smith, H. T. Kalinoski, H. R. Udseth and B. W. Wright, *Anal. Chem.*, 56, 2476(1984).

22. B. W. Wright, H. T. Kalinoski and R. D. Smith, *Anal. Chem.*, 57, 2823-2829 (1985).

23. P. A. Peaden, J. C. Fjeldsted, M. L. Lee, S. R. Springston and M. Novotny, *Anal. Chem.*, 54, 1090(1982).

24. J. C. Fjeldsted, W. P. Jackson, P. A. Peaden and M. L. Lee, *J. Chromatogr. Sci.*, 21, 222(1983).

25. D. Y. Peng, and D. B. Robinson, *J. AICHE*, 23, 132(1977).

26. A. S. Teja, R. L. Smith and S. I. Sandler, *Fluid Phase Equil.*, 14, 265 (1983).

27. B. W. Wright and R. D. Smith, *Chromatographia*, 18, 542(1984).

28. R. D. Smith, J. C. Fjeldsted and M. L. Lee, *J. Chromatogr.*, 247, 231(1982).

29. E. Brunner, *J. Chem. Therm.*, 17, 671 (1985).

30. L. G. Randall, "Ultrahigh Resolution Chromatography," S. Ahuja (Ed.), ACS Symposium Series: Vol. 250, Chpt. 11 (1984).

31. J. M. Levy and W. M. Ritchey, "Proceedings of the Sixth International Symposium on Capillary Chromatography," Huethig, Heidelberg, 925(1985).

32. R. N. Hazlett and J. M. Hall, "Chemical Aspects of Jet Fuel Thermal Oxidation Stability," p. 501-510, In: Fouling of Heat Transfer Equipment, ed. E. F. C. Somerscales and J. G. Knudsen, Hemishere Pub. Co., Washington, D.C., 1981.

33. J. H. Worstell and S. R. Daniel, *Fuel*, 60, 481-484 (1981).

34. J. R. Solash, R. N. Hazlett, J. C. Burnett, E. Beal, and J. M. Hall, in: ACS Symposium Series, No. 163, *Oil Shale, Tar Sands, and Related Materials*, H. C. Stauffer (Ed.), Chapter 16.

35. C. J. Nowack, R. J. Delfosse, G. Speck, J. Solash, and R. N. Hazlett, in: ACS Symposium Series No. 163, *Oil Shale, Tar Sands, and Related Materials*, H. C. Stauffer (Ed.), Chapter 18.

36. J. R. Solash, R. N. Hazlett, J. M. Hall and C. J. Nowack, *Fuel*, 57, 521-528 (1978).

37. K. E. Dahlin, S. R. Daniel, and J. H. Worstell, *Fuel*, 60, 477-480 (1981).

38. J. H. Worstell, S. R. Daniel, and G. Frauenhoff, *Fuel*, 60, 485-487 (1981).

39. F. R. Mayo and B. Y. Lan, Ind. Eng. Chem. Prod. Res. Dev., 25, 333 (1986).

40. J. Li and N. C. Li, Fuel, 56, 1041 (1985).

41. M. C. Loeffler and N. C. Li, Fuel, 56, 1047 (1985).

42. T. H. Gouw and R. E. Jentoft, Advan. Chromatogr., 13, 1 (1975).

43. B. W. Wright, H. R. Udseth and R. D. Smith, "Investigation of Super-critical Fluid Chromatography-Mass Spectrometry for Fuels Character-ization," Final Report from Battelle Pacific Northwest Laboratories to Naval Research Laboratory, Contract No. N0014-82-K-2065, March 16, 1984.

44. J. W. Goetzinger, C. J. Thompson and D. W. Brinkman, "A Review of Storage Stability Characteristics of Hydrocarbon Fuels, 1952-1983", 1983, DOE/BETC/IC-83/3.

45. R. D. Smith, H. R. Udseth and R. N. Hazlett, Fuel, 64, 810 (1985).

46. R. D. Smith and H. R. Udseth, Fuel, 62, 466 (1983).

47. R. A. Yost and C. G. Enke, J. Amer. Chem. Soc., 100, 2274 (1978).

48. J. V. Cooney, R. N. Hazlett, and E. J. Beal, "Mechanisms of Syncrude/Synfuel Degradation," NRL 2nd Annual Rpt. on DOE/Contract, Rpt. No. DOE/BC/10525-8, May 1984 and NRL 3rd Annual Rpt. on DOE/Contract, Rpt. No. DOE/BC/10525-15, March 1986.

49. L. Jones, D. R. Hardy, and R. N. Hazlett, Am. Chem. Soc. Div. Petrol. Chem. Prepr., 28, 1157-1164 (1983).

50. R. D. Smith and H. R. Udseth, Anal. Chem. 55, 2266-2272 (1983).

51. R. D. Smith, J. L. Fulton, R. C. Petersen, A. J. Kopriva and B. W. Wright, Anal. Chem. 58, 2057-2064 (1986).

52. T. L. Chester, D. P. Innis, G. P. Owens, Anal. Chem. 57, 2243-2247 (1985).

53. G. Eglinton, S. K. Haj Ibrahim, J. R. Maxwell, J.M.E. Quirke, G. J. Shaw, J. K. Volkman and A.M.K. Wardroper, Philos. Trans. R. Soc. London, Ser. A., 293, 69-91 (1979).

54. G. J. Shaw, J.M.E. Quirke, and G. Eglinton, J. Chem. Soc. Perkins Trans. 1, 1655-1659 (1978).

55. G. J. Shaw, G. Eglinton and J.M.E. Quirke, Anal. Chem., 53, 2014-2020 (1981).

56. R. Sundararaman, E. J. Gallegos, E. W. Baker, J.R.B. Slayback and M. R. Johnson, Anal. Chem. 56, 252 (1984).

57.   B. R. Tolf, X. Y. Jiang, A. Wegmann-Szente, L. A. Kehres, E. Bunnenberg and C. Djerassi, J. Amer. Chem. Soc. 108, 1363 (1986).

58.   D. H. Aue and M. T. Bowers, "Stabilities of Positive Ions from Equilibrium Gas-Phase Basicity Measurements", in: Gas Phase Ion Chemistry, M. T. Bower (Ed.), Academic Press, NY, 1979.

59.   J. W. Brankenteld, W. F. Taylor and D.W. Brinkman, "Fundamental Synthetic Fuel Stability Study," 1981, DOE/BC/10045-12.

60.   L. Jones, R. N. Hazlett, N. C. Li, and J. Ge, Am. Chem. Soc. Div. Fuel Chem. Prepr. 28, 196-202 (1983).

61.   L. Oller, C. C. Gleason, M. J. Kenworthy, J. D. Cohen and D. W. Bahr, AFWAL-TR-81-2100, Wright-Aeronautical Laboratory, May 1982. (AD B066 2076).

62.   P. L. Russel, Wright Patterson AFB, Rpt. No. AFWAL-TR-82-2114, Pt. II, June 1983. (AD B076 4601).

63.   "Manual on Hydrocarbon Analysis," 3rd Ed., American Society for Testing and Materials: Philadelphia, PA (1977).

64.   J. Solash, R. N. Hazlett, J.M. Hall and L. J. Nowack, Fuel, 57, 521(1978).

65.   J. C. Suatoni, H. R. Garber and B. G. Davis, J. Chromatogr. Sci., 13, 367(1975).

66.   C. W. Sink, D. R. Hardy and R. N. Hazlet, Naval Research Laboratory Memorandum Report 5407, Sept. 1984. (AD-A-145 754).

67.   C. W. Sink, D. R. Hardy and R. N. Hazlett, Naval Research Laboratory Memorandum Report 5497, Dec. 1984.

68.   T. A. Norris and M. G. Rawdon, Anal. Chem., 56, 1767(1984).

END

1 - 81

DTIC